UNIVERSITAT POLITÈCNICA DE VALÈNCIA

Doctoral Thesis

Optimal deep learning assisted design of socially and environmentally efficient steel-concrete composite bridges under constrained budgets

Valencia, July 2023

Author: David Martínez Muñoz

Advisors: D. Víctor Yepes Piqueras
D. Jose Vicente Martí Albiñana

Acknowledgements

I would like to express my sincere gratitude to all those who have assisted and encouraged me throughout the extensive process that has culminated in the fulfillment of my doctoral thesis. To begin with, I am grateful to Universitat Politècnica de València for allowing me to undertake this research project, which has proven to be a valuable experience in my academic and professional development. I would like to extend my heartfelt gratitude to my thesis advisors, Víctor Yepes and José Vicente Martí, whose unwavering support and guidance have been invaluable throughout the research process.

Words cannot express the depth of my gratitude to José García for his unwavering collaboration and support during the most arduous stages of this project. I would like to acknowledge his continued support and the tremendous opportunity he provided me to join his research team at the Pontificia Universidad Católica de Valparaíso, which has enhanced my research insight and professional growth. This project would have been considerably more difficult without his invaluable guidance.

Furthermore, I would like to thank the Spanish Ministry of Science and Innovation. This research would not have been possible without the support of grant FPU-18/01592, funded by MCIN/AEI/10.13039/501100011033, "ESF invests in your future", as well as the financial assistance provided by DIMALIFE (BIA2017-85098-R) and HYDELIFE (PID2020-117056RB-I00), both funded by MCIN/AEI/10.13039/5011-00011033, and "ERDF A way of making Europe".

I could not forget to thank all my colleagues in the research group. I am incredibly thankful to Nadia and Vicent, who warmly welcomed me when I first arrived at ICITECH, and to all those who have joined the group since then, including Iñaki,

Alex, Andrés, Mehrdad, Salva, Byron, Paola, Iván, and Antonio. I appreciate their support and the time they have spent with me, and it has been a pleasure to share this experience with them.

I want to thank my colleagues at ICITECH, who have shared many years with me. Their encouragement and support have been instrumental in helping me progress. I would like to thank Ester, Marta, Celia, Manolo, Eduard, Lisbel, Hesam, Ghobad, and all those who have since moved on from ICITECH to pursue their professional endeavors.

Finally, I would like to acknowledge the invaluable support of my family, which has played a crucial role in enabling me to achieve everything. I am incredibly grateful to Carolina, who has been a constant source of encouragement, pushing me to persevere through the most challenging moments of this project.

Doctoral thesis by article compendium

This doctoral thesis is presented as a compendium of previously published articles. The complete references of each paper comprising the body of the thesis are provided below:

- MARTÍNEZ-MUÑOZ, D.; MARTÍ, J.V.; YEPES, V. (2020). **Steel-concrete composite bridges: design, life cycle assessment, maintenance and decision making**. Advances in Civil Engineering, 2020:8823370.

  DOI:10.1155/2020/8823370

- MARTÍNEZ-MUÑOZ, D.; MARTÍ, J.V.; YEPES, V. (2021). **Comparative life cycle analysis of concrete and composite bridges varying steel recycling ratio**. Materials, 14(15):4218.

  DOI:10.3390/ma14154218

- MARTÍNEZ-MUÑOZ, D.; MARTÍ, J.V.; YEPES, V. (2022). **Social Impact Assessment Comparison of Composite and Concrete Bridge Alternatives**. Sustainability, 14(9):5186.

  DOI:10.3390/su14095186.

- MARTÍNEZ-MUÑOZ, D.; GARCÍA, J.; MARTÍ, J.V.; YEPES, V. (2022). **Optimal design of steel-concrete composite bridge based on a transfer function discrete swarm intelligence algorithm**. Structural and Multidisciplinary Optimization, 65:312.

  DOI:10.1007/s00158-022-03393-9

- MARTÍNEZ-MUÑOZ, D.; GARCÍA, J.; MARTÍ, J.V.; YEPES, V. (2022). **Discrete swarm intelligence optimization algorithms applied to steel-concrete composite bridges**. Engineering Structures, 266:114607.

  DOI:10.1016/j.engstruct.2022.114607

- MARTÍNEZ-MUÑOZ, D.; GARCÍA, J.; MARTÍ, J.V.; YEPES, V. (2023). **Hybrid swarm intelligence optimization methods for low-embodied energy steel-concrete composite bridges**. Mathematics, 11(1):140.

  DOI:10.3390/math11010140

- MARTÍNEZ-MUÑOZ, D.; GARCÍA, J.; MARTÍ, J.V.; YEPES, V. (2023). **Deep learning approach for life cycle optimization of steel-concrete composite bridges**. Applied Soft Computing.

  Manuscript Under Review

- MARTÍNEZ-MUÑOZ, D.; MARTÍ, J.V.; YEPES, V. (2023). **Game theory approach for environmental and social LCA multi-objective optimization of steel-concrete composite bridges**. Engineering Structures.

  Manuscript Under Review

Abstract

Infrastructure design is strongly influenced by the search for solutions considering the impact on the economy, the environment, and society. These criteria were strongly related to the definition of sustainability by the Brundtland Commission in 1987. This milestone posed a challenge for technicians, scientists, and legislators alike. This challenge consisted of generating methods, criteria, tools, and regulations that would allow the inclusion of the concept of sustainability in developing and designing new infrastructures. Since then, small advances have been made in the search for sustainability, but they need more in the short term. As an action plan, the United Nations established the Sustainable Development Goals, setting the year 2030 as the target for achieving them. Within these goals, infrastructure is postulated as a critical point. Traditionally, methods have been developed to obtain optimal designs from the point of view of economic impact. However, although recent advances have been made in implementing and using complete life cycle analysis methods, there still needs to be a clear consensus, especially in the social pillar of sustainability. Given that sustainability encompasses different criteria, which in principle do not necessarily go hand in hand, the problem of finding sustainability is posed not only as an optimization problem but also as a multi-criteria decision-making problem.

The main objective of this doctoral thesis is to propose different methodologies for obtaining optimal designs that introduce the pillars of sustainability in the design of steel-concrete composite bridges. A three-span box-girder bridge is proposed as a representative structural problem. Given the complexity of the structure, which involves 34 discrete variables, optimization with mathematical methods is unaffordable. Therefore, the use of metaheuristic algorithms is proposed. This complexity also translates into a high computational cost for the model, so a deep neural net-

works model is implemented to allow the validation of the design without the need for computation. Given the problem's discrete nature, discretization techniques are proposed to adapt the algorithms to the structural optimization problem. In addition, to improve the solutions obtained from these discrete algorithms, hybridization methods based on the K-means technique and mutation operators are introduced depending on the type of algorithm. The algorithms used are classified into two branches. The first are those based on trajectories such as Simulated Annealing, Threshold Accepting, and Old Bachelor Acceptance. Moreover, swarm intelligence algorithms such as Jaya, Sine Cosine Algorithm, and Cuckoo Search are used. The Life Cycle Assessment methodology defined in the ISO 14040 standard is used to evaluate the social and environmental impact of the proposed designs. The application of this methodology allows the evaluation of the impact and comparison with other designs. The single-objective evaluation of the different criteria leads to the conclusion that cost optimization is associated with a reduction of the environmental and social impact of the structure. However, optimizing environmental and social criteria does not necessarily reduce costs. Therefore, to perform a multi-objective optimization and find a compromise solution, a technique based on Game Theory is implemented, proposing a cooperative game strategy. The multi-criteria technique used is the Entropy Theory to assign criteria weights for the aggregate objective function. The criteria considered are the three pillars of sustainability and the constructive ease of the top slab. Applying this technique results in an optimal design concerning the three pillars of sustainability and from which the constructive ease is improved.

Resumen

El diseño de infraestructuras está fuertemente influido por la búsqueda de soluciones que tengan en cuenta el impacto en la economía, el medio ambiente y la sociedad. Estos criterios están muy relacionados con la definición de sostenibilidad que hizo la Comisión Brundtland en 1987. Este hito supuso un reto para técnicos, científicos y legisladores. Este reto consistía en generar métodos, criterios, herramientas y normativas que permitieran incluir el concepto de sostenibilidad en el desarrollo y diseño de nuevas infraestructuras. Desde entonces, se han producido pequeños avances en la búsqueda de la sostenibilidad, pero se necesitan más a corto plazo. Como plan de acción, las Naciones Unidas establecieron los Objetivos de Desarrollo Sostenible, fijando el año 2030 como meta para alcanzarlos. Dentro de estos objetivos, las infraestructuras se postulan como un punto crítico. Tradicionalmente, se han desarrollado métodos para obtener diseños óptimos desde el punto de vista del impacto económico. Sin embargo, aunque en los últimos tiempos se ha avanzado en la aplicación y utilización de métodos de análisis del ciclo de vida completo, aún falta un consenso claro, especialmente en el pilar social de la sostenibilidad. Dado que la sostenibilidad engloba diferentes criterios, que en principio no van necesariamente de la mano, el problema de la búsqueda de la sostenibilidad se plantea no sólo como un problema de optimización, sino también como un problema de toma de decisiones multi-criterio.

El objetivo principal de esta tesis doctoral es proponer diferentes metodologías para la obtención de diseños óptimos que introduzcan los pilares de la sostenibilidad en el diseño de puentes mixtos acero-hormigón. Como problema estructural representativo se propone un puente viga en cajón de tres vanos mixto. Dada la complejidad de la estructura, en la que intervienen 34 variables discretas, la optimización con

métodos matemáticos resulta inabordable. Por ello, se propone el uso de algoritmos metaheurísticos. Esta complejidad también se traduce en un alto coste computacional para el modelo, por lo que se implementa un modelo de redes neuronales profundas que permite la validación del diseño sin necesidad de computación. Dada la naturaleza discreta del problema, se proponen técnicas de discretización para adaptar los algoritmos al problema de optimización estructural. Además, para mejorar las soluciones obtenidas a partir de estos algoritmos discretos, se introducen métodos de hibridación basados en la técnica K-means y operadores de mutación en función del tipo de algoritmo. Los algoritmos utilizados se clasifican en dos ramas. La primera son los basados en trayectorias como el Simulated Annealing, Threshold Accepting y el Algoritmo del Solterón. Por otra parte, se utilizan algoritmos de inteligencia de enjambre como Jaya, Sine Cosine Algorithm y Cuckoo Search. La metodología de Análisis del Ciclo de Vida definida en la norma ISO 14040 se utiliza para evaluar el impacto social y medioambiental de los diseños propuestos. La aplicación de esta metodología permite evaluar el impacto y compararlo con otros diseños. La evaluación mono-objetivo de los diferentes criterios lleva a la conclusión de que la optimización de costes está asociada a una reducción del impacto medioambiental y social de la estructura. Sin embargo, la optimización de los criterios medioambientales y sociales no reduce necesariamente los costes. Por ello, para realizar una optimización multi-objetivo y encontrar una solución de compromiso, se implementa una técnica basada en la Teoría de Juegos, proponiendo una estrategia de juego cooperativo. La técnica multi-criterio utilizada es la Teoría de la Entropía para asignar pesos a los criterios para la función objetivo agregada. Los criterios considerados son los tres pilares de la sostenibilidad y la facilidad constructiva de la losa superior. Aplicando esta técnica se obtiene un diseño óptimo relativo a los tres pilares de la sostenibilidad y a partir del cual se mejora la facilidad constructiva.

Resum

El disseny d'infraestructures està fortament influït per la cerca de solucions que tinguen en compte l'impacte en l'economia, el medi ambient i la societat. Aquests criteris estan molt relacionats amb la definició de sostenibilitat que va fer la Comissió Brundtland en 1987. Aquesta fita va suposar un repte per a tècnics, científics i legisladors. Aquest repte consistia a generar mètodes, criteris, eines i normatives que permeteren incloure el concepte de sostenibilitat en el desenvolupament i disseny de noves infraestructures. Des de llavors, s'han produït xicotets avanços en la cerca de la sostenibilitat, però es necessiten més a curt termini. Com a pla d'acció, les Nacions Unides van establir els Objectius de Desenvolupament Sostenible, fixant l'any 2030 com a meta per aconseguir-los. Dins d'aquests objectius, les infraestructures es postulen com un punt crític. Tradicionalment, s'han desenvolupat mètodes per a obtindre dissenys òptims des del punt de vista de l'impacte econòmic. No obstant això, encara que en els últims temps s'ha avançat en l'aplicació i utilització de mètodes d'anàlisis del cicle de vida complet, encara falta un consens clar, especialment en el pilar social de la sostenibilitat. Atés que la sostenibilitat engloba diferents criteris, que en principi no van necessàriament de la mà, el problema de la cerca de la sostenibilitat es planteja no sols com un problema d'optimització, sinó també com un problema de presa de decisions multi-criteri.

L'objectiu principal d'aquesta tesi doctoral és proposar diferents metodologies per a l'obtenció de dissenys òptims que introduïsquen els pilars de la sostenibilitat en el disseny de ponts mixtos. Com a problema estructural representatiu es proposa un pont viga en calaix de tres vans mixt. Donada la complexitat de l'estructura, en la qual intervenen 34 variables discretes, l'optimització amb mètodes matemàtics resulta inabordable. Per això, es proposa l'ús d'algorismes metaheurísticos. Aque-

sta complexitat també es tradueix en un alt cost computacional per al model, per la qual cosa s'implementa un model de xarxes neuronals profundes que permet la validació del disseny sense necessitat de computació. Donada la naturalesa discreta del problema, es proposen tècniques de discretització per a adaptar els algorismes al problema d'optimització estructural. A més, per a millorar les solucions obtingudes a partir d'aquests algorismes discrets, s'introdueixen mètodes d'hibridació basats en la tècnica K-*means i operadors de mutació en funció del tipus d'algorisme. Els algorismes utilitzats es classifiquen en dues branques. La primera són els basats en trajectòries com la Simulated Annealing, Threshold Accepting i el Old Bachelor Acceptance. D'altra banda, s'utilitzen algorismes d'intel·ligència d'eixam com Jaya, Sine Cosine Algorithm i Cuckoo Search. La metodologia d'Anàlisi del Cicle de Vida definida en la norma ISO 14040 s'utilitza per a avaluar l'impacte social i mediambiental dels dissenys proposats. L'aplicació d'aquesta metodologia permet avaluar l'impacte i comparar-lo amb altres dissenys. L'avaluació mono-objectiu dels diferents criteris porta a la conclusió que l'optimització de costos està associada a una reducció de l'impacte mediambiental i social de l'estructura. No obstant això, l'optimització dels criteris mediambientals i socials no redueix necessàriament els costos. Per això, per a realitzar una optimització multi-objectiu i trobar una solució de compromís, s'implementa una tècnica basada en la Teoria de Jocs, proposant una estratègia de joc cooperatiu. La tècnica multi-criteri utilitzada és la Teoria de l'Entropia per a assignar pesos als criteris per a la funció objectiu agregada. Els criteris considerats són els tres pilars de la sostenibilitat i la facilitat constructiva de la llosa superior. Aplicant aquesta tècnica s'obté un disseny òptim relatiu als tres pilars de la sostenibilitat i a partir del qual es millora la facilitat constructiva.

Contents

List of Figures

List of Tables

Chapter 1

Introduction and objectives

1.1 Background

There has been growing recognition of the impact of raw material consumption and emissions from various industrial processes in recent years. Society has become aware that uncontrolled resource depletion could endanger the planet's future. The concept of sustainable development was introduced by the Brundtland Commission in 1987 to address this concern. Sustainable development is a form of development that meets the needs of the present without compromising the ability of future generations to meet their own needs [1]. Since then, significant efforts have been made to develop cleaner production processes and materials with fewer contaminants.

However, the construction industry remains one of the most carbon-intensive industries [2], [3]. Furthermore, construction activities also contribute significantly to environmental pollution [4]. According to Choi [5], the construction industry accounts for 30% of global energy consumption, 30% of greenhouse gas emissions, and 40% of raw material extraction. Therefore, optimizing human activities regarding material consumption and emissions is crucial to ensure more sustainable processes that minimize environmental impact. As sustainability is paramount, numerous researchers have studied existing construction processes to enhance and optimize their sustainability.

It is widely acknowledged that infrastructure is a critical driver of economic prosperity and social development, as it provides essential services and promotes territorial integration. According to the International Monetary Fund, investing an additional 1% of the Gross Domestic Product (GDP) in infrastructure would lead to an average increase of 1.5% in the world's GDP within four years. This estimate aligns with the observation that around 20% of World Bank loans in recent years have been directed towards transport infrastructure [6]. Moreover, the construction sector accounts for approximately 9% of Europe's GDP and provides 18 million direct jobs [7].

Given the infrastructure's economic, environmental, and social impact, sustainability must be considered in its design to achieve the 2030 Agenda goals. Bridges, in particular, are critical infrastructure in civil engineering, contributing to economic growth and connecting distinct geographical areas. Therefore, their structural design must consider the concept of sustainability.

Engineers are tasked with designing structures that fulfill their intended purpose and consider various other factors. In the case of bridge design, factors such as the construction process and the structure's potential for reuse or demolition must be evaluated. This necessitates a thorough understanding of the materials' behavior and the stresses that will undergo throughout the service life [8]. Furthermore, constructing

these structures has a significant environmental impact that cannot be overlooked [9]. However, this impact can be minimized through careful design and planning [10].

Steel-concrete composite bridges (SCCBs) could be suitable to accomplish the current design objectives. The steel components of these bridges are recyclable, as highlighted by Gervasio [11]. Since developing composite structure theories in the 20th century, SCCBs have been widely used, as noted by Bernabeu [12]. According to Musa and Diaz, SCCBs are highly efficient because steel and concrete can be placed in the cross-section zones where they perform best. In addition, SCCBs provide aesthetic appeal, as observed by Musa and Diaz [13]. However, the design of such structures can be quite complex due to the numerous design variables involved [14].

Researchers have developed various methods to achieve optimal structures using algorithms. These procedures involve changing the structure's variables to guide the search for optimal solutions. Accepting new solutions depends on the objective function's value and the algorithm's specific characteristics. Optimization methods have been applied to all kinds of structures, including bridges, as evidenced by the work of Martí et al. [15], Martins et al. [16], [17], and Penadés-Plà [18]. However, research on optimization has primarily focused on concrete bridges, with limited knowledge available for SCCBs. In this field, only the economic dimension of sustainability has been explored, considering it as a single objective.

In contrast, sustainability should be considered more broadly to encompass the social and environmental impacts, as previously mentioned. Furthermore, the complexity of structural problems is associated with high computational costs. This makes, on the one hand, the application of mathematical methods to solve the problems unavoidable and, on the other hand, the need for large amounts of time when considering the application of metaheuristic optimization techniques. This problem can be solved by using metamodels to assist the optimization process. The application becomes more critical in the multi-objective SCCBs optimization problem approach since the evaluation of different objective functions directly translates into increased computational time.

Considering the importance of sustainability in the design of SCCBs structure, it is imperative to propose a methodology that encompasses a comprehensive sustainability profile. Such a methodology should aim at achieving a compromise solution by leveraging the benefits of optimization, machine learning, and multi-criteria decision-making techniques to address the challenges posed by complex structural problems. In recent research, the Life Cycle Assessment (LCA) methodology has emerged as a prominent approach for evaluating the environmental and social impact of such structures [19]

This doctoral thesis was conducted at the University Institute of Concrete Science and Technology (ICITECH) at the Universitat Politècnica de València (UPV). The research group has extensive experience in this field. It has produced numerous publications related to the topic, which provided a solid foundation for this study.

Furthermore, several public funding sources supported the thesis's preparation, including the Spanish Ministry of Science and Innovation (BIA2017-85098-R, PID2020-117056RB-I00, and FPU-18/01592).

1.2 Research objectives

This PhD thesis proposes a comprehensive sustainable profile design strategy for structures using the LCA methodology to evaluate the environmental and social impacts. Furthermore, the economic dimension have been taken into account to consider the typical inclination of governments to enforce budgetary constraints on infrastructure. The method is applied to a three-span steel-concrete composite bridge using discrete hybrid optimization techniques guided by a neural network artificial intelligence model. The following research questions are formulated in light of the current context and identified knowledge gaps to assess the sustainable design:

- **Question 1:** Are steel-concrete composite bridges a viable alternative in terms of their environmental and social impact and how the steel recycling affect in the assessment?
- **Question 2:** Can optimization techniques be aligned with sustainable development goals in the design of steel-concrete composite bridges?
- **Question 3:** Is there a direct relationship between the cost and environmental and social impact in the design of steel-concrete composite bridges?
- **Question 4:** Do the design results, encompassing the three dimensions of sustainability, affect the ease of construction for certain elements of the solution obtained?
- **Question 5:** How can advances in artificial intelligence and predictive modeling be leveraged to improve designs and reduce computational time for bridge optimization?

This PhD thesis proposes an LCA-oriented Game Theory approach for providing sustainable designs following ISO 14040 standard and using discrete hybrid metaheuristic techniques assisted by a deep neural network metamodel for improving both computational and performance design results.

The following goals were set for this doctoral dissertation:

1. Review the existing literature related with steel-concrete composite bridges design, sustainability assessment, maintenance and decision making techniques used for finding the lacks of knowledge in SCCB design.
2. Compare composite bridges' environmental and social impact with other types to determine whether they represent a viable solution considering different steel recycling ratios.
3. Propose procedures for searching optimal designs using discrete metaheuristic algorithms applying discretization and hybridization techniques.
4. Conclude the relationship between the three pillars of sustainability when optimizing them in isolation in SCCBs.
5. Apply game theory and entropy theory to enable a search for optimal solutions considering the three dimensions of sustainability and the constructive ease of certain elements.
6. Study the behavior of the proposed methods when deep learning techniques such as deep neural networks are introduced to improve computational time.

1.3 Methodology

This dissertation methodology employs five different techniques to achieve the research objectives.

The first step involves reviewing the State of the Art of SCCBs design from a sustainability perspective. This is accomplished through exploring and evaluating existing research in various fields related to SCCBs design. This study examines research related to composite bridges, including their design, behavior, optimization, construction processes, maintenance, impact assessment, and decision-making approaches to provide a comprehensive approach to design. The review summarizes the findings and employs multivariate analysis to identify patterns and knowledge gaps relevant to sustainable SCCBs design.

Next, meta-heuristic techniques have been selected as design methods to automate the process. Two main branches have been chosen: swarm intelligence and trajectory-based methods. Swarm intelligence utilizes a population of individuals that interact with each other to generate new solutions. The meta-heuristic algorithms used in this method are Jaya, Sine Cosine Algorithm, and Cuckoo Search. On the

other hand, trajectory-based algorithms make minor changes between iterations to modify the individual and search for the optimum solution. The main feature of these algorithms is the definition of a threshold for accepting or rejecting a new solution. In this case, the algorithms used are Simulated Annealing, Threshold Accepting, and Old Bachelor Acceptance. The latest algorithm can increase or decrease the threshold during iterations, depending on the number of solutions accepted.

Moreover, discretization and hybridization techniques have been employed to adapt the algorithms to the discrete nature of the SCCB optimization problem and improve their performance. The first technique employs V-shaped functions to convert the continuous swarm intelligence algorithms into discrete ones. Additionally, two hybridization techniques have been utilized. For the swarm intelligence algorithms, a K-means clustering technique has been applied. Meanwhile, for trajectory-based metaheuristics, a mutation operator has been utilized to take advantage of the exploration of genetic algorithms by inducing random mutations in individuals.

These design techniques have been utilized to achieve an optimal and sustainable design for a three-span box-girder SCCB with three spans of 60-100-60. The process involved the automation of model generation, stress analysis, measurement, and structural verification using a Python program with modules that produce results for the considered objective functions. Five objective functions were employed to evaluate sustainability in all dimensions, including cost, CO_2 emissions, embodied energy, and environmental and social life cycle assessment. An additional objective function was included to improve construction feasibility by considering the number of reinforcement bars required for bridge resistance.

Environmental and social impact evaluations were conducted utilizing the cradle-to-grave approach with the LCA methodology. Besides employing this tool for calculating objective functions, it was also used to compare SCCB with slab and box-girder concrete bridges. The software, openLCA, was utilized for modeling the complete life cycle, and the environmental and social impact databases used were ecoinvent and soca, respectively. The life cycle inventory analysis methods employed were ReCiPe and Social Impact Weighting.

Due to the structural modeling and objective function calculation, this approach has a high computational cost. A Deep Neural Networks model has been trained to predict the feasibility of solutions to address this issue.

The selected objective functions were implemented as both single and multi-objective approaches. To achieve a three-dimensional sustainable design, a cooperative strategy utilizing the Game Theory approach was developed, taking into account cost, environmental and social LCA, in addition to constructive ease. This approach enables

the search for a compromise solution among all the alternatives using a mathematical framework. To achieve this, the Entropy Theory multi-criteria decision-making method was also utilized to reach a solution.

1.4 Dissertation structure

The structure of this dissertation presents the research into 12 chapters:

- **Chapter 1:** Explains the research backdrop, aims, and major contributions of the actual PhD dissertation, as well as the research methods used.
- **Chapter 2:** Shows the state of art of SCCB design and assess how the sustainability have been applied for reaching those designs by using optimization, MCDM and LCA techniques.
- **Chapter 3:** Presents a life cycle environmental assessment comparing alternatives of box-girder SCCB with different types of concrete bridges for studying its feasibility depending on the span length. Furthermore, applies different steel recycling ratios in order to compare the variability in the impact produced.
- **Chapter 4:** Presents a social impact evaluation using the life cycle assessment methodology and comparing SCCB with concrete alternatives with different steel recycling ratios for the SCCB steel. Moreover, compares the results with a environmental LCA analysis.
- **Chapter 5:** Describes the optimization problem and applies both cost and CO_2 single-objective optimizations using a v-shape transfer function as discretization techniques for Sine Cosine and Jaya algorithms. Moreover, compares the results with a Simulated Annealing with a mutation operator and shows the differences between cost and CO_2 optimum designs.
- **Chapter 6:** Applies both the v-shape transfer function and the K-means hybridization technique to Sine Cosine and Cuckoo Search algorithms and compares the results to the ones obtained by same algorithms without the K-means clustering technique and the Simulated Annealing with a Mutation Operator for both cost and CO_2 single objective optimization.
- **Chapter 7:** Uses the hybrid techniques proposed using as objective function the embodied energy and compares the results with a cost optimization.
- **Chapter 8:** Utilizes deep learning models to predict the feasibility of the bridge. These machine-learning models are applied to the hybrid techniques proposed

in previous chapters. The objective functions considered are cost and social and environmental life cycle assessment considered as a single objective. The chapter aims to compare the design differences and computation time improvements.

- **Chapter 9:** Applies a cooperative strategy based on the game theory applied mathematics branch to carry out a multi-objective optimization considering cost, the environmental and social life cycle assessment, and the constructive ease of the upper slab. This chapter compares the results obtained by the multi-criteria optimization with the single objective optimization results of the previous chapters.
- **Chapter 10:** Presents a detailed analysis of the outcomes obtained in the preceding chapters.
- **Chapter 11:** Provides a concise overview of the key aspects and case-specific findings derived from this doctoral dissertation and proposed avenues for further investigation.

Figure 1.1 summarizes the methodologies employed in this dissertation for reaching the SCCB study case sustainable design.

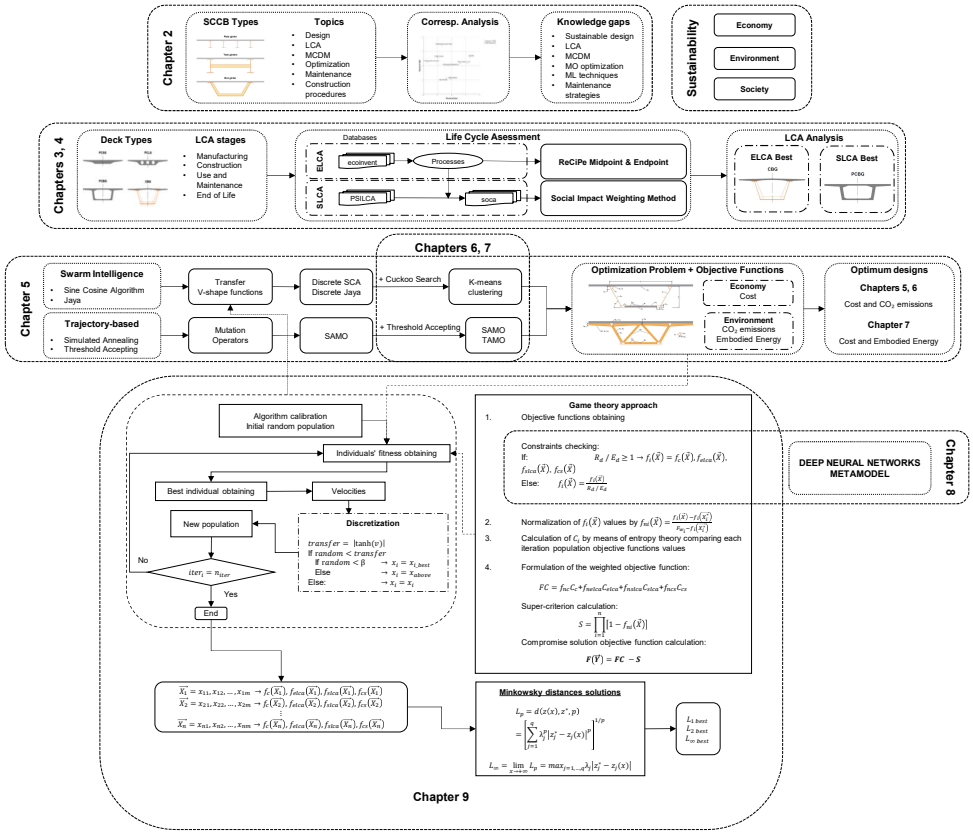

Figure 1.1: Dissertation methodology flowchart

Chapter 2

Steel-concrete composite bridges: design, life cycle assessment, maintenance, and decision-making

Authors:	D. Martínez-Muñoz , J.V. Martí, and V. Yepes		
Status:	Manuscript published		
Journal:	Advances in Civil Engineering, 8823370		
Year:	2020		
DOI:	10.1155/2020/8823370		
JCR IF (2021):	1.843		
	JCR Category	Ranking	Quartile
	Construction & Building Technology	48/68	Q3
	Engineering, Civil	102/138	Q3
Presentation:	Post-print (author version)		

Abstract

Steel-concrete composite bridges are used as an alternative to concrete bridges because of their ability to adapt their geometry to design constraints and the possibility of reusing some of the materials in the structure. In this review, we report the research carried out on the design, behavior, optimization, construction processes, maintenance, impact assessment, and decision-making techniques of composite bridges in order to arrive at a complete design approach. In addition to a qualitative analysis, a multivariate analysis is used to identify knowledge gaps related to bridge design and to detect trends in research. An additional objective is to make visible the gaps in the sustainable design of composite steel-concrete bridges, which allows us to focus on future research studies. The results of this work show how researchers have concentrated their studies on the preliminary design of bridges with a mainly economic approach, while at a global level, concern is directed towards the search for sustainable solutions. It is found that life cycle impact assessment and decision-making strategies allow bridge managers to improve decision-making, particularly at the end of the life cycle of composite bridges.

Keywords: steel-concrete composite bridges; design; optimization; maintenance; MCDM; LCA

2.1 Introduction

Bridges are one of the most important structural typologies made by civil engineers and have a great impact on society by favoring territorial connection. The design of bridges must integrate different requirements to reach a design according to the required needs. In addition, the design of bridges must consider the context in which the structure is framed. This context is related to the characteristics of the place where the structure will be located and the determining factors from economic, cultural and environmental point of views. Engineers are faced with making designs that must take into account factors that go beyond the simple fact that their work fulfills the function for which it is designed [8]. In bridge design, other aspects, such as the construction process or the structure's reuse or demolition strategies, must be evaluated. This requires a clear understanding of the behavior and stresses that their materials will be subjected to throughout their service life [8]. In addition, these infrastructures have an associated environmental impact during their construction [9] that must also be considered. This impact can be mitigated with good design and planning [10]. Since the World Commission of Environment and Development defined sustainable development guidelines [1], national policies have focused on obtaining infrastructures that accomplish the sustainable development terms. In addition, the

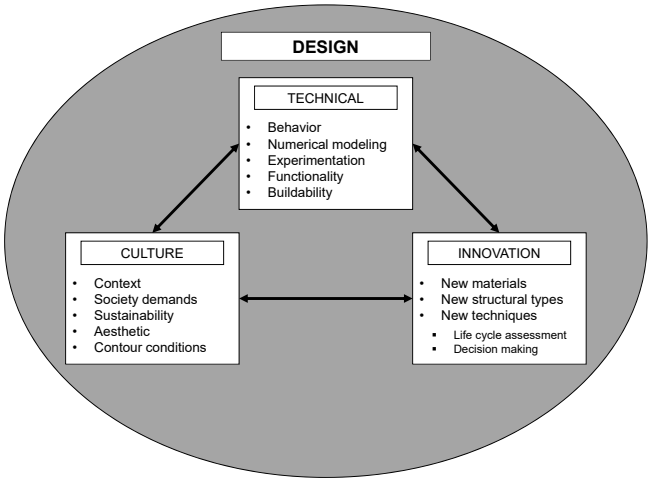

Figure 2.1: Scheme of design criteria

United Nations defined the Sustainable Development Goals [20] as objectives for 2030. Because of this, it can be understood that one of the demands of society is the incorporation of sustainability in infrastructure design. Authors such as Rams [21] add environmental friendliness as one of their design principles. Furthermore, innovation in building materials and structural shapes give designers more tools to make designs more in line with current design criteria. In figure 2.1, the scheme of design criteria have been displayed.

To achieve the objectives of the current design, steel-concrete composite bridges (SCCBs) can be a good alternative due to the recyclability of the steel parts of the structure [11]. SCCBs have been used extensively since the 20th century, when composite structure theories were developed more generally [12]. In addition, Musa and Diaz state that this type of bridge is highly efficient due to the possibility of placing the steel and concrete in the parts of the cross section where they perform best. They also provide added value due to their attractive appearance [13].

The aim of this review is to collect knowledge regarding SCCBs to identify the approach that designers and researchers have given to design. This work provides designers and technicians with a guide where current information is collected regarding the behavior of this type of structure, the methods used by authors to reach the optimum design, the construction methods and maintenance, as well as the repair strategies. Furthermore, a lack of knowledge related to SCCBs is found, offering researchers the possibility of focusing their efforts on the weakest areas. The gaps

are obtained by using statistical techniques that analyze the correlation between different variables. Furthermore, all the information considered in this study gives a broader vision of the possibilities of the sustainable design of SCCBs, considering sustainability in the whole process.

2.2 Data sampling strategy

The searches related to the subject of this work were carried out with the scientific bibliographic databases of SCOPUS and the Web of Science. The search period was limited from 1995 to 2019. The terms used for the search of the different articles were the combination of "Steel-concrete composite bridges" with the following words: *"Optimization", "Decision making", "Multi-attribute decision making", "Multi-target decision making", "Multi-criteria decision making", "Life cycle assessment", "Life cycle", "Maintenance", "Fatigue", "Reliability", "Uncertainty", "Robustness", "Fire resistance", "Construction process", "Safety", "Strength", "Seismic"* and *"Buckling"*, finding a total of 4784 articles.

In order to filter the works that are directly related to the relevant topics, a first exclusion criterion was applied considering only peer-reviewed scientific papers and conference works. In addition, studies that do not consider the complete composite action of the structure or that deal with the behavior of independent composite elements were discarded. Finally, we only considered articles written in English for this study. This screening strategy resulted in 90 articles.

2.2.1 Statistical analysis

To identify the fields that have been extensively studied and those that present a lack of knowledge, a simple correspondence analysis was carried out using IBM SPSS Statistics 25 (IBM Corp., Armonk, NY, USA) software [22]. This method allows us to represent the relationship between two variables. In this case, it was used to relate the fields of knowledge related to the design with the type of section of the SCCB and the stages of the design process. This statistical method has been applied in other literature review studies [23].

2.3 Steel-concrete composite bridge design

2.3.1 General overview

SCCBs have been studied extensively due to the good behavior of this type of structure. The information obtained from the literature review was divided into six fields of study: *Design and Behavior, Optimization, Construction Process, Maintenance and Repair, Life Cycle Assessment (LCA) and Multi-Criteria Decision Making (MCDM)*. This division is not arbitrary. The division is related to the sustainable design phases that Penadés-Plà and others proposed in their work [23]: *Planning and Design, Construction, Operation and Maintenance and Demolition and Recycle*.

The first stage encompasses the Design and Behavior field of knowledge, where researchers study the behavior of the structure and propose calculation methods and structural solutions to improve the behavior of specific areas or the whole set. In the next phase of the process, designers use techniques to achieve better solutions and study how to bring their designs to reality. At this stage of the design process, the optimization and construction processes play a crucial role and must be considered together to reach the best solution for the construction phase. Once the structure materializes, the design should consider maintenance periods and methods to evaluate the condition of the structure, in order to assess the actions to be taken, either for repair or maintenance. When the service life has come to an end, the construction has to be demolished and recycled. All these processes and decisions have an associated impact, which is where the LCA method allows technicians to assess the impact of the structures. Throughout the design process, decisions have to be made to reach the best solution for each stage. MCDM methods offer a powerful tool for designers to select the solution that most closely matches the constraints [24].

In addition, the SCCBs found in the articles of this review can be grouped by the type of cross section into three categories, plate girder, twin girders or box girder, according to the classification of Vayas and Iliopoulos [25]. In Figure 2.2, the three bridge sections described are displayed. The plate girder bridge consists of a number of steel girders that are connected to a concrete slab by shear connectors that allow composite behavior. The twin girders bridge has two or more steel girders that are usually I-shaped girders, which, like the plate girder bridge, are connected to a concrete slab. The difference between the slab bridge and the beam bridge is the behavior of the steel beams. On the one hand, slab bridges have a larger number of smaller beams. Because of their slenderness, these beams are classified as class 1 or 2 sections according to the Eurocodes [26]. On the other hand, in beam bridges, the larger dimensions of the beams make it impossible for the steel beams to behave as class 1 or 2 sections these are classified as class 4 sections and a reduction must

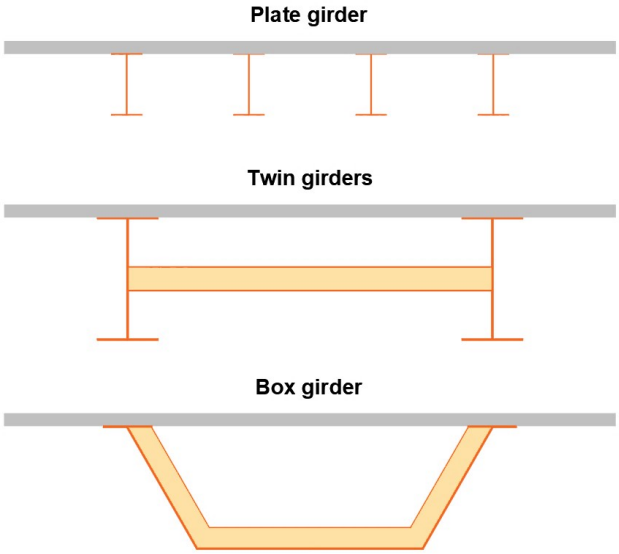

Figure 2.2: Bridge cross sections considered

be taken into account for calculations [26]. The geometry of the concrete slab is also reduced considering an effective width due to the phenomenon of shear lag according to regulations [26]. Finally, the box girder bridge is made up of an open steel box girder connected to a concrete slab on the top. The difference lies in the torsional behavior of this type of cross section, which is better than for twin girders bridges [13].

The distribution of studies found in every field is displayed in Figure 2.3. As shown, the greatest number of studies is focused on the Design and Behavior of bridges (66%), followed by the Optimization (13%) and the LCA (8%). Furthermore, the studies can be grouped by the year of publication and research field, as shown in Figure 2.4. The period of greatest production related to SCCBs was between 2010 and 2019. In 2019, there was a change in trend, with more studies carried out in fields related to optimization and decision making instead of continuing with the study of the behavior of bridges and the generation of new designs.

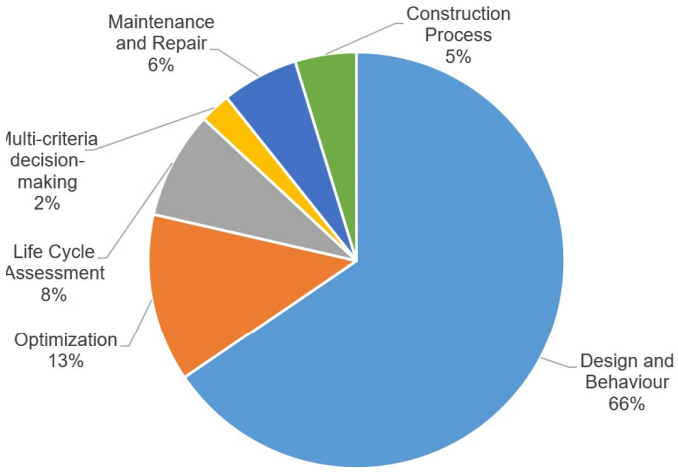

Figure 2.3: Distribution of publications in every research field

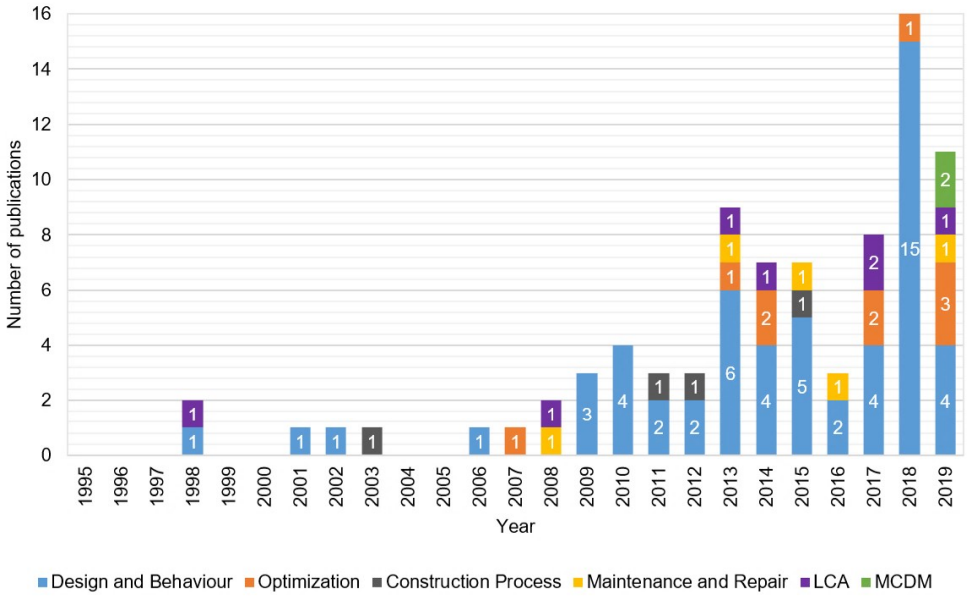

Figure 2.4: Number of publications grouped by year and research field

2.3.2 Design and behavior

The field of design and behavior includes all the studies related to the behavior of SCCBs towards traffic loads, torsion, fire, fatigue and seismic actions. In addition, this field includes new designs proposed by authors for the global design of the bridge deck or other local parts that have unique behavior.

In this field, three main approaches have been found: design proposals, behavior studies and calculation methods. Design proposals are focused on the conception of new geometries or the distribution of materials that improve the behavior of SCCBs [27]–[37]. Behavior studies are centered on the application of experimental or numerical approaches to study the bridge response when submitted to fire [38]–[42], seism [43]–[51], fatigue [52]–[64], secondary torsion [65], vibrations [66]–[71], blasting loads [72] or other phenomena [73]–[79]. Alternatively, some authors have focused their studies on implementing new calculation methods for SCCBs [80]–[87].

Table 2.1: Summary of SCCB design publications

Ref.	Author	Topic	Cross section	Method
[27]	Nakamura et al.	Cross-section designs	Twin girders	Experimental
[31]	Kim and Jeong	Cross-section and shear connector design	Plate girder	Experimental & Numerical
[29]	Xie et al.	Steel sections depth for mid-span in concrete bridges	Box girder	Numerical
[32]	Kim and Jeong	Cross-section and shear connector design	Plate girder	Experimental & Numerical
[30]	Vasseghi	Shear connectors in negative bending region	Plate girder	Numerical
[33]	Shao et al.	Cross-section design with reactive powder concrete	Box girder	Experimental & Numerical
[34]	Wu et al.	Cross-section U-shaped design	Box girder	Experimental & Numerical
[35]	Nie et al.	Corrugated steel web cross-section	Box girder	Experimental
[36]	Esteves, Almeida and Oliveira Pedro	union between concrete and composite sections	Box girder	Numerical
[37]	Peng-Zhen et al.	Negative bending region	Twin girders	Experimental
[28]	Xie et al.	Steel sections length for mid-span in concrete bridges	Box girder	Numerical

Table 2.1 summarizes the studies carried out for bridge design, with the majority of the studies dealing with proposals for the design of bridge cross sections and shear connectors. The most studied cross-section type is the box girder. According to the amount of studies found, it can be seen that work is focused on analyzing the behavior of SCCBs. Fire resistance studies are focused on modeling fire action with numerical models [38], [42] or fluid mechanics [39]. Other studies, related to the analysis of the fire behavior of SCCBs, they have also carried out experimental tests to calibrate the numerical models [40], [41]. However, all the authors conclude that there are very few studies on the fire behavior of SCCBs. This lack of studies is also reflected in issues such as blasting loads [72] or the torsional behavior of curved SCCBs [65]. On the contrary, the behavior of SCCBs to fatigue and seism has been largely studied.

Studies related to new calculation methods focus on adding new concepts to the design of SCCBs. Zona et al. [80] proposed a probabilistic non-linear analysis method for bridge design using the first-order second-moment approximation [88] and the direct differentiation method [89]–[92] for the sensitivity analysis. Nie and Zhu [82]

created a beam-truss model for box girder SCCBs based on classical shear-flexible grillage analysis, obtaining a 10% difference between this model and traditional ones. Jia et al. [84] included in their method the system reliability to failure with a ten degrees of freedom finite element model. Other authors have focused their method on evaluating the shear lag [81], shrinkage, creep and cracking [85] or flexural lateral loads [86], [87].

2.3.3 Optimization

The design of structures is based on the search for solutions that allow the structures to be able to fulfil their function using as fewer resources as possible. The designers use an iterative process that consists of the modification of the geometry and a later verification to arrive at a better design of the structure. This procedure is clearly based on the experience and judgement of the designer. Researchers have developed different methods to achieve optimal structures by means of algorithms. These procedures guide the search for optimal solutions by changing the variables that define the structure. The acceptance of new solutions depends on the value of the objective function and the characteristics of the algorithm. These optimization methods have been applied to all types of structures, including bridges [15], [18], [93], [94].

Some researchers have focused their studies on the search for optimum designs, taking as an objective the cost reduction of the structure [95], starting from basic studies carried out by applying techniques that include penalty functions for the search of the optimum [96]. Since then, techniques have become increasingly more complex, with the use of optimization algorithms, like in the study of Musa and Diaz [13] who used the Excel optimization module to reach a preliminary design without cracking and fatigue checks. The optimization process generally uses a numerical model to evaluate the stresses of the bridge, which has a high computational cost, with the authors having developed methods that divide the optimization process into two stages. Briseghella et al. [97] used a simple model to reach the optimum geometry with the *Ansys* optimization tool and later applied topological optimization [98]–[102] to a more complex numerical model using the finite element method to reduce the steel sections that are subjected to local buckling.

Pedro et al. [103] applied different algorithms in a two-stage optimization process. The results of their analysis gave good behavior for the optimization techniques for SCCB optimization, with good results. Other authors have applied the fmincon Matlab functions [104] to SCCB I girder bridges, taking good results for span lengths up to 20 m. In other studies, the life cycle cost of the structure were evaluated, comparing the SCCB solution with pre-stressed concrete solutions and stating that the

pre-stressed concrete solutions are better than the composite ones [105]. These results could depend on the life cycle phases that have been considered. Rempling et al. [106] propose a set-based parametric design [107], [108] applied to SCCB optimization. Kaveh et al. applied and compared different algorithms to composite bridges in their studies successfully [109], [110]. The optimization techniques are summarized in Table 2.2.

Table 2.2: Optimization techniques used by authors

Ref.	Author	Cross section	Method
[110]	Kaveh	Box girder	Colliding bodies optimization [111] Enhanced colliding bodies optimization [112] Vibrating partial systems [113]
[106]	Rempling et al.	Twin girders	Set-based parametric design [107], [108] Set-based design [107], [108]
[103]	Pedro et al.	Twin girders	Backtracking search algorithm [114] Firefly algorithm [115] Genetic algorithm [116] Imperialist competitive algorithm [117] Search group algorithm [118]
[110]	Kaveh et al.	Box girder	Cuckoo search [119] Harmony search [120] Particle swarm optimization [121]
[104]	Lv et al.	Plate girder Twin girders	Matlab fmincon function
[97]	Briseghella et al.	Box girder	Ansys optimization tool Topological optimization [98]–[102]
[13]	Musa and Diaz	Box girder	Excel solver

Nowadays, the value of structures is not assessed only by their economy, but also by their social and environmental impact. Optimization studies carried out in the current literature focus on the optimization of a single objective and fundamentally on the reduction of weight and therefore on an economic improvement. The social and environmental pillars of sustainability are not studied from the point of view of optimization. Furthermore, in studies carried out on concrete bridges, multi-objective optimization has been applied [122], [123], while in SCCBs, these methods are not applied, nor are those of accelerated optimization [124]. Therefore, it can be said that there is a lack of knowledge in the field of multi-criteria optimization and the use of methodologies that allow the optimization of the structure from a social and environmental point of view for the SCCBs. Moreover, the approach given to the optimization of structures consists mainly of the application of different algorithms to the problems. There are no studies related to the knowledge of the algorithms in a more scientific way in the field of bridge optimization. Arnold [125] exposes this

phenomenon in his work and indicates that the trend to be taken is towards the understanding of the behavior of algorithms. The application of optimization algorithms in the field of structures and especially in the field of SCCBs is quite recent and therefore further studies of different optimization methods is needed to have the possibility to compare. However, the study of how these techniques work and why some are better than others for this field of study should not be left aside.

2.3.4 Construction process

The construction process of the SCCB is unique because the construction has a differentiation between the steel and concrete parts of the structure. The most common process is to build and place the steel part first using support systems to reduce the deflections of the steel part of the bridge. Then, the concrete slab formwork and the reinforcement are placed and the concrete is poured. This unique procedure gives the structure a characteristic behavior and researchers are currently developing and studying different construction processes for SCCBs [126]–[131]. The construction processes can be summarized as continuous precast girder bridges, incremental launching, span-by-span construction and cantilever construction [132].

Here, we review the effects of the construction processes. Marí, Mirambell and Estrada studied the effects of construction process and slab prestressing on the serviceability behavior using a finite element model of one dimension [132], with a 14% increase in negative bending zones and a reduction of 50% in positive bending reported. Jung, Kim and Sim [133] studied the behavior of a prestressed concrete box girder bridge with corrugated steel webs built by incremental launching. The results of the study conclude that this type of structural cross section allows the maximum span-to-depth ratio due to the self-weight reduction of the structure to be extended compared with a prestressed concrete box girder. Other authors have studied the precast construction of bridges in Europe and America [134]. They state that the construction of prefabricated bridges accelerates the construction of bridges and that the possibility of doing so with steel-concrete bridges is a good solution for the use of the material. This also occurs because such precast structures usually work in an isostatic way and therefore the upper concrete slab is compressed and the steel section is pulled. Another possibility is the use of removable prefabricated elements, allowing for connection of the precast concrete slabs with the steel beams, as in the study by Valipour et al. [135]. This study reveals that good results are obtained in the construction process in terms of ductility and strength using prefabricated elements.

In this field, the literature on SCCBs is scarce, so a detailed study is needed of their structural behavior with different construction methods. In addition, there are new methods being used to build mixed bridges that differ from the traditional ones. In

addition, it is important to consider the new construction procedures as a further boundary condition for the models and work to find optimal solutions.

2.3.5 Maintenance and repair

To reach a sustainable design, a complete study of all the stages of the service life of the bridge is required. Service life is a concept that allows designers and engineers to define the period of time that is considered to use the infrastructure. However, maintenance activities are necessary to keep the structure in a state that allows it to be used in a safe way. These activities can be preventive when related with the design of infrastructures preventing the possibility of damage [136] or corrective, with a repair approach. Focusing on the search in SCCBs, two main trends have been established: repair and renovation [137], [138] and the evaluation of bridge conditions [139]–[141].

In contrast, Albrecht and Lenwari propose three methods of fatigue damage repair [137]. The method that gives better results is to tension a steel wire in the low part of the steel section to compress the section, so that when loads are applied the section will always be compressed. This gives a fatigue resistance higher than the one imposed by the AASTHO. Sugimoto, Yoshida and Tanigaka [138] proposed the reinforcement of steel railway bridges, placing a concrete slab on the top of the steel beams, transforming the steel bridge in a composite one, taking advantage of the composite action between steel and concrete and improving the behavior against deflections. Alternatively, authors have proposed different methods to assess bridge conditions, giving stakeholders infrastructure management data to make decisions regarding the maintenance of the bridge. Gheitasi and Harris [139], using a finite element model, assess the composite action that is still working in bridges with damage in the concrete slabs, this method allows us to evaluate if the structure needs maintenance or, on the contrary, it still has sufficient resistance capacity. In other studies, authors proposed a decision making method according to the data obtained by instrumented bridges that have corrosion damage on the steel beams [140]. The numerical model proposed by the author is capable to assess the maintenance needs of the bridge by the infrastructure manager. Moreover, Matos et al. [141] proposed a model that is capable of introducing data from the bridge condition and uses Bayesian inference [142], [143] to reduce the uncertainty of model parameters, allowing stakeholders to take better decisions according to maintenance.

2.3.6 Life cycle assessment

Bridges have an associated impact during all phases of their life cycle. Therefore, researchers have searched for different ways to evaluate the impact of bridges in an objective way. Widman [144] applied the Environmental Priority Strategies in Product Design (EPS), the Environmental Theme Method (ETM) and the Ecoscarcity Method (EM) to assess the life cycle of a box girder SCCB. This evaluation resulted in a low maintenance impact of the bridge. The author states that the maintenance phase is very small and, therefore, it is not necessary to protect the structures, it is better to repair it. ISO 14040:2006 [145] defines the methodology to assess the life cycle of bridges for the first time, in this way a framework is generated that allows researchers to have a guide for their studies. Gervasio and da Silva compared concrete with composite bridge solutions, analyzing the cost and the environmental impact, with the results showing that SCCBs have a higher cost but a low environmental impact [11]. Du and Karoumi [146] state that SCCBs are better from the point of view of the environmental impact due to the possibility of materializing slender sections and the higher capability to recycle of structural steel. The steel recycling rate for structural steel is 98% [147], which allows us to reduce the impact of SCCBs. In other research, author have done a literary review of the LCA methods and software and implemented new LCA methods to reach the impact evaluations of SCCB railway bridges [148] and short span bridges [149].

Table 2.3: Summary of SCCB LCA publications

Ref.	Year	Author	Structural Type	Pillar	Method	Approach
[144]	1998	Widman	Box girder	Environmental	EPS ETM EM	Cradle to grave
[11]	2008	Gervasio and da Silva	Twin girders	Environmental Economic	Lippiatt [150]	Cradle to grave
[146]	2013	Du and Karoumi	Twin girders	Environmental	ReCiPe [151]	Cradle to grave
[95]	2017	Batikha et al.	Twin girders	Economic	Cost of materials and maintenance	Cradle to grave
[149]	2020	Milani and Kripka	Plate girder	Environmental	ReCiPe [151]	Cradle to gate

As seen in Table 2.3, the studies carried out for the LCA of SCCBs have been focused on the economic and environmental pillars. For SCCBs, there exists a knowledge gap in the approach social of LCA. Furthermore, researchers have considered a cradle to grave approach. It is necessary to carry out studies with a broader vision to take into account the entire life cycle process, including the phases of dismantling and demolition of the structure and the recycling and reuse of materials.

2.3.7 Multi-Criteria Decision-Making

Decision making is a process that allows solutions to be obtained that satisfy different objectives. This process can be carried out in many ways. Hwang and Yoon [152] classified the multi-criteria decision making processes into multi-attribute decision making (MADM), and multi-objective decision making. MADMs are used to decide on a discrete number of solutions that is what usually occurs in bridge design and more specifically at SCCBs.

Penadés-Plà et al. carried out a review of MCDM methods applied to bridges [23], but in SCCBs, these methods have not been extensively applied. Only two publications have been found related with that field. The first applies SCORE [153] and PANTURA [154] methods to choose the best alternative between concrete and composite I girder bridges [155]. In the other study, the method AHP [156] and Vikor [157] have been applied to short span bridges. In this second study, the results obtained gives as the most suitable solutions for the two methods the steel-concrete composite one. Furthermore, authors state that the application of MCDM in short span bridges can provide good design for small-span bridges to fulfil the needs of connection between areas in undeveloped countries [149].

According to the small number of well-founded investigations related to this research topic; it can be said that there is a lack of knowledge in this field. This must be completed with future studies that take into account the MCDM methodologies in each of the phases of the SCCB design cycle, introducing uncertainty and robustness in the decision-making process [158], [159].

2.4 Discussion

Most of the studies focus on preliminary design and structure behavior as these represent 66% of the total with 55 articles. Inside this category, three main trends have been found: bridge design (18%), behavior (42%) and calculation methods (13%). The bridge design studies have been focused on the definition of the transverse section of bridges and the connection between the steel and concrete parts of the structures. In the behavior approach, a lack of research is observed in accidental actions, like fire and blasting loads, compared with other topics considered by authors, such as seism and fatigue behavior. In addition, other works have focused on the new calculation method considering sensitivity or reliability and carrying out statistical methods applied to the design of the structure.

Optimization research, which means the 13% of the total with 11 articles, has focused on cost optimization. There is a lack of knowledge in applying multi-criteria

optimizations methods and considering other criteria for the optimization, such as environmental or social. Furthermore, the optimization is only focused on the application of different algorithms to take results; however, authors are not considering the study of the behavior of algorithms in structural optimization. There is a lack of knowledge according to the search for causes and reasons why some heuristics work better than others. Related with that field, authors do not emphasize in the construction process, which is decisive in many cases. This may be due to the lack of study of the behavior of SCCBs in the construction processes with only a 5% of papers of the total considered.

Once the final design is defined, the structure has a defined service life. To reach this, it is important to define the maintenance periods and, if it were necessary, the repairs. There are few studies focused on the repair and maintenance of SCCBs, representing the 6% of the total. Work in this field focuses on evaluating the condition of bridges and defining the repairs to be carried out. There is a lack of knowledge in the preventive maintenance of this type of structures. There are currently techniques for evaluating the impact of these actions and methods for making decisions regarding maintenance, repair and demolition. These methods are LCA and MCDM.

LCA and MCDM studies, which represents the 8% and 2% respectively, are closely related in the studies included in this review. These methods are used to choose the best alternative, comparing between concrete, steel, composite and timber bridges. These methods always give SCCBs as a good alternative compared with concrete. Because of this, it is important not only to apply these methods for the type of bridge selection, but also to use these methods to assess the needs of the bridges built, in maintenance, repair or demolition according to different criteria.

To identify the relation between the research fields, the sustainable design phases and the structural type of the cross sections of bridges, a statistical analysis has been carried out. The method used to study the relation between that variables have been the simple correspondence analysis [160]. To use this method, every publication has to be classified according to the research field, the design phase and the structural type considered in every study. Once the classification is completed, the frequency of each combination of variables has to be obtained. The method uses the Chi-square distance to give as a result the relation between every categories of each variable. IBM SPSS Statistics for Windows, Version 25.0 [22] software have been used to carry out the statistical analysis. For clearer results, the variables have been compared in pairs, obtaining the results shown in Figures 2.5 and 2.6.

In Figure 2.5, the results of the simple correspondence analysis are shown for the Research field and Sustainable design stage variables. The graphic shows a clear relationship between Design and Behavior with Planning and Design stages, and

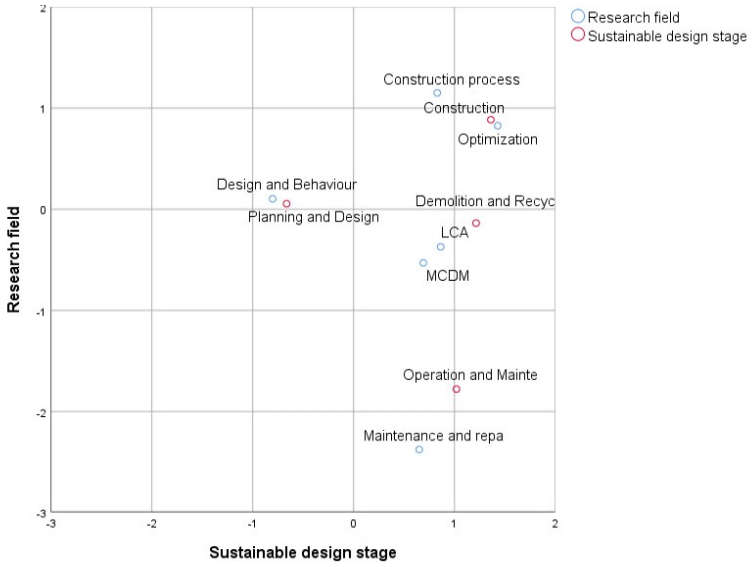

Figure 2.5: Simple correspondence analysis for research field and sustainable design stages.

between Construction and Optimization. These results are logical because the Planning and Design stage is related with obtaining a first design that has to be improved at later stages. To reach that first design, it is necessary to consider the structural behavior of the SCCB. To obtain the final design to build the bridge, the construction process of the bridge and the optimization procedure must be considered. These concepts are in line with the graph, but it is observed that in the studies considered in this review the construction design is focused more on optimization than on the construction process. This result shows a lack of consideration of the construction process in the optimization. Furthermore, it can be seen that the LCA and MCDM are quite linked to the Demolition and Recycle design stage. This is because a large part of these studies focus on making decisions between maintenance and repair of SCCBs or demolition. This is an important topic that should be developed in subsequent studies due to the lack of studies related to these topics for SCCBs.

Figure 2.6 shows the relation between the research fields and the structural type of the transverse section. Articles that consider the box girder sections for the studies are 28. Otherwise, plate girder and twin girder sections are considered in 23 and 64 of the articles in this paper. There is a relation between the box girder cross section and the Optimization field, while the twin girders section is more related with the LCA. The distance between the box girder section with other research field shows a need to carry out studies related with the construction process, the maintenance and

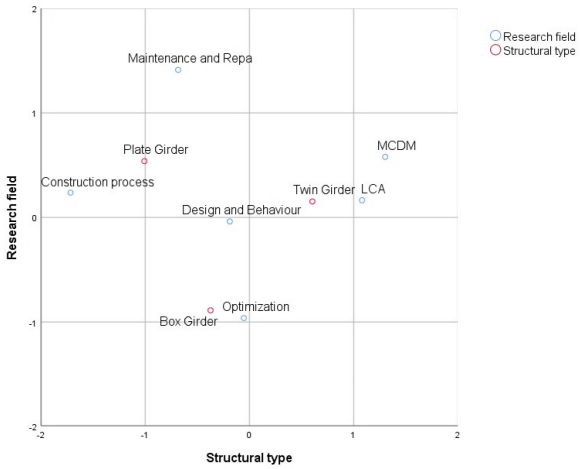

Figure 2.6: Simple correspondence analysis for research field and structural type

repair and the study of the design and behavior considering MCDM and LCA. The results of the analysis between the field of knowledge and the structural type of the cross section, in general do not show a clear relation between them. This is a sign of a lack of studies in most fields, which is an opportunity for researchers to develop these topics in greater depth.

The statistical analysis accomplished in this review shows the relation between the fields of knowledge with every design phase. Based on the results obtained, it can be state that construction should be considered in optimization as a determining factor. The LCA and MCDM method are related with maintenance and repair and demolition phases due to the need of decision making and assessment methods to ease the decision of stakeholders in infrastructure management. The studies have not a clear relation between the research fields and the cross-section type of SCCBs. A larger study should be done to complete the lack of knowledge identified in this work.

2.5 Conclusions

This review has focused on a design approach for steel-concrete composite bridges. Four design stages have been considered and the research fields related with that phases have been reviewed. These research fields are Design and Behavior (66%), Optimization (13%), Construction Process (5%), Maintenance and Repair (6%), Life Cycle Assessment (5%) and Multi-Criteria Decision-Making (2%). To improve the lit-

erature review, a statistical analysis has been carried out to look for relations between fields of study, design stages and bridge cross-section types.

Most of the studies focus on preliminary design and structure behavior. The bridge design studies have been focused on the definition of the transverse section of bridges and the connection between the steel and concrete parts of the structures. It is observed a lack of research in the behavior of SCCBs summited to accidental actions. Furthermore, the trend of new calculation methods is related with adding sensitivity or reliability to the analysis. Optimization research has focused on cost optimization. There is lack of knowledge in applying multi-criteria optimizations methods and considering other criteria for the optimization, such as environmental or social. This is far from the current trend of searching for sustainable solutions considering all the pillars of sustainability. The studies focused on the repair and maintenance evaluate the condition of bridges and define the repairs to be carried out. There is a lack of knowledge in the preventive maintenance of this type of structures and LCA and MCDM methods for maintenance management. These methods are applied only to compare between types of bridge. It is observed that the results of these methods give SCCBs as a good alternative from an environmental point of view.

The SCCB literature review carried out shows the gaps in the fields related with bridge design. This work can be a useful tool for researcher to focus their analysis in those gaps. In this way, research related to the design of steel-concrete composite bridges will be able to focus on those topics that have not yet been dealt with in depth.

Chapter 3

Comparative life cycle analysis of concrete and composite bridges varying steel recycling ratio

Authors:	D. Martínez-Muñoz , J.V. Martí, and V. Yepes		
Status:	Manuscript published		
Journal:	Materials, 14(15):4218		
Year:	2021		
DOI:	10.3390/ma14154218		
JCR IF (2021):	3.748		
	JCR Category	Ranking	Quartile
	Metallurgy & Metallurgical Engineering	18/79	Q1
	Physics, Applied	56/161	Q2
Presentation:	Post-print (author version)		

Abstract

Achieving sustainability is currently one of the main objectives, so a consensus between different environmental, social, and economic aspects is necessary. The construction sector is one of the main sectors responsible for environmental impacts worldwide. This paper proposes the life cycle assessment (LCA) and comparison of four bridge deck alternatives for different span lengths to determine which ones are the most sustainable solutions. The ReCiPe method is used to conduct the life cycle analysis, by means of which the impact value is obtained for every alternative and span length. The Ecoinvent 3.3 database has been used. The life cycle has been divided into four phases: manufacturing, construction, use and maintenance, and end of life. The associated uncertainties are considered, and the results are shown in both midpoint and endpoint approaches. The results of our research show that for span lengths less than 17 m, the best alternative is the prestressed concrete solid slab. For span lengths between 17 and 25 m, since the box-girder solution is not used, then the prestressed concrete lightened slab is the best alternative. For span lengths between 25 and 40 m, the best solution depends on the percentage of recycled structural steel. If this percentage is greater than 90%, then the best alternative is the composite box-girder bridge deck. However, if the percentage is lower, the cleanest alternative is the prestressed concrete box-girder deck. Therefore, the results show the importance of recycling and reusing structural steel in bridge deck designs.

Keywords: life cycle assessment; sustainability; structures; ReCiPe; environment; bridges

3.1 Introduction

Over the last few years, awareness of the consequences of the consumption of raw materials and the emissions of various processes has risen. Society has realized that if we continue with the uncontrolled consumption of resources, our current actions will compromise the future of the planet. For this reason, the sustainable development concept appeared, a term that was introduced in 1987 by the Brundtland Commission, defining it as *"development that meets the needs of the present without compromising the ability of future generations to meet their own needs"* [1]. Since then, a significant effort has been invested to achieve cleaner production processes for known materials and the development of new materials with the same characteristics but fewer contaminants.

Construction is one of the most carbon-intensive industries [2], [3], and in terms of CO_2 emissions, its cement requirements alone produce 5% of the total emissions [161]. Furthermore, construction contributes to environmental pollution [4]. This negative contribution is mainly produced by cement and concrete production [161], [162]. The impact of these activities is produced by their energy consumption, and in the construction sector, concrete is one of the most important materials used in buildings. Due to this circumstance, concrete consumption, and therefore the associated pollution, will increase over the next years [163]. Because of this, human activities must be optimized in terms of material consumption and emissions to ensure more sustainable processes that will not compromise the environment as much.

Due to the importance of achieving this objective, many researchers have been studying current construction processes in order to improve and optimize their sustainability. Researchers have studied the emissions produced by concrete projects [164]–[166] or construction procedures [167]–[169]. Other studies have focused on the optimization of concrete structures such as prestressed bridges [170], [171] and earth-retaining walls [172]–[175]. Other researchers have studied CO_2 fixation by carbonation processes and their influence on the emissions [176], [177] and the concrete recycling ratio [148], [178], [179].

However, to study the environmental impact, life cycle analysis (LCA) is performed. This is a powerful and versatile method capable of evaluating any type of construction or process [180] or the materials used therein [181]–[183], from concrete and earth retaining walls [184], [185] to optimal bridge decks [159], house structures [186], and facades [187], [188]. However, some reviews state that there is a lack of LCA in steel–concrete composite bridges [189].

The aim of this study is to carry out analyses of the life cycle of four bridges: prestressed concrete solid slab (PCSS), prestressed concrete lightened slab (PCLS), prestressed concrete box-girder (PCBG), and steel–concrete composite box-girder (CBG). The aim is to determine which of them, depending on the span length, has the lowest environmental impact [148], [178], [190]. Additionally, a sensitivity analysis is carried out to evaluate the impact of the life cycle of a composite bridge depending on its steel recycling ratio in order to study the feasibility of this structural type compared to concrete alternatives. This allows us to provide a broader approach and to make a comparison of the amount of recycled steel that has been used in the manufacturing processes. Steel manufacturing comprises two main production methods: basic oxygen furnace (BOF) and electric arc furnace (EAF). In both processes, iron is combined with steel scrap, which is the product that is obtained by the steel recycling process. In EAF production, the percentage of steel scrap (recycled steel) used is between 90 and 100%, while in the BOF production process, the percentage of steel scrap (recycled steel) is reduced to 10–30% [147]. The rates of BOF and EAF and, in

consequence, the rate of recycled steel used for steelmaking depend largely on the technological development of countries. Therefore, this makes this study useful not only for countries with a high technological development in the steelmaking process but also for other countries where steel contains a smaller amount of recycled raw material.

3.2 Materials and Methods

The life cycle analysis (LCA) method consists of obtaining the environmental impact of an activity, evaluating the potential contribution of the processes that make up that product. These processes together encompass all the activities required to complete the main product. The procedures begin by obtaining the raw material and end with the waste management. The LCA of the bridge decks has been carried out according to ISO 14040:2006 [145]. It comprises four phases to obtain the assessment: definition of goal and scope, inventory analysis, impact assessment, and interpretation of the results. The life cycle impact assessment (LCIA) that has been chosen for this research is the ReCiPe 2008 method [151]. The database used to obtain the environmental impact information is Ecoinvent v3.3.

3.2.1 Goal and Scope Definition

The main goal of this research is to compare, from the environmental point of view, four different bridge deck types. The structural system selected is a continuous beam, and the analyses have been carried out on six span lengths: 15, 20, 25, 30, 35, and 40 m. The purpose of this research is to compare different deck types with different span lengths to evaluate the differences between them, and the LCA method makes it possible to obtain a quantitative assessment of the different solutions proposed. Pang et al. [191] affirm that there are three main reasons for performing an LCA analysis on bridges: comparison of different alternatives, comparison of different bridge component alternatives, and comparison of new material with conventional material. To compare different bridge alternatives, these have to be similar in terms of load capacities, deck dimensions, and span if all the alternatives are in the same geographical area. If they are not, then it is necessary to take into account other conditions such as the geotechnical information of the ground, the seismicity of the building location, and the corrosion capacity of the environment, among others. In this study, the same location has been considered for all the alternatives.

Bridge Deck Type Selection

Bridges are very important infrastructures that allow society to avoid obstacles and enable users to close the gap between two points. Furthermore, these structures have a direct impact on society in terms of their economic, social, and environmental role. For beam bridges, the most important part is the deck, because it has to resist the stresses produced by the traffic loads. The deck type depends on different conditionings: functional, constructive, economic, and environmental, among others. In this paper, four deck types have been compared: prestressed concrete solid slab (PCSS), prestressed concrete lightened slab (PCLS), prestressed concrete box-girder (PCBG), and composite box-girder (CBG). Figure 3.1 presents a sketch of each of the alternatives.

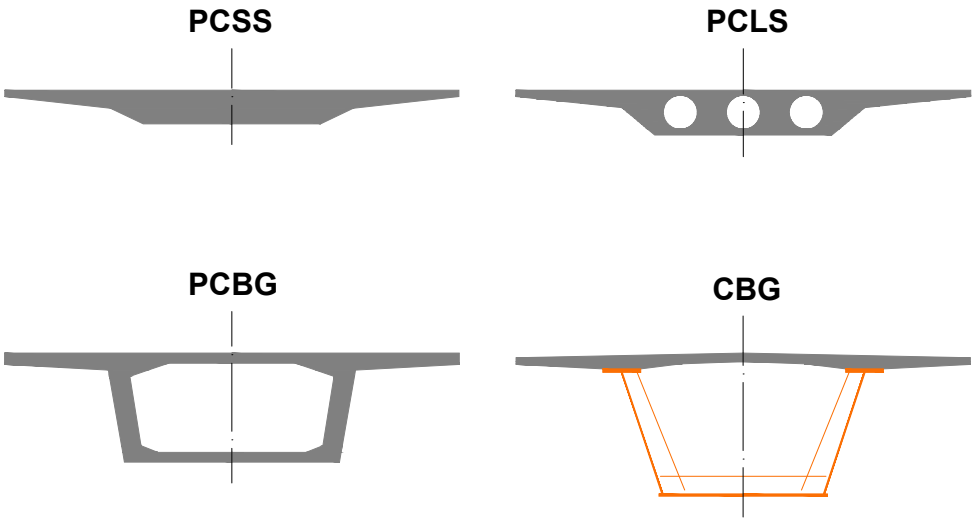

Figure 3.1: Bridge deck cross sections

The use of these decks depends on the span length. On the one hand, continuous slab depth decks are used for lengths between 5 and 50 m, but the usual range of application is from 15 to 35 m. However, the box-girder bridges have lengths between 25 and 125 m, and the most used range is 35–80 m. In box-girder bridges, two main materials are used to form the resistant section of the bridge: concrete, which can be reinforced or prestressed, and steel. The choice of material may depend on various factors, including the environment to which the structure is exposed, the road alignment, and geotechnical constraints, among others.

Slab bridges are usually used for shorter distances, because for greater lengths, the amounts of concrete, passive reinforcing steel (PRS), and active reinforcing steel (ARS) increase to a large extent, which translates into a higher cost, which is even more acute in PCSS. On the other hand, box-girder bridges can be used for greater lengths due to the ease of increasing their bridge deck depth, taking advantage of the mechanical arm increase and making the most of the mechanical characteristics of the materials. This study focuses on the comparison of these four bridge deck types with span lengths from 15 to 40 m, assessing them from the environmental point of view. This selection of alternatives comprises two slab and two box-girder decks, providing a wide range of choice and an estimation of the environmental cost of the structures for structural engineers and designers, depending on the dimensions of the structure.

Phases of the Analysis

Four stages are defined to assess the bridge's life cycle. To carry out the complete analysis of the structure, the processes that encompass all the activities should be considered, starting with the design, going through the manufacturing and the construction of the structure, and finally, the demolition and collection of the used materials. To consider all these activities, the life cycle of the structure is divided into four phases: manufacturing, construction, use and maintenance, and end of life, depending on the moment at which every activity is carried out. In this paper we have focused on PCSS, PCLS, PCBG, and CBG deck types, but it could be used for all bridge deck types by making minor modifications.

Manufacturing The manufacturing stage includes all activities needed to produce the materials that will be used for the resistant section, since the raw materials are extracted to be ready for use in the construction phase. The most widely used materials in bridge structures are concrete and steel. Databases usually refer to products that allow for the modeling of these materials, but it is possible to create a new product with real manufacturing processes and distances or in the case of concrete, with different dosages. The general processes to obtain one cubic meter of concrete and one kilogram of steel are shown in Figure 3.2.

The concrete matrix is created from different components that allow the quantity of each product that forms the concrete matrix to be controlled. Furthermore, it permits the control of the distance that every raw material is transported to the concrete manufacturing factory, allowing the study to be more specific, depending on the location where the concrete is created. Once all the materials of the concrete matrix are brought together, to simulate the concrete mixing, another process is created, includ-

ing the concrete matrix along with the energy, the mixing factory, or other activities that are needed to create one cubic meter of the final concrete product.

To produce a cubic meter of concrete, the mass of the final product and the wastes produced in the process must be considered. Marceau et al. [192] concluded that for the production of one cubic meter of concrete, the solid waste is 24.5 kg and the wastewater is 0.0348 m^3, the solid waste being small amounts of concrete. The real amount of each material that forms the concrete matrix can be calculated in Equations (3.1–(3.5) [159].

$$Total\ solid = Cement + Gravel + Sand \tag{3.1}$$

$$Primary\ cement = Cement + \left(\frac{Cement}{Totalsolid}\right) \cdot Waste\ concrete \tag{3.2}$$

$$Primary\ gravel = Gravel + \left(\frac{Gravel}{Totalsolid}\right) \cdot Waste\ concrete \tag{3.3}$$

$$Primary\ sand = Sand + \left(\frac{Sand}{Totalsolid}\right) \cdot Waste\ concrete \tag{3.4}$$

$$Primary\ water = Water + Wastewater \tag{3.5}$$

Steel manufacturing comprises two main production methods: basic oxygen furnace (BOF) and electric arc furnace (EAF). In both processes, iron is combined with steel scrap, which is the product that is obtained by the steel recycling process. In EAF production, the percentage of steel scrap (recycled steel) used is between 90 and 100%, while in the BOF production process, the percentage of steel scrap (recycled steel) is reduced to 10–30% [147]. The use of steel scrap has a direct relation with the environmental impact, and for this reason, the EAF and BOF have very different impacts. The ratio of steel scrap used for BOF and EAF production is known, so by controlling the EAF and BOF ratio to produce a kilogram of steel, the quantity of recycled steel for each steel product can be controlled in the manufacturing processes. The BOF and EAF waste production is considered in the product manufacturing part of the database.

The steel recycling ratio is especially important for steel and steel–concrete composite bridges. Because of the great amounts of steel used in their construction, slight

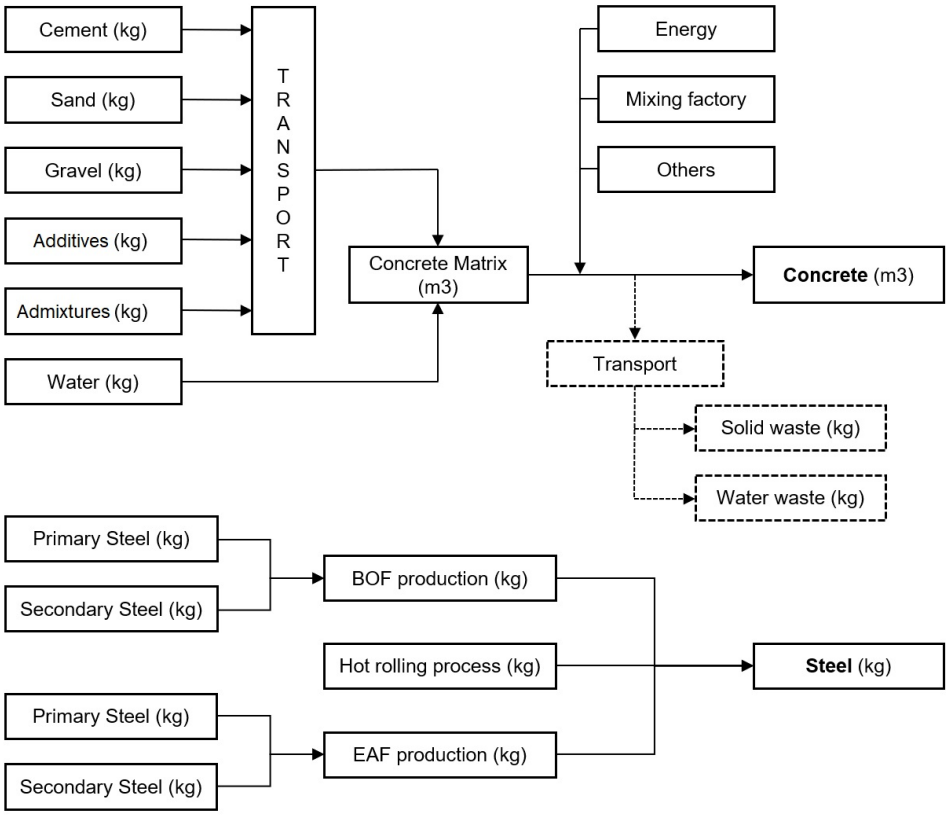

Figure 3.2: Concrete and steel manufacturing processes

variations in the steel recycling ratio produce great differences in the environmental impact of the bridge, as it is produced in general with a great amount of steel. From this point of view, it is important to distinguish between structural and rebar steel, as the USA steel recycling ratio for rebar steel is 71%, while the structural steel recycling ratio is 98% [193]. The difference between the recycling ratios of these two types of steel is occasioned by the difficulty of separating rebar steel from the concrete, because of which the recycling ratio for rebar steel is lower. Furthermore, the separation between the EAF and BOF steel production processes allows the specific steel recycling ratio of the study area to be introduced [184].

Construction The construction phase includes all the activities that are necessary to build the bridge, considering the machinery, depending on the chosen construction method and the location of the structure. The construction method must be defined at this stage. At this stage, the formwork, scaffolding, vibrators, and concrete pouring must be considered. In addition, for steel and steel–concrete composite bridges, the processes of welding the different parts that have not been considered in the manufacturing phase must be introduced. The construction method is introduced in the LCA model through the diesel consumption of the machinery obtained from the manufacturer's data, the literature, or other databases.

Use and Maintenance The use and maintenance stage contains all the activities that will be needed throughout the life of the structure. These activities can be classified into three different categories: maintenance activities, CO_2 fixation, and traffic detour. To carry out the different maintenance activities, the partial or total closure of the bridge may be necessary. If closure of the bridge is necessary, it implies that the vehicles will need to take an alternative route to reach their destination. This increase of the distance is translated into an increment of the environmental impact. The traffic detour impact is affected by different factors such as the location of the structure, the ratio of heavy vehicles, and the detour distance.

Authors have two different options to handle the maintenance stage. On the one hand, researchers assess the maintenance operations through a literature review to consider these operations [148], [178], [194]. On the other hand, different possible scenarios have been considered to analyze which one has the lowest environmental impact [191]. If the closure of the bridge is necessary for the maintenance activities, and their duration is defined, then this activity will be considered by introducing the processes that simulate those activities. These processes depend on the material used in the design of the bridge. The maintenance of steel bridges depends on the type of steel; if the steel is resistant to corrosion, this operation will be irrelevant, but if the steel needs to be treated for corrosion, this treatment will be repeated along the bridge life. For concrete bridges, these operations include the demolition of the external layer and their replacement with a reparation mortar. All these operations are considered by introducing the materials necessary for the repair, the diesel consumption of the machinery, and the emissions produced by the traffic detour if it occurs.

On the other hand, studies have concluded that concrete can fix CO_2 through carbonation [164], [176], [195]. Carbonation is one of the principal damage mechanisms of reinforced concrete bridges, and it is determined by three main factors [177]: the w/b ratio, the concentration of CO_2 in the surrounding air, the specific climate conditions, and the depth of embedded steel. Carbonation damages the concrete structure, but

if we focus on the environmental impact, carbonation reduces the structure's environmental impact. Lagerblad et al. [196] studied the CO_2 fixed by carbonation during the life-cycle based on Fick's first law. Equation 3.6 allows the fixed CO_2 to be calculated, in which k is the carbonation coefficient, t is the service life, A is the exposed area of concrete, r is the ratio of CaO that is going to become carbonated, C is the content of cement in one cubic meter of concrete, *k* is the content of clinker in the cement, L is the content of CaO in the clinker, and ϵ is the molecular weight ratio of CO_2/CaO. This equation is simplified grouping the constants. Lagerblad et al. [196] consider that r takes the value of 0.75 and L of 0.65 and assume that ϵ takes the value of 0.7857. Clearing out the equation with these constants, the expression changes to (3.7). García-Segura et al. [177] state that concrete structures can fix CO_2 along their service life.

$$CO_2 fixed(kg) = \frac{k\left(\frac{mm}{\sqrt{year}}\right)\cdot\sqrt{t(year)}}{1000}\cdot A(m^2)\cdot r\cdot C\left(\frac{kg}{m^3}\right)\cdot k(\%)\cdot L(\%)\cdot\epsilon \quad (3.6)$$

$$CO_2 fixed\,(kg) = 0.383\cdot\frac{k\left(\frac{mm}{\sqrt{year}}\right)\cdot\sqrt{t(year)}}{1000}\cdot A(m^2)\cdot C\left(\frac{kg}{m^3}\right)\cdot k(\%) \quad (3.7)$$

$\mathrm{End\ of\ Life}$ The end of life stage includes all the activities related to the dismantling of the structure, i.e., with the processes that occur when the life of the structure has ended. The principal processes involved in that stage of the bridge life are the machinery used to carry out the demolition of the structure and the transport and the treatment of the generated waste products.

Consequently, it is necessary to define the distances between the bridge construction location and the landfill or the waste treatment plants. There are three main possibilities for the waste materials: to reuse them, to recycle them, or to dispose of them in a landfill, depending on their characteristics. In this case study, and generally in bridges, the most commonly used materials are concrete and steel, and depending on the needs of the society of the region studied, there will be several possibilities for the waste treatment.

The steel recycling ratio has been studied by many researchers. Hammervold et al. [194] considered a 100% steel recycling ratio, while other authors such as Du et al. [178] and Hettinguer et al. [179] considered a lower value. Penadés-Plà et al. [19] considered the Spanish average steel recycling ratio of 71%. Other authors use the average value of larger areas of study. As you can see above, the steel recycling ratio depends on the location of the construction, and it is possible to refine the assessment of the steel used in the LCA model by controlling the ratio.

The concrete case is different from steel, because it can be recycled and reused with ease, especially in bridges. The Spanish concrete regulations recommend using at most 20% of concrete recycled coarse aggregates to produce new concrete [197]. Different concrete recycling ratios are considered [148], [178], [179]. As described before, the carbonation processes of concrete are carried out. If all the concrete is crushed [177], the surface available to perform the carbonation processes increases; therefore, the carbonation of the all concrete volume can be produced. Lagerblad [196] states the coefficient for concrete carbonation depending on concrete's strength. In this study, two types of concrete have been used, with 30 and 40 MPa strengths. The carbonation coefficient (k) is 1.5 mm/year$^{0.5}$, 4 mm/year$^{0.5}$, 6 mm/year$^{0.5}$, 0.75 mm/year$^{0.5}$, and 1 mm/year$^{0.5}$, depending on whether the concrete is exposed, sheltered, indoors, wet, or buried, for 30 MPa concrete strength, and 1 mm/year$^{0.5}$, 2.5 mm/year$^{0.5}$, 3.5 mm/year$^{0.5}$, 0.5 mm/year$^{0.5}$, and 0.75 mm/year$^{0.5}$ for 40 MPa concrete strength. The crushed concrete aggregate is assumed to have a 10 mm diameter.

Functional Unit

The study has been realized considering a square meter as the functional unit to enable the comparison of the different bridges. It is necessary to carry out a comparison between bridges to consider other factors such as the geotechnical parameters of the soil, seismic conditions, or contour restraints. If the location of the studied bridges is different, then the impact can differ depending on the processes used in the manufacturing of the materials. Another possibility is to consider the linear meter as the functional unit, as Penadés-Plà et al. [19] did. To compare the linear meter with the square meter, the values of the parameters must be divided by the deck width.

3.2.2 Inventory Analysis

The inventory analysis consists of the data collection of all the materials and energy consumption that are needed to develop all the processes involved in the bridge life cycle; in this case, all the values are referred to a square meter of bridge. These processes produce an output in terms of emissions to the environment, and the consideration of the output of every process together gives the environmental impact associated with the product that is being assessed.

Software

The model has been developed with the OpenLCA software from GreenDelta. This is an open source program that allows LCA applications to be performed, especially for the scientific community [198]. Furthermore, this software allows the introduction of the uncertainty attached to the processes previously imported from a database.

The database used to import the processes was Ecoinvent [199] in its version 3.3. This database was selected for this study because of its scientific reliability and constant updating [200].

3.2.3 Uncertainty

Uncertainty appears in LCA analyses due to the differences between the processes that are implemented in the database and the real ones [201]. These differences are caused by different factors, but the most important are the geographical location [202] and the time period over which the data were collected. For instance, it is not the same producing a kilogram of steel in Germany or in Spain, because the technology of the production process or the distances between the quarry and the facilities differ, and the manufacturing processes of steel in Spain in 2000 or in 2017 cannot be considered the same. These variations of location and time will introduce uncertainty in the processes.

To accommodate this uncertainty, the pedigree matrix [203] has been used. This method allows uncertainty factors to be introduced by means of five indicators: reliability, completeness, temporal correlation, geographical correlation, and further technological correlation. In addition, a basic uncertainty factor will be considered depending on the nature of the processes [199].

3.2.4 Bridge Deck Design

In Table 3.1, the quantity of materials per square meter has been provided. The amounts of materials for the PCSS and PCLS bridge decks have been obtained from the study by Yepes et al. [204]. The materials used to define the PCBG and CBG deck alternatives have been obtained from the instruction “Obras de paso de nueva construcción” of the Spanish Ministry of Public Works [205].

Table 3.2 shows the dosage of 30 and 40 MPa strength concrete used for this study. The PCSS, PCLS, and PCBG decks have been designed with HP-40 prestressed concrete, while for the CBG bridge deck, HA-30 reinforced concrete has been considered. The biggest difference in the use of materials is that in the CBG alternative,

Table 3.1: Amount of materials per square meter of deck.

	Unit	15	20	25	30	35	40
PCSS							
Concrete HP-40	m^3	0.473	0.561	0.649	0.738	0.826	0.914
Reinforcement Steel	kg	51.728	61.380	71.033	80.686	90.339	99.992
Prestressed Reinforcement Steel	kg	9.223	17.133	25.043	32.953	40.863	48.773
Formwork	m^2	1.500	1.500	1.500	1.500	1.500	1.500
PCLS							
Concrete HP-40	m^3	0.509	0.557	0.605	0.654	0.702	0.750
Reinforcement Steel	kg	52.165	57.109	62.052	66.996	71.939	76.883
Prestressed Reinforcement Steel	kg	5.069	10.914	16.759	22.604	28.449	34.294
Formwork	m^2	1.700	1.700	1.700	1.700	1.700	1.700
PCBG							
Concrete HP-40	m^3	0.441	0.461	0.482	0.503	0.523	0.544
Reinforcement Steel	kg	28.790	32.601	36.632	40.884	45.356	50.048
Prestressed Reinforcement Steel	kg	3.042	4.917	6.792	8.667	10.542	12.417
Formwork	m^2	1.900	1.900	1.900	1.900	1.900	1.900
CBG							
Concrete HA-30	m^3	0.220	0.230	0.240	0.250	0.261	0.272
Reinforcement Steel	kg	20.976	22.250	23.603	25.037	26.559	28.173
Structural Steel	kg	59.400	63.700	68.175	81.000	80.600	88.375
Shear Connector Steel	kg	0.310	0.346	0.381	0.423	0.437	0.494
Formwork	m^2	1.000	1.000	1.000	1.000	1.000	1.000

a steel–concrete composite structure, the structural steel beam that supports the slab, is added.

Table 3.2: Concrete dosage considered for bridge decks

Material	Unit	C30/37	C40/50
Gravel	kg	1110.00	829.00
Sand	kg	730.00	1102.00
Cement	kg	300.00	320.00
Water	kg	201.00	160.00
Superplasticizer	kg	0.27	5.00

Life Cycle Model Description

The life cycle model comprises four stages, the processes considered for the modeling of the decks have been obtained mainly from the Ecoinvent database, and those that were not included there have been generated, such as some types of machinery that have been modeled by their diesel consumption considering their operation times.

Manufacturing In the production phase, all the processes to produce materials have been included. In addition, the transport of the materials to the construction site has been considered, where the distances between the facilities and the bridge construction location are 30 km for concrete and 150 km for both the structural and rebar steels. Two types of concrete have been introduced depending on the deck type. Concrete of 30 MPa strength has been introduced directly from the Ecoinvent database, while the 40 MPa strength concrete process has been created as shown in Figure 3.2.

Steel production has been considered, creating two different steel production processes to consider the differences between the steel recycling ratio of the rebar and the structural steels. Ecoinvent's BOF process considers 19% of steel scrap (recycled steel), while the EAF process considers 100% of steel scrap. If the steel scrap amount is known, it is possible to control the total steel recycling ratio for the rebar and the structural steels. For the former, a 71% steel recycling ratio has been considered, while for the structural steel, many different recycling ratios have been determined to study their different impacts. Those ratios are 71% (CBG_71), 90% (CBG_90), and 98% (CBG_98). This varying of the steel recycling ratios has been considered in order to reflect differences between countries reusing materials, because in developing countries, policies that consider reuse are lower [206].

Furthermore, the CBG bridge deck needs to take into account the welding of the steel sheets in the manufacturing process, so this has been introduced in the CBG model considering the Ecoinvent database process.

Construction Construction was considered to be in situ. The activities considered in this stage are those related with concrete pouring and vibrating, the assembly of the different steel parts of the CBG, and the handling of the active reinforcement steel. A concreting with no special concrete curing requirements has been considered. The machinery is modeled introducing the diesel consumption data, which have been obtained from the Bedec database [207]. The diesel consumption is 123.42 MJ of energy per cubic meter of concrete and 10.2 MJ per kg of active reinforcement steel. The CO_2 emissions are 32.24 kg and 2.62 kg, respectively.

Use and Maintenance For the use and maintenance phase, it has been considered that traffic detours are not necessary to carry out the maintenance operations and that only the concrete needs to be maintained because the steel that has been considered is a weathering steel that does not need maintenance. The machinery for the maintenance was estimated considering two different periods of maintenance. The machinery consumption contemplated in this phase of the life cycle is 584.28 MJ, and the CO_2 emissions are 46.58 kg of CO_2 per square meter repaired.

End of Life At this stage, the activities related to the demolition and transport to landfill have been introduced in the LCA model. On the one hand, for the concrete elements, the machinery needed for their demolition has been considered. In addition, to be able to consider that all the concrete is carbonated, the crushing process has been included. On the other hand, only the transportation to the landfill has been reflected in the model because the recycling process of the steel has already been taken into account in the manufacturing process. For the CBG bridge deck alternative, steel sheet cutting with a flame cutting process has been considered.

3.2.5 Impact Assessment

The impact assessment consists of converting the impact of the processes considered to model the life cycle with an indicator that allows researchers, scientists, or readers to interpret them more easily. These indicators differ depending on the life cycle impact assessment (LCIA) method selected. The results of each process are shown as a list of emissions and consumed resources, and the LCIA methods distribute the emissions and consumed resources in a shorter list of indicators.

The LCIA method chosen is the ReCiPe method. There are two main impact assessment approaches, the midpoint and the endpoint, and the LCIA method transforms the emissions and the resource consumptions into an indicator, depending on the approach. For example, CML is an LCIA method that gives a midpoint approach, a list of indicators that shows a complete environmental profile that is difficult to interpret [208]. On the other hand, the eco-indicator LCIA method gives an endpoint approach. This approach takes the midpoint approach indicators and concentrates them in three damage categories: resources measured in dollars, human health measured in disability-adjusted life years, and ecosystem impact measured in species·year. This endpoint approach allows researchers to analyze the impact of the activity more easily. The ReCiPe LCIA method provides both the endpoint and the midpoint approaches and has therefore been chosen for the LCIA.

The ReCiPe midpoint approach provides a list of 18 environmental indicators. These indicators are useful if the study carried out is focused on one specific impact, such

as the global warming potential or the metal depletion. The categories supplied by this method are: agricultural land occupation (ALO), global warming potential (GWP), fossil depletion (FD), freshwater ecotoxicity (FEPT), freshwater eutrophication (FEP), human toxicity (HTP), ionizing radiation (IRP), marine ecotoxicity (MEPT), marine eutrophication (MEP), metal depletion (MD), natural land transformation (NLT), ozone depletion (OD), particulate matter formation (PMF), photochemical oxidant formation (POFP), terrestrial acidification (TAP), terrestrial ecotoxicity (TEPT), urban land occupation (ULO), and water depletion (WD). In this study, the recycling and further use of the materials has been considered and therefore the hierarchist (H) version is chosen [209]. To assess the total impact, the normalization of the endpoint impact is needed in order to add the three categories. The normalization set used in this research is the Europe ReCiPe H/A person/year.

3.2.6 Interpretation

The interpretation phase is the last stage of the LCA, in which the impact results of the analyzed activity are evaluated and compared with other activities or studies. The interpretation depends on the objective of the study. The study can be focused on the contribution of each life cycle phase to the final impact, on the impact of every material compared with the others, or on the comparison between the emissions or the resource consumption between alternatives, among others. In this study, the comparison between the different bridge deck alternatives is carried out.

3.3 Life Cycle Assessment

In this research, the uncertainty has been considered using a Monte Carlo simulation with 1000 iterations to obtain the probabilistic uncertainty values of the LCA results. In the comparison graphs, only the mean values are shown to make them easier to interpret. The life cycle flowchart for bridge decks is summarized in Figure 3.3.

3.3.1 Midpoint Approach

The midpoint impact categories, as stated before, provide more reliable results due to the wide range of indicators provided. The data obtained allows the study to be focused on particular impacts, such as the global warming potential, evaluating the CO_2 emissions of the activity. The full results of a 35 m span length bridge are provided in Table 3.3, including the coefficients of variation of all indicators. A global warming potential (GWP) study has been done to compare the emissions of each alternative, as shown in Figure 3.4. The difference between the slab decks

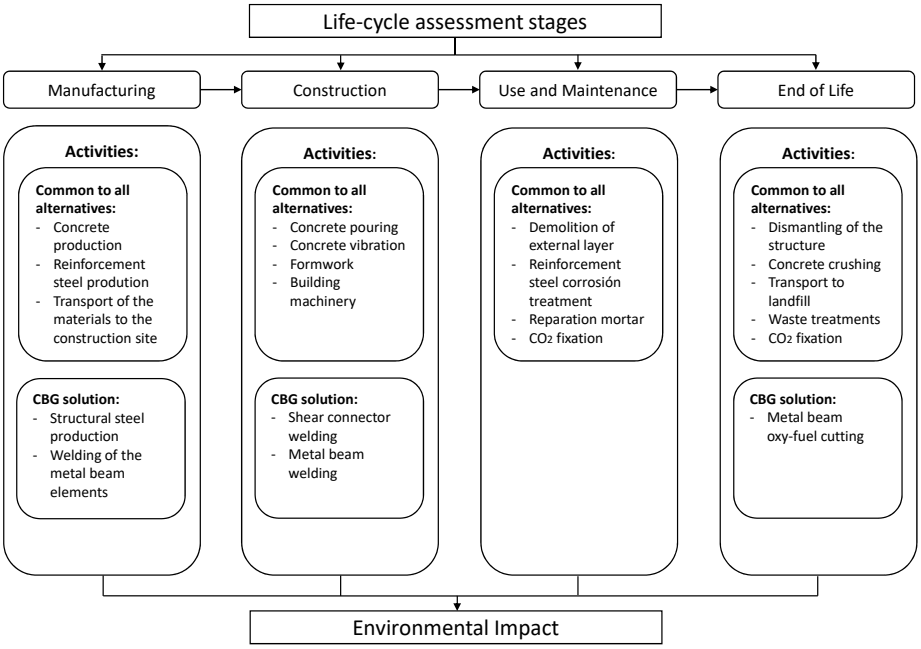

Figure 3.3: Life cycle of the bridge decks

and the box-girder can be clearly distinguished. For span lengths in which the box-girder decks are built, these are the best alternatives from the GWP point of view. The PCLS emits lower quantities of CO_2 than the PCSS for span lengths of less than 17 m. In larger span length ranges, we can state that the CBG bridges are better than the PCBG, even though we consider a 71% steel recycling ratio for the structural steel (CBG_71). If we focus on the contribution of every life cycle stage to the GWP indicator, it is observed that in the end of life phase, all the alternatives have a negative impact on the GWP, due to the CO_2 fixation caused by the carbonation of concrete.

Figure 3.5 shows that the concrete alternatives (PCSS, PCLS, and PCBG) have a greater negative impact in the end of life phase, because the high amounts of concrete that they contain allow a great CO_2 fixation by the carbonation processes. The PCBG alternative has a greater impact on the GWP during the use and maintenance phase because it has a larger surface to repair.

Table 3.3: Midpoint approach impacts of 35 m long bridges. Mean and coefficient of variation (cv).

		PCSS		PCLS		PCBG		CBG_98	
Acronym	**Unit**	**Mean**	**cv (%)**	**Mean**	**cv (%)**	**Mean**	**cv (%)**	**Mean**	**cv (%)**
ALO	m2*a	31.35	59.31%	31.67	63.27%	29.09	71.18%	22.583	55.17%
GWP	kg CO_2 eq	636.76	45.72%	556.19	44.00%	392.14	40.28%	322.776	35.37%
FD	kg oil eq	148.79	26.09%	129.51	24.25%	95.97	20.58%	83.494	26.26%
FEPT	kg 1,4-DB eq	7.53	41.45%	6.01	40.54%	3.76	39.15%	6.285	43.37%
FEP	kg P eq	0.16	40.84%	0.13	39.08%	0.08	37.43%	0.100	37.76%
HTP	kg 1,4-DB eq	276.00	44.56%	218.63	44.03%	135.98	42.66%	253.954	47.37%
IRP	kg U235 eq	56.39	44.71%	49.34	44.12%	35.33	40.17%	25.067	31.96%
MEPT	kg 1,4-DB eq	7.41	40.88%	5.92	39.98%	3.71	38.60%	6.140	43.13%
MEP	kg N eq	0.14	23.59%	0.13	21.70%	0.10	17.53%	0.079	24.98%
MD	kg Fe eq	98.26	50.78%	78.60	47.04%	46.66	44.54%	42.531	35.66%
NLT	m2	0.13	25.82%	0.12	24.29%	0.09	20.45%	0.094	39.37%
ODP	kg CFC-11 eq	0.00	19.32%	0.00	17.68%	0.00	14.55%	0.000	21.31%
PMFP	kg PM10 eq	1.74	27.47%	1.51	24.64%	1.10	20.31%	0.948	26.43%
POFP	kg NMVOC	3.63	19.95%	3.29	17.87%	2.63	14.03%	1.761	18.52%
TAP	kg SO2 eq	2.90	26.53%	2.57	24.56%	1.95	20.35%	1.504	24.73%
TETP	kg 1,4-DB eq	0.08	33.95%	0.07	33.60%	0.04	32.70%	0.122	48.71%
ULO	m2*a	7.18	34.96%	6.10	34.11%	4.19	33.32%	4.070	32.24%
WD	m3	1540.31	45.90%	1294.58	45.72%	851.61	44.25%	852.564	38.79%

A comparison between all the alternatives for every midpoint approach impact is presented in Figure 3.6 for a 35 m span length bridge, providing their impact relative to the biggest one. The alternative that has the most impact in all the categories is the PCSS, excluding the TEP where the highest impact alternative is the CBG_98. In MD, the CBG_71 reaches the impact of the PCLS alternative because of the large amount of steel that is needed for this bridge deck section. However, the CBG_91 alternative, from which a high impact was expected, does not produce such a high one because of the steel recycling, which allows for the generation of a new product with the same characteristics using low amounts of raw material. These steel recycling processes, excluding the raw material reduction, produce a greater impact on the HTP indicator.

Furthermore, the contribution of every life cycle stage on every indicator is illustrated in Figures 3.7–3.10. In all the alternatives, the life cycle phase that has the highest impact in most categories is manufacturing, but there are many exceptions. For the ALO indicator, the phase with the greatest impact is the construction for all the alternatives. The contribution of the use and maintenance stage has a greater impact in the MEP, NLT, ODP, PMFP, POFP, and TAP indicators, especially in the PCBG bridge deck alternative, due to having the highest surface exposed to the environmental conditions, which requires more maintenance. In Figures 3.7–3.10, the results of the midpoint approach for PCSS, PCLS, PCBG, and CBG_98 are shown.

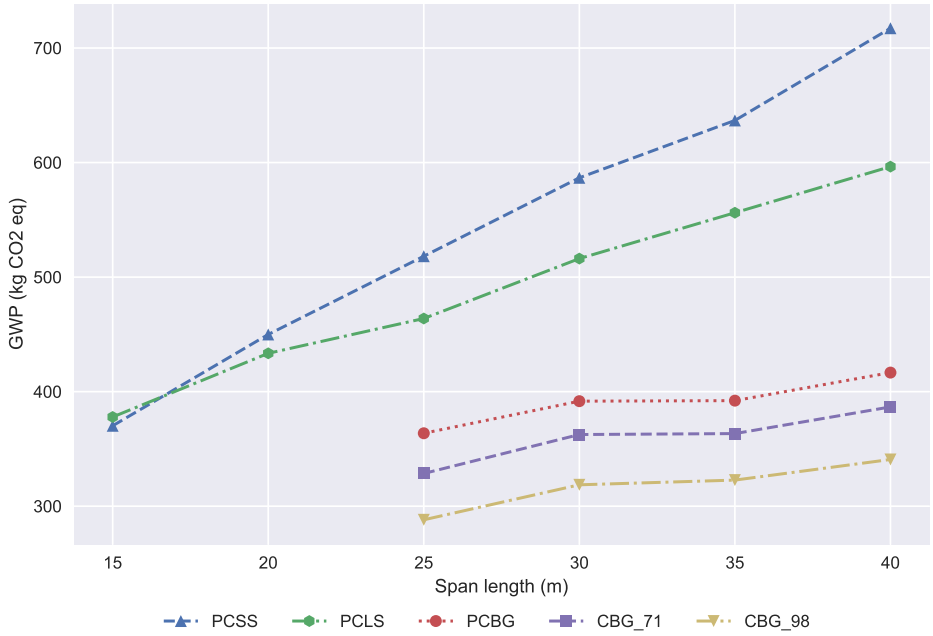

Figure 3.4: Development of GWP according to the span length

3.3.2 Endpoint Approach

To obtain the assessment results in a way that is easier to interpret to compare between different categories, the endpoint approach is provided. The three categories can be significant for choosing the best alternative depending on the situation. If the study area is close to a protected area, then the environmental impact of the structure will be the most important one for the study. If it is built close to a population center, the human health impact will be the most significant, and if the location lacks resources, then the resources category will be the most important one. In this study, a normalization set has been applied to these three impact category results to obtain a global impact. This is useful when there is no preference between the environmental criteria, and equal importance is considered for all the criteria. In this way, a total impact score for the bridge deck alternatives was obtained. The normalization and weighting set adopted was the Europe ReCiPe H/A person/year.

A comparison between the PCSS, PCLS, PCBG, and CBG bridge deck solutions was done. For the CBG alternative, three structural steel recycling ratios were considered,

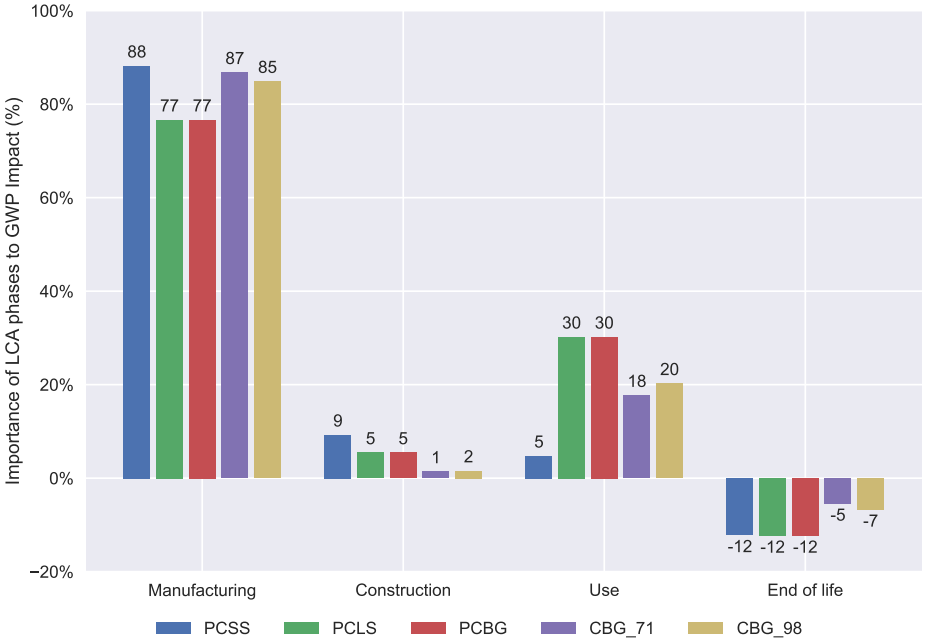

Figure 3.5: Contribution of deck alternatives to life cycle stages for 35 m span length

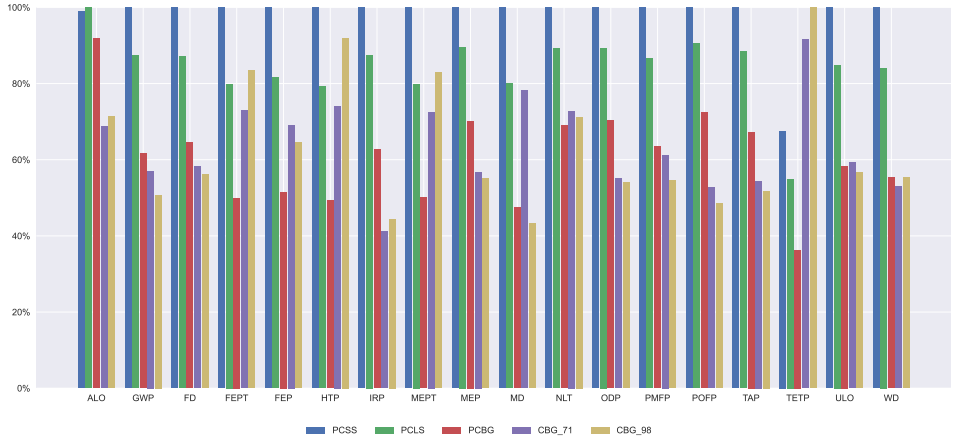

Figure 3.6: Midpoint impacts for 35 m span length

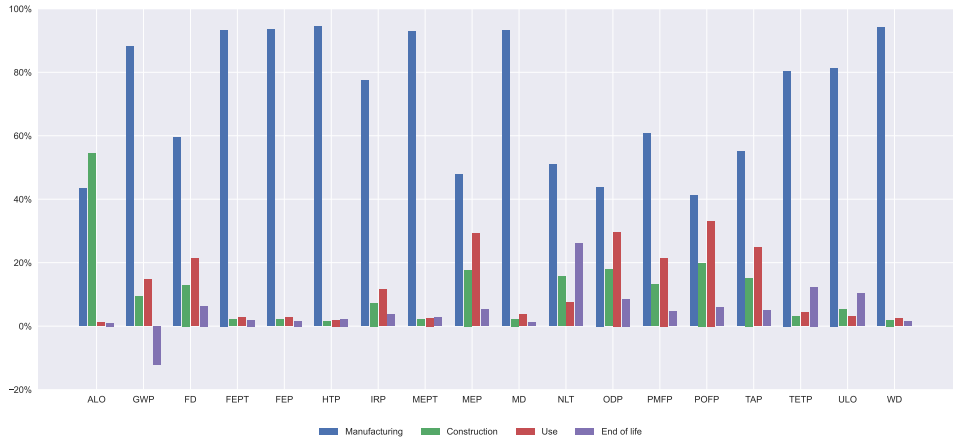

Figure 3.7: Impact categories for 35 m span length PCSS solution

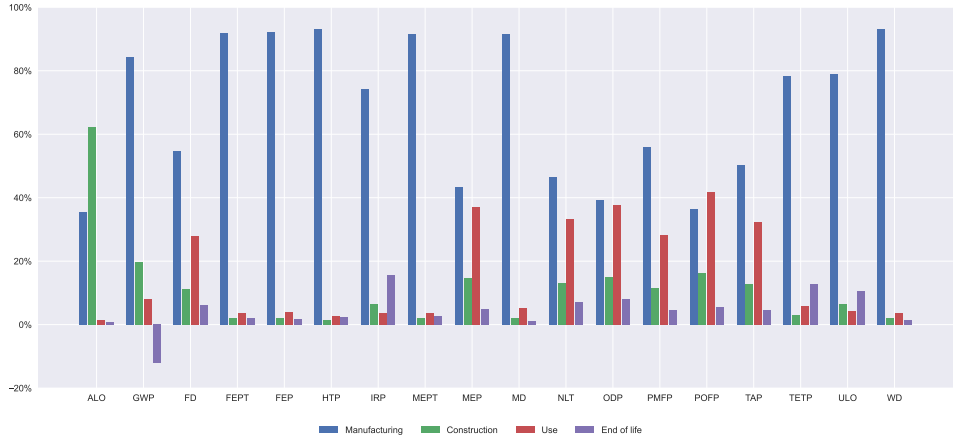

Figure 3.8: Impact categories for 35 m span length PCLS solution

71% (CBG_71), 90% (CBG_90), and 98% (CBG_98), to analyze the differences between the composite box-girder bridge decks and the concrete alternatives.

First, the ecosystems impact is provided in Figure 3.11 in species.year. The best solution is the PCBG, the PCSS is competitive for span lengths shorter than 18 meters, and for longer ones, the PCLS is even better than the CBG alternative. If the steel recycling ratio of the structural steel is 98%, then the PCLS is better until 30

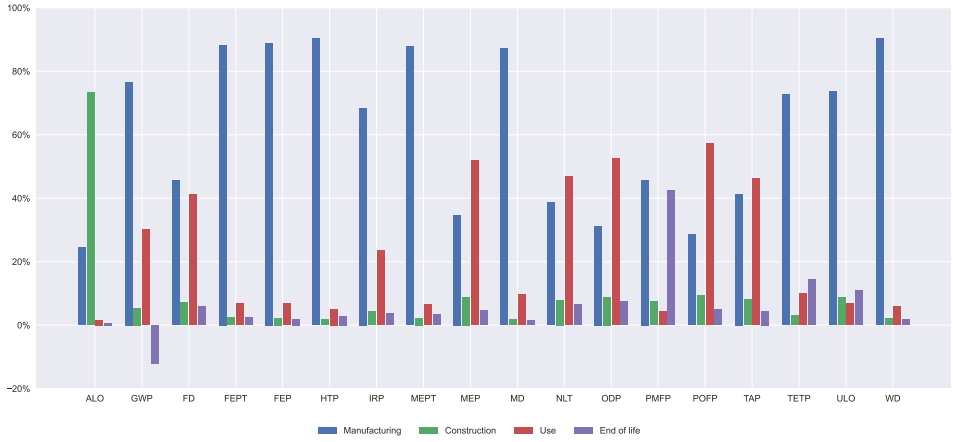

Figure 3.9: Impact categories for 35 m span length PCBG solution

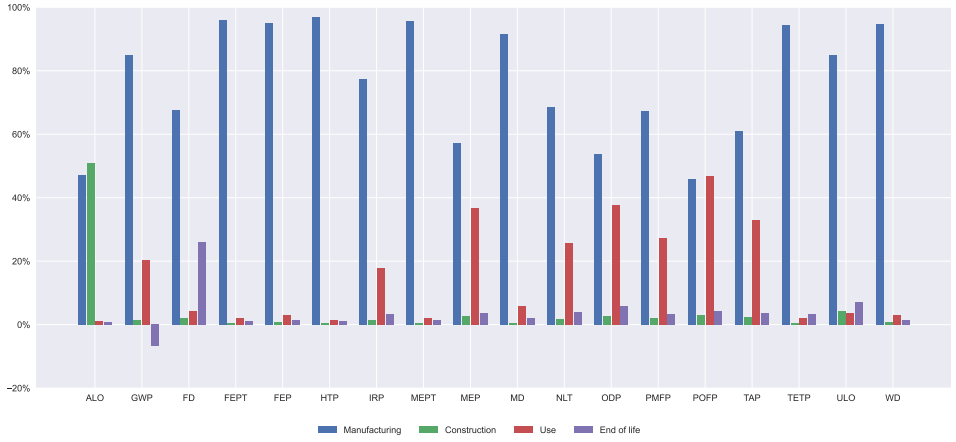

Figure 3.10: Impact categories for 35 m span length CBG_98 solution

m, but if we reduce that ratio, then the PCLS is the best solution until 35 m. These results are because the PCSS needs great amounts of steel when the span length increases. If we compare the PCLS and the CBG, the high increment of materials for the PCLS is compensated by the high environmental cost of the steel production when the recycling ratio of this process is lower.

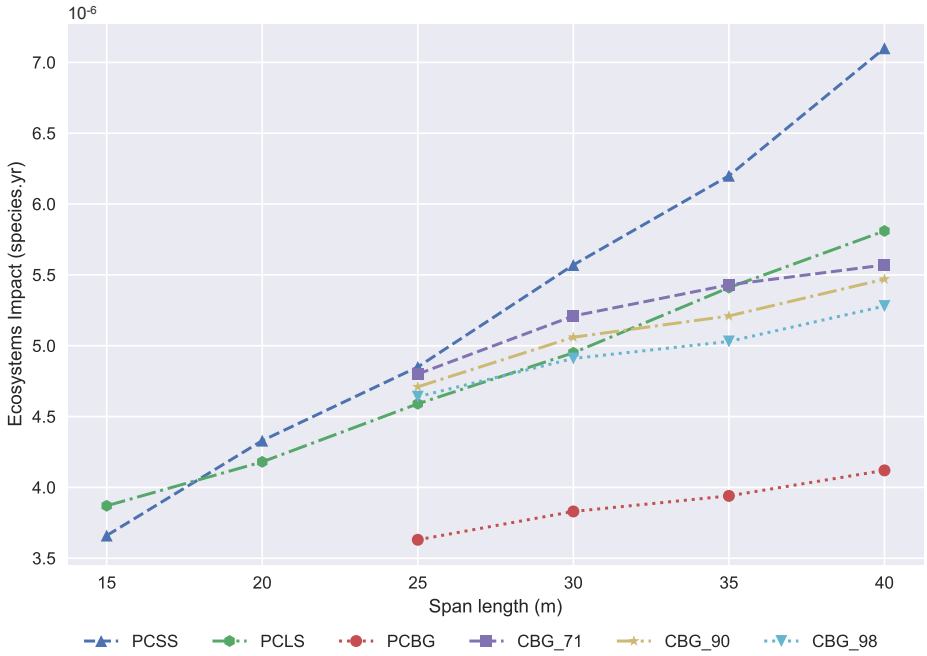

Figure 3.11: Development of the ecosystems impact with regard to span length

The damage caused to human health is measured in disability-adjusted life years, and it is shown in Figure 3.12. PCSS is a competitive alternative up to 17 m, then the PCLS is the best alternative from that span length up to 25 m. The PCBG alternative is competitive with CBG when the structural steel recycling ratio is 71%. If the recycling ratio is greater, then the CBG alternative is the best solution.

The damage caused by the resources, measured in dollars, is shown in Figure 3.13. The PCSS remains the best solution for span lengths shorter than 17 m, and from there up to 25 m, the best solutions are the box-girders. From the resources point of view, the best solution is the CBG if the structural steel recycling ratio is 90%; if it is not, then the PCBG is a competitive solution compared with the CBG.

Normalization has been done to compare the total impact results. These results are provided in Figure 3.14 measured in points. The best solutions are usually the CBG with structural steel recycling ratios higher than 90% in the ranges where they are usually built. If the ratio is lower, then the PCBG is the best solution. The PCSS and PCLS solutions are much worse in terms of the environmental impact due to the great increase of materials as the span length increases. These alternatives must

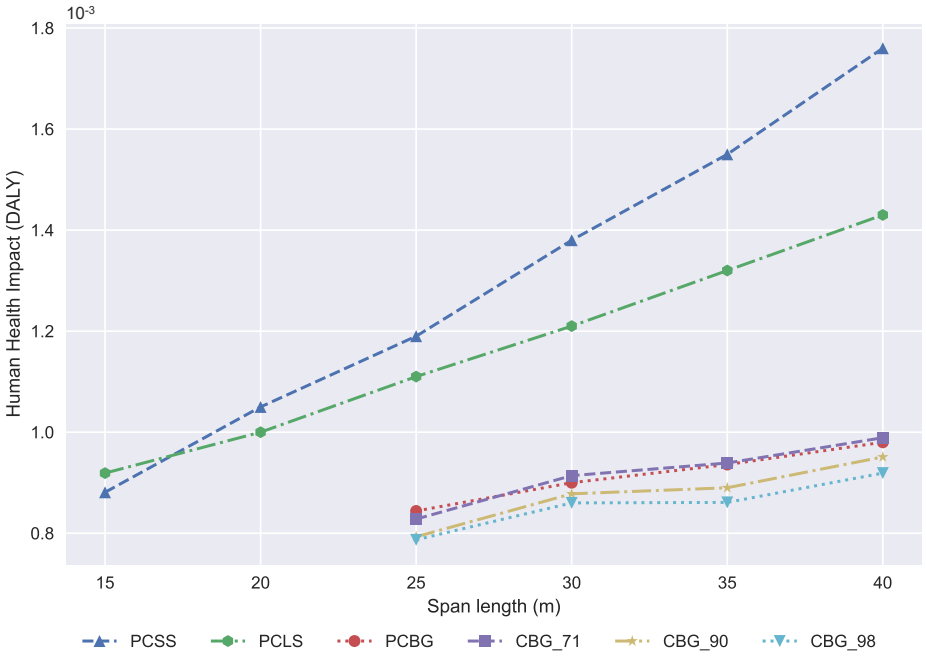

Figure 3.12: Development of the human health impact with regard to span length

be used for lengths less than 25 m from the environmental point of view, and, tuning even more, the PCSS alternative is the most sustainable one for span lengths below 17 m.

A comparison between the contributions of the life cycle stages considered in this study is shown in Figure 3.15 for the three main environmental categories. For all categories, the manufacturing process is the most important one and the construction the least. It is observed that in the end of life stage, the concrete carbonation of the crushed concrete gives a negative value, which becomes even lower for the CBG_98 alternative, due to the smaller amounts of concrete used for this bridge deck section. The use and maintenance stage is more important for the PCBG alternative. The contribution of the construction phase is almost null for the composite alternative in all categories.

Finally, a comparison between the impacts of every material on the total impact is provided in Figure 3.16. Steel and concrete are the most important materials in terms of the environmental impact. In the PCBG, the diesel consumption also becomes

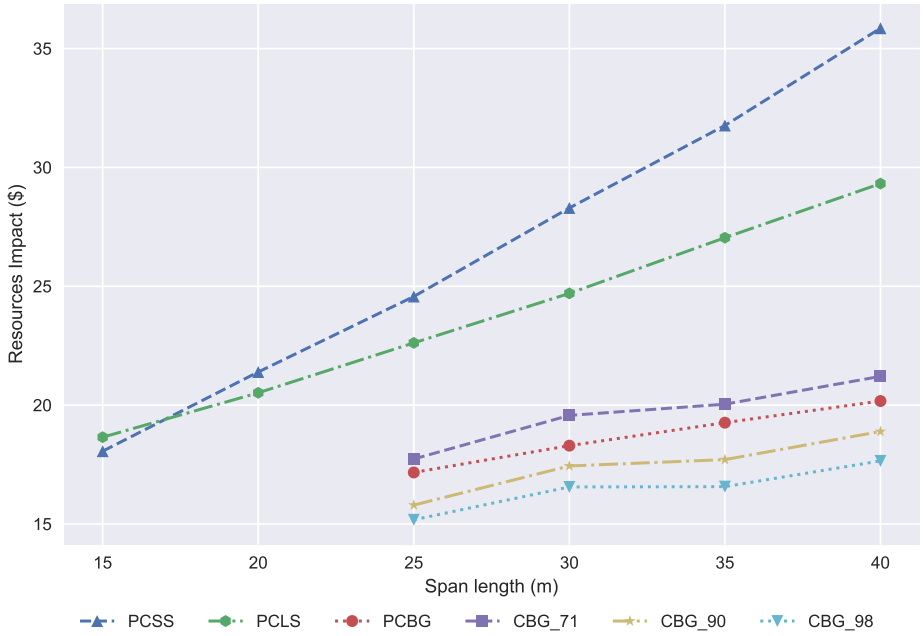

Figure 3.13: Development of the resources impact with regard to span length

important. It is observed that the contribution of steel takes a value of 50.44% for the composite alternative.

3.4 Conclusions

One of the most important sectors that influences climate change is construction. For this reason, environmental assessments are required to analyze the impact of construction and to select options that do not affect the future of the planet. In this study, an LCA has been done for four different bridge deck sections, with an endpoint and midpoint approach.

A comparison between the impacts of the alternatives has been carried out. For span lengths less than 25 m, the box-girder solutions have not generally been used, but they are the best alternatives in terms of the environmental impact for these lengths. The PCSS and PCLS alternatives are competitive from 15 to 25 m, and between 15 and 17 m, the best solution is the PCSS. The difference between these slab bridge

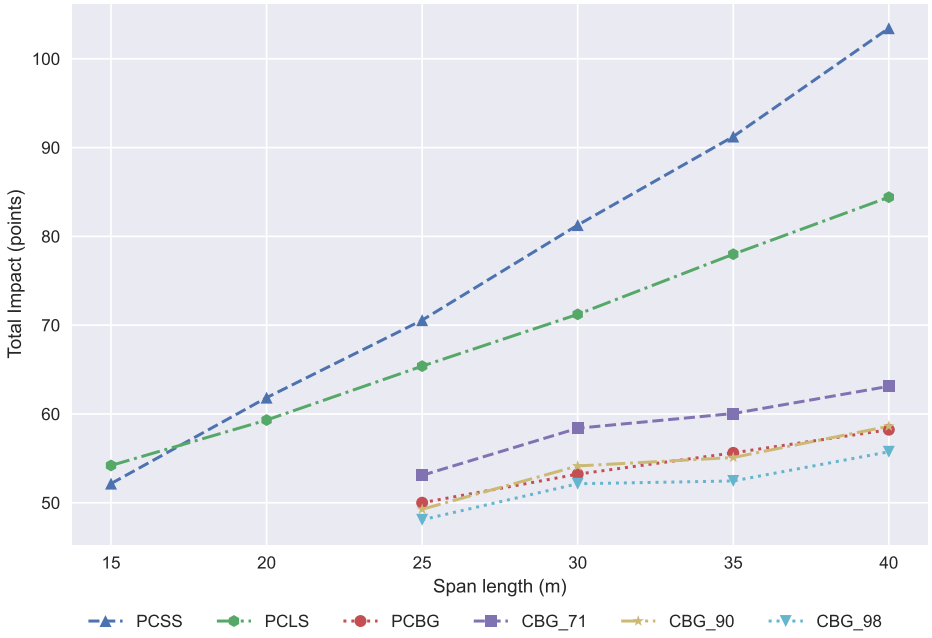

Figure 3.14: Development of the total impact with regard to span length

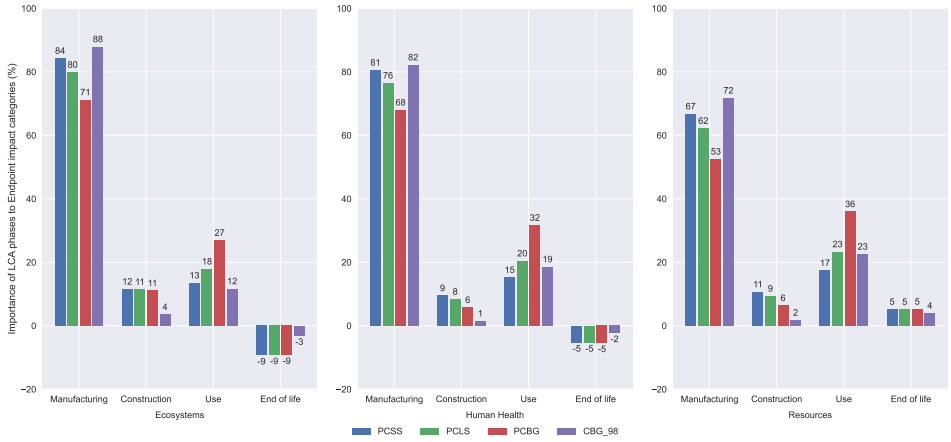

Figure 3.15: Importance of the LCA stages according to the endpoint impact categories

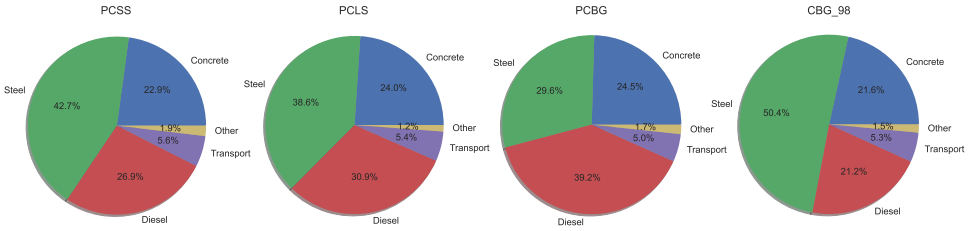

Figure 3.16: Importance of materials to total impact

deck alternatives is caused by the increment of materials for the PCSS alternative, mainly steel.

The steel recycling ratio is determinant in comparing steel and composite bridge decks. The structural recycling ratio is usually greater than the rebar one, and this difference is reflected in the impact values. If we consider the same steel recycling ratio for structural and rebar steel, the box-girder concrete alternatives are better than the composite ones. If we consider a 98% steel recycling ratio, this being the value in the USA, then the best alternative is the CBG.

The consideration of CO_2 fixation by carbonation processes has an important impact on the evaluation and comparison of the alternatives, because the composite structures use a smaller amount of concrete, which is reflected as lower CO_2 emissions in the environmental impact assessment. For concrete structures, the carbonation processes, even though they are negative for the steel reinforcements, make concrete solutions more competitive than the steel structures.

The most important LCA phase for all the alternatives is the manufacturing, and for the concrete alternatives (PCSS, PCLS, and PCBG), the use and maintenance phase has a great impact due to the greater surface of concrete that has to be maintained. In this study, the steel does not require maintenance because it is a weathering steel. In further studies, the steel maintenance can be considered. The concrete maintenance activities are an important factor in the impact; if the durability of the material increases, then this maintenance will be reduced.

Every graph and result shown in this paper will help engineers, designers, and constructors to select cleaner alternatives, and if they consider their own countries' material production processes, they can choose the best environmental solution. For countries where there is less steel recycling, concrete structures will be the best solution, but in countries with cleaner steel production processes, composite and steel solutions will be the best ones from the environmental point of view.

Chapter 4

Social impact assessment comparison of composite and concrete bridge alternatives

Authors:	D. Martínez-Muñoz , J.V. Martí, and V. Yepes		
Status:	Manuscript published		
Journal:	Sustainability, 14(9):5186		
Year:	2022		
DOI:	10.3390/su14095186		
JCR IF (2021):	3.889		
	JCR Category	Ranking	Quartile
	Environmental sciences	133/279	Q2
	Environmental studies	57/127	Q2
Presentation:	Post-print (author version)		

Abstract

The definition of sustainability includes three fundamental pillars: economic, environmental, and social. Studies of the economic impact on civil engineering infrastructures have been focused on cost reduction. It is not necessarily in line with economic sustainability due to the lack of other economic factors. Moreover, the social pillar assessment has been weakly developed compared to the economic and the environmental ones. It is essential to focus on the social pillar and evaluate clear indicators that allow researchers to compare alternatives. Furthermore, bridge life cycle assessment studies have been focused on concrete options. This has resulted in a lack of analysis of the impact of composite bridge alternatives. This study is conducted in two stages. The first part of the study makes a cradle-to-grave social and environmental sustainability evaluation with the SOCA v2 and ecoinvent v3.7.1 databases. This assessment is carried out on four concrete and composite bridge alternatives with span lengths between 15 and 40 m. The social impact weighting method and recipe have been used to obtain the social and environmental indicators. The second part of the study compares the results obtained from the social and environmental assessment of the concrete and the composite alternatives varying the steel recycling rate. The bridge alternatives are prestressed concrete solid slab, prestressed concrete lightened slab, prestressed concrete box-girder, and steel–concrete composite box-girder. The results show that composite options are the best for environmental impact, but the concrete box girder solutions are better for social impact. Furthermore, an increase in the steel recycling rate increases the social impact and decreases the environmental one.

Keywords: sustainability; bridges; structures; LCA; recipe; soca

4.1 Introduction

Sustainability has grown since its definition by the World Commission on Environment and Development in 1987 [1]. This worry has been transmitted to developers in some social sectors. However, Sustainable Development Goals were not defined until 2015 as a response to the social demand related to environmental impact [210].

Three main pillars define this sustainability concept. The most studied is the economic one. This pillar is related to the cost associated with one process, product, or service and has been the traditional choice criterion for deciding between alternatives. The second is the environmental pillar, related to the impact on the environment. Finally, the social pillar completes the sustainability profile. This part assesses how the society stakeholders are affected by one process, product, or service.

As stated before, the most studied sustainability criterion has been the economic impact. Researchers have been carrying out different studies to reduce the economic impact of their projects. The primary method of reducing the economic impact carried out by researchers has been through optimization techniques. This method has been applied extensively in construction sector elements, such as reinforced concrete bridge piers [211], concrete road vaults [212], buttressed walls [172], [173] or facades [213], among others. Other authors have applied different techniques to reach sustainable solutions considering other criteria besides the cost [94], [122]. To evaluate the environmental impact of construction processes, researchers have been studying the life cycle assessment (LCA) of different construction activities [19], [148], [169], [178] due to its contribution to the total carbon emissions to the environment [2], [3]. This industry's high impact is due to its cement requirements, which represent 5% of the global CO_2 emissions contribution [161]. As a consequence, construction substantially impacts environmental pollution [4]. Moreover, if the focus is on the sustainability assessment of the social pillar, there is a lack of study in comparison with the economic or the environmental pillars [214], [215].

Researchers state that the lack of knowledge in the social assessment pillar is due to the ambiguity in the definition of the sustainability criteria related to social impact [214], [216]. Nevertheless, the United Nations have set aside 6 of its 17 sustainable development goals for this part of sustainability. This marks a clear trend for public agencies to consider the social pillar an essential part of the overall sustainability analysis. As a response to this demand, there is a recent trend in studying the social assessment to give it the same importance as the study of economic and environmental sustainability [159], [215].

Construction projects' social sustainability assessment has an additional complication due to its stakeholder's situation [215]. Regarding social demands for the construction sector, this must satisfy not only the clients or the employees, but also the industry and community users' needs [217]. Furthermore, the final product obtained must consider the impact on future and present generations, considering the health and safety of the implied agents in the process [218].

One of the most representative infrastructures of the constructions sector is bridges. Because of this, researchers have been developing different studies to assess its sustainability [219]. As stated in Martínez-Muñoz et al. [189] the central part of sustainability studies is focused on concrete bridges. This study also advises a lack of study in environmental and social LCA of composite bridges. A recent environmental LCA study focused the scope on the comparison of concrete and steel–concrete composite bridge (SCCB) alternatives [220]. This study states that the percentage of recycled steel is crucial for the feasibility of SCCBs from an environmental point of view and presents SCCBs as an eco-friendly alternative for bridge design. De-

spite this, no LCA has yet been carried out that considers the social impact of SCCB. Some researchers have carried out different studies assessing different criteria for social assessment, such as noise, dust, and time [221]–[223].

This study aims to assess the social feasibility of SCCBs compared with concrete bridges, using the LCA methodology. To reach this goal, four alternatives of bridges have been proposed for the comparison: prestressed concrete solid slab (PCSS), prestressed concrete lightened slab (PCLS), prestressed concrete box-girder (PCBG), and steel–concrete composite box-girder (CBG). A parametric study considered span lengths between 15 and 40 m to allow a broader comparison. Both environmental and social LCAs have been modeled for each span length to compare the results between both evaluations. Different steel recycling rates have been proposed for CBG alternatives to assess the relevance of the steel recycling process in SCCBs social LCA. The steel recycling rate is contingent upon the process of manufacturing the steel. The two main processes available to produce steel are basic oxygen furnace (BOF) and electric arc furnace (EAF). This process combines the iron with steel scrap obtained from the steel recycling process. The amount of steel scrap is between 90% and 100% for EAF and 10% and 30% for BOF. Modifying the BOF and EAF for steel production can model different manufacturing processes and, consequently, different steel recycling amounts. This difference in manufacturing processes is directly linked to the differences between countries' steel production and technological development. This justifies the usefulness of this study to compare the impact of different bridge alternatives and their feasibility considering several steel manufacturing processes. With all of the above, the objective of this study is to compare different concrete and composite bridge solutions from the environmental and social impact points of view and, in addition, how the steel recycling ratio variation modifies the contribution of composite bridges to these impacts.

4.2 Materials and Methods

The life cycle analysis (LCA) methodology consists of modeling a process, product, or service, and assessing the contribution of every activity to the environment or the society, among others. All activities must be included since the raw material is extracted until the product finishes its service life to model the principal activity. This study conducted two assessments: the environmental life cycle assessment (E-LCA) and the social life cycle assessment (S-LCA). The methodology applied in this study follows the ISO 14040:2006 [145] that describes the process to carry out the environmental analysis. It comprises four stages to obtain the assessment: goal and scope definition, inventory analysis, impact assessment, and interpretation of the results. For assessing the social impact, the most common guide is followed [224].

The life cycle impact assessment (LCIA) chosen for this research is the recipe 2008 method [151] for E-LCA and the social impacts weighting method for S-LCA. The selected databases for modeling are ecoinvent v3.7.1 and SOCA v2 to E-LCA and S-LCA, respectively.

The LCA methodology allows converting the data introduced from the life cycle inventory to impact and damage categories that help understand how the process affects specific indicators. The life cycle impact assessment (LCIA) methods are responsible for carrying out this transformation. With the information extracted from the models, the actors involved in the decision process between solutions can compare them to make their decision.

4.2.1 Goal and Scope Definition

This research poses two primary goals. The first one compares different bridge deck alternatives from environmental and social points of view. The second is related to the feasibility of these various alternatives between the environment and the social perspective. All bridge decks were considered as continuous beams so that the span length represents the highest of every span. This research considered six span lengths between 15 m and 40 m, increasing five meters from the initial to the final distance. The LCA method allows quantifying the impact of every deck solution objectively and comparing them. As stated by the bridges of Pang et al. [191], the LCA analysis is helpful for three main purposes: comparison between designs options, comparison between different bridge materials alternatives, and assessment of new materials compared with traditional ones. All the other options must be similar in load, width, and location to compare accurately. This last criterion is crucial because if not met, the geotechnical or seismic conditions could change and, therefore, the design requirements of the bridge. The same location is considered for every bridge deck alternative to compare bridge decks.

Bridge Deck Type Definition

The structural beam system is one of the most common bridge types due to its simplicity and economic feasibility. The most crucial part of this type of bridge is the deck since it is responsible for resisting all the stresses associated with the acting loads. The choice of the deck type depends on different factors, such as constructability, aesthetics, or economy, among others. The bridge decks chosen are the same as those in the work of Martínez-Muñoz et al. [220]: prestressed concrete solid slab (PCSS), prestressed concrete lightened slab (PCLS), prestressed concrete

box-girder (PCBG), and composite box-girder (CBG). In Figure 4.1, the standard geometry of these deck types is represented.

Its economic feasibility has defined traditional bridge deck type choosing. Considering this, PCSS and PCLS slabs have been applied in ranges between 15 m and 35 m. On the other hand, the box-girder bridges' scope of use is defined between 25 m and 125 m, its regular use being from 35 m to 80 m. Concrete and steel are the most common materials used for box-girder alternatives. In this case, PCBG is made from prestressed concrete, such as slab-type alternatives. The primary material is concrete and steel to solve concrete tensile strength problems in these alternatives.

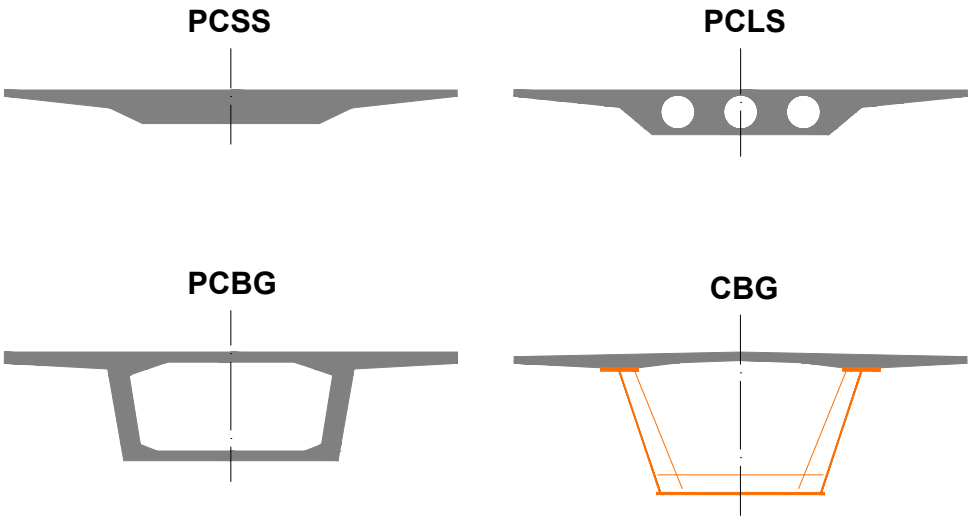

Figure 4.1: Bridge deck cross sections.

On the contrary, the CBG alternative is mainly made of a rolled steel beam to which a concrete slab is added on the upper part. This last alternative design concept is to locate every material in the zones that are more resistant, i.e., concrete in the areas with compressed fibers and steel in the areas with tensioned ones. As described before, two slab and two box-girder decks were selected. This study aims to provide several alternatives for environmental and social impact assessment to give designers information on which option is better in terms of the span length.

Phases of the Analysis

To consider a complete bridge LCA, it is defined in four stages. These stages consider all the activities necessary from the starting design to the final structure service life. These processes consider the manufacturing of the materials, the bridge construction, its maintenance, and its demolition and transportation of the materials to landfills. To view all this information, the structure of the LCA model considers the following stages: manufacturing, construction, use and maintenance, and end of life. This LCA follows the format of other bridge LCA studies [159], [220].

Manufacturing This stage includes all processes from the raw material extraction to the final building materials on the construction site. The most used materials in the construction industry are concrete and steel. Because of this, databases include processes that allow the introduction of these materials to the model. In this study, those processes are defined, adding the raw materials and determining the dosage. This process is described in Figure 4.2.

$$Total\ solid = Cement + Gravel + Sand\ \ (per\ m^3\ of\ concrete) \tag{4.1}$$

$$Total\ cement = Cement + \left(\frac{Cement}{Totalsolid}\right) \cdot Waste\ concrete\ \ (per\ m^3\ of\ concrete) \tag{4.2}$$

$$Primary\ gravel = Gravel + \left(\frac{Gravel}{Totalsolid}\right) \cdot Waste\ concrete\ \ (per\ m^3\ of\ concrete) \tag{4.3}$$

$$Primary\ sand = Sand + \left(\frac{Sand}{Totalsolid}\right) \cdot Waste\ concrete\ \ (per\ m^3\ of\ concrete) \tag{4.4}$$

$$Primary\ water = Water + Wastewater\ \ (per\ m^3\ of\ concrete) \tag{4.5}$$

The concrete matrix is composed mainly of cement, sand, gravel, and water. In addition, additives and additions can be added to the concrete matrix to give the concrete specific properties. Furthermore, the distance between the extraction site of every material must be added to the model. The final process includes the concrete matrix and the energy, the mixing factory, and the activities necessary to make one cubic meter of the modeled concrete to simulate the concrete mixing.

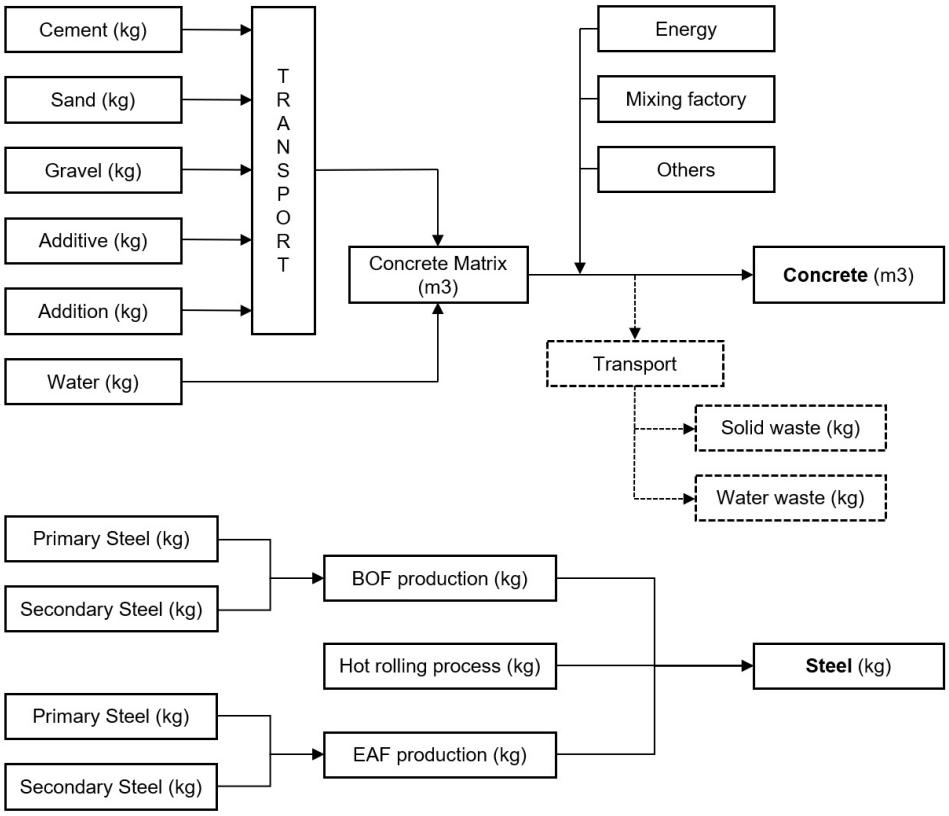

Figure 4.2: Concrete and steel manufacturing processes.

Marceau et al. [192] state that for one cubic meter of concrete production, there is 24.5 kg of material waste, and the wastewater is 0.0348 m^3. To consider both the final concrete and the debris associated with the production, the exact amount of each material is defined by Equations (4.2)–(4.5) [220].

The two main processes available to produce steel are basic oxygen furnace (BOF) and electric arc furnace (EAF). This process combines the iron with steel scrap obtained from the steel recycling process. The amount of steel scrap is between 90% and 100% for EAF and 10% and 30% for BOF [147]. The use of recycled steel directly affects the sustainability of the alternative, and as a consequence, the EAF and BOF impacts give different results. Modifying the BOF and EAF for steel production can model other manufacturing processes and, consequently, different steel recycling amounts. This difference in manufacturing processes is directly linked to

the differences between countries' steel production and technological development. The BOF and EAF waste are considered in the database processes.

The percentage of recycled steel is essential for SCCBs due to the significant steel needed for its construction. Slight variations in the recycling rate give substantial differences in the SCCBs impact. From this point of view, it is essential to distinguish between hot rolled and rebar steel. Consequently, a percentage of 71% is considered for reinforcement bars, and 98% for hot rolled steel [193]. This difference rate is due to the difficulty separating reinforcement bars steel from the concrete. Consequently, the steel scrap obtained from the reinforcement bars steel is lower.

Construction The construction stage considers all the necessary processes to make the deck, considering the auxiliary elements and machinery, which depend on the bridge placement and type of construction. These processes are included in this LCA phase. In the SCCB case, welding processes are introduced. The construction method is modeled by considering the diesel consumption of the machinery obtained from the manufacturers' data, the literature, or other databases.

Use and Maintenance This stage encompasses all the processes necessary throughout the bridge life. These processes can be classified into three different categories: maintenance activities, CO_2 fixation, and traffic detour. To make this maintenance work, sometimes bridge closure is needed. In this case, it implies a traffic detour, and as a consequence, an increase in the distance required to reach the same location generates a higher impact. This impact is affected by different factors, such as the location of the traffic type.

The maintenance phase can be managed in two different ways. Researchers have been reviewing different maintenance possibilities [148], [178], [194]. In other studies, different scenarios have been assessed to evaluate its sustainability [191]. If the bridge's closure is needed, the closure time is defined. Processes required for maintenance depend on the bridge material. For example, if the steel selected is not corrosion-resistant in steel bridges, the maintenance operations must be repeated many times. These activities include removing the external layer and replacing them with a reparation mortar for concrete bridges. In this study, maintenance operations, including auxiliary machinery, materials, diesel consumption, and emissions due to traffic detours, are considered.

Some studies state that concrete fixes CO_2 during its carbonation process [164], [176], [195]. Carbonation significantly affects reinforced concrete bridges, and three main factors determine it [177]: the w/b ratio, the concentration of CO_2 in the environment, the climate conditions, and the steel depth. Carbonation produces passivation loss of reinforcement bars, reducing the impact on the environment. Lagerblad et

al. [196] researched CO_2 fixed by carbonation during the life cycle based on Fick's first law. Equation (4.6) allows to calculate the fixed CO_2 in which k is the carbonation coefficient, t is the service life, A is the exposed area of concrete, r is the ratio of CaO that is going to become carbonated, C is the content of cement in one cubic meter of concrete, k is the content of clinker in the cement, L is the content of CaO in the clinker, and ϵ is the molecular weight ratio of CO_2/CaO. This equation is simplified by grouping the constants. Lagerblad et al. [196] consider that r takes the value of 0.75, L of 0.65 and assume that ϵ takes the value of 0.7857. Clearing out the equation with these constants, the expression changes to (4.7). Concrete structures can fix CO_2 along its service life [177].

$$CO_2 fixed\,(kg) = \frac{k\left(\frac{mm}{\sqrt{year}}\right)\cdot\sqrt{t(year)}}{1000}\cdot A(m^2)\cdot r\cdot C\left(\frac{kg}{m^3}\right)\cdot k(\%)\cdot L(\%)\cdot\epsilon\ (per\ m^2) \quad (4.6)$$

$$CO_2 fixed\,(kg) = 0.383\cdot\frac{k\left(\frac{mm}{\sqrt{year}}\right)\cdot\sqrt{t(year)}}{1000}\cdot A(m^2)\cdot C\left(\frac{kg}{m^3}\right)\cdot k(\%)\ (per\ m^2) \quad (4.7)$$

$\mathrm{End\ of\ Life}$ This phase includes all processes needed to dismantle the bridge. The principal method is demolishing the system, landfill transport, and waste treatment. Consequently, these processes are modeled by transportation distances and specific machinery. There are three main possibilities for materials waste: reuse, recycle or transportation to a landfill. In this research, concrete and steel are the most commonly used materials. This waste processing will depend on the needs of society in every case.

Many researchers have studied the steel recycling ratio. Hammervold et al. [194] considered a 100% steel recycling ratio, and other authors such as Du et al. [178] and Hettinguer et al. [179] considered a lower value. Penadés-Plà et al. [19] considered the Spanish average steel recycling ratio, 71%. The steel recycling ratio is associated with the construction location. It is possible to adjust the evaluation of the steel by controlling the recycling ratio in the LCA model.

The Spanish concrete regulation allows using 20% of concrete recycled coarse aggregates in new concretes [197]. Different concrete recycling rates are defined [148], [178], [179]. As described before, the concrete carbonation process always occurs. If all the concrete is crushed, the full concrete carbonation is produced due to the accessible surface increase [177]. The concrete carbonation coefficient depends on the concrete's strength [196]. In this study, two concrete strengths, 30 and 40 MPa,

are considered. The carbonation coefficients (k) are 1.5 mm/year$^{0.5}$, 4 mm/year$^{0.5}$, 6 mm/year$^{0.5}$, 0.75 mm/year$^{0.5}$ and 1 mm/year$^{0.5}$, depending on whether the concrete is exposed, sheltered, indoors, wet or buried for 30 MPa concrete strength, and 1 mm/year$^{0.5}$, 2.5 mm/ year$^{0.5}$, 3.5 mm/year$^{0.5}$, 0.5 mm/year$^{0.5}$ and 0.75 mm/year$^{0.5}$ for 40 MPa concrete strength. The crushed concrete maximum aggregate size is assumed to have a 10 mm diameter.

Functional Unit

This research considered a square meter as the functional unit to compare bridge deck alternatives. Different bridge locations can produce other impacts due to the placement conditions regarding geotechnical properties and seismicity. Moreover, the material's production processes can be different.

4.2.2 Inventory Analysis

The inventory analysis consists of collecting data on materials and energy consumption to model the processes of the bridge life cycle. This study case takes the square meter of the bridge as a functional unit. These processes produce output in terms of emissions to the environment. The consideration of the production of every process gives the environmental impact associated with the product that is being assessed.

Software

The software used to model the bridge's life cycle is OpenLCA from GreenDelta. This is an open-source program that allows LCA models to create and run. This was used extensively by the researcher's community [198].

This study has used two databases. The first one is the ecoinvent database [199], version 3.7.1. This database is constantly updating and very reliable from the scientific point of view [200]. Data given by the ecoinvent database are related to the environmental impact of processes. On the other hand, the social database used for this research is SOCA, version 2. This database takes data from PSILCA social database and assigns the processes in the ecoinvent 3.7.1 database their corresponding social impact. This allows researchers to use the ecoinvent database to model the social implications of their studies efficiently. The life cycle impact assessment (LCIA) chosen for this research is the recipe 2008 method [151] for E-LCA and the social impacts weighting method for S-LCA. The selected databases for modeling are ecoinvent v3.7.1 and SOCA v2 to E-LCA and S-LCA, respectively. Table 4.1 encompasses all the information about the databases, the LCIA methods used,

the impact categories, and the damage categories. The impact categories give a more detailed view of various specific indicators. However, the damage categories group these indicators and show a more widespread impact. In this study, damage categories are used to compare the different alternatives to conclude. In Table 4.1, the environmental assessment gives a result of three damage categories related to the impact on the ecosystems, the human health, and resources, while the social evaluation shows the implications associated with four different stakeholders: local community, society, value chain actors, and workers.

Table 4.1: Environmental and social life cycle assessment categories.

Database	LCIA	Impact Categories	Damage Categories
ecoinvent	ReCiPe (E-LCIA)	Agricultural land occupation Climate Change Fossil depletion Freshwater ecotoxicity Freshwater eutrophication Human toxicity Ionizing radiation Marine eutrophication Metal depletion Natural land transformation Ozone depletion Particulate matter formation Photochemical oxidant formation Terrestrial acidification Terrestrial ecotoxicity Urban land occupation Water depletion	Ecosystems Human Health Resources
SOCA	Social Impacts Weighting Method (S-LCIA)	Access to material resources Environmental Footprints GHG Footprints Local employment Migration Respect of indigenous rights Safe and healthy living conditions Contribution to economic development Health and Safety Corruption Fair competition Promoting social resposibility Child labor Discrimination Fair Salary Forced labour Freedom of association and collective bargaining Health and Safety Social benefits, legal issues Working time	Local Community Society Value Chain Actors Workers

4.2.3 Bridge Deck Design

Table 4.2 shows the amounts of materials determined by each deck type and span length. These amounts were taken from the study of Martínez-Muñoz et al. [220]. In this study, the quantity of materials was obtained from Yepes et al. [204] for PCSS and PCLS alternatives. In contrast, for PCBG and CBG ones, the data were taken by applying the criteria defined in the Spanish Ministry of Public Works named "Obras de paso de nueva construcción" [205].

Table 4.3 shows the material amount for the concretes considered in this research. The concrete decks are designed with C40/50 prestressed concrete, while for the CBG bridge deck, C30/37 reinforced concrete is considered. The most significant is the CBG alternative, where the structural steel beam that supports the slab is added.

Table 4.2: Amount of materials per square meter of deck.

	Unit	15	20	25	30	35	40
PCSS							
Concrete C40/50	m^3	0.473	0.561	0.649	0.738	0.826	0.914
Reinforcement Steel	kg	51.728	61.380	71.033	80.686	90.339	99.992
Prestressed Reinforcement Steel	kg	9.223	17.133	25.043	32.953	40.863	48.773
Formwork	m^2	1.500	1.500	1.500	1.500	1.500	1.500
PCLS							
Concrete C40/50	m^3	0.509	0.557	0.605	0.654	0.702	0.750
Reinforcement Steel	kg	52.165	57.109	62.052	66.996	71.939	76.883
Prestressed Reinforcement Steel	kg	5.069	10.914	16.759	22.604	28.449	34.294
Formwork	m^2	1.700	1.700	1.700	1.700	1.700	1.700
PCBG							
Concrete C40/50	m^3	0.441	0.461	0.482	0.503	0.523	0.544
Reinforcement Steel	kg	28.790	32.601	36.632	40.884	45.356	50.048
Prestressed Reinforcement Steel	kg	3.042	4.917	6.792	8.667	10.542	12.417
Formwork	m^2	1.900	1.900	1.900	1.900	1.900	1.900
CBG							
Concrete C30/37	m^3	0.220	0.230	0.240	0.250	0.261	0.272
Reinforcement Steel	kg	20.976	22.250	23.603	25.037	26.559	28.173
Structural Steel	kg	59.400	63.700	68.175	81.000	80.600	88.375
Shear Connector Steel	kg	0.310	0.346	0.381	0.423	0.437	0.494
Formwork	m^2	1.000	1.000	1.000	1.000	1.000	1.000

As usual in bridge LCA modeling, four stages are considered for the life cycle model. The processes considered for the E-LCA modeling were collected from the ecoinvent database. The diesel consumption of machinery generated those processes that are not included in the database. For S-LCA, the database chosen is SOCA due to the ecoinvent processes PSILCA database social assessment addition.

Table 4.3: Concrete dosage considered for bridge decks.

Material	Unit	C30/37	C40/50
Gravel	kg	1110.00	829.00
Sand	kg	730.00	1102.00
Cement	kg	300.00	320.00
Water	kg	201.00	160.00
Superplasticizer	kg	0.27	5.00

Manufacturing All the activities needed to manufacture materials are considered in the production phase. In addition, the transport is included, considering 30 km for concrete and 150 km for steel. The original ecoinvent database process considered concrete of the 30 MPa process. The 40 MPa concrete process is introduced following the description in Figure 4.2.

Steel manufacturing is produced differently for modeling reinforcement bar and hot rolled steel. Ecoinvent database considers 19% of steel scrap for the BOF process and 100% for the EAF. Modifying these processes, a specific steel recycling ratio can be considered. Consequently, a 71% steel recycling ratio is modeled for reinforcement bars, while for hot rolled steel, two different recycling ratios are determined. Those ratios are 71% (CBG_71) and 98% (CBG_98). This rate difference is modeled to consider different countries' materials reuse. In countries with lower developments, the reuse policies are less strict [206].

Furthermore, the SCCB deck welding of the steel sheets is modeled. This is considered by using the ecoinvent database's process.

Construction Bridges building is modeled as on-site. The processes contemplated in this phase are concrete pouring, vibration and assembling of the different parts of SCCB alternatives and, furthermore, in concrete solutions, the tension of the active reinforcement steel. The auxiliary elements are modeled by introducing the diesel consumption data from the Bedec database [207]. The diesel consumption is 123.42 MJ of energy per cubic meter of concrete and 10.2 MJ per kg of active reinforcement steel [220]. The CO_2 emissions are 32.24 kg and 2.62 kg, respectively. The concrete selected does not have unique curation processes.

Use and Maintenance Traffic detours are not considered necessary at this stage. Only the concrete needs repairs on activities because the steel chosen does not require maintenance activities. The machinery for the upkeep is estimated considering two different periods of actuation. The machinery consumption contemplated in this life cycle phase is 584.28 MJ, and the CO_2 emissions are 46.58 kg of CO_2 per square meter repaired [220].

End of Life In this stage, all demolition and transport to landfill processes are considered in the LCA model. The machinery needed for the deconstruction is considered for the concrete elements. In addition, the crushing process is considered to assume the full carbonation of concrete. On the other hand, only landfill transportation is modeled. The recycling process of steel is reflected in the manufacturing process. For SCCBs alternatives, steel sheet cutting is introduced.

4.2.4 Impact Assessment

The impact assessment results depend on the LCIA method chosen. LCIA methods transform from specific resources consumption and emissions to indicators. This transformation allows designers and researchers to understand the impact of activities better. As described in Section 4.2.2, two LCIA methods are chosen for both E-LCA and S-LCA evaluations. As described in Table 4.1, the technique selected for E-LCA is recipe. This method gives, as a result, 18 indicators related to different environmental impacts. These indicators can be grouped into three main damage categories that focus on more general effects. Consequently, the interpretation of results is straightforward due to the lowest amount of information. Similarly, the social impact weighting method gives specific indicators and four damage categories. In Figure 4.3, a schema of the relations between databases and methods used in this study is defined.

This research aims to compare the feasibility of different decks from the environmental and social points of view and the difference between those results. Accordingly, only the damage categories are considered for the study to understand the results quickly.

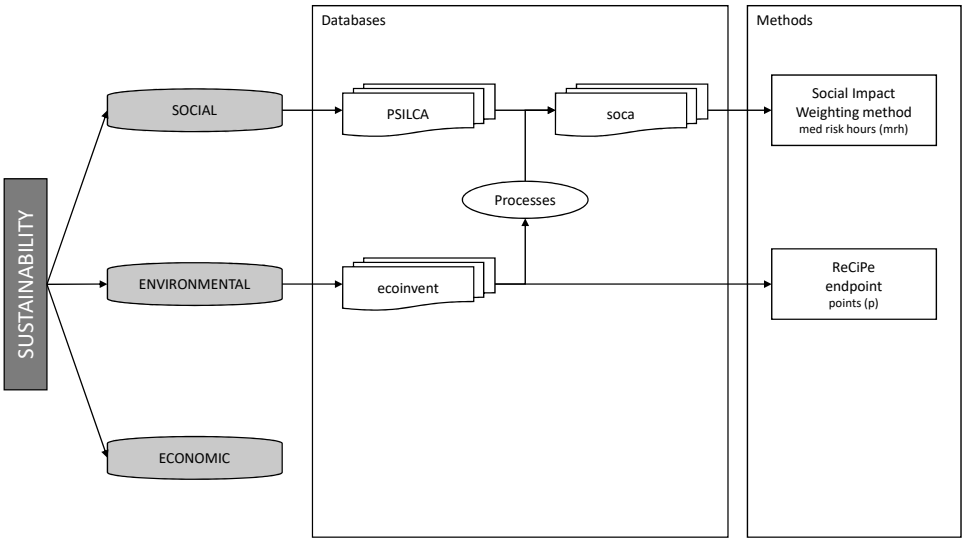

Figure 4.3: Databases and methods flowchart.

4.2.5 Interpretation

At this phase, the comparison of the different bridge alternatives is carried out. All processes and activity's impact results are analyzed and compared. This interpretation depends on the research goal defined.

4.3 Lyfe Cycle Assessment

This research carried out the complete LCA of four different bridge decks. It is a cradle-to-grave analysis. This type of analysis considers all bridge processes, starting with the raw material extraction and ending with the demolition of the structure and the transportation of the materials obtained to landfills. Only the damage categories results are exposed in all graphs and tables to ease the comparison of alternatives. In Figure 4.4, the processes considered for modeling the complete life cycle of every deck option are summarized. This processes follows the proposal in Martínez-Muñoz et al. [220].

4.3.1 Environmental LCA

The LCIA method used to carry out the environmental assessment is recipe. As mentioned before, this LCIA method gives two alternatives of obtaining results. This study chooses the endpoint approach to obtain more easily comparable results. The results of the E-LCA show three damage categories: ecosystems impact, human health impact, and resources impact. The units of this damage category are species.yr, disability-adjusted life years (DALYs), and dollar ($), respectively. As the three damage categories give their results in different units, a normalization and weighting method is required to compare them. The Europe recipe H/A person/year is set as the weighting method in this research.

In this work, four bridge deck alternatives are proposed for its comparison: PCSS, PCLS, PCBG, and CBG. Two steel recycling ratios to consider different steel manufacturing processes for CBG alternatives are 71% (CBG_71) and 98% (CBG_98). These steel recycling rates correspond to those of reinforcement bars in Spain and the maximum recycling rate for hot rolling steel according to the World Steel Association [147].

Results for the environmental analysis are represented in Figure 4.5. As can be seen from the ecological point of view, PCSS is the best solution between 15 m and 18 m. PCLS becomes the best alternative up to 25 m, where box solutions are used from this point on. In span lengths between 25 m and 40 m, it can be seen in Figure 4.5 that solutions with lower environmental impact are the best compared to others. For concrete solutions, the best alternative is the PCBG. In this case, the comparison between damage categories makes no sense due to the similarity of every damage category. The three damage categories are normalized and summed to give the same importance to total impact. From the results obtained for each damage category, the most ecofriendly solution is CBG_98. Furthermore, the more recycled steel is used, the more environmentally friendly the alternative is.

4.3.2 Social LCA

Social evaluation of bridge deck alternatives is carried out using the social impact weighting method as the LCIA method. This method, in a similar way to recipe, gives a series of indicators related to specific impact categories, as can be seen in Table 4.1. For this case study, the indicators are collected in four categories related to the leading social stakeholders following the method in Penadés-Plà et al. [159]. This impact categories grouping allows us to understand better the social impact of the alternatives and their comparison. The social stakeholders chosen are local community, value chain actors, society, and workers as defined in Table 4.1.

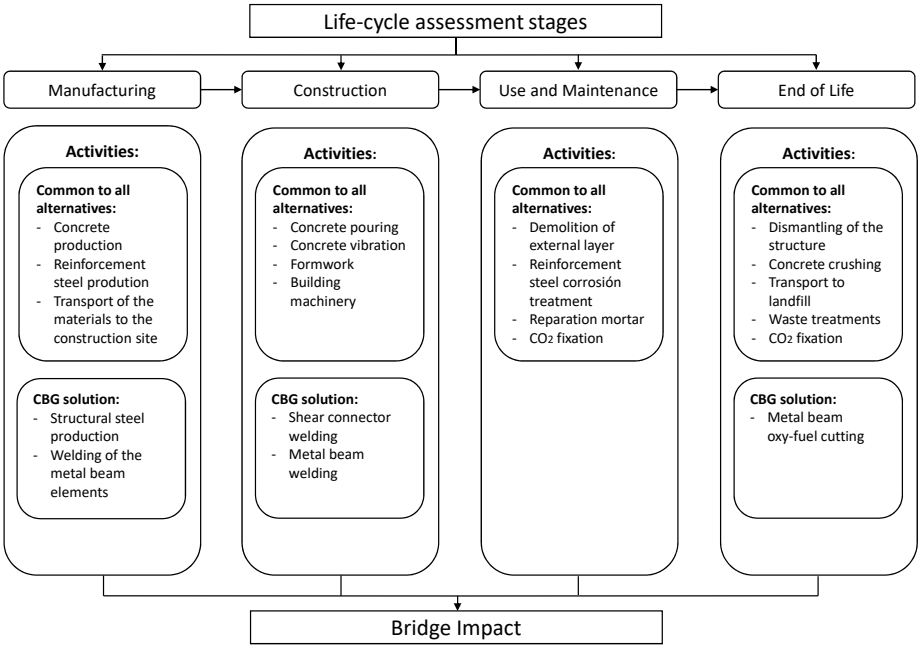

Figure 4.4: Life cycle of the bridge decks.

Results from S-LCA give precise results regarding the feasibility of alternatives for each span length. From 15 m to 25 m, the best option is the PCLS. From this length, the PCBG is the best alternative from a social point of view. Regarding the CBG alternatives, it can be seen that its social feasibility is very low compared to PCBG, even below the PCLS solution with higher recycling rates (CBG_98). It can be observed that solutions with higher steel recycling ratios give higher social impact values for social damage categories, as can be seen in Figure 4.6. If the analysis is focused on the slopes of the obtained lines, it can be seen that the impact on resources increases to a greater extent than the impact on human health, and this, in turn, is greater than the impact on the ecosystems.

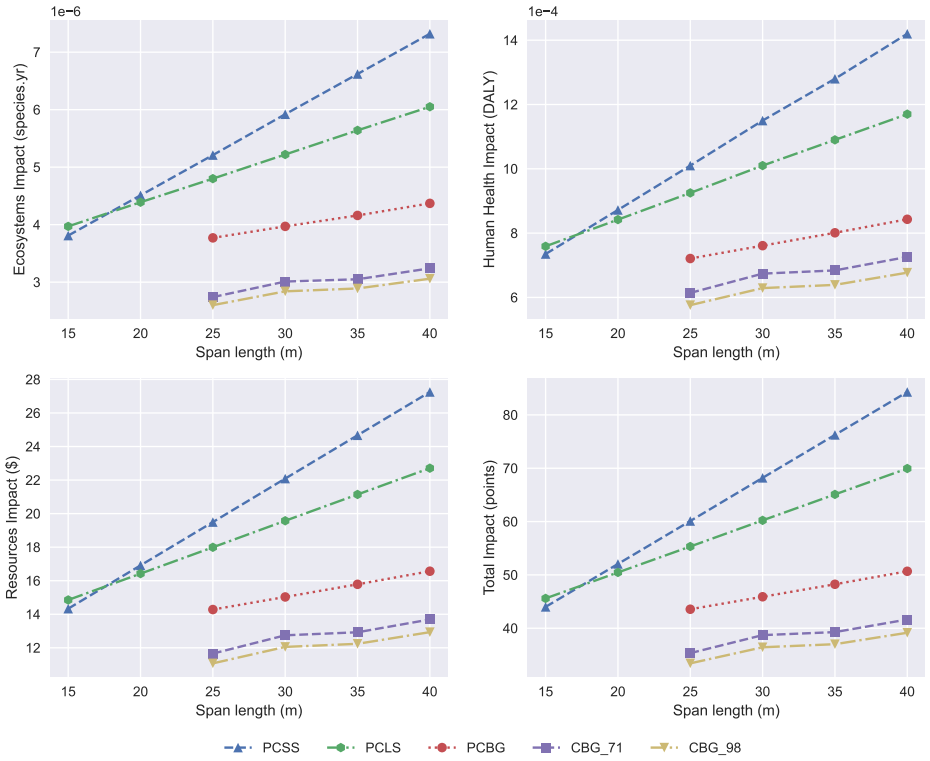

Figure 4.5: Development of environmental impacts regarding the span length.

4.4 Discussion

This research carried out a social and environmental impact assessment of four bridge deck alternatives. As it can be seen in Section 4.3, results from both evaluations give opposite results. Regarding the feasibility of E-LCA options, the most suitable alternative for 25 m to 40 m span lengths is the CBG. Moreover, the increase in the steel scrap used for the steel manufacturing process reduces the impact of the CBG alternatives, with the CBG_98 alternatives being the best from the environmental point of view. On the contrary, for social assessment, this is a worse alternative than PCBG, and in addition, a higher steel recycling ratio gives, as a consequence, a higher social impact.

To get an idea of the cause of this contrast between LCA criteria, a more detailed study was carried out regarding the importance of stages for global analysis. In Table

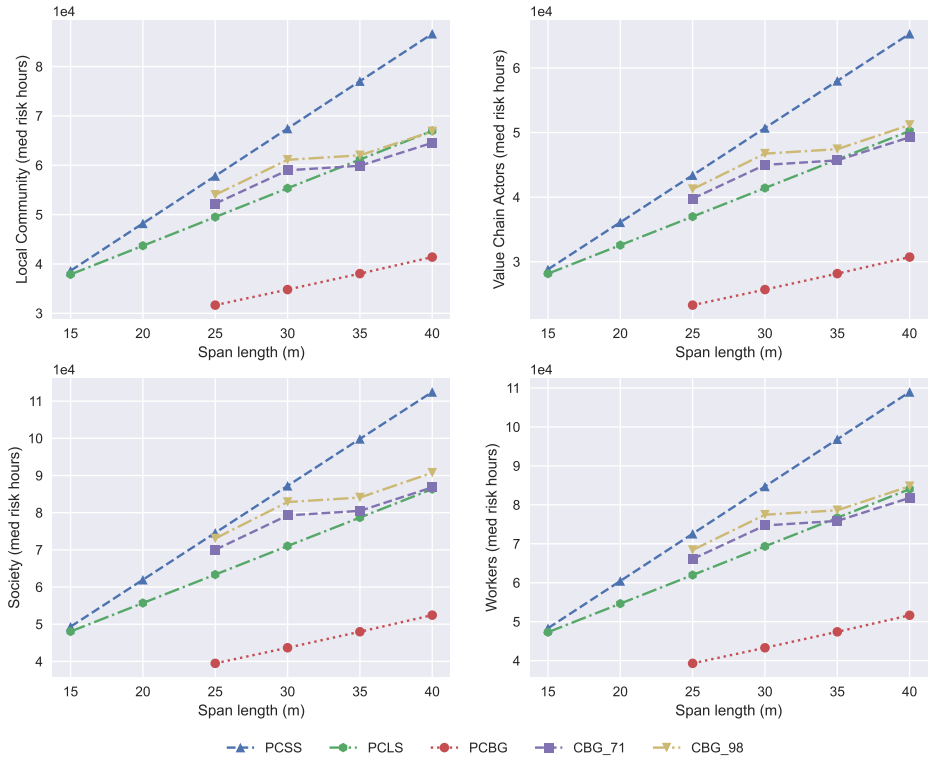

Figure 4.6: Development of social impacts regarding the span length.

4.4, the total assessments for both social and environmental criteria are summarized for a 35 m solution. It can be observed that the solution with the most impact for both ecological and social assessments is the PCSS. However, the feasibility of solutions changes drastically between criteria. The CBG with 98% of recycled steel is the best, eco-friendly solution. It should be remembered that this is the usual steel recycling rate for hot rolled steel according to the World Steel Association [147]. For social impact assessment, this changes, and the most socially sustainable solution is the PCBG, with the 98% of recycled steel CBG solution lagging behind the PCLS one.

The difference between these two assessments is produced by the importance of steel to the total impact in both environmental and social assessments. In Figure 4.7, the importance of every process is defined according to the results obtained from the LCA models. As can be seen, steel is the process that has the most significant impact on the total for both assessments. However, for social impact, this importance

Table 4.4: Sustainability assessment for 35 m span length solutions.

Deck Alternative	Assessment	Unit	Manufacturing	Construction	Use and Maintenance	EoL	Total
PCSS	Environmental	p	57.03	7.68	11.86	−0.33	76.24
	Social	mrh	91,346.24	2062.11	2242.40	1197.07	96,847.81
PCLS	Environmental	p	46.11	5.83	13.44	−0.29	65.09
	Social	mrh	71,340.94	1799.18	2544.54	1002.49	76,687.16
PCBG	Environmental	p	30.33	3.12	15.02	−0.23	48.24
	Social	mrh	42,442.18	1377.60	2853.89	721.98	47,395.64
CBG_98	Environmental	p	28.04	1.25	7.96	−0.24	37.01
	Social	mrh	75,914.48	575.45	1479.21	635.76	78,604.89

grows from 51.1% to 80.8% in the case of the CBG_98 alternative. Furthermore, regarding the steel manufacturing process in the environmental assessment, the impacts of one kg of steel considering 71% and 98% of steel scrap are 0.152 and 0.104 points. If the same analysis is carried out from the social perspective, the results are 1941.08 and 2066.51 med risk hours for one kg of steel considering 71% and 98% of steel scrap, respectively. Suppose we add that the importance of steel is more remarkable for the social analysis and that considering a higher percentage of steel recycling generates a more significant impact. In that case, we find the cause of these differences in effects. Suppose the analysis is focused on the slopes of the obtained lines. In that case, it can be seen that the impact growing the most is the impact on society, followed by the effect on workers, local community, and value chain actors.

Figure 4.7: Importance of materials processes to total environmental and social impact models.

Finally, the importance of every bridge deck LCA stage of this study is defined in Figure 4.8. Regarding the similarities of both assessments, it can be stated that manufacturing is the most critical stage for both social and environmental impacts. The next order by importance is the use and maintenance phase, followed by the construction and the end of life. One difference is observed between these two sustainability assessment criteria. The carbonation process reduces the use and maintenance and end-of-life stages for environmental assessment. In contrast, the carbonation reduction does not affect the total impact of the social evaluation. Another difference is observed between alternatives in the construction stage. For E-LCA, the PSCC alternative is the most impacting, while for the S-LCA, it is the PCBG.

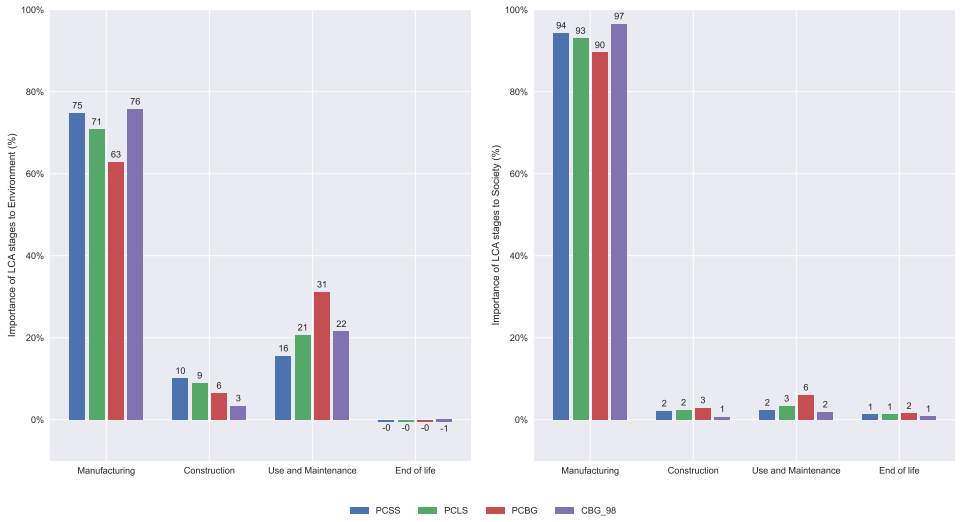

Figure 4.8: Importance of the LCA stages for environmental and social impact models for 35 m span length solutions.

4.5 Conclusions

This research compared the environmental and social impacts of different bridge deck alternatives. Usually, in span lengths between 15 m and 25 m, the options used are the PCSS and PCLS, taking economic feasibility as the criterion. In these studies, PCSS and PCLS are compared from the social and environmental points of view. This comparison gave the result taht the PCLS is a better alternative. In the span, the length ranges from 15 m to 18 m; PCSS is better than PCLS for the

environmental assessment, but PCLS overcomes the PCSS in all length ranges for social impact.

The steel recycling ratio variation modifies the impact of alternatives. Still, in contrast with other studies made with older versions of this database, it is not crucial to define the feasibility of the options. From the environmental point of view, the more steel is recycled, the lower the ecological impact. On the contrary, for the social sustainability of deck alternatives, lower amounts of steel scrap reduce the global impact of the structure.

CO_2 fixation by carbonation processes only impacts the environmental analysis, reducing the impact of the structure in use and maintenance and end of life stages. This reduction is less critical in composite solutions because the amount of concrete in this board type is minor to concrete alternatives. Regarding the social sustainability of the alternatives, carbonation, and consequently, the CO_2 fixation produced in this process, does not affect the total assessment of the structure. This leads to the fact that the end-of-life phase, where the concrete is crushed, positively impacts the environmental analysis. At the same time, it does not positively impact the social analysis.

Regarding the material importance in the assessment, the steel impact is higher in environmental and social aspects. Finally, we assume higher values concerning other material contributions. Finally, the manufacturing stage has the most significant life cycle impact of all the alternatives, as found in other research studies with the same scope.

This research compares different bridge deck alternatives from the environmental and social sustainability points of view. In the main conclusion, the composite box girder alternatives are the most sustainable from the ecological point of view. However, the most suitable for social impact is the prestressed concrete box-girder solution. Consequently, the most sustainable choice of alternatives for bridge decks is mainly a multi-criteria decision-making problem that will depend on the weights assigned to every economic, environmental, and social pillar.

As a result of this study, researchers and designers can obtain information about the feasibility of concrete and composite alternatives proposed for analysis. The information regarding this feasibility is limited to the defined cross-section types of slab and box-girder bridges, their assessment from environmental and social points of view, and the span lengths between 15 m and 40 m. In future research studies, other composite bridge cross-section alternatives can be studied, such as twin I-girder bridges or plate girders, to examine if they improve the feasibility of composite options for social impact. Furthermore, optimization techniques can be applied to

cross sections to obtain new designs, considering the social and environmental LCA impacts as objective functions.

Chapter 5

Optimal design of steel-concrete composite bridge based on a transfer function discrete swarm intelligence algorithm

Authors:	D. Martínez-Muñoz , J. García, J.V. Martí, and V. Yepes		
Status:	Manuscript accepted		
Journal:	Structural and Multidisciplinary Optimization, 65:312		
Year:	2022		
DOI:	10.1007/s00158-022-03393-9		
JCR IF (2021):	4.279		
	JCR Category	Ranking	Quartile
	Engineering, Multidisciplinary	20/92	Q1
	Mechanics	31/138	Q1
Presentation:	Post-print (author version)		

Abstract

Bridge optimization can be complex because of the large number of variables involved in the problem. In this paper, two box-girder steel–concrete composite bridge single objective optimizations have been carried out considering cost and CO_2 emissions as objective functions. Taking CO_2 emissions as an objective function allows to add sustainable criteria to compare the results with cost. SAMO2, SCA, and Jaya metaheuristics have been applied to reach this goal. Transfer functions have been implemented to fit SCA and Jaya to the discontinuous nature of the bridge optimization problem. Furthermore, a Design of Experiments has been carried out to tune the algorithm to set its parameters. Consequently, it has been observed that SCA shows similar values for objective cost function as SAMO2 but improves computational time by 18% while also getting lower values for the objective function result deviation. From a cost and CO_2 optimization analysis, it has been observed that a reduction of 2.51 kg CO_2 is obtained by each euro reduced using metaheuristic techniques. Moreover, for both optimization objectives, it is observed that adding cells to bridge cross-sections improves not only the section behavior but also the optimization results. Finally, it is observed that the proposed design of double composite action in the supports allows to remove continuous longitudinal stiffeners in the bottom flange in this study.

Keywords: Swarm intelligence; Steel–concrete composite structures; Bridges; Optimization; Metaheuristics; Sustainability

5.1 Introduction

Traditionally, structural design processes depend on methods based on common practice. Once the analysis of this first design is done, the geometry of the sections and the grade of the materials are modified based on the experience of the technician [174]. Researchers have implemented optimization methods to obtain structural designs through automated processes to reduce this need for expertise. Optimization techniques can be classified into two large groups, the first of complete techniques and the second of approximate or incomplete methods. The exact or complete approaches are the ones that produce the best result regardless of the processing time. The most commonly used strategies in integer programming are branch-and-cut and branch-and-bound. Many combinatorial optimization problems can be expressed as mixed-integer linear programming problems [225]. These exact algorithms have had good results solving complex problems, however, when the type of constraints does not meet certain conditions or the size of the problem is very large, these algorithms do not necessarily work well. On the other hand, Incomplete techniques are those

that find a suitable solution that is not always the best but does so in a reasonable amount of time. Among these incomplete techniques are heuristic and metaheuristic algorithms.

These methods use heuristic or metaheuristic algorithms that allows to explore the space of possible solutions while considering both rules and randomness. A peculiarity of structural design problems is that the variables on which the problem depends are discrete, making the optimization problem more complex. Optimization methods have been used extensively in structural problems, as can be seen in some of the literature reviews [226]–[228]. These structures include Reinforced Concrete (RC) building frames [229], wind turbine foundations [230] or bridge decks [231]. These methods have also been applied to beam [165], [232] and cable-stayed [16] bridges among others.

In bridges, some very complex structural optimization problems can arise due to the high number of variables. This complexity can be even greater in composite bridges, where the number of possible solutions increases due to a large number of variables [14]. Furthermore, Steel-Concrete Composite Bridges (SCCB) can be divided into three groups according to the cross-section: plate-girder, twin-girders, and box-girder [25], and its behavior differs between these types. Consequently, literature review have collected the techniques used in SCCBs' optimization [189]. In simplified problems, an Excel solver [13] or the fmincom Matlab® function [104] have been applied. Meanwhile, other methods have been used for more complex SCCBs, such as set-based parametric design [106], Harmony Search (HS) [109], Genetic Algorithm (GA), or the Imperialist competitive algorithm [103]. In the optimization algorithms, there is a family that uses swarm intelligence methods. These algorithms have also been applied to SCCB, such as Cuckoo Search (CS), Particle Swarm Optimization (PSO) [109], Colliding Bodies Optimization (CBO), Enhanced Colliding Bodies Optimization (ECBO), or Vibration Particle System (VPS) [110]. Methods such as GA or Simulated Annealing (SA) have been widely used in structural optimization problems due to their easy adaptation to discrete optimization problems. On the other hand, swarm intelligence methods are usually built to optimize on continuous spaces, such as the sine cosine algorithm (SCA) [233] or Jaya [234]. Recent optimization research has applied transfer functions to these algorithms to adapt them to binary [235], [236] problems, which is common in engineering optimization problems. These latest algorithms, under certain conditions, have made it possible to exceed the results of algorithms such as GA or SA.

To get an optimum, it is first necessary to define one objective function. In bridges, this objective function has traditionally been related to the cost or weight reduction. In SCCB optimization, the research objective function has cost in all studies [189]. Considering only cost as an optimization objective function means that other criteria,

such as the environmental or social impact, have not been considered. In concrete bridges, many authors have applied objective functions to get more sustainable solutions, such as embodied energy [124] or the bridge lifetime reliability [165].

In this study, as a first contribution, a bridge composed of steel and concrete with three sections and a single box girder of 60-100-60 meters has been modeled and optimization of costs and emissions CO_2 has been carried out. Both optimization criteria have been considered as single-goal optimizations to compare the results. By incorporating CO_2emissions, the impact has been analyzed from the point of view of economic resources and the sustainability of the infrastructure. Additionally, three optimization algorithms have been considered: Simulated Annealing with a Mutation Operator (SAMO2), Sinus Cosinus Algorithm (SCA) and Jaya. The first is a traditional trajectory-based algorithm that has efficiently solved structural optimization problems [14]. The other two algorithms implemented in this study are SCA and Jaya, these correspond to swarm intelligence algorithms and naturally work in continuous search spaces. As a second contribution, a discretization method based on transfer functions (used to solve binary problems) has been proposed to adapt SCA and Jaya algorithms in order to solve the discrete optimization problem of the bridge. To evaluate the results of the discretizations, they were compared with SAMO2, which has efficiently solved structural design problems. We should also point out that this discretization method can be extended to solve other types of discrete problems. Finally, to perform the cost and emissions analysis, the SCA is used, which was the one that obtained the best result.

5.2 Optimization: problem description

Optimization maximizes or minimizes one objective function. This search can be done by considering the objective functions separately or together; if the criteria are considered separate, the process is called single objective optimization. On the contrary, if all criteria are considered together is known as multi-objective optimization. In this research, the optimization objective functions are cost and CO_2 emissions considered as two different single objective optimizations. In equation 5.1, the cost objective function is defined by multiplying the unit cost of every material in the bridge by its measurement. The CO_2 emissions target function is formulated in equation 5.2. The data for CO_2 emissions considers cradle-to-gate analysis. Thus, it is necessary to consider the emissions of every process to get bridge materials on-site and execute the project. The data of prices and CO_2 emissions that are shown in Table 5.1 have been obtained from the Construction Technology Institute from Catalonia by the BEDEC database [207]. Both optimization expressions need to fulfill, throughout the entire process, the constraints imposed by the regulations or recommendations

Table 5.1: Cost and CO_2 emission values

Unit	Cost (€)	Emissions (kg of CO_2)
m^3 of concrete C25/30	88.86	256.66
m^3 of concrete C30/37	97.80	277.72
m^3 of concrete C35/45	101.03	278.04
m^3 of concrete C40/50	104.08	278.04
m^2 of precast pre-slab	27.10	54.98
kg of steel B400S	1.40	0.70
kg of steel B500S	1.42	0.70
kg of rolled steel S275	1.72	4.33
kg of rolled steel S355	1.85	4.33
kg of rolled steel S460	2.01	4.33
kg of shear-connector steel	1.70	2.8

represented by equation 5.3 in a general manner. The specific constraints for this optimization problem are defined in section 5.2.3 and more concretely by equation 5.5 and Table 5.4 of the aforementioned section.

$$C(\vec{x}) = \sum_{i=1}^{n} p_i \cdot m_i(\vec{x}) \tag{5.1}$$

$$E(\vec{x}) = \sum_{i=1}^{n} e_i \cdot m_i(\vec{x}) \tag{5.2}$$

$$G(\vec{x}) \geq 1 \tag{5.3}$$

5.2.1 Variables

A 220 m continuous steel-concrete composite box-girder three-span bridge is proposed for optimization. The problem variables correspond to each bridge element's geometry, reinforcement, and concrete and steel grades. To reach a buildable solution, all of these variables have been discretized, configuring a discrete optimization problem. The variables discretization has been defined in Table 5.2. Considering this variable discretization, the number of combinations for the optimization problem corresponds to $1.38 \cdot 10^{46}$. Due to many possible combinations, metaheuristic techniques are justified to obtain the optimum. In total, 34 variables are considered for the global definition of this bridge optimization problem. These bridge variables have

been represented in Figure 5.1. According to the nature of the variables, they can be grouped into six categories. The first correspond to cross-section geometric variables, which are: upper distance between wings (b), wings and cells angle (α_w), top slab thickness (h_s), beam depth (h_b), floor beam minimum high (h_{fb}), top flange thickness (t_{f_1}), top flange width (b_{f_1}), top cells high (h_{c_1}) and thickness (t_{c_1}), wing thickness (t_w), bottom cells high (h_{c_2}), thickness (t_{c_2}), and width (b_{c_2}) and bottom slab thickness (h_{s_2}). Beam depth bounds correspond to L/40 and L/25, being L, the largest span length.

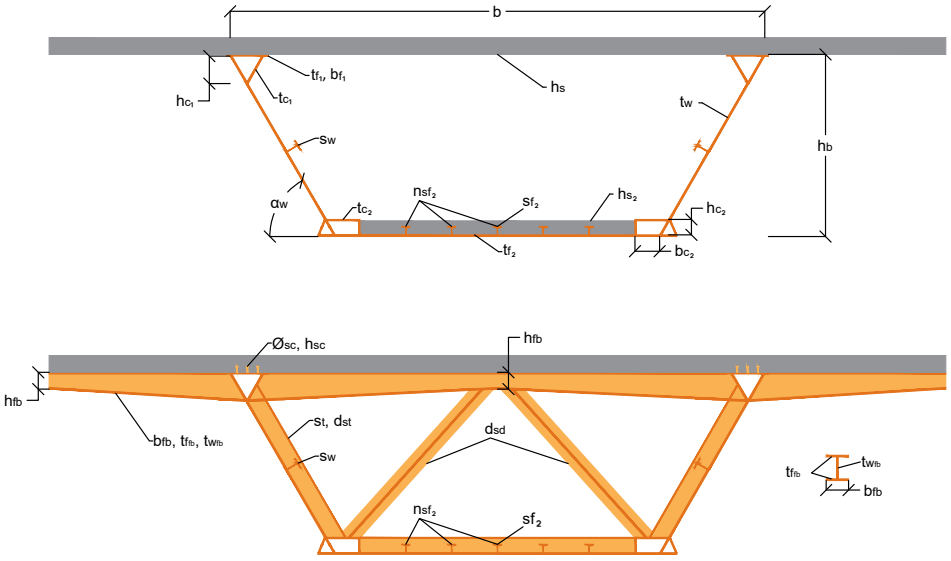

Figure 5.1: Cross-section variables for SCC bridge

SCCB can take advantage of materials to a greater extent because each material that makes it up is subjected to the stresses that best resist. This would be true in an SCCB working as an statically determinate girder. In this case, the upper concrete slab would be compressed along the entire length of the bridge. This upper slab is connected to the top flanges by shear connectors. This would also stiffen the flanges plate, which avoids buckling. Moreover, in the isostatics case, the lower flanges would be subjected to tensile stress, avoiding buckling instability phenomena. However, in the present case and with the usual loads to which the bridges are subjected

(mostly gravitational), negative bending stresses will occur in supported areas. This will result in reversing the forces and tensile stresses in the upper concrete slab and the compression in the lower flange. In this case, to improve the behavior of the bridge cross-section, it has been decided to materialize a concrete bottom slab in these areas in addition to the usual increase of the top slab reinforcement. To optimize the top slab reinforcement, it has been divided into a base reinforcement that is the minimum required by regulations [26], [237], [238] and two more areas, in negative bending sections, where the reinforcement is increased. The bottom slab and reinforcement increasing area lengths are described in section 5.2.2. Accordingly, the second group of variables corresponds to base reinforcement, first reinforcement and second reinforcement bar diameters (ϕ_{base}, ϕ_{r_1}, ϕ_{r_2}), and the corresponding bar number of the reinforcement areas (n_{r_1}, n_{r_2}).

The next variable group correspond to stiffeners. The elements considered in these work as stiffeners are half IPE profiles for wings (s_w), bottom flange(s_{f_2}) and the transverse ones (s_t). For bottom flange stiffeners, the number of stiffeners ($n_{s_{f_2}}$) has also been considered as a variable. As can been seen in Figure 5.1, there are two more variables that define the distance between diaphragms (d_{sd}) and transverse stiffeners (d_{st}).

The last categories correspond to floor beam variables geometry, the shear connector's characteristics, and the materials' grades. Floor beam variables are defined by the floor beam width (b_{fb}), and the flanges ($t_{f_{fb}}$) and wing ($t_{w_{fb}}$) thicknesses. The shear connectors have been defined by their height(h_{sc}) and diameter (ϕ_{sc}). Finally, the yield stress from rolled steel (f_{yk}), concrete strength (f_{ck}) and reinforcement steel bars yield stress (f_{sk}) complete the variable definition. The variables are the same for all the spans of the bridge.

5.2.2 Parameters

To narrow down the problem, some variables or properties need to be fixed in every optimization problem. These fixed variables are named parameters, and they remain invariant during the whole optimization process. In this case, these parameters correspond to boundaries defined to some bridge elements, including dimension, thicknesses, reinforcement distributions, external ambient conditions, or density (among others). The values of these parameters are summarized in Table 5.3.

The bridge deck width (B) corresponds to 16 meters, and the depth does not vary over the entire length of the bridge. In the cross-section, it has been defined by four cells: two on the upper side of the wings and two more on the bottom, as can be seen in Figure 5.1. These cells allow these parts of the wing to be stiffened,

Table 5.2: Design variables and boundaries

Variables	Unit	Lower Bound	Increment	Upper Bound	Values number
b	m	7	0.01	10	301
α_w	deg	45	1	90	46
h_s	mm	200	10	400	21
h_b	cm	250 (L/40)	1	400 (L/25)	151
h_{fb}	mm	400	100	700	31
t_{f_1}	mm	25	1	80	56
b_{f_1}	mm	300	10	1000	71
h_{c_1}	mm	0	1	1000	101
t_{c_1}	mm	16	1	25	10
t_w	mm	16	1	25	10
h_{c_2}	mm	0	10	1000	101
t_{c_2}	mm	16	1	25	10
b_{c_2}	mm	300	10	1000	71
t_{f_2}	mm	25	1	80	56
h_{s_2}	mm	150	10	400	26
$n_{s_{f_2}}$	u	0	1	10	11
d_{st}	m	1	0.1	5	41
d_{sd}	m	4	0.1	10	61
b_{fb}	mm	200	100	1000	9
$t_{f_{fb}}$	mm	25	1	35	11
$t_{w_{fb}}$	mm	25	1	35	11
n_{r_1}	u	200	1	500	301
n_{r_2}	u	200	1	500	301
ϕ_{base}	mm	6, 8, 10, 12, 16, 20, 25, 32			8
ϕ_{r_1}	mm	6, 8, 10, 12, 16, 20, 25, 32			8
ϕ_{r_2}	mm	6, 8, 10, 12, 16, 20, 25, 32			8
s_{f_2}	mm	From IPE 200 to IPE 600*			12
s_w	mm	From IPE 200 to IPE 600*			12
s_t	mm	From IPE 200 to IPE 600*			12
h_{sc}	mm	100, 150, 175, 200			4
ϕ_{sc}	mm	16, 19, 22			3
f_{ck}	MPa	25, 30, 35, 40			4
f_{yk}	MPa	275, 355, 460			3
f_{sk}	MPa	400, 500			2

*Following the standard series of IPE profiles [239].

creating a sheet of class one to three that does not need to be reduced according to Eurocodes [26], [238]. To allow the optimization process to define if these cells

Table 5.3: Optimization problem main parameters

Geometrical parameters		
Bridge deck width (W)	16	m
Span number	3	
Central span length	100	m
External span length	60	m
Minimum web thickness ($t_{w_{min}}$)	15	mm
Minimum flange thickness ($t_{f_2 min}$)	25	mm
Reinforcement cover	45	mm
Material parameters		
Maximum aggregate size	20	mm
Concrete longitudinal strain modulus (E_{cm})	$22 \cdot ((f_{ck} + 8)/10)^3$	MPa
Concrete transverse strain modulus (G_{cm})	$E_{cm}/(2 \cdot (1 + 0.2))$	MPa
Steel longitudinal strain modulus (E_s)	210000	MPa
Steel transverse strain modulus (G_s)	80769	MPa
Regulation requirement parameters		
Regulations	Eurocodes[26], [237], [238], [240], IAP-11[241]	
Exposure environment	XD2	
Structural class	S5	
Service life	100	years
Loading parameters		
Reinforced concrete density	25	kN/m^3
Steel density	78.5	kN/m^3
Asphalt density	24	kN/m^3
Asphalt layer thickness	100	mm
Bridge traffic protections	5.6	kN/m

improve the structural behavior of the cross-section (and consequently are relevant to obtain a minimum of the objective function), the minimum height of these cells is fixed to zero. The boundaries of all of the variables, including the cells heights (h_{c_1}, h_{c_2}), can be seen in Table 5.2. The variable's boundaries have been defined following Monleón bridge design publication [242]. The cell height(h_{c_1}, h_{c_2}) defines the floor beam depth in the zone of contact with the wings. If the cell height is smaller than the floor beam minimum depth (h_{fb}), then it takes that minimum value for beam depth in that zone. Profiles placed to materialize the diaphragm sections are 2L 150x15. Furthermore, pre-slabs have been considered for use as a formwork. It should be noted that this element is designed to be part of the resistant section. Therefore, the measurement module of the software subtracts it from the total amount of concrete.

Base reinforcement for both the upper and the lower concrete slabs is obtained according to the minimum need for reinforcement defined in Eurocode 2 [238]. The connection between the steel beam and concrete slab is designed to resist the whole stress of the concrete slab considering the effective width that is given by Eurocode 4 [26] due to shear lag. Because the only width considered as resistant (both in the concrete slab and in the lower flange) is effective, the defined steel bar reinforcement is placed only in that width.

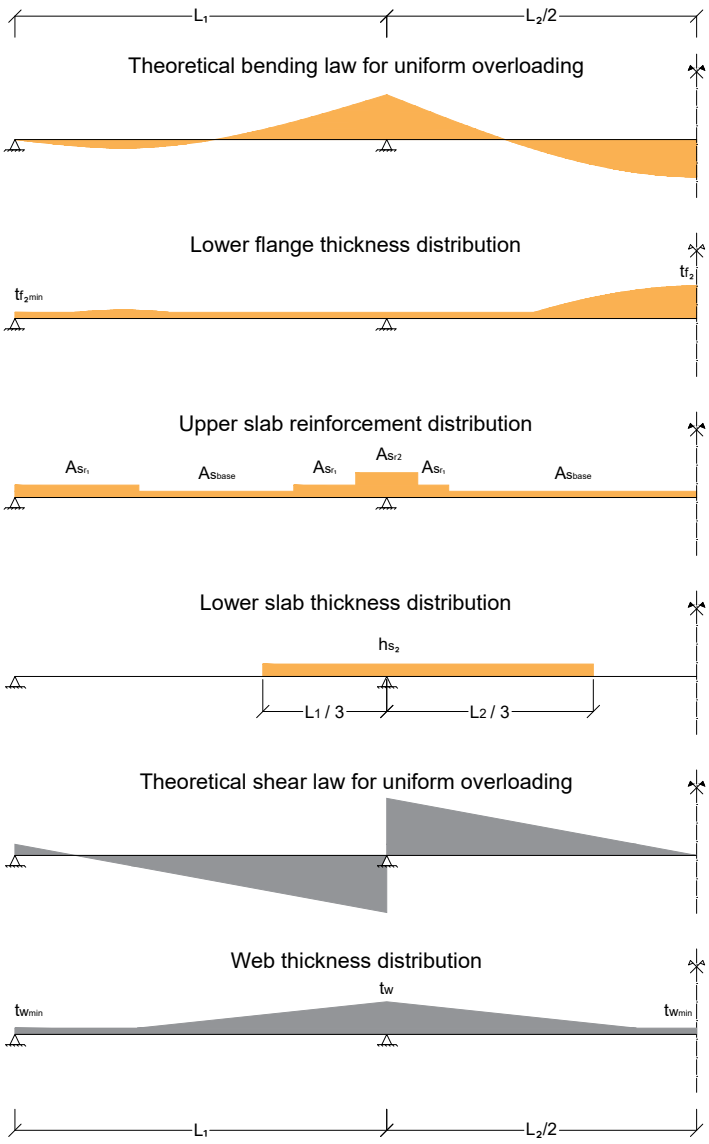

Figure 5.2: Longitudinal distribution of thicknesses and steel bar reinforcements

To optimize some materials in SCCB, it is usual to modify the thicknesses of webs and flanges to reduce their amount. In this work, the variation of thicknesses has been programmed by considering a theoretical bending and shear law for a distributed load over the entire surface of the bridge. In Figure 5.1, the lower flange thickness is modified along the bridge, varying from a minimum value t_{f_2min} to the one defined as t_{f_2}. This variation corresponds to the theoretical bending law. In contrast, the wing's thickness varies according to the shear law from $t_{w_{min}}$ to t_w. The minimum value of these thicknesses has been defined according to recommendations in Monleón [242].

Finally, steel bar reinforcements and lower slab areas are defined. The lower slab is placed in negative bending sections to mobilize the composite dual-action. To define lengths where negative bending can be produced, it has been considered the distance defined by Eurocode 4 [26] for shear lag stresses that correspond with one-third of the span length. It is necessary to increase the upper slab reinforcement to resist the tension stresses produced. In this case study, it has been considered two reinforcement areas. The first is placed in zones where the section can be subjected to negative bending, and base reinforcement cannot resist the stresses. The second is placed on top of supports, corresponding to one-third of the distance between the support and the point of change of sign of the bending of the theoretical law. This decision is related to the position of the center of gravity of the parabola, which is at one-third of its total length. Figure 5.2 shows the top slab's reinforcement distributions.

5.2.3 Constraints

As mentioned in section 5.2, optimization procedures must comply about the constraints imposed on the problem. In bridge optimization, these constraints are set by the regulations [26], [237], [238] and recommendations [25], [242].

Constraints imposed by regulations can be divided into two main groups: the Ultimate Limit States (ULS) and Serviceability Limit States (SLS). All of the loads applied and their combination are defined in regulations [240]. Table 5.3 summarizes the structural checks and load values that have been considered.

To check ULS for all bridge elements, it has been considered both global and local analysis. The checks considered for global analysis include flexure, shear, torsion, and flexure-shear interaction as defined in Table 5.4. A linear elastic analysis has been used to obtain the deflections and stresses. To get section resistance, the effective area has been considered by applying both reductions due to shear lag [26] and section reduction of the steel plates classified as class 4 [237]. This last re-

duction is carried out by an iterative process. This procedure produces a variation of the neutral fiber of the section due to the area reduction. This process must be repeated until the difference between the neutral fiber obtained between iterations is null or negligible. To attain this, a difference of 10^{-6} meters has been imposed as termination criteria for the iterative process. To obtain the value of the mechanical characteristics of the homogenized section, the relationship (n) between the modulus of longitudinal deformation of concrete (E_{cm}) and steel (E_s) has been obtained according to equation 5.4. Concrete creep and shrinkage have been considered according to regulations [26], [238]. The procedure used for the time-dependent effects evaluation of concrete is the Ageing coefficient method defined in the annex KK of EN 1992-2:2013 [238]. Furthermore, a local model has been considered to check ULS in-floor beams, stiffeners, and diaphragms by considering flexure, shear, buckling, and minimum mechanical characteristics checks.

$$n = \frac{E_s}{E_{cm}} \tag{5.4}$$

The SLS considered for the analysis are the stress limit for materials, fatigue, and deflection as defined in Table 5.4. There is no explicit limit for deflection in Eurocodes. Still, the IAP-11 Spanish road bridges regulation [241] gives a maximum of $L/1000$ for the frequent value of live loads deflection value, with L representing the span length. This frequent value is defined in the IAP-11 as $\psi_1 Q_k$, where ψ_1 is the simultaneity factor and Q_k are the values of each live load. This loads value corresponds to the actions associated with a one-week return period. The values of this ψ_1 coefficients are: 0.75 for the concentrated traffic load 0.40 for the distributed traffic load, 0.2 for wind load and 0.6 for the thermal loads [241]. This has been considered as the maximum value of the deflection. In addition geometrical and constructibility requirements have been deemed.

A numerical model has been implemented in the Python [243] programming language to get the stresses and carry out all ULS, SLS, and geometrical and constructibility checks defined in regulations [26], [237], [238], [240] and recommendations [25], [242] as defined in Table 5.4. To calculate the deflections and stresses, this software applies the displacement method considering the vertical displacements (U_z) and the spins in y and x-axes (θ_y, θ_x), taking as input data the 34 bridge variables defined in section 5.2.1 and the loads specified in regulations. To obtain the effects due to the moving loads, all possible load combinations have been considered to get their envelope as defined in section 5.2.3. This software divides every bridge span into a defined number of bars. In this case, the total number of bars is 44, distributed in 12-20-12 corresponding to the three spans of the bridge; thus, discretizing the bridge into 5-meter length bars. Once the stresses have been ob-

Table 5.4: Structural checks and load values

Checkings		
ULS	Flexure	$M_{Ed} \leq M_{Rd} = \frac{W_{el,min} f_y}{1.05}$
	Shear	$V_{Ed} \leq V_{Rd} = \frac{A_v \left(f_y/\sqrt{3}\right)}{1.05}$
	Torsion	$M_{T,Ed} \leq M_{T,Rd} = \frac{A_T \left(f_y/\sqrt{3}\right)}{1.05}$
	Flexure-shear interaction	$M_{Ed} \leq M_{Rd} = \frac{W_{el,min}\left(1-\left(\frac{2V_{Ed}}{V_{pl,Rd}}-1\right)^2\right) f_y}{1.05}$
	Stiffeners	$Ist \geq \frac{\sigma_m}{E}\left(\frac{b}{\pi}\right)^4 \left(1 + w_0 \frac{300}{b} u\right)$
SLS	Stress limitation	$\sigma_y \leq fyk$
		$\sigma_c \leq 0.6fck$
		$\sigma_s \leq 0.8fsk$
	Fatigue	$\frac{\gamma_{Ff}\ \Delta\sigma_{E,2}}{\Delta\sigma_C/\gamma_{Mf}} \leq 1$
		$\frac{\gamma_{Ff}\ \Delta\tau_{E,2}}{\Delta\tau_C/\gamma_{Mf}} \leq 1$
	Deflection	$L/1000$
Loads		
Dead	Self Weight	Depends on the geometry
	Dead Loads	46.72 kN/m
Live	Traffic concentrated	(300, 200, 100) kN
	Traffic distributed	(9, 2.5, 2.5) kN/m^2
	Thermal heating	18℃
	Thermal cooling	-10℃
	Wind	$F_{wz} =$ 60.84 kN/m
		$F_{wy} =$ 10.78 kN/m
		$F_{wx} =$ 43.12 kN/m

tained, the program performs structural checks and returns the measurements, cost, CO_2 emissions, and checking coefficients. These checking coefficients correspond to the quotient between the design values of the effects of actions (E_d) and its corresponding resistance value (R_d), as shown in equation 5.5. If these coefficient values are greater or equal to one, then the section complies with the imposed restriction defined in Table 5.4.

$$\frac{R_d}{E_d} \geq 1 \tag{5.5}$$

Computational model description

The procedure used to obtain the deflections and stresses has been the displacement method. This method consists in solving the equation 5.6.

$$\mathbf{f} = \mathbf{K} \cdot \mathbf{d} + \mathbf{f_0} \tag{5.6}$$

In this equation, $\mathbf{f_0}$ correspond to the perfect embedding forces vector. These forces would be obtained if each of the system bars had all the degrees of freedom constrained. $\mathbf{K}$ is the stiffness matrix of the system, generated by assembling the stiffness matrices of all bar elements. To get the stiffness matrix of each element, the average between both frontal and dorsal nodes' mechanical properties has been calculated. The complete section without considering the shear lag and panel reduction has been considered to obtain these mechanical properties. Finally, $\mathbf{d}$ and $\mathbf{f}$ are the deflections and stress vectors, respectively. The computational model process flowchart for stresses obtaining have been defined in figure 5.3.

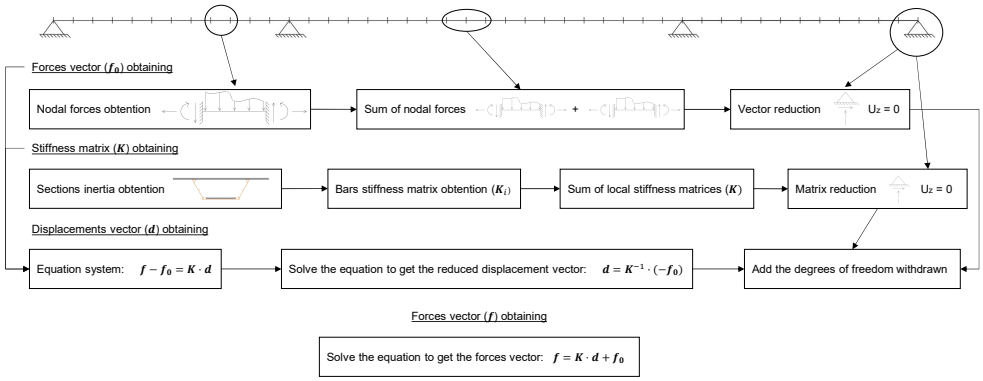

Figure 5.3: Computational model process flowchart

This procedure is repeated with all load cases defined in Table 5.4. The following load cases have been considered loading the entire bridge length as a single load case: Self Weight, Dead Loads, Thermal Heating, Thermal Cooling, and Wind. In order to consider the different positions of traffic loads, every 5-meter bar has been loaded separately, considering two separated loading cases, the concentrated load and the distributed. This gives, as a result, 88 load cases for traffic load and a total of 93 if all load cases are considered. The results obtained from loading each bar have been combined to consider all loading possibilities regarding traffic load. After this,

the load case envelope has been calculated to consider each section's maximum and minimum results.

Regarding combinations and envelopes, the envelope of all persistent and transitory situations combinations have been obtained for ULS. These combinations have been considered dominant action all live loads in different combinations. The envelope of all characteristic combinations has been considered for SLS regarding stress limitation.

5.3 Methodology

In this section, the algorithms used are detailed. SAMO2 and a discrete version of the Sine Cosine and Jaya Algorithms were used to develop the experiments. The algorithms were chosen due to the differences in their movement methods and the ease of parameterization in the case of Jaya and SCA.

5.3.1 Trajectory-based algorithm: SAMO2

Simulated Annealing was developed by [244]. This algorithm is an analogy based on the thermodynamic behavior of a group of atoms forming a crystal. "Annealing" refers to the chemical process of heating and cooling materials in a controlled manner. This study has chosen a variant to carry out the optimization, which includes the benefits of genetic algorithms. The genetic algorithm seeks the best solution through selection, crossover, and mutation operators. To include these strategies, it has been used the SAMO2. This metaheuristic introduces the probabilistic acceptance of the poorer quality solutions to flee from local optimums and directs the search towards better objective function values. For this reason, it accepts inadequate solutions with probability P_a. The expression is given by the expression of Glauber (5.7), where T is a parameter that decreases with time. Consequently, the probability of accepting a poor solution is reduced from the initial value, T_0. Furthermore, it includes a mutation operator that allows the algorithm to change some variables to explore the optimization process.

$$P_a = \frac{1}{1 + e^{\frac{-\Delta E}{T}}} \tag{5.7}$$

The initial temperature is set according to the method proposed by Medina [245]. This algorithm depends on several parameters: Markov Chain Length (MCL), which defines the number of iterations before temperature decreases, and the Cooling Co-

efficient (CC), which is always less than one and represents the temperature variation. Furthermore, the mutation operator depends on the Variables Number (VN) and the Standard Deviation (SD). To fix the end of the optimization, two termination criteria have been defined for this metaheuristic: the first is the Unimproved Chains (UC) that limit the number of Markov Chains allowed without any improvement before finishing the optimization, and the second ends the process if the temperature reaches 5% of the initial (T_0). This algorithm has been chosen as it has achieved good results in other bridge optimization problems [124].

5.3.2 Swarm intelligence algorithms: SCA and Jaya

Sine Cosine Algorithm (SCA)

Sine Cosine Algorithm (SCA) was proposed in [233] and corresponded to a swarm intelligence algorithm that considers the sine and cosine functions to carry out the process of exploring and exploiting the search space. To carry out the movement of the solutions, P_j^t is additionally used, which corresponds to the position of the destination solution for iteration t and dimension j, and typically uses the best solution obtained so far. In addition to P_j^t, the algorithm uses three random numbers r_1, r_2, r_3, which take values between 0 and 1. The update method used is shown in Equations 5.8 and 5.9.

$$x_{i,j}^{t+1} = x_{i,j}^t + r_1 \times sin(r_2) \times \mid r_3 P_j^t - x_{i,j}^t \mid \tag{5.8}$$

$$x_{i,j}^{t+1} = x_{i,j}^t + r_1 \times cos(r_2) \times \mid r_3 P_j^t - x_{i,j}^t \mid \tag{5.9}$$

Jaya

Jaya is a swarm intelligence algorithm that allows to tackle continuous optimization problems, with and without constraints naturally. Jaya was proposed in [246] to solve benchmark problems. However, it has been used to solve complex optimization problems in different areas. The peculiar distinctive feature of Jaya from the other swarm intelligence algorithms is that it updates agents' positions in the population by considering the best and worst individuals. Additionally, binary versions of Jaya have been developed. For example, in [247] an XOR operator was integrated to be able to tackle binary problems. Another attractive quality of Jaya is that it does not have specific control parameters, and only the size of the population and the number of

generations need to be defined. In Figure 5.4 and Equation 5.10, the flowchart and the movement of Jaya are shown, respectively.

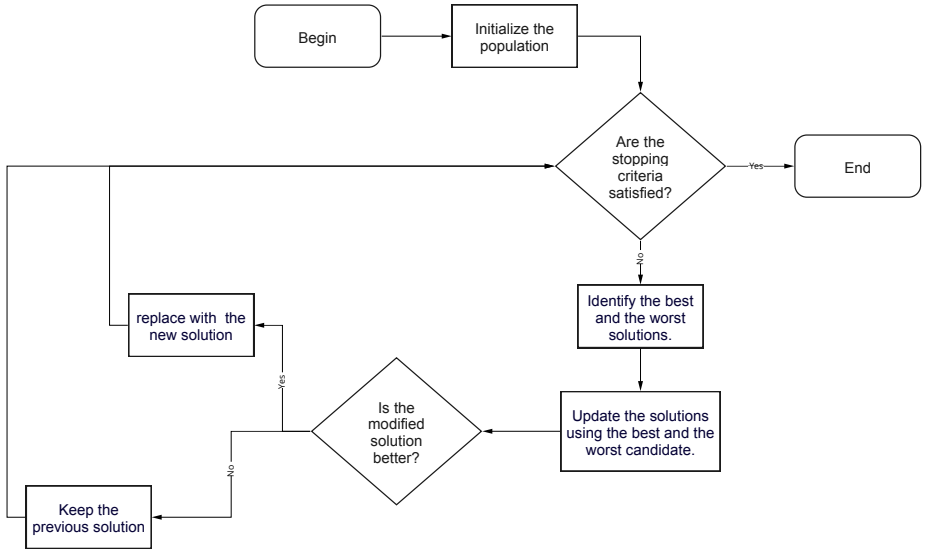

Figure 5.4: The standard Jaya algorithm flowchart.

$$x_{i,j}^{t+1} = x_{i,j}^{t} + r_1(x_{best,j}^{t} - \mid x_{i,j}^{t} \mid - r_2(x_{worst,j}^{t} - \mid x_{i,j}^{t} \mid)) \tag{5.10}$$

Discretization algorithm

The discretization algorithm is applied in the case of swarm intelligence metaheuristics because both metaheuristics work naturally in continuous spaces. As input parameters, it uses the metaheuristic, MH, and the list of discrete solutions obtained in the previous iteration, $lSol$. As an output, it returns a new list of discrete solutions, $lSol$. As the first case, the discretization algorithm obtains the velocities of the MH. This specifically corresponds to the component that modifies $x_{i,j}^{t}$ in Equations 5.8 to 5.10 . For example, in the case of Jaya, it corresponds to what is obtained from the operation $r_1(x_{best,j}^{t} - \mid x_{i,j}^{t} \mid - r_2(x_{worst,j}^{t} - \mid x_{i,j}^{t} \mid))$.

Subsequently, a transfer function is applied that aims to bring the velocity values, which can take values in $\mathbb{R}$, to values between [0, 1). A v-shape transfer function have been used in this study case, $\mid \tanh(v) \mid$. With the obtained values $lSolProbability$,

when applying the transfer function, each solution and dimension are considered, and the value is compared with a random number r_1 between [0,1). If the value of $lSolProbability$ is greater than the random number, an update occurs in that dimension; otherwise, it is not modified. The update procedure has two possibilities: a β value is considered, and a random number r_2 is generated. If this r_2 is less than β, the value is replaced by the value of the best obtained so far for that dimension. Otherwise, a random update is performed. This last option is intended to improve the exploration of the search space.

Algorithm 1 Discretization algorithm

```
1: Function Discretization(lSol, MH)
2: Input lSol
3: Output lSol
4: vlSol ← getVelocities(Lsol, MH)
5: lSolProbability ← appliedTransferFunction(vlSol)
6: for (each SolProbability in lSolProbability) do
7:    for (each dimSolProbability in SolProbability) do
8:       if dimSolProbability > r1 then
9:          if beta > r2 then
10:            Update lSol_{i,j} considering the best.
11:         else
12:            Update lSol_{i,j} with a random value allowed.
13:         end if
14:      else
15:         Don't update the element in lSol_{i,j}
16:      end if
17:   end for
18: end for
19: return lSol
```

5.3.3 Parameter tuning

The results obtained from the metaheuristics depend on their parameter values. Consequently, a parameter selection process is needed to choose those that give the best results for the objective function. This depends strongly on the optimization problem. Therefore, different optimization problems will result in different parameter values. The search for parameters that best fit the optimization problem is called parameter tuning.

SAMO2 tuning

Depending on the metaheuristic, the parameter number varies. There are algorithms with more parameters, such as SAMO2 than others with a smaller number. First, searching for the best fitting ones can become a complex problem. Consequently, existing procedures allow the researcher to get the most statistically significant parameters to focus the search on the variation of these. These procedures are called *Design of Experiments (DoE)*. In this case, a 2^k *fractional factorial design* has been carried out to get the SAMO2 parameter tuning.

In factorial designs, each factor level's possible combinations are studied in each trial or replication. This makes it possible to evaluate the change in response when the level of the factor is varied. This variation is called the effect of the factor and is related to its statistical significance [248]. Two levels need to be assigned to the studied algorithm parameters to carry out this procedure. The studied parameters and the levels are chosen are shown in Table 5.5.

Table 5.5: SAMO2 variables bound for DoE

Parameter	Lower Bound (-)	Upper bound (+)
MCL	100	1000
SD	0%	30%
VN	1	5
CC	0.80	0.95
UC	1	5

Because two levels are defined for each variable, 32 (2^5) runs are needed to get a complete factorial design. Furthermore, five replications need to be considered to get the average and the deviation for each experiment, obtaining 160 runs. To reduce the number of runs, it has been decided to carry out a fractional factorial DoE of resolution V. This reduces the number of runs to 80 because of the reduction

of combinations to 16. A summary of the parameter value combinations is given in Table 5.6.

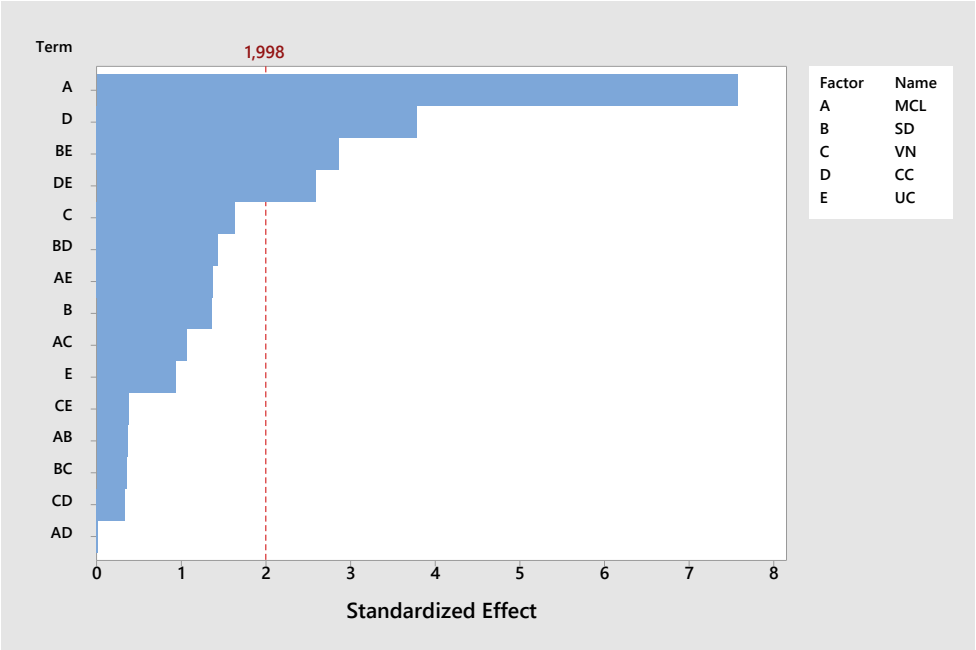

Figure 5.5: Pareto chart of the standardized effects

DoE Minitab [249] software has been used to carry out the statistical analysis. For the statistical analysis, the first-order interaction has also been considered. Accordingly, in Figure 5.5, it can be seen that the parameters with more effect are MCL and CC. In addition, the interaction between UC with SD and UC is also significant. The average results of the five replicates for each of the 16 experiments are shown in Table 5.6.

Table 5.6: Parameter values combination and results for DoE

	MCL	SD	VN	CC	UC	Cost (€)	Time (s)	%Desv	%Min
1	-	-	-	-	+	4620844,60	1055,93	5,80%	20,61%
2	+	-	-	-	-	4033264,82	9833,70	7,46%	5,27%
3	-	+	-	-	-	5109179,62	989,63	3,37%	33,35%
4	+	+	-	-	+	3831318,29	9810,90	0,10%	0,00%
5	-	-	+	-	-	4609783,20	804,36	13,33%	20,32%
6	+	-	+	-	+	4088143,85	7819,85	7,90%	6,70%
7	-	+	+	-	+	4694176,90	787,77	11,78%	22,52%
8	+	+	+	-	-	4622308,95	7846,10	6,32%	20,65%
9	-	-	-	+	-	4164394,64	3043,06	11,89%	8,69%
10	+	-	-	+	+	3831268,79	28688,65	0,11%	0,00%
11	-	+	-	+	+	4430917,82	3252,46	10,75%	15,65%
12	+	+	-	+	-	3831788,82	28818,08	0,07%	0,01%
13	-	-	+	+	+	4743449,44	3182,93	9,49%	23,81%
14	+	-	+	+	-	3851070,22	30519,37	0,50%	0,52%
15	-	+	+	+	-	4463121,26	2977,47	13,46%	16,49%
16	+	+	+	+	+	3839681,73	26664,77	0,11%	0,22%

As can be seen in Table 5.6, the best results correspond to experiment number 10. However, considering the cost and the optimization time, it can be observed that with a worsening of 0.001% in the objective function, it can be got the result in 34.28% less time if the parameters of experiment four are used. Furthermore, the deviation between experiments ten and four is similar, 0.11% and 0.10%, respectively. Due to the improvement in computation time and slight difference in deviation and objective function value, the parameters chosen for the SAMO2 optimization correspond to experiment four, as shown in Table 5.7.

Table 5.7: Parameter chosen for SAMO2 algorithm

MCL	SD	VN	CC	UC
1000	30%	1	0,8	5

Swarm intelligence metaheuristics tuning

The methodology proposed in [250] was used in the selection of the parameters. To obtain an adequate selection of the parameters, this methodology uses four measures defined by the Equations (5.11) to (5.14). $GBestValue$ corresponds to the best value obtained from all executions considering all of the parameter settings. $BestValue$ and $WorstValue$ correspond to the best and the worst value obtained for a given parameter setting. The parameters and explored values are shown in Table 5.8. In the Range column, the explored values are displayed for each parameter. The Value column corresponds to the selected value. For the generation of values, each combination of parameters was executed five times. For the calculation of the best performance, each of the indicators is constructed to have values between 0 and 1. The closer to 1, the better the performance. These values are plotted on a radar chart, and the area under the curve is calculated. The set of indicators that takes the largest area corresponds to the best performance. To determine the number of iterations, 600 and 800 iterations were considered. In the latter case, there were no significant differences in the optimal, but it did have an important impact on the time used.

1. The percentage deviation of the best value obtained compared to the best known value:

$$bSolution = 1 - abs(\frac{GBestValue - BestValue}{GBestValue}) \tag{5.11}$$

2. The percentage deviation of the worst value obtained compared to the best known value:

$$wSolution = 1 - abs(\frac{GBestValue - WorstValue}{GBestValue}) \tag{5.12}$$

3. The percentage deviation of the average value obtained compared to the best known value:

$$aSolution = 1 - abs(\frac{GBestValue) - AverageValue}{GBestValue} \tag{5.13}$$

4. The convergence time for the best value:

$$nTime = 1 - abs(\frac{convergenceTime - minTime}{maxTime - minTime}) \tag{5.14}$$

Table 5.8: Scanned parameters for swarm metaheuristics

Parameters	Description	Value	Range
N	Number of solutions	10	[10, 20]
Iteration Number	Maximum iterations	600	[600, 800]
β	Exploration-exploitation	0.8	[0.7, 0.8]

5.4 Results

5.4.1 Parameter tuning

In this section, the results obtained from the parameterization of the metaheuristics are shown. It should be noted that SCA and Jaya have no necessary parameters for their movements. In Figure 5.6, the results of the first four configurations are shown. Of the four configurations, chart 2 and chart 3 have considerably worse nTime indicators than the other two configurations. Graphs 1, 2, and 3 have similar values for aSolution, wSolution, and bSolution. Therefore 1 has a better performance than the other two. When comparing 1 with 4, we see that nTime is similar, however, 1 is superior in the other indicators, with which the configuration $N = 10$, iteration = 600, and $\beta = 0.8$ was chosen.

5.4.2 Cost minimization metaheuristic comparison

This section aims to describe and analyze the results obtained by the SAMO2, discrete Jaya, and discrete SCA algorithms. For an adequate analysis, descriptive statistics are used together with boxplot visualizations. Additionally, the Kolmogorov-Smirnov-Lilliefors and the signed-rank Wilcoxon statistical tests are used to determine the statistical significance of the results. These tests were chosen according to the statistical methodology shown in Figure 5.7, [251], [252].

In this research work, 30 executions were used. The choice of 30 cases is related to the conditions for the statistical methods to be reliably applicable. Particularly according to [253], in the case of the parametric statistical test $n > 30$ is suggested. On the other hand, in the case of the Wilcoxon test, the minimum value is 15, [254]. However, the value of 30, in the case of non-parametric tests, is widely used in cases of comparison of algorithms in the area of computer science and operations research.

The results of the 30 executions of each of the algorithms are shown in Table 5.9, with the settings selected for the problem of minimizing the cost of the structure. The Cost column corresponds to the minimum value obtained in the execution. Column

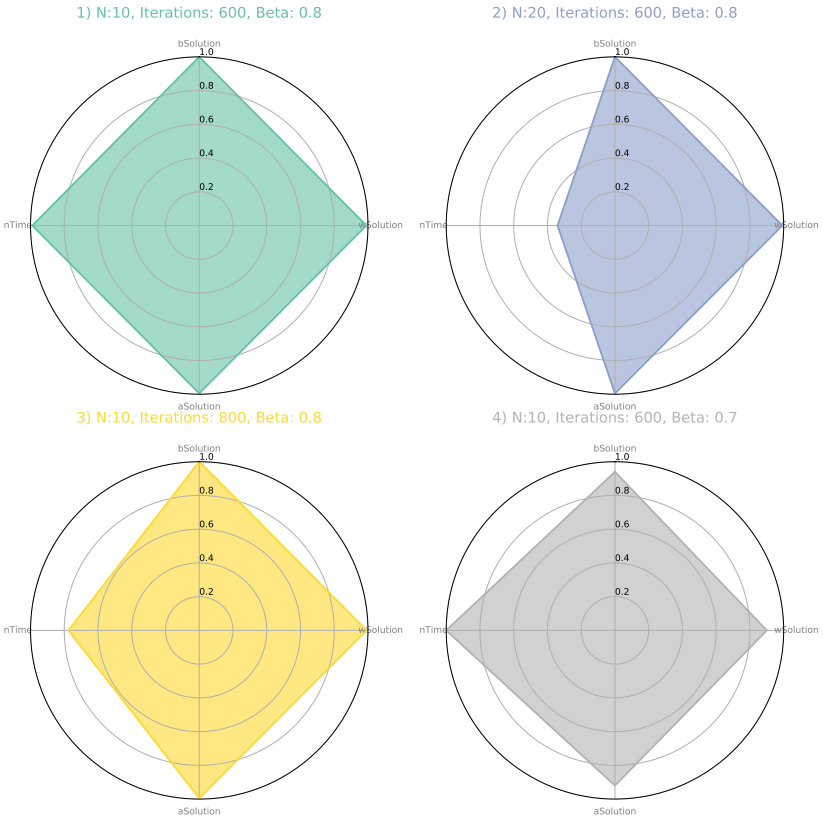

Figure 5.6: Adjustment of swarm parameters by means of radar chart

CO_2 corresponds to the value of emissions of CO_2 for the minimum cost structure obtained. The time corresponds to the time required to obtain the minimum.

When analyzing the table, it can be observed that the best value was obtained with the SAMO2 algorithm with a cost of 3826142 €, followed by the minimum obtained by SCA of 3829666 €. However, on average, SCA is systematically higher than SAMO2, obtaining an average value for the 30 executions of 3850445 €, whereas SAMO2 got 3870302 €. The Jaya algorithm was quite a bit further away with an av-

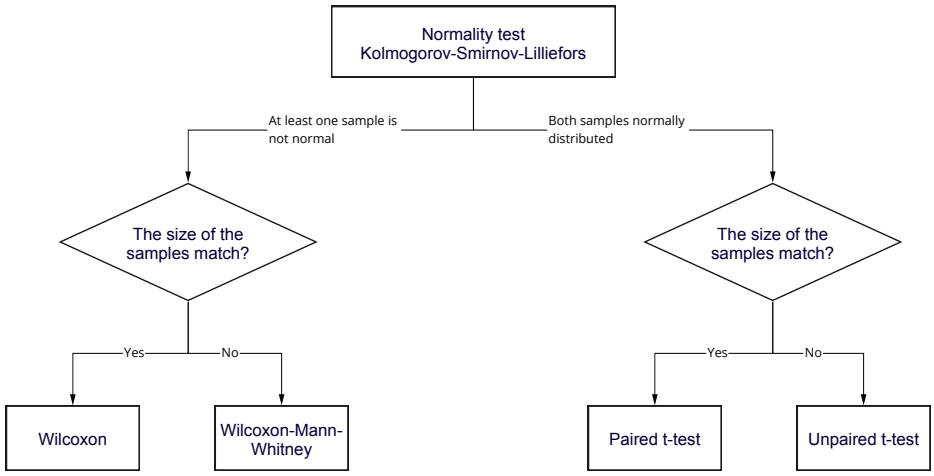

Figure 5.7: Statistical methodology

erage of 4175991 €. When applying the Kolmogorov-Smirnov-Lillefors test and later the Wilcoxon test, it can be seen that the difference between SCA and SAMO2 is significant. In Figure 5.8, it has been compared the cost minimization boxplots obtained by the different algorithms. It has been observed that in the case of SAMO2 and SCA, the interquartile range is very similar; however, SAMO2 has a significant number of outliers. The latter observation reinforces the robustness of SCA concerning SAMO2.

Table 5.9: Cost minimization results for 30 executions of SAMO2, discrete Jaya and discrete SCA algorithms

	SAMO2			Discrete Jaya			Discrete SCA		
Run	**Cost (€)**	**CO_2 (kg)**	**Time(s)**	**Cost (€)**	**CO_2 (kg)**	**Time(s)**	**Cost (€)**	**CO_2 (kg)**	**Time(s)**
1	3829112	9393007	9196	4143961	10114677	7842	3854631	9441993	7497
2	3845663	9422139	7590	4768396	11451567	7010	3841685	9423182	7822
3	3829828	9390570	9687	4274386	9681541	5682	3868348	9487298	7890
4	3834439	9395042	9719	4167039	9494257	7700	3837468	9411814	7635
5	3836721	9393995	9431	4296276	9832819	7863	3863494	9467940	7786
6	3832833	9394394	9198	3966049	9664702	6634	3838032	9396761	7795
7	3837599	9398873	9291	3867355	9439086	6690	3835377	9395270	7318
8	3841418	9408629	9271	3923888	9536557	7945	3839078	9400419	7876
9	3826260	9391263	9226	3942003	9495904	7704	3844805	9422679	7832
10	3837246	9398956	9691	3862458	9465666	5887	3867325	9485202	7880
11	3838964	9399137	9507	4193812	9480247	6545	3833502	9406118	7557
12	3844258	9420046	9669	4507870	10273813	7231	3840298	9419024	7904
13	3840202	9408438	9557	3900545	9469228	6024	3844078	9432582	7509
14	4701903	11582022	9857	3919121	9538184	7932	3848079	9419256	7790
15	4004603	9837622	9957	4191451	10219877	7916	3920211	9618810	7821
16	3837030	9407815	9504	4426445	10272926	7568	3840156	9402993	7886
17	3838077	9398395	9706	3988854	9625319	7738	3851332	9451619	7740
18	3826143	9389610	9794	4628723	10388171	7639	3829666	9398361	7905
19	3836306	9393541	9326	3884798	9425667	7015	3844407	9425169	7902
20	3829965	9397333	9913	4260373	9525527	7995	3853756	9458527	7736
21	3834064	9395196	9591	4704005	11472333	6842	3846266	9424806	7922
22	3838869	9397516	9535	3953660	9626126	7902	3856002	9455145	7502
23	3840493	9410517	9239	4363499	9990653	7275	3858728	9455868	7583
24	3836563	9399930	9618	4589899	10380952	7753	3839780	9410778	7904
25	3833027	9394227	9495	4025218	9846483	3307	3866162	9481381	7730
26	3834233	9397504	9413	4133015	9433096	7848	3853062	9444842	7790
27	3845712	9417868	9566	3889122	9532552	7550	3867166	9474659	7781
28	3832970	9403292	9985	4116324	9418032	7931	3847715	9447151	7552
29	3829559	9389435	8800	4482044	10843764	7022	3844695	9425683	7660
30	3834992	9398076	9775	3909149	9511426	6425	3838057	9417710	7891
average	3870302	9487480	9470	4175991	9881705	**7147**	**3850445**	**9440101**	7747
Wilcoxon p-value	0.012	0.0012		1.92e-06	4.29e-06				

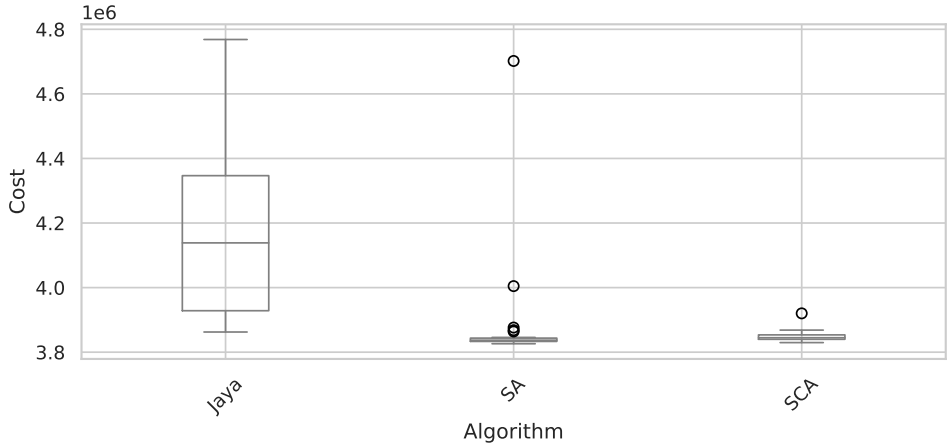

Figure 5.8: Cost boxplots for SAMO2, Jaya, and SCA Algorithms

The computational time required by each algorithm to find the minimum is another interesting variable to analyze. In this case, the best time was obtained by Jaya with a value of 3306, but with very bad values (probably due to the fast convergence of the algorithm). In a comparison between SAMO2 and SCA, it is seen that it consistently performs better in all SCA executions. SCA gets an average time of 7747 seconds and SAMO2 9470 seconds. Additionally, Figure 5.9 shows the histograms of the convergence times for the three algorithms. The SAMO2 histogram is shifted towards higher values, getting the worst performance. In the case of Jaya, a much more dispersed histogram reinforces the possibility of a fast convergence that implies bad results in the optimization. In the case of SCA, a much less dispersed histogram is obtained than the previous ones, with values mainly between 7500 and 7900. Finally, when the emission values associated to cost optimization results are analyzed, a clear correlation is founded between cost and CO_2 optimization. Therefore, the designs minimized by SCA also obtain minimum emission values of CO_2. On average, SCA got emissions of 9440101 and SAMO2 of 9487480 kg of CO_2.

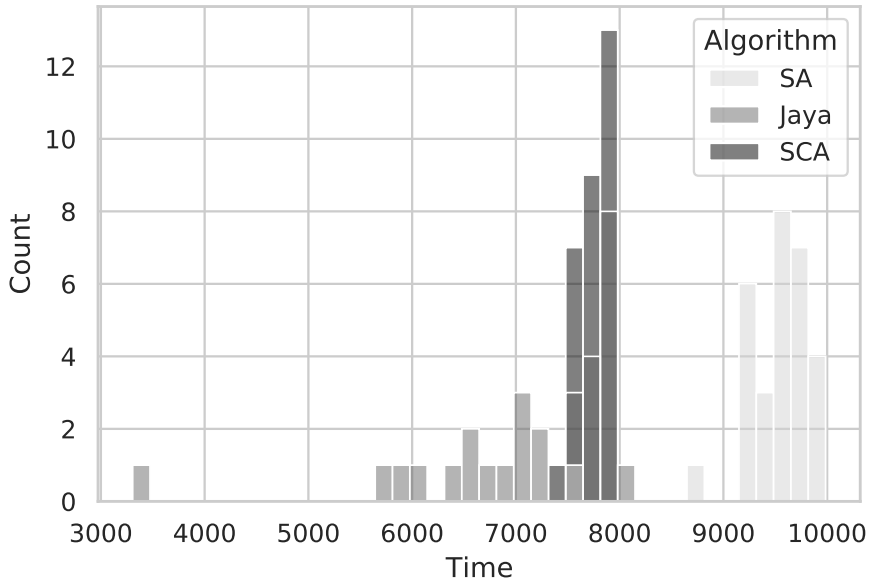

Figure 5.9: Time histogram for SAMO2, Jaya, and SCA Algorithms

The results obtained from cost optimization show that SCA gets the best results in cost and computation time compared with Jaya and SAMO2. Accordingly, SCA results have been considered for the cost optimization analysis. Furthermore, the correlation between cost and CO_2 optimization in these algorithms is consistent with the results obtained in other bridge optimization works. Because of this relationship between both targets, the same algorithm parameters have been chosen to get results for CO_2 optimization.

5.4.3 Insight into the discrete algorithm

This section aims to investigate some features of the procedure given in Algorithm 1. The first attribute to investigate relates to the transfer function application in line 5 of the algorithm. Particularly, it is desired to determine whether the transfer function contributes to the discretization procedure. This is accomplished by replacing the transfer function with a uniform random operator that generates values between 0 and 1. In addition, line 8 of the algorithm configures two values for $dimSolProbability$. The first value is set to 0.5 ($Random0.5$), corresponding to a

50% chance of executing a transition. The second value is set to 0.7 ($Random0.3$), corresponding to a 30% chance of executing a transition. The results are presented in Table 5.10. The table shows that, on average, the values obtained by Discrete SCA are higher than those obtained by the random operator for its different parameters. In particular, it was 0.75% higher than Random 0.3 and 0.86% higher than Random 0.5. The same situation occurs when analyzing the maximums; in the case of the Random operator, these are greater than in the case of SCA. The standard deviation also shows a considerable difference, where the dispersion of the random operator has values close to 55,000, and in the case of SCA, it is 17,048. Finally, the execution times are quite similar in all cases.

A second experiment involves the parameter $beta$ used in line 9 of the Algorithm 1. This parameter has to do with exploration and exploitation. If the criterion is met, the update considers the best solution; otherwise, a random update is carried out. In addition to the value used (0.8), the values 0.5 and 0.3 were also investigated. The outcomes are shown in Table 5.11. According to the averages, the parameter with the best outcome was 0.8. This holds true when examining the maximum. In the event of the minimum, SCA 0.3 earned the best value, but SCA 0.8 was not far behind. Another notable result is the value of the standard deviation, which is significantly lower for SCA 0.8, indicating higher stability in locating the optimal ones. This is also associated with the convergence times. In the case of SCA 0.5 and 0.3 are considerably less than 0.8, but their dispersion is greater. All of the above points to a decrease in the stability of the algorithm when using these parameters.

Table 5.10: Cost minimization results for 30 executions of Random 0.3, Random 0.5 and discrete SCA algorithms

	Random 0.5		Random 0.3		Discrete SCA	
Run	**Cost**	**Time (s)**	**Cost**	**Time (s)**	**Cost**	**Time (s)**
1	3841686	7545	3854631	7435	3854631	7497
2	3838057	8121	3841686	7893	3841685	7822
3	3856002	6979	3868348	7113	3868348	7890
4	4004604	7985	4041118	8001	3837468	7635
5	3837585	6922	3863494	6893	3863494	7786
6	3920211	8021	4009757	8021	3838032	7795
7	3863494	7215	3835377	7325	3835377	7318
8	4004604	7498	3973917	7568	3839078	7876
9	3920211	8210	3844806	7901	3844805	7832
10	3867325	7646	3938024	7924	3867325	7880
11	3920211	7645	3912499	7235	3833502	7557
12	3847798	8024	3840298	8024	3840298	7904
13	3844078	7644	3847990	7701	3844078	7509
14	3848079	7891	3844078	7903	3848079	7790
15	3927551	7798	3920211	7923	3920211	7821
16	3853756	7234	3847713	8002	3840156	7886
17	3854631	8102	3851332	8115	3851332	7740
18	4004604	7744	3829666	6903	3829666	7905
19	3844695	7894	3844407	7745	3844407	7902
20	3840156	7745	3853756	7801	3853756	7736
21	3858728	7875	3846266	7932	3846266	7922
22	3846266	7534	3856002	7345	3856002	7502
23	3868348	7655	3858728	7792	3858728	7583
24	3853062	7943	3930520	8002	3839780	7904
25	4004604	7653	3866162	7755	3866162	7730
26	3920211	7897	3853062	7932	3853062	7790
27	3844407	7746	3867166	7743	3867166	7781
28	3847874	7653	3847715	7510	3847715	7552
29	3851332	7695	3844695	7655	3844695	7660
30	3867166	7894	3938024	8032	3838057	7891
Average	3883378	7714	3879048	7704	3850445	7747
Max	4004604	8210	4041118	8115	3920211	7922
Min	3837585	6922	3829666	6893	3829666	7318
std	55639	312	54164	340	17048	159

Table 5.11: Cost minimization results for 30 executions of Discrete SCA 0.8, Discrete SCA 0.5 and Discrete SCA 0.3 algorithms

	Discrete SCA 0.8		**Discrete SCA 0.5**		**Discrete SCA 0.3**	
Run	**Cost**	**Time (s)**	**Cost**	**Time(s)**	**Cost**	**Time(s)**
1	3854631	7497	3843524	5676	3852498	5621
2	3841685	7822	3845599	5894	3851261	4947
3	3868348	7890	3832283	6109	3859721	5076
4	3837468	7635	3829373	5964	3854194	5938
5	3863494	7786	3840952	5826	3870990	5367
6	3838032	7795	3839057	6028	3849196	3840
7	3835377	7318	3849643	5444	3839412	4984
8	3839078	7876	3839271	5470	3850429	3134
9	3844805	7832	3839664	6062	3857432	5189
10	3867325	7880	3840787	5122	3847051	5963
11	3833502	7557	3845540	2349	3851258	5992
12	3840298	7904	3844938	5631	3876165	5515
13	3844078	7509	3834878	5901	3861690	5767
14	3848079	7790	3846365	5554	3852585	4235
15	3920211	7821	3833527	4493	3859730	3051
16	3840156	7886	3827056	5701	4056478	4554
17	3851332	7740	4029735	6070	3840542	6077
18	3829666	7905	3846775	5445	3855213	5681
19	3844407	7902	3834013	5946	3859171	5079
20	3853756	7736	3838546	5027	3841768	5056
21	3846266	7922	3838290	5659	3853698	4084
22	3856002	7502	3833359	4896	3875181	4084
23	3858728	7583	3846665	5643	3844489	2744
24	3839780	7904	3849429	5611	3858573	5245
25	3866162	7730	3841566	5998	3845703	6115
26	3853062	7790	3830238	6047	3842629	4220
27	3867166	7781	3856881	6057	3840573	5631
28	3847715	7552	4158713	6045	3862079	5616
29	3844695	7660	3832127	5833	3843622	3737
30	3838057	7891	3848890	4531	3864325	4549
Average	3850445	7747	3862589	5834	3865589	5170
Max	3920211	7922	4158713	6109	4056478	6115
Min	3829666	7318	3827056	2349	3839412	2744
std	17048	159	66973	746	38284	997

5.4.4 Optimization results

This work has compared both cost and CO_2 single objective optimizations of a continuous box-girder steel-concrete composite bridge of 220 m with three spans divided in 60, 100 and 60 m length. As stated earlier, and backed by data obtained from the algorithm comparison, the results correspond to SCA optimization. In total, 30 algorithm runs have been carried out to perform a statistical analysis of the results obtained. To get results from CO_2 emission, the same procedure as in cost optimization has been used while considering CO_2 emissions as the objective function. Because the optimization problem is similar, the same algorithm parameters have been applied for the CO_2 target.

This section gives the bridge variables values obtained considering cost and CO_2 as two single objective optimizations while briefly comparing both results. Furthermore, cost and CO_2 relation for both optimizations is shown in Figure 5.16, while in Figures 5.14 structural and reinforcement steel amounts have been shown for both cost and CO_2 optimizations best results. In section 5.5, a more extensive discussion of these results is provided.

The first results are related to the material's resistance, reinforcement, and shear connector diameter. For cost optimization results, concrete compressive strength (f_{ck}) and yield stress for structural steel (f_{yk}) correspond to 25 and 275 MPa for all individuals. However, for CO_2 optimization, the value of steel yield (f_{yk}) shows greater dispersion. The best individual has a 355 MPa value, as can be seen in Table 5.12. Reinforcement diameters (ϕ_{base}, ϕ_{r_1} and ϕ_{r_2}) obtained from optimization correspond to 6 mm for both base and reinforcement layers. Consequently, optimization gets three reinforcement layers on the top slab. Regarding shear connectors, as in reinforcement bars, the optimization gets both lowest diameter (ϕ_{sc}) and connector length (h_{sc}). For CO_2 the optimization results show the same results.

Once the materials have been defined, the results from the geometrical variables are obtained. Steel beam depth (h_b), web angle (α_w) and distances between transverse stiffeners (d_{st}) and diaphragms (d_{sd}) are shown in Figure 5.10. It should be emphasized that the thickness of the upper (h_s) and lower (h_{s_2}) concrete slabs gives the same result for both optimizations and takes the minimum possible value of 0.20 and 0.15 m, respectively. Meanwhile, CO_2 optimization gets higher beam depths (h_b), and stiffener (d_{st}) and diaphragm (d_{sd}) distance values than cost. The next variable values are related to the webs and flanges of the cross section. As can be seen in Figure 5.11, CO_2 takes a higher range of values than cost for both width (b_{f_1}) and thickness (t_{f_1}) of the upper flanges; while for webs (t_w) and lower flange (t_{f_2}), thickness gets lower values.

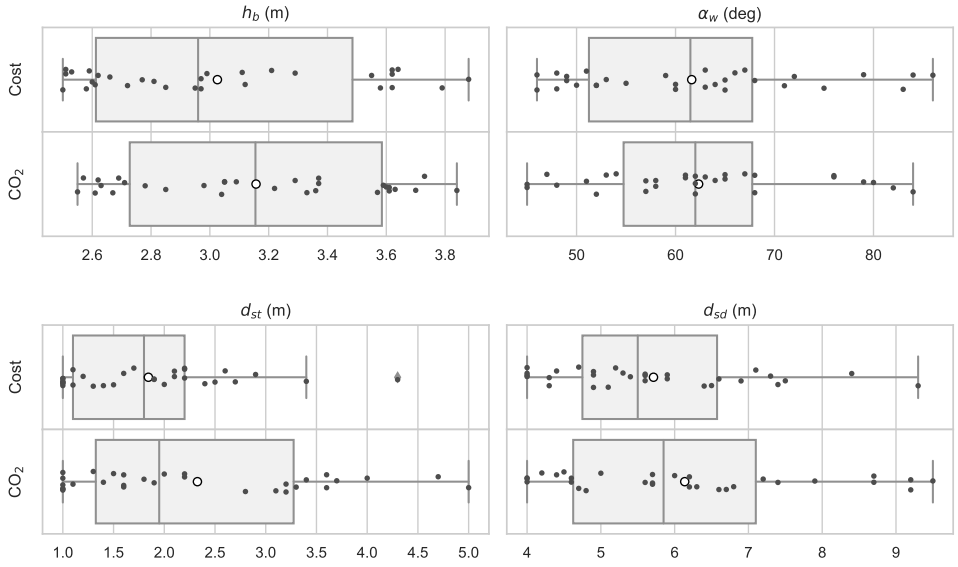

Figure 5.10: Cross section geometrical variables for cost and CO_2 optimization

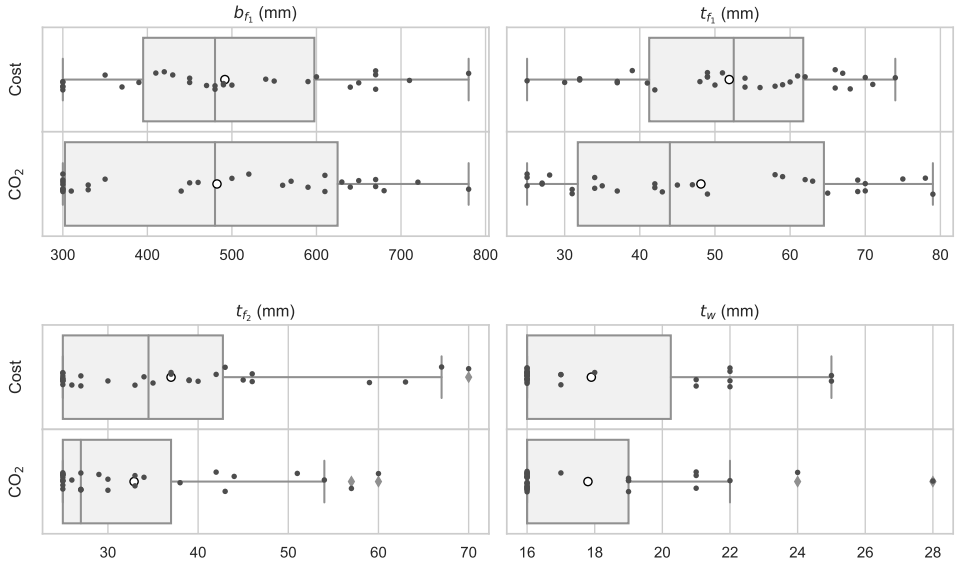

Figure 5.11: Flanges and web variables for cost and CO_2 optimization

As stated in Section 5.2.2, and in accordance with Figure 5.1, the cross-section of this optimization problem involves the inclusion of four cells: two uppers and two lower. The aim of these cells is to improve structural cross-section behavior, which allows better values of the objective function to be obtained. Figure 5.12 shows the results obtained for cell variables (h_{c_1}, t_{c_1}, h_{c_2}, t_{c_2}, b_{c_2}). It should be noted that the algorithm is left to eliminate these cells by allowing them to take a null value in variables that define its geometry. As can be seen in Figure 5.12, both optimization objectives get values larger than zero for cell variables. It can be observed that CO_2 optimization gives in average lower values for upper cell height (h_{c_1}) and thickness (t_{c_1}). Meanwhile, for lower cells, although the average value of the results obtained is similar, the cost optimization gives a wider range of values for variables of this element (h_{c_2}, t_{c_2}, b_{c_2}).

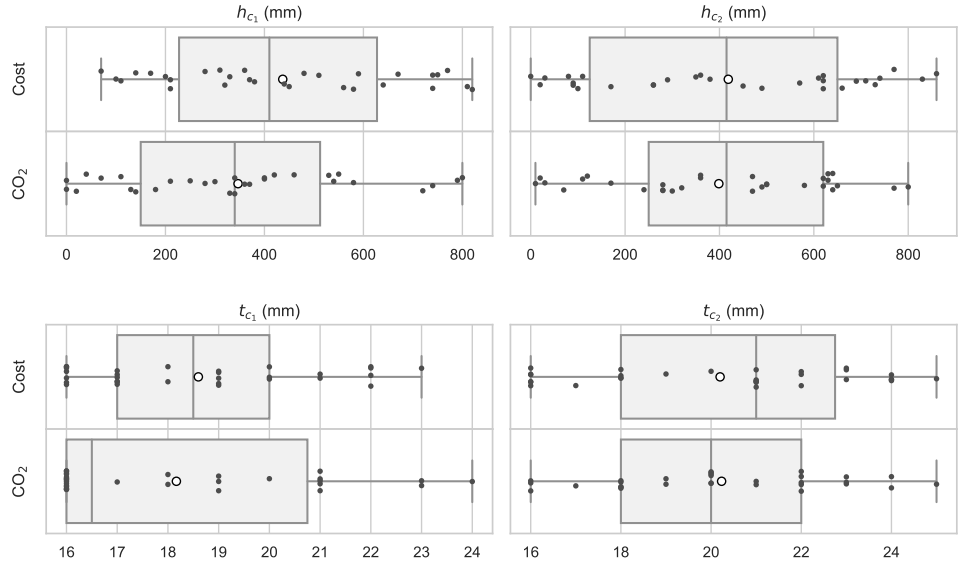

Figure 5.12: Cell variables results for cost and CO_2 optimization

Figure 5.13 gives the floor beam variables results. As can be seen in this figure, and consequently with results in Figure 5.10, CO_2 optimization gives higher values of depths (h_{fb}) and widths (b_{fb}) due to the higher distances between diaphragm sections, where these floor beams are materialized. Against that, thicknesses ($t_{f_{fb}}$, $t_{w_{fb}}$) values are similar in both optimizations.

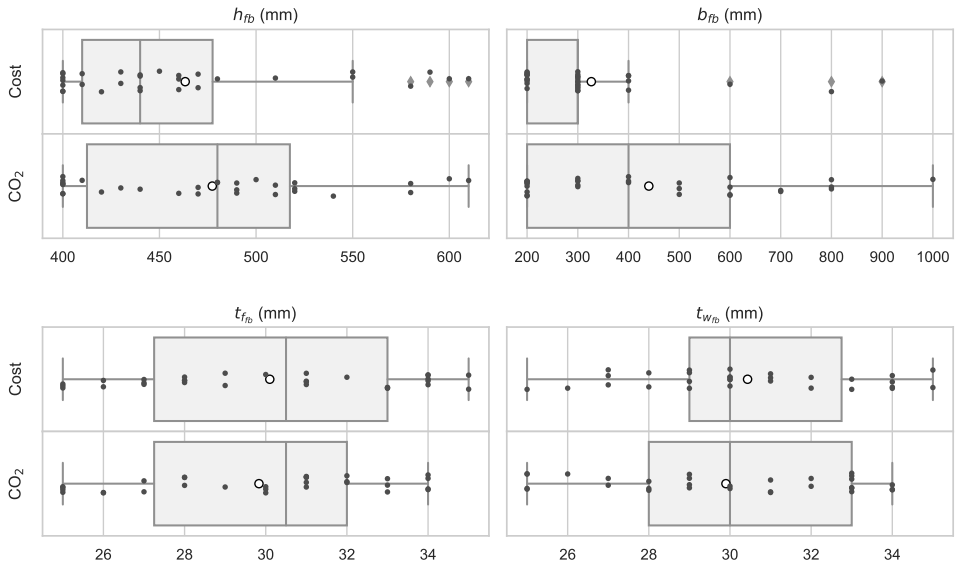

Figure 5.13: Floor beam variables results for cost and CO_2 optimization

Finally, the results from material amounts and cost are represented in Figures 5.14 and 5.16, respectively. The first figure shows that the cost target function gives higher values for rolled steel and lower values for reinforcement steel in slabs. However, CO_2 optimization gives the opposite result. The first part of Figure 5.14 gives boxplots that show the values reached by the 30 individuals obtained from the algorithm runs. In the second part, the trajectory of steel amounts has been represented for the best individuals obtained from cost and CO_2 optimization. Regarding the relationship between cost and CO_2 obtained in Figure 5.16, it can be seen that there is a clear relationship between both criteria for cost optimization. For this case, a straight line with equation $CO_2 = 2.5144 \cdot Cost - 241,642$ with a $R^2 = 0.98$ expresses a good fit of the straight line. By applying cost optimization for each euro reduced, a reduction of 2.5144 kg of CO_2 is obtained by applying heuristic optimization techniques. In contrast, for CO_2 optimization for the same cost, there is a large dispersion between the CO_2 values obtained. This difference between cost and CO_2 objective functions optimization is shown in figure 5.15. In this figure, cost and CO_2 trajectories have been plotted for the best individual of both optimization objectives. It can be seen that when optimizing cost, both cost and CO_2 amounts decreases following the same trend. However, when the objective function is CO_2 , cost have a high variation during

the optimization getting a clear difference in terms of cost at the end. Furthermore, in Table 5.13 the lowest values for ULS and SLS constraints have been shown.

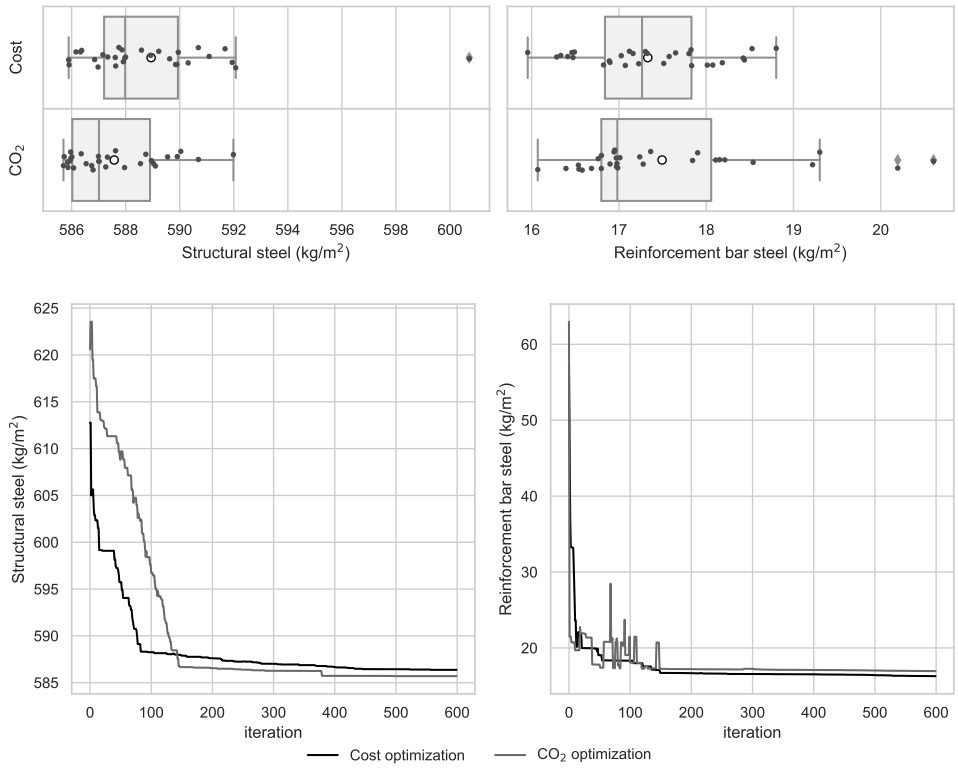

Figure 5.14: Reinforcement bars and structural steel amounts for both optimization objectives

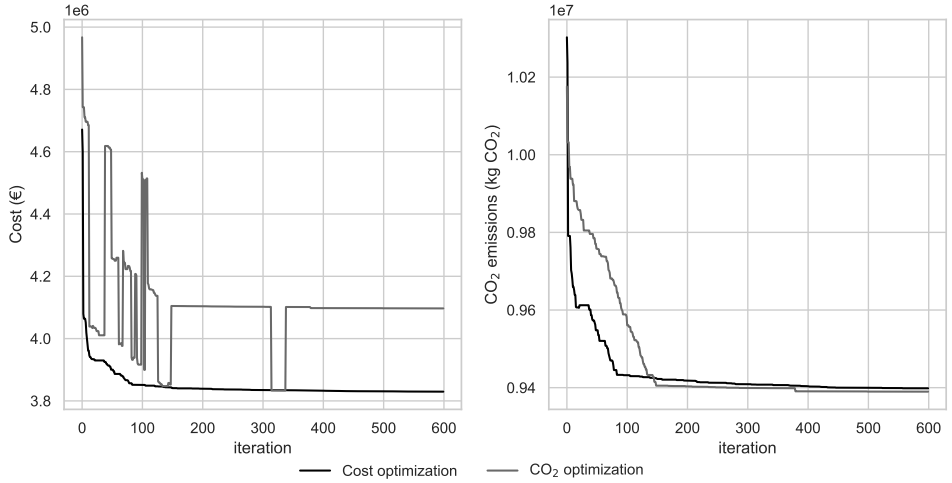

Figure 5.15: Cost and CO_2 variation during the optimization process for both optimization objective functions

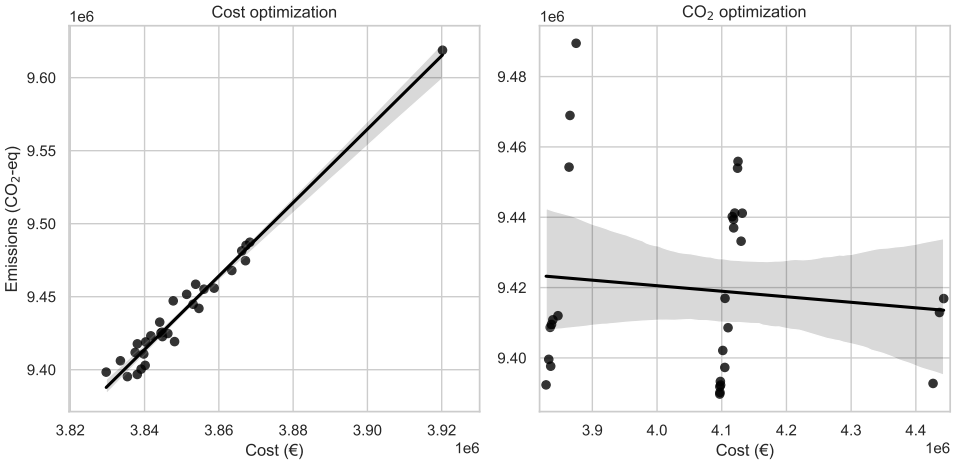

Figure 5.16: Cost and CO_2 correlation considering both optimization objectives

Table 5.12: Design variables results for best individual and minimum and maximum values

		Cost optimization			CO_2 optimization		
Variables	**Unit**	**Best**	**Min**	**Max**	**Best**	**Min**	**Max**
b	m	7	7	7.16	7	7	7
α_w	deg	63	46	86	65	45	84
h_s	mm	200	200	200	200	200	200
h_b	cm	312	250	388	298	255	384
h_{fb}	mm	430	400	610	400	400	610
t_{f_1}	mm	70	25	74	34	25	79
b_{f_1}	mm	780	300	780	350	300	780
h_{c_1}	mm	440	70	820	420	0	800
t_{c_1}	mm	21	16	23	16	16	24
t_w	mm	16	16	25	16	16	28
h_{c_2}	mm	80	0	860	630	10	800
t_{c_2}	mm	16	16	25	20	16	25
b_{c_2}	mm	310	300	700	300	300	610
t_{f_2}	mm	25	25	70	27	25	60
h_{s_2}	mm	150	150	180	150	150	240
$n_{s_{f_2}}$	u	0	0	0	0	0	0
d_{st}	m	1	1	4.3	1.6	1	5
d_{sd}	m	4.3	4	9.3	4.7	4	9.5
b_{fb}	mm	300	200	900	200	200	1000
$t_{f_{fb}}$	mm	28	25	35	28	25	34
$t_{w_{fb}}$	mm	27	25	35	31	25	34
n_{r_1}	u	200	200	439	259	200	446
n_{r_2}	u	337	200	431	403	200	424
ϕ_{base}	mm	6	6	8	6	6	6
ϕ_{r_1}	mm	6	6	6	6	6	6
ϕ_{r_2}	mm	6	6	6	6	6	6
${s_{f_2}}^*$	mm	270	200	600	330	200	600
${s_w}^*$	mm	400	200	600	200	200	550
${s_t}^*$	mm	360	200	550	500	200	600
h_{sc}	mm	100	100	100	100	100	100
ϕ_{sc}	mm	16	16	22	16	16	22
f_{ck}	MPa	25	25	25	25	25	25
f_{yk}	MPa	275	275	275	355	275	460
f_{sk}	MPa	500	500	500	500	500	500

* Values of the standard series of IPE profiles [239]

Note: Min and Max correspond to the maximum and minimum values obtained. Best correspond to the value obtained for the best individual.

Table 5.13: Lower checking coefficients values obtained from for both cost and CO_2 optimization best individuals

Contraints	Cost	CO_2
ULS		
Flexure	1.132	1.476
Flexure-shear interaction	1.155	-
SLS		
Stress in steel	1.768	1.831
Stress in concrete	1.817	1.793

Note: This checking coefficients correspond to the expression that compares the design stresses and the resistant ones defined in equation 5.3

5.5 Discussion

In this section, the results shown in section 5.4.4 will be discussed. These results have been compared with earlier optimization studies of [97] and [109], where box-girder SCCB has been optimized. As can be seen in Table 5.12, the concrete strength (f_{ck}) obtained from both cost, and CO_2 optimizations is 25 MPa. This concrete strength value is a result of the high inertia of the resistant section in compressed zones that make the concrete compression lower than the strength limit defined by regulations [26], [238]. For steel, the value obtained by cost optimization is unusual. For structural steel in bridges, the expected value is 355 MPa, as in [97]. This reduction in yield stress (f_{yk}) makes a difference between a traditional design between a cost optimization design. Meanwhile, [109] used 275 MPa steel for the bridge solution. Moreover, if the CO_2 optimization is analyzed, it can be observed that the best individual takes a 355 MPa value for yield stress (f_{yk}). This is produced because there is no difference in CO_2 emissions between different yield stress; consequently, taking higher resistance steel does not increase the value of the objective function. This higher value allows to use less material due to the higher steel resistance. Regarding reinforcing bars steel, it can be seen that the results given for both optimization objectives are yield stress (f_{sk}) of 500 MPa, which is the usual value for concrete structures [25], [242]. Continuing with reinforcing bar analysis, it can be seen that the optimization always gets a 6 mm diameter. The program can add up to three layers of reinforcement to the top slab. The optimization algorithm uses this possibility to adjust as far as possible the reinforcing needs, decreasing the bar diameter as a consequence. For shear connectors, it can be seen that the program takes the lowest

boundary values for both heights (h_{sc}) and diameter (ϕ_{sc}) in cost and CO_2 emissions optimization of best individuals.

Next is the analysis of the main cross-section variables. It can be seen in Section 5.4.4 that cost optimization, in general, gets lower deck depth values compared with CO_2 optimization. Moreover, the CO_2 best optimization individual gets a greater web angle (α_w), which leads to a higher value of the bottom flange, obtaining a higher value of steel amount. Regarding top flanges, the results in Figure 5.11 are confirmed in Table 5.12. CO_2 obtains lower values of width (b_{f_1}), and it is observed that this plate thickness (t_{f_1}) also takes a lower value than cost.

Table 5.14: Cost and emissions for the best individual of both optimization objectives

		Cost optimizatión			CO_2 optimization		
Material	**Unit**	**Measurement**	**Cost (€)**	**CO_2 (kg)**	**Measurement**	**Cost**	**CO_2**
Concrete	m^3	528	46918 (1.2%)	135516 (1.4%)	528	46918 (1.1%)	135516 (1.4%)
Structural Steel	kg	2064029	3550130 (92.7%)	8937246 (95.1%)	2061655	3814062 (93.1%)	8926966 (95.1%)
Reinforcement Steel	kg	57328	80259 (2.1%)	40130 (0.4%)	59668	83535 (2.0%)	41768 (0.4%)
		Total	3829666	9398360	**Total**	4096922	9389721

One of the aims of this study has been to analyze if cells added to the cross-section help reduce costs and emissions. It can be stated that this is true. The values from the cell variables show that their values are not zero in every case. Therefore, cells improve the structural behavior of the cross-section because they allow buckling of the plates to be controlled by reducing the distances between elements without stiffening. These elements allows to add a more resistant section and become longitudinal stiffening elements. The opposite occurs for bottom flange longitudinal stiffeners. If the values shown in Table 5.12 are observed, then, in every case the value of this element's number ($n_{s_{f_2}}$) takes the value of zero. This may lead to a contradiction because these elements prevent the lower flange from buckling when compressed (i.e., in the support areas on piles). But if the results of this research are compared with [109], then it can be seen that in his study, he obtains the same result. In this optimization case, it is logical to obtain this result because, in sections subjected to sagging, a lower slab materializes that works in compression and do not allow the plate's buckling. Furthermore, in hogging sections (i.e., in span centers), this plate's main effort is tension and, therefore, buckling will not occur. Moreover, the center part of the bottom flanges is not taken into account for the strength calculation of the section due to the shear lag reductions imposed by the standards [26] used for the calculation. In [97], where a topological optimization is carried out, the material in these bottom flange areas is removed because it exceeds the maximum working stress.

Finally, material amounts and objective function values obtained have been analyzed. The material summary results are shown in Table 5.15, while cost and CO_2

emissions are in Table 5.14. The relation between both objective functions have been represented in Figure 5.16. As stated in Section 5.4, there is a clear relationship between cost and CO_2 optimization when choosing cost as the objective function, while on the contrary, it is not. This is due to the equality between different steel grade emissions in data obtained from BEDEC database [207]. This allows the CO_2 optimization process to obtain different yield stress values for structural steel without producing major variations in its target function, but on the higher ones in terms of cost. This contrast with related traditional concrete bridges optimization works [166], [175] where it is found that both cost and CO_2 optimization leads to the optimization of the other.

Table 5.15: Material amount summary for both optimization objectives

		Cost optimization			**CO_2 optimization**		
Material	**Unit**	**Best**	**Min**	**Max**	**Best**	**Min**	**Max**
Concrete	m^3	528	528	528	528	528	528
Structural Steel	kg	2064029	2062333	2114520	2061655	2061656	2083789
Reinforcement Steel	kg	57328	56161	66184	59668	56566	72530
Cost	€	3829666	3829666	3920211	4096922	3828450	4443057
CO_2	kg	9398360	9395269	9618810	9389721	9389721	9489469

Note: Min and Max correspond to the maximum and minimum values obtained. Best correspond to the value obtained for the best individual.

5.6 Conclusions

In this article, the design of a Steel-Concrete Composite Bridge has been considered. This design has considered the analysis of costs and emissions of CO_2 . The proposed bridge considers 34 discrete variables that correspond to $1.38 \cdot 10^{46}$ combinations. A discretization method was proposed through the use of transfer functions, which was applied to the SCA and Jaya metaheuristics. To evaluate the method, they were compared with SAMO2, which has previously solved structural problems efficiently. The results showed that discrete SCA was the one that obtained the best results both in the optimization values and in the execution times. SCA was 24.5% faster than SAMO2 and in the case of cost optimization, considering the average, SCA obtained 0.5% lower values than SAMO2.

Subsequently, SCA was used to compare cost and CO_2 optimizations. Regarding the results obtained, it was observed that in both optimizations bottom flange stiffeners has been removed due to the double composite action of concrete slabs on supports. Furthermore, the use of inner cells in the bridge cross-section has been considered. These cells improve the section stress resistances and reduce the distance between non-stiffened areas in steel plates. In addition, there is a clear relationship between

cost and CO_2 optimization. In this case, it can be observed that one euro decrease in cost translates into 2.5144 kg of CO_2 reduction when applying heuristic optimization techniques.

Chapter 6

Discrete swarm intelligence optimization algorithms applied to steel-concrete composite bridges

Authors:	D. Martínez-Muñoz , J. García, J.V. Martí, and V. Yepes
Status:	Manuscript published
Journal:	Engineering Structures, 266:114607
Year:	2022
DOI:	10.1016/j.engstruct.2022.114607
JCR IF (2021):	5.582

JCR Category	Ranking	Quartile
Engineering, Civil	20/138	Q1

Presentation:	Post-print (author version)

Abstract

Composite bridge optimization might be challenging because of the significant number of variables involved in the problem. The optimization of a box-girder steel–concrete composite bridge was done in this study with cost and CO_2 emissions as objective functions. Given this challenge, this study proposes a hybrid algorithm that integrates the unsupervised learning technique of k-means with continuous swarm intelligence metaheuristics to strengthen the latter's performance. In particular, the metaheuristics sine-cosine and cuckoo search are discretized. The contribution of the k-means operator regarding the quality of the solutions obtained is studied. First, random operators are designed to use transfer functions later to evaluate and compare the performances. Additionally, to have another point of comparison, a version of simulated annealing was adapted, which has solved related optimization problems efficiently. The results show that our hybrid proposal outperforms the different algorithms designed.

Keywords: combinatorial optimization; bridge; metaheuristics; composite structures; k-means

6.1 Introduction

Bridge optimization is an interesting problem to address both because of the technical challenges that the problem presents and because of the potential applications in reducing costs, CO_2 emissions, and energy consumption. The technical difficulties are related to the large number of discrete variables required in its design and the complex objective functions and restrictions that these must satisfy [94]. Due to the more significant number of variables necessary for their design, Steel-Concrete Composite Bridges (SCCB) present a considerable challenge. According to the SCCB literature, they can be classified into three groups according to their cross-section: Plate-beam, Twin-Girders, and Box-Girder [25], and their behavior are different between these types.

Due to the type of objective function and the constraints used in structural design problems, metaheuristics (MH) have had good results in optimizing structures. These techniques have been applied in steel structures [255], arch bridges [256], [257] or reinforced concrete columns [258] among others. In some studies, metaheuristic has been applied as first optimization step for topological optimization [259] due to the computational cost of this last method [97]. In particular, metaheuristic techniques have performed well in addressing complex SCCBs optimization [189]. For example, in [109] a discrete harmony search algorithm was proposed and applied to the design

of multi-span composite box girder bridges. In the article, the authors obtained a 15 % reduction of materials when compared to a traditional design. In [103], a two-stage based optimization methodology is developed for the design of simply supported steel-concrete composite I-girder bridges. In the first stage, a simplified structural model based on expert criteria is developed and used with the aim of providing a starting point for the local search. In the second stage, a search group algorithm is chosen based on statistical analysis. The proposed method was shown to reduce the structural cost by up to 9.17%. Three metaheuristic algorithms were studied in [110] and used for reaching the optimal design of steel-concrete composite i-girder bridges. The algorithms used were Collision Bodies (CBO), Collision Body Enhanced Optimization (ECBO), and Vibration Particle System (VPS). Among the results, it was obtained that the final optimized design does not need longitudinal stiffeners.

Despite the excellent performance of metaheuristics and the large size of many combinatorial problems, the strengthening of metaheuristics is also necessary. Among the different strategies to strengthen the metaheuristics, the hybrid methods have stood out. Several of the most frequently utilized hybridization techniques, include *hybrid heuristic*, [260], where different metaheuristic algorithms are combined to enhance their capabilities. *Mateheuristics*, [261], where mathematical programming methods are integrated with metaheuristics techniques. *Simheuristics*, [262], which encompass a combination of simulations with metaheuristic modeling.

Metaheuristics generate important ancillary data in the solution search process, which can be exploited by machine learning methods. This opens a line of research in which machine learning techniques can be integrated into metaheuristic algorithms to strengthen the performance of the latter.

When searching for integration types in which machine learning techniques improve the performance of metaheuristic algorithms, three main categories are found. Low-level integrations, high-level integrations, and optimization problems [263], [264]. In the case of the hybrid algorithm proposed in this article, the type of integration designed is a low-level integration. The low-level integrations involve local search operators, population initiation, binarization, parameter control, in which ML approaches improve particular operators of the MH algorithm. For example in parameter tuning, in [265], an iterated racing method was employed; a reset mechanism was combined with an elitist procedure (to assure the optimal configuration), and the use of a truncated sampling distribution to allow for automated parameter setting. Decision trees were utilized in [266] to modify particular parameters in the traveling salesman problem. Compared to fixed parameter values, the decision tree technique improved the quality of the solutions and the computing time. Another case of low-level integration is used to initialize solutions. For the shop scheduling problem [267], decision trees were utilized to produce early solutions for new instances, in conjunction with Op-

position Based Learning (OBL), to begin complementary solutions. Reinforcement Learning (RL) and other approaches can also be utilized to create solutions. In these situations, the solution building may be thought of as a series of additions of decisions, for which an RL algorithm can be trained. For example, a Deep Q-network was constructed and utilized for the optimization of the Job-Shop Scheduling Problem [268]. Similarly, in [269], transfer learning approaches were utilized to generate initial solutions using three evolutionary multi-objective algorithms and applied to 12 benchmark functions. Finally, another successful application of low-level integration has been used to generate binary versions of algorithms that work on continuous spaces.

Another essential field of study is the creation of binary versions of algorithms that function in continuous areas naturally. There are some examples of ML and metaheuristics working together in this field. The K-means approach was utilized to build binary versions of the cuckoo search algorithm (CS) and used to the matrix covering problem in [270]. For the multidimensional knapsack problem, in [271] a hybrid algorithm using k-means as the binarization method and KNN as the local search operator is proposed. The hybridization between metaheuristic techniques with the aim of improving the convergence or quality of the solutions is another interesting line of low-level integration. In [272], the hybridization of hybrid metaheuristic algorithms was proposed with the aim of addressing the optimal dimensioning of steel beam structures with numerous discrete variables. The numerical results indicate that the hybrid algorithm of adaptive dimensional search and exponential big bang-big crunch is the most promising of the techniques investigated. In [273], it is integrated the convergence curve of each subsequent execution of the algorithm in relation to the information gained from prior executions. It is monitored at specified times during each subsequent execution, referred to as the solution monitoring period. The solution monitoring period is chosen in such a way that each run allows the algorithm to explore the search space in order to increase the quality of the solution, while also periodically forcing the algorithm to return to the most promising prior visit. If it is unable to improve the solution after a specified number of iterations, it will terminate. Numerical investigations with tough test examples containing up to 354 design variables reveal that, in general, the proposed approach improves the solution quality and the robustness or stability of the outcomes in metaheuristic structure optimization.

Following this last line of generating binary versions to efficiently solve binary optimization problems. In this article, the integration method has been adapted to address discrete problems. In particular, a discrete hybrid algorithm is proposed. This algorithm incorporates the k-means technique into the discretization solution phase

of continuous swarm intelligence metaheuristics. The contribution of this work includes:

- In this study, a cost, and CO_2 emissions optimization of a 60-100-60 three-span single box-girder steel-concrete composite bridge has been performed.
- It should be noted that it considers 35 design variables on average 55 possible choices for each variable, which implies a computationally demanding structure.
- A discrete hybrid k-means swarm intelligence algorithm is proposed, and the contribution of the k-means technique to the robustness of the algorithm is studied. In particular, it should be noted that in previous works [250], [271], k-means has been used to solve binary optimization problems, that is, whether the variable is present or not. In the optimization developed in this article, the technique was adapted to allow more than two states for each of the variables.
- The results of the hybrid algorithm are compared with discrete simulated annealing that has been efficient in solving related problems [173], in addition to considering the comparison with algorithms that perform discretization through transfer functions that are frequently used to binarize or discretize solutions [274].

A brief content structure of the following sections: In Section 6.2, the box-girder steel-concrete composite bridge problem is detailed. Later, in Section 6.3, the discrete k-means swarm intelligence algorithm is developed. Our numerical experiments and comparisons are detailed in Section 6.4. Finally, in Section 6.5, the conclusions and future lines of research are discussed.

6.2 The Optimization problem and computational model

This section aims to define and detail the optimization problem. In the case of bridges, there are different objective functions to be minimized, among which there is a particular interest in the costs of the bridge and the CO_2 emissions released in the manufacture of its materials. In this work, two mono-objective functions are defined. The first shows the bridge's overall cost, which is formalized in Equation 6.1 and is calculated by multiplying the unit cost of each material c_i, multiplied by the units used, m_i. In the case of CO_2 emissions, the calculation is similar to the previous one, with the difference that instead of considering cost, the emissions e_i considers cradle-to-gate analysis for each unit of material i multiplied by the amount of material i used. The emissions calculation is formalized in Equation 6.2. For the cost

Table 6.1: Cost and CO_2 emission values

Unit	Cost (€)	Emissions (kg of CO_2)
m^3 of concrete C25/30	88.86	256.66
m^3 of concrete C30/37	97.80	277.72
m^3 of concrete C35/45	101.03	278.04
m^3 of concrete C40/50	104.08	278.04
m^2 of precast pre-slab	27.10	54.98
kg of steel B400S	1.40	0.70
kg of steel B500S	1.42	0.70
kg of rolled steel S275	1.72	4.33
kg of rolled steel S355	1.85	4.33
kg of rolled steel S460	2.01	4.33
kg of shear-connector steel	1.70	2.8

function, the values from Table 6.1 are used, which were obtained from the Construction Technology Institute from Catalonia by the BEDEC database [207]. Finally, the bridge design process is subject to constraints imposed by expert recommendations and regulations related to the standard. Generically, these are shown in Equation 6.3.

$$C(\vec{x}) = \sum_{i=1}^{n} c_i \cdot m_i(\vec{x}) \tag{6.1}$$

$$E(\vec{x}) = \sum_{i=1}^{n} e_i \cdot m_i(\vec{x}) \tag{6.2}$$

$$G(\vec{x}) \leq 0 \tag{6.3}$$

For the description of the problem, the variables, parameters, and constraints of the problem will be considered. In the case of variables, they correspond to the values modified in the optimization procedure to achieve the optimum. In the case of parameters, they are values that are considered fixed in the optimization, and that usually represent boundary conditions. Finally, the constraints are imposed by regulations [26], [237], [238] and recommendations of specialists [25], [242].

6.2.1 Variables of the problem

Our optimization problem is a Steel-Concrete Composite Bridge (SCCB) with a box-girder cross section divided in three spans of 60-100-60 meters. The problem variables can be grouped into two groups. The first group correspond to the geometric variables of the bridge and the second group with grades of steel and concrete. In order to design bridges that are feasible to build, these variables cannot take any value, but only allowed values, with which our search space corresponds to a discrete space. Variables are shown in Table 6.2. These variables, depending on their characteristics, are grouped into five categories. The first category correspond to geometric variables of the transverse section. Upper distance between wings (b), wings and cells angle (α_w), top slab thickness (h_s), beam high (h_b), floor beam minimum high (h_{fb}) , top flange thickness (t_{f_1}), top flange width (b_{f_1}), top cells high (h_{c_1}) and thickness (t_{c_1}), wing thickness (t_w), bottom cells high (h_{c_2}), thickness (t_{c_2}), and width (b_{c_2}) and bottom slab thickness (h_{s_2}). For clarity, these variables are outlined in Figure 6.1.

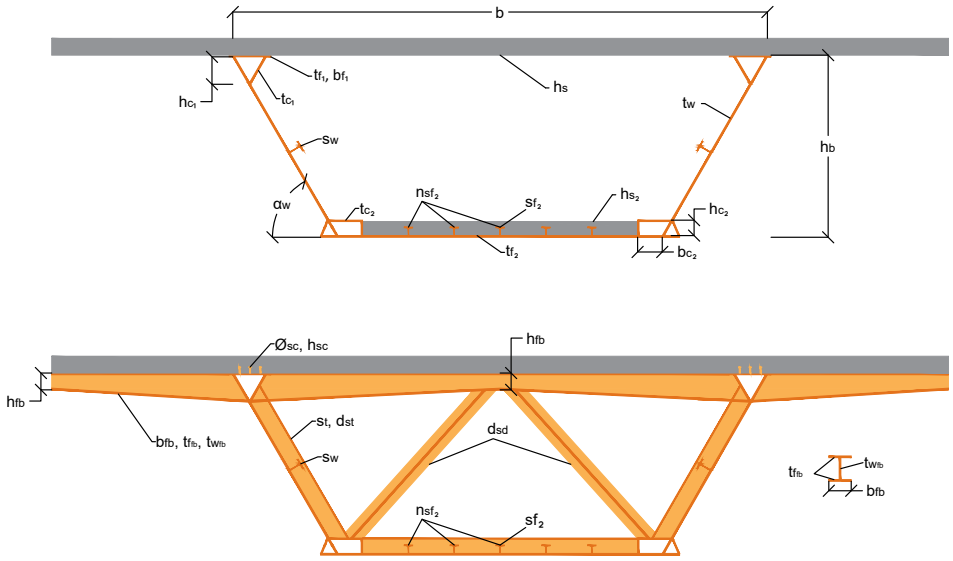

Figure 6.1: Transverse section variables for SCC bridge

Table 6.2: Design variables and boundaries

Variables	Unit	Lower Bound	Increment	Upper Bound	Values number
b	m	7	0.01	10	301
α_w	deg	45	1	90	46
h_s	mm	200	10	400	21
h_b	cm	250	1	400	151
h_{fb}	mm	400	100	700	31
t_{f_1}	mm	25	1	80	56
b_{f_1}	mm	300	10	1000	71
h_{c_1}	mm	0	1	1000	101
t_{c_1}	mm	16	1	25	10
t_w	mm	16	1	25	10
h_{c_2}	mm	0	10	1000	101
t_{c_2}	mm	16	1	25	10
b_{c_2}	mm	300	10	1000	71
t_{f_2}	mm	25	1	80	56
h_{s_2}	mm	150	10	400	26
$n_{s_{f_2}}$	u	0	1	10	11
d_{st}	m	1	0.1	5	41
d_{sd}	m	4	0.1	10	61
b_{fb}	mm	200	100	1000	9
$t_{f_{fb}}$	mm	25	1	35	11
$t_{w_{fb}}$	mm	25	1	35	11
n_{r_1}	u	200	1	500	301
n_{r_2}	u	200	1	500	301
ϕ_{base}	mm	6, 8, 10, 12, 16, 20, 25, 32			8
ϕ_{r_1}	mm	6, 8, 10, 12, 16, 20, 25, 32			8
ϕ_{r_2}	mm	6, 8, 10, 12, 16, 20, 25, 32			8
s_{f_2}	mm	From IPE 200 to IPE 600*			12
s_w	mm	From IPE 200 to IPE 600*			12
s_t	mm	From IPE 200 to IPE 600*			12
h_{sc}	mm	100, 150, 175, 200			4
ϕ_{sc}	mm	16, 19, 22			3
f_{ck}	MPa	25, 30, 35, 40			4
f_{yk}	MPa	275, 355, 460			3
f_{sk}	MPa	400, 500			2

* Following the standard series of IPE profiles.

The second category of variables corresponds to the diameters of the base reinforcement, first reinforcement and second reinforcement bar diameters (ϕ_{base}, ϕ_{r_1}, ϕ_{r_2}),

and the corresponding bar number of the reinforcement areas (n_{r_1}, n_{r_2}). These variables are intended to improve the bridge transverse section. To optimize the top slab reinforcement, it has been divided into a base reinforcement that is the minimum required by regulations [26], [237], [238] and two more areas, in negative bending sections, where the reinforcement is increased. The lower slab and the lengths of the increasing area of reinforcement will be described in section 6.2.2.

The stiffeners correspond to the third category of variables. In this design, half IPE profiles for wings (s_w), bottom flange (s_{f_2}) and the transverse ones (s_t) are considered variable stiffeners. For bottom flange stiffeners, the number of stiffeners ($n_{s_{f_2}}$) has also been considered as a variable. As can be seen in Figure 6.1, there are two more variables that define the distance between diaphragms (d_{sd}) and transverse stiffeners (d_{st}).

The last two categories correspond to the geometry of the shear connector's characteristics, and the floor beam variables. The floor beam variables are defined by the width of the floor beam (b_{fb}) and the thicknesses of the flanges ($t_{f_{fb}}$) and webs ($t_{w_{fb}}$). Shear connectors have been defined by their height (h_{sc}) and diameter (ϕ_{sc}). Finally, the elastic limit of rolled steel (f_{yk}), the strength of concrete (f_{ck}) and the elastic limit of reinforcing steel bars (f_{sk}) complete the definition of the variables.

6.2.2 Parameters of the problem

In each optimization problem, it is necessary to set some variables, typical of the conditions to which the structure will be subjected, defined by some regulation, environmental conditions, or some geometric definition that has no need or the possibility of changing. These fixed attributes are called parameters and remain unchanged throughout the optimization process. The parameters and values defined in the bridge design are summarized in Table 6.3.

Considering the Eurocode regulations [26], [237], that our bridge is a 60-100-60 meters three-span box-girder steel-concrete composite bridge with a deck width (B) of 16 meters without height variation, for cells have been defined in the transverse section for improving the resistant behaviour. These cells are shown in Figure 6.1. Two cells are at the upper side of the wings, and the other two are at the bottom. The minimum height of these cells, (h_{c_1}, h_{c_2}), has been set to zero in order to identify if they contribute to the reduction of costs or emissions of CO_2 additionally for set the upper limit of these, the bridge design rules defined in [242] has been considered.

The base reinforcement for the upper and lower concrete slab is set according to the minimum need for reinforcement defined in Eurocode 2 [238]. The connection between the concrete slab and the steel beam is dimensioned to resist the shear lag

Table 6.3: Optimization problem parameters

Geometrical parameters		
Bridge deck width (W)	16	m
Span number	3	
Central span length	100	m
External span length	60	m
Minimum web thickness ($t_{w_{min}}$)	15	mm
Minimum flange thickness ($t_{f_2 min}$)	25	mm
Reinforcement cover	45	mm
Material parameters		
Maximum aggregate size	20	mm
Concrete longitudinal strain modulus (E_{cm})	$22 \cdot ((f_{ck} + 8)/10)^3$	MPa
Concrete transverse strain modulus (G_{cm})	$E_{cm}/(2 \cdot (1 + 0.2))$	MPa
Steel longitudinal strain modulus (E_s)	210000	MPa
Steel transverse strain modulus (G_s)	80769	MPa
Regulation requirement parameters		
Regulations	Eurocodes[26], [237], [238], [240], IAP-11[241]	
Exposure environment	XD2	
Structural class	S5	
Service life	100	years
Loading parameters		
Reinforced concrete density	25	kN/m^3
Steel density	78.5	kN/m^3
Asphalt density	24	kN/m^3
Asphalt layer thickness	100	mm
Bridge traffic protections	5.6	kN/m
Traffic load	According to the codes	
Thermal load	According to the codes	
Wind load	According to the codes	

stresses produced in the top flanges. For bending resistance the effective width given by Eurocode 4 [26] have been considered. Also, because the only width considered resistant is effective, the defined steel bar reinforcements are placed only in that width.

Finally, steel bar reinforcement increase and lower slab areas are defined. The lower slab is placed in negative bending sections to mobilize the composite dual-action. To define lengths where negative bending can be produced, we have considered the distance defined by Eurocode 4 [26] for shear lag stresses that correspond with one-third of the span length. As stated earlier, it is necessary to increase the upper

slab reinforcement to resist the tension stresses produced. In this case study, we have considered two reinforcement areas. The first is placed in zones where the section can be subjected to negative bending, and base reinforcement cannot resist the stresses. The second is placed on top of supports, corresponding to one-third of the distance between the support and the point of change of sign of the bending of the theoretical law.

6.2.3 Constraints of the problem

In designing a structure, the constraints imposed by regulations and specific conditions to the structure, such as safety factors, must be considered. Mainly, in the optimization of this bridge, the necessary constraints to consider are defined in the regulations, [26], [237], [238] and additionally, recommendations defined in, [25], [242] have been incorporated.

When analyzing the regulations, it is found that the constraints imposed make up two groups: The first one corresponds to the Ultimate Limit States (ULS) and the second group, to the Service Limit States (SLS). In the case of ULS, the restrictions are related to the structural resistance of the bridge elements subjected to the stresses caused by the acting loads. In the case of SLS, the restrictions are intended to ensure the serviceability of the structure during its useful life. All applied loads and their combination are defined in the [240] regulation. The table 6.3 summarizes the load cases considered.

In order to verify the ULS restrictions in all the elements of the bridge, both the global and the local analyses have been considered. In the case of the global analysis, the checks consider shear, flexure, torsion, and flexure-shear interaction. To obtain stresses and deflections, a linear elastic analysis has been considered. When considering [237] and [26], these indicate that the resistance of the section must be included, in our design, the effective section has been selected and applying it both the shear lag reductions and the reduction of the section of steel plates classified as class 4. To achieve the above, a precision of 10^{-6} meters has been considered for the iterative process. To obtain the value of the mechanical characteristics of the homogenized section, the relationship (n) between the longitudinal deformation modulus of concrete (E_{cm}) and steel (E_s) has been obtained according to Equation 6.4. For the case of concrete creep and shrinkage, they were defined following the [26], [238] standard. Likewise, a local model was developed to verify the beams, reinforcements, and diaphragms in the ULS floor, considering controls for shear, flexure, buckling, and minimum mechanical characteristics.

$$n = \frac{E_s}{E_{cm}} \tag{6.4}$$

The SLS considered for the analysis is the tension limit for materials, fatigue, and deflection. There is no apparent limit for deflection in Eurocodes, but the IAP-11 Spanish regulation [241] gives a maximum of $L/1000$ for the frequent combination of live loads deflection value, with L representing the span length. This has been considered as the maximum value of the deflection. In addition, we have considered geometrical and constructibility requirements.

Additionally, a numerical model has been implemented to obtain the stresses and carry out all the ULS, SLS, and geometric and constructibility checks. In the case of deflections and stresses, the model applies the perfect embedding forces method, taking the 34 bridge variables we selected as input data. The model divides each span of bridge into a defined number of bars. In this case, the total number of bars is 44, distributed in 12-20-12 corresponding to the three spans of the bridge; thus, discretize the bridge into bars of 5 meters in length. Once the stresses have been obtained, the program performs structural checks and returns the measurement results, cost, emissions, and verification coefficients. These verification coefficients correspond to the quotient between the design values of the effects of the actions (E_d) and their corresponding resistance value (R_d), as shown in the equation 6.5. If these coefficient values are greater than or equal to one, then the Section complies with the imposed restriction.

$$\frac{R_d}{E_d} \geq 1 \tag{6.5}$$

6.2.4 Structure computational model description

The procedure used to obtain the deflections and stresses has been the perfect embedding forces method. This method consists in solving equation 6.6.

$$\mathbf{f} = \mathbf{K} \cdot \mathbf{d} + \mathbf{f_0} \tag{6.6}$$

In this equation, $\mathbf{f_0}$ correspond to the perfect embedding forces vector. These forces would be obtained if each of the system bars had all the degrees of freedom constrained. $\mathbf{K}$ is the stiffness matrix of the system, generated by assembling the stiffness matrices of all bar elements. To get the stiffness matrix of each element, the

average between both frontal and dorsal nodes' mechanical properties has been calculated. The complete section without considering the shear lag and panel reduction has been considered to obtain these mechanical properties. Finally, $\mathbf{d}$ and $\mathbf{f}$ are the deflections and stress vectors, respectively.

This procedure is repeated with all load cases. The following load cases have been considered loading the entire bridge length as a single load case: Self Weight, Dead Loads, Thermal Heating, Thermal Cooling, and Wind. In order to consider the different positions of traffic loads, every 5-meter bar has been loaded separately, considering two separated loading cases, the punctual load and the distributed. This gives, as a result, 88 load cases for traffic load and a total of 93 if all load cases are considered. The results obtained from loading each bar have been combined to consider all loading possibilities regarding traffic load. After this, the load case envelope has been calculated to consider each section's maximum and minimum results.

Regarding combinations and envelopes, the envelope of all persistent and transitory situations combinations have been obtained for ULS. These combinations have been considered dominant action all live loads in different combinations. The envelope of all characteristic combinations has been considered for SLS regarding stress limitation.

6.3 Optimization algorithms

The detail of the discretization algorithms will be explained in this Section. First, the metaheuristics used to perform the optimization will be detailed in Section 6.3.1. Then the proposed hybrid algorithm, Section 6.3.2, which uses k-means as the discretization method will be explained. Later in Section 6.3.3, the algorithm that uses a transfer function as a discretization method is detailed. The following reference is recommended for a greater depth of transfer functions and their applications in combinatorial optimization [274]. We must emphasize that the k-means discretization method takes all the solutions, groups them, and later assigns the probabilities. In the case of transfer functions, each probability is assigned individually, without looking at the other solutions.

Figure 6.2 shows the flowchart used to perform the optimization using cuckoo search and the sine cosine algorithms (SCA). As a starting point, the set of solutions is initialized, this set corresponds to a valid set, that is, it complies with the constraints imposed by the problem. Once the solutions have been initialized, it is asked whether the stopping criteria of the algorithm are met. In this case, the stopping criterion of the algorithm corresponds to the maximum number of defined iterations. In the event that the maximum number of iterations has not been met, the hybrid algorithm

is executed. As a first stage of the hybrid algorithm, the set of velocities for the different generated solutions is obtained. Subsequently to the set of solutions, the k-means clustering technique is applied in order to group the solutions and assign a transition probability to each group in the transition probabilities stage. The detail of these three stages will be explained in Section 6.3.2. Finally, a solution update criterion is established, in which it is evaluated if each of the variables or dimensions associated with a solution is updated. This is intended to balance the exploitation and exploitation of the search space. Solutions with good values of the fitness function will have few updates to be able to exploit the space. The detail of this update will also be made in Section 6.3.2

6.3.1 Swarm intelligence algorithms: SCA and CS

This section details the swarm intelligence algorithms used to address optimization. Specifically, the cuckoo search was chosen as it has successfully solved a large number of optimization problems, particularly in the area of civil engineering. Additionally, the parameterization of the original algorithm is quite simple. In the case of the sine cosine algorithm, the type of move it executes is based on the sin and cosine functions and is completely different from the move of cuckoo search. On the other hand, this last metaheuristic does not require proper parameter tuning.

Sine Cosine Algorithm (SCA)

Sine Cosine Algorithm (SCA) was proposed in [233] and corresponded to a swarm intelligence algorithm that considers the sine and cosine functions to carry out the process of exploring and exploiting the search space. To carry out the movement of the solutions, P_j^t is additionally used, which corresponds to the position of the destination solution for iteration t and dimension j, and typically uses the best solution obtained so far. In addition to P_j^t, the algorithm uses four random numbers r_1, r_2, r_3, r_4. As the algorithm starts to iterate, r_1 decreases. It starts at 2 and converges to 0 at the end of the optimization. On the other hand, r_2 takes values between 0 , 2π. r_3 considers values between 0 and 2, and finally r_4 is used to select Equations 6.7 and 6.8 taking values between 0 and 1 and a threshold of 0.5.

The update method used is shown in Equations 6.7 and 6.8.

$$x_{i,j}^{t+1} = x_{i,j}^t + r_1 \times sin(r_2) \times \mid r_3 P_j^t - x_{i,j}^t \mid \tag{6.7}$$

$$x_{i,j}^{t+1} = x_{i,j}^t + r_1 \times cos(r_2) \times \mid r_3 P_j^t - x_{i,j}^t \mid \tag{6.8}$$

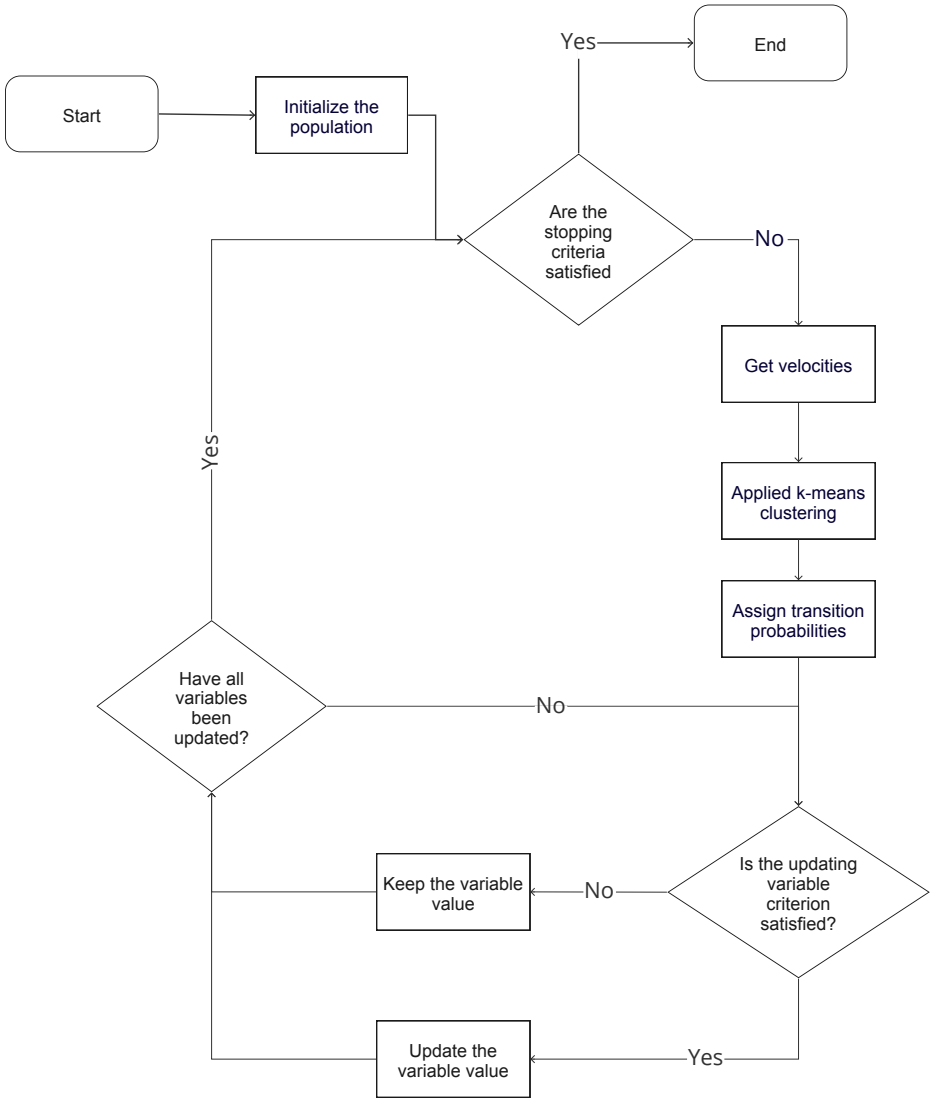

Figure 6.2: Discrete hybrid k-means algorithm flow chart.

Cuckoo Search Algorithm (SC)

The reproductive strategy phenomena observed in cuckoo species, which lay their eggs in the nests of other bird species, has inspired the CS algorithm. Such is the level of sophistication of cuckoo birds that in some cases even the colors and patterns of the eggs of the chosen host species are mimicked. In the analogy, an egg corresponds to a solution. The concept behind the analogy is to use the best solutions (cuckoos) to replace those that do not perform well. The CS algorithm uses three basic rules:

1. Each cuckoo lays one egg at a time and deposits its egg in a randomly chosen nest.
2. The nests with the best results, that is, with high-quality eggs, will be considered in the next generation.
3. The number of nests available is a fixed parameter. The egg laid by a cuckoo can be discovered by the host bird with a probability $p_a \in (0, 1)$

In Equation 6.9 the movement of CS is defined. The symbol $\oplus$, denotes entry-wise multiplication, whereas $\alpha > 0$ denotes the step size. This step size specifies the maximum distance that a particle can travel in a random walk over a set number of iterations. The Lévy distribution modulates the transition probability of the Lévy flights in Equation 6.10.

$$x_{i,j}^{t+1} = x_{i,j}^{t} \alpha \oplus levy(\lambda) \tag{6.9}$$

$$levy(\lambda) \sim g^{-\lambda}, (1 < \lambda < 3) \tag{6.10}$$

6.3.2 K-means discrete algorithm

In this subsection, the detail of the algorithm that allows discretizing the SCA and CS metaheuristics is explained, these MH, naturally work in continuous search spaces. The k-means discrete algorithm (KMDA), uses the unsupervised learning technique k-means to cluster the solutions. As input parameters, KMDA considers the list of solutions $lSol$, the metaheuristic MH to be discretized, and the list of transition probabilities $transitionProbs$, where each group obtained by applying k-means is associated with a value of transition probability. In line 4, KMDA uses the metaheuristic that is being discretized, for this case, SCA or CS, however, it can be any continuous swarm intelligence metaheuristic, and together with the list of solutions

$lSol$ obtained in the previous iteration, the movement of the metaheuristic is applied, obtaining the velocity for each solution in the list of solutions. The calculation of the velocity for each dimension of the solution vector is done using the equations 6.7 and 6.9. The velocity in the metaheuristics is considered by $lSol_{i,j} = |x_{i,j}^{t+1} - x_{i,j}^{t}|$. $vlSol$ identifies the list of velocities associated with the list of solutions $lSol$.

Once the list of solutions $vlSol$ has been obtained, the next step corresponds to grouping the velocities using the k-means technique for a number K of clusters. This applies in line 5 of the algorithm. The objective of applying k-means is to generate groups where the elements of each group have similar characteristics. In this case the groups that have velocities with small values and that therefore in continuous space would move very little, will be related to small transition values in our discrete space. As a result of clustering, $lSolClustered$ is obtained, where the cluster is stored for each of the components of each speed associated with the list of solutions $lSol$.

Subsequently, each component's $dimSol$ cluster is considered for each solution, and a transition probability is assigned. For the case studied here, a $K = 5$ was used and with transition probabilities [0.1, 0.2, 0.4, 0.8, 0.9]. The smallest value of the transition probability is assigned to the cluster with the lowest average velocity, and in that order, the probabilities are assigned. The assignment of the transition probabilities was established intuitively and supported by previous experiences when solving binary problems. Following the idea that the first two clusters have the smallest velocities, small transition probabilities are assigned, with the aim of favoring the exploitation of space. The last two clusters that have the highest velocities, are assigned high probabilities to favor exploration of the search space, and the middle cluster has a probability of 0.4.

Finally, using a random number r_1 it is determined if the component $lSol_{i,j}$, is updated or stays the same. The higher the probability of transition, the greater the probability of change. Additionally, it is used a random number r_2, making the update be considering the best value or randomly. In our case $\beta = 0.8$. The KMDA pseudocode is shown in algorithm 2.

Algorithm 2 k-means discrete algorithm (KMDA)

1: **Function** KMDA($lSol$, MH,$transitionProbs$)
2: **Input** $lSol$, MH, $transitionProbs$
3: **Output** $lSol$
4: $vlSol \leftarrow$ getVelocities($lSol$, MH)
5: $lSolClustered \leftarrow$ appliedKmeansClustering($vlSol$, K)
6: **for** (each Sol_i in $lSolClustered$) **do**
7: **for** (each $dimSol_{i,j}l$ in Sol_i) **do**
8: $dimSolProb_{i,j}$ = getClusterProbability($dimSol$, $transitionProbs$)
9: **if** $dimSolProb_{i,j} > r_1$ **then**
10: **if** $beta > r_2$ **then**
11: Update $lSol_{i,j}$ considering the best.
12: **else**
13: Update $lSol_{i,j}$ with a random value allowed.
14: **end if**
15: **else**
16: Don't update the element in $lSol_{i,j}$
17: **end if**
18: **end for**
19: **end for**
20: **return** $lSol$

6.3.3 Transfer function discrete algorithm

In the case of the algorithm that uses transfer functions, the structure is very similar to KMDA. Specifically, a transfer function is applied that aims to bring the velocity values, which can take values in $\mathbb{R}$, to values between [0, 1). In this case, a v-shape transfer function, $\mid \tanh(v) \mid = \mid \frac{e^x - e^{-x}}{e^x + e^{-x}} \mid$, was used. The fundamental difference is that KMDA calculates the speeds and then applies clustering by analyzing all the values of the solutions. This can be seen in lines 4 and 5 of algorithm2. In the case of transfer functions, this is done individually within the for loops on lines 6 and 7 of algorithm 3.

Algorithm 3 Transfer function discrete algorithm

Function Discretization($lSol$, MH)
Input $lSol$
Output $lSol$
for (each Sol in $lSol$) **do**
  for (each $dimSol$ in Sol) **do**
    $vdimSol \leftarrow$ getVelocity($dimSol$, MH)
    $dimSolProb \leftarrow$ appliedTransferFunction($vdimSol$)
    if $dimSolProb > r_1$ **then**
      if $beta > r_2$ **then**
        Update $lSol_{i,j}$ considering the best.
      else
        Update $lSol_{i,j}$ with a random value allowed.
      end if
    else
      Don't update the element in $lSol_{i,j}$
    end if
  end for
end for
return $lSol$

6.4 Results

In this Section, the experiments developed to evaluate the behavior of the discrete hybrid algorithm are detailed, in addition to analyzing the findings found when optimizing the bridge. The results are divided into four subsections. In Section 6.4.1 it is explained how the selection of the hyperparameters used by the algorithm was made. Later in Section6.4.2, the results of the experiments that identify the contribution of the algorithm in the optimization result are detailed. Later in Section6.4.3, the results are compared with other implementations.

Python 3.6 was used to create the algorithm, along with a PC running Windows 10, a core i7 processor, and 32GB of RAM. To see if the difference is statistically significant, the Wilcoxon signed-rank [275]method was used. The 0.05 p-value was chosen. The methods described in [251] was used to choose the test. The Shapiro–Wilk normality

test is used initially in this process. The Wilcoxon signed-rank is recommended to check the difference if one of the populations is not normal and has the same number of points.

6.4.1 Parameter setting

The methodology used to select the correct parameters was adapted from the procedure defined [250]. To obtain an adequate selection of the parameters, we used three measures defined by the Equations (6.11) to (6.13). For the generation of values, each combination of parameters was executed five times. The set of parameters explored and selected for CS is shown in Table 6.4. For the calculation of the best performance, each of the indicators is constructed to have values between 0 and 1. The closer to 1, the better the performance. These values are plotted on a radar chart and the area under the curve is calculated. The set of indicators that takes the largest area, corresponds to the best performance.

1. The percentage deviation of the best value obtained in the specific execution, compared to the best value obtained of all the runs:

$$bSolution = 1 - \frac{BestTotalValue - BestValue}{BestTotalValue} \tag{6.11}$$

2. The percentage deviation of the worst value obtained in the specific execution, compared to the best value obtained of all the runs:

$$wSolution = 1 - \frac{BestTotalValue - WorstValue}{BestTotalValue} \tag{6.12}$$

3. The percentage deviation of the average value obtained in the specific execution, compared to the best value obtained of all the runs:

$$aSolution = 1 - \frac{BestTotalValue - AverageValue}{BestTotalValue} \tag{6.13}$$

Table 6.4: Parameter setting for the hybrid cuckoo search algorithm

Parameters	Description	Value	Scanned range
N	Number of Nest	10	[5, 10, 20]
γ	Step Length	0.01	0.01
κ	Levy distribution parameter	1.5	1.5
K	Number of clusters	5	[4, 5]
Iteration Number	Maximum iterations	600	[200,400,600]

6.4.2 Insight into discrete algorithm

This Section aims to evaluate the contribution of the KMDA operator in the result of the optimization of the bridge. Two random discretization operators were designed, $Random0.5$ and $Random0.3$. Specifically, these operators do not execute the clustering in line 5 of the algorithm 2or the probability assignment in line 8. The value of $dimSolProb_{i,j}$ is replaced by 0.5 in the case of $Random0.5$ and 0.7 in the case of $Random0.3$ (30% probability of transition). The rest of the code remains unchanged. These operators were applied to the SCA metaheuristics and the bridge cost optimization problem. The results are shown in Table 6.5 and Figure 6.3.

In Table 6.5, the result of 30 executions for each of the operators mentioned above, together with the descriptive statistics, are shown. In this experiment, the objective function corresponds to cost optimization. From each of the optimizations, the bridge that obtained the best cost is registered, the emissions obtained for that bridge, and the time it took for the optimization. In the case of the cost results, we see that Hybrid SCA obtains the best values and smaller dispersion of the results. When emissions are analyzed, we see that the Hybrid SCA case is more robust in all indicators. Additionally, the latter suggests an essential correlation between optimizing the cost of the bridge and reducing its emissions. The Wilcoxon test shows that the results are statistically significant. When the execution times are analyzed, the results are similar in the three evaluated operators. When comparing the cost boxplots, Figure 6.3, we visually observe the robustness of Hybrid SCA against random operators.

6.4.3 Algorithm comparisons

This Section will evaluate KMDA's performance against other implementations that have effectively solved combinatorial problems. The first algorithm used was an implementation of simulated annealing (SA) proposed in [276] and used to optimize prestressed concrete precast road bridges and later applied to other structural design problems [14], [173]. For the second comparison, the algorithm detailed in Section 6.3.3 is used, which performs the discretization procedure using the v-shape

Table 6.5: Cost minimization results for 30 executions of Random 0.5, Random 0.3, and discrete hybrid SCA algorithms

	Random 0.5			Random 0.3			Hybrid SCA		
Run	**Cost (€)**	**CO_2(kg)**	**Time(s)**	**Cost (€)**	**CO_2(kg)**	**Time(s)**	**Cost (€)**	**CO_2(kg)**	**Time(s)**
1	3841685.5	9423182.3	7545.1	3854631.0	9441992.7	7434.5	3830092.8	9390104.1	7835.5
2	3838056.5	9417710.5	8121.4	3841685.5	9423182.3	7892.6	3864886.9	9480536.6	7945.0
3	3856001.6	9455145.0	6978.9	3868347.8	9487298.0	7112.7	3826395.0	9388407.3	7873.4
4	4004603.5	9837622.5	7984.7	4041117.6	9915536.1	8001.2	3825919.0	9385589.0	7929.9
5	3837584.6	9406572.5	6921.5	3863494.3	9467939.5	6893.2	3823801.1	9385004.6	7916.1
6	3920211.2	9618810.5	8021.3	4009757.4	9837067.3	8021.3	3835442.1	9391386.1	7911.4
7	3863494.3	9467939.5	7214.8	3835377.4	9395269.5	7324.6	3826324.6	9389542.7	7920.3
8	4004603.5	9837622.5	7498.1	3973917.2	9747159.4	7568.3	3826206.4	9385730.7	7935.5
9	3920211.2	9618810.5	8210.4	3844805.5	9422679.4	7901.4	3830234.3	9387716.3	7858.2
10	3867325.2	9485202.2	7645.7	3938023.8	9657116.7	7923.5	3825188.7	9385235.2	7931.7
11	3920211.2	9618810.5	7645.2	3912499.4	9593267.2	7234.8	3828878.5	9387047.9	7748.9
12	3847797.6	9432071.6	8024.1	3840298.2	9419023.8	8024.1	3831864.4	9388519.9	7719.6
13	3844078.0	9432582.0	7643.7	3847990.2	9432380.4	7701.4	3823462.5	9384378.1	7637.7
14	3848079.2	9419256.1	7891.4	3844078.0	9432582.0	7903.2	3828178.8	9386856.2	7819.4
15	3927551.4	9631163.6	7798.4	3920211.2	9618810.5	7923.2	3826847.5	9386123.4	7933.9
16	3853756.2	9458527.3	7234.1	3847713.1	9431886.6	8001.5	3824311.6	9384796.6	7687.4
17	3854631.0	9441992.7	8102.3	3851331.6	9451618.9	8114.7	3822723.1	9384013.6	6165.3
18	4004603.5	9837622.5	7743.6	3829666.1	9398360.6	6902.6	3824024.1	9384655.0	7767.6
19	3844695.3	9425683.0	7893.9	3844407.2	9425168.7	7745.2	3824115.0	9384852.9	7918.0
20	3840156.4	9402992.6	7745.1	3853756.2	9458527.3	7801.4	3829979.1	9387820.3	7891.1
21	3858728.1	9455868.2	7874.5	3846266.3	9424806.5	7931.6	3823245.0	9384270.9	7870.4
22	3846266.3	9424806.5	7534.2	3856001.6	9455145.0	7345.2	3828654.6	9388464.0	7945.4
23	3868347.8	9487298.0	7654.9	3858728.1	9455868.2	7791.5	3827333.5	9386286.3	7895.7
24	3853062.4	9444842.4	7943.4	3930520.1	9638238.9	8002.3	3824394.8	9384837.7	7876.2
25	4004603.5	9481380.6	7653.2	3866161.5	9481380.6	7754.8	3830913.2	9388051.0	7855.7
26	3920211.2	9618810.5	7896.7	3853062.4	9444842.4	7931.9	3829366.5	9387824.7	7668.7
27	3844407.2	9425168.7	7745.7	3867165.6	9474659.0	7742.5	3833463.0	9391767.1	7731.3
28	3847873.6	9432179.5	7653.3	3847714.8	9447150.9	7509.8	3824394.8	9384837.7	7845.4
29	3851331.6	9451618.9	7694.9	3844695.3	9425683.0	7654.7	3823562.7	9384427.5	7696.0
30	3867165.6	9474659.0	7893.5	3938023.8	9657116.7	8032.4	3830124.4	9388127.9	7947.6
Average	3883377.8	9512198.4	7713.6	3879048.3	9512058.6	7704.1	3828477.6	9389907.0	7789.3
Max	4004603.5	9837622.5	8210.4	4041117.6	9915536.1	8114.7	3864886.9	9480536.6	7947.6
Min	3837584.6	9402992.6	6921.5	3829666.1	9395269.5	6893.2	3822723.1	9384013.6	6165.3
Std	55639.3	130762.0	312.2	54164.3	134417.5	340.2	7622.2	17251.2	320.7
Wilcoxon p-value	4.1 e-4		1.7 e-4						

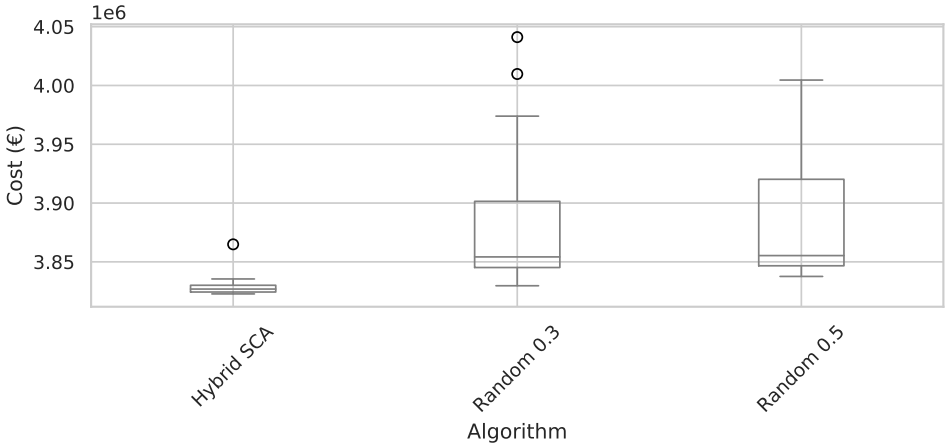

Figure 6.3: Cost boxplots for Random 0.5, Random 0.3, and SCA Algorithms.

$|tanh(v)|$ function. To make the comparison, all the algorithms are executed 30 times to optimize costs and 30 times to optimize CO_2 emissions. The results are recorded in Tables 6.6, and 6.7. Additionally, the results are shown through box diagrams in Figures 6.4, and 6.5.

In Table 6.6, the cost optimization for SA, transfer SCA, hybrid SCA, and hybrid CS is shown. When analyzing the descriptive statistics, we see that the cost results obtained by the hybrid algorithms are very similar and superior to those for SA and transfer CSA in the minimum, maximum, average, and deviation obtained. When applying the Wilcoxon test, it indicates that the difference is not significant between the hybrid algorithms and if it is significant between hybrid SCA with respect to SA and transfer SCA. When applying the Wilcoxon test, it indicates that the difference is not significant between the hybrid algorithms and if it is significant between hybrid SCA with respect to SA, transfer SCA and transfer CS. In the case of the emissions obtained in cost optimization, we observe that both hybrid algorithms consistently obtain very similar results and are more robust than SA and transfer SCA. Again, the strong relationship between optimizing costs and reducing emissions of CO_2 is observed in the hybrid algorithms. When analyzing the times, we see that SA is 21.5% slower than Hybrid SCA, being this very similar to transfer SCA and hybrid CS. When comparing the boxplots, Figure 6.4, the similarity of the hybrid methods is visually observed, and the robustness of the results concerning the other methods.

Table 6.6: Cost minimization comparison for 30 executions of SA, discrete transfer function SCA and CS, discrete hybrid SCA, and CS algorithms. Time is measured in seconds.

	SA			Transfer SCA			Transfer CS			Hybrid SCA			Hybrid CS		
Run	**Cost (€)**	**CO_2(kg)**	**Time**	**Cost (€)**	**CO_2(kg)**	**Time**	**Cost (€)**	**CO_2(kg)**	**Time**	**Cost (€)**	**CO_2(kg)**	**Time**	**Cost (€)**	**CO_2(kg)**	**Time**
1	3829112	9393007	9196	3854631	9441992	7497	3853274	9447811	7621	3830092	9390104	7835	3825644	9385453	7975
2	3845663	9442138	7589	3841685	9423182	7822	3853926	9449454	7741	3864886	9480536	7945	3825115	9385192	7976
3	3829827	9390569	9687	3868347	9487298	7889	3861618	9468696	7812	3826395	9388407	7873	3825644	9385453	7891
4	3834439	9395041	9719	3837467	9411814	7635	3837015	9413229	7635	3825919	9385589	7929	3830529	9387861	7959
5	3836720	9393995	9430	3863494	9467939	7786	3859823	9464319	7653	3823801	9385004	7916	3822875	9384095	7930
6	3832832	9394394	9198	3838032	9396760	7795	3933952	9636170	7563	3835442	9391386	7911	3827681	9386457	7983
7	3837598	9398873	9291	3835377	9395269	7317	3844299	9425351	7752	3826324	9389542	7920	3824141	9384712	8008
8	3841417	9408629	9271	3839077	9400419	7876	3832605	9397118	7976	3826206	9385730	7935	3827522	9386379	7971
9	3826259	9391263	9225	3844805	9422679	7832	3853274	9447811	7698	3830234	9387716	7858	3827541	9386388	7949
10	3837246	9398956	9691	3867325	9485202	7880	3857615	9458840	8043	3825188	9385235	7931	3825756	9387883	8055
11	3838964	9399136	9507	3833501	9406118	7556	3829202	9389102	7467	3828878	9387047	7748	3824519	9384899	8267
12	3844258	9420045	9668	3840298	9419023	7903	3861618	9468696	7894	3831864	9388519	7719	3831847	9388511	8292
13	3840202	9408438	9557	3844078	9432582	7509	3854516	9450954	7735	3823462	9384378	7637	3827980	9386681	8291
14	4701903	11582022	9856	3848079	9419256	7789	3836478	9406458	7642	3828178	9386856	7819	3823891	9384589	8267
15	4004603	9837622	9956	3920211	9618810	7820	3853274	9447811	7756	3826847	9386123	7933	3825444	9385765	8148
16	3837030	9407814	9504	3840156	9402992	7886	3860073	9450935	7985	3824311	9384796	7687	3823063	9384870	8210
17	3838077	9398394	9705	3851331	9451618	7740	3851195	9427987	7463	3822723	9384013	6165	3832782	9401328	8308
18	3826142	9389610	9793	3829666	9398360	7905	3848626	9422617	7683	3824024	9384655	7767	3828246	9386736	8370
19	3836306	9393541	9326	3844407	9425168	7902	3839130	9400681	7843	3824115	9384852	7918	3831724	9388450	8249
20	3829965	9397333	9912	3853756	9458527	7736	3839701	9402112	7722	3829979	9387820	7891	3824459	9384869	8236
21	3834063	9395196	9590	3846266	9424806	7921	3851195	9427987	7463	3823245	9384270	7870	3830466	9387831	7897
22	3838868	9397515	9535	3856001	9455145	7502	3879874	9500752	7985	3828654	9388464	7945	3825593	9385428	7645
23	3840493	9410516	9238	3858728	9455868	7583	3861537	9457936	7583	3827333	9386286	7895	3826446	9385925	7912
24	3836563	9399930	9617	3839779	9410778	7903	3881525	9505995	7793	3824394	9384837	7876	3827796	9386514	7914
25	3833027	9394227	9494	3866161	9481380	7729	3849452	9428558	7642	3830913	9388051	7855	3822766	9384035	7896
26	3834233	9397503	9412	3853062	9444842	7790	3841782	9409898	7856	3829366	9387824	7668	3822723	9384013	7024
27	3845712	9417868	9565	3867165	9474659	7781	3854384	9440750	7843	3833463	9391767	7731	3822723	9384013	5218
28	3832969	9403292	9984	3847714	9447150	7552	3858984	9467252	7748	3824394	9384837	7845	3825907	9385583	7943
29	3829559	9389435	8800	3844695	9425683	7660	3851331	9448449	7654	3823562	9384427	7696	3823593	9384442	7923
30	3834992	9398075	9775	3838056	9417710	7891	3841344	9423805	7962	3830124	9388127	7947	3830083	9388051	7914
Average	3870301	9487479	9470	3850445	9440101	7746	3854421	9446251	7740	3828477	9389907	7789	3826483	9386414	7921
Max	4701903	11582022	9984	3920211	9618810	7921	3933952	9636170	8043	3864886	9480536	7947	3832782	9401328	8370
Min	3826142	9389435	7589	3829666	9395269	7317	3829202	9389102	7463	3822723	9384013	6165	3822723	9384013	5218
Std	160135	403661	443	17047	43542	159	19179	45846	158	7622	17251	320	2954	3137	570
Wilcoxon p-value	3.6 e-4			1.4 e-4											

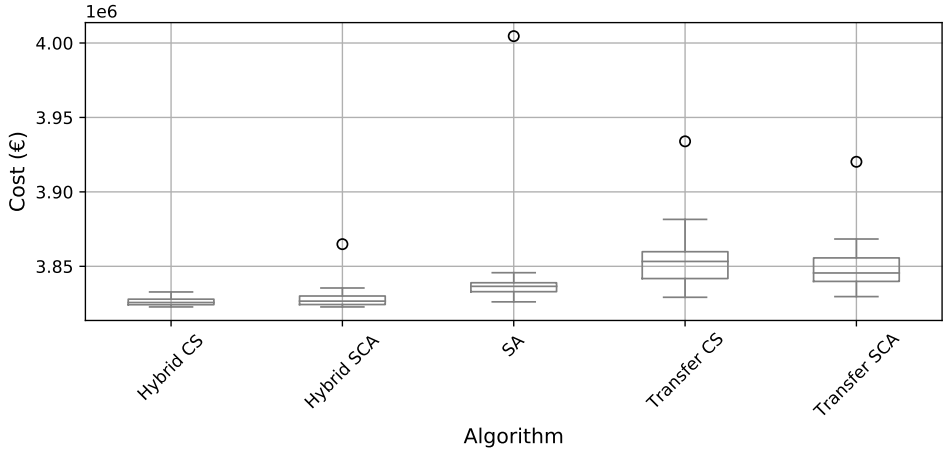

Figure 6.4: Cost boxplots for SA, discrete transfer SCA, discrete hybrid SCA, and discrete hybrid CS Algorithms.

Table 6.7 shows the comparison between discrete algorithms that use k-means (Section 6.3.2), SA, and transfer functions (Section 6.3.3), optimizing CO_2 emissions. When analyzing the amount of CO_2produced during the emissions optimization process, we see that the results of the hybrid method are better than the one that uses transfer functions and SA in all indicators. This is also visually verified by comparing the different boxplots in Figure 6.5. However, when analyzing the costs obtained in the optimization of emissions, it does not behave equivalent to the optimization of costs. In this case, a significant dispersion is observed in all algorithms. The range between Max and Min is significant in all five algorithms. This correlation between cost optimization and emission reduction of CO_2 identified in Table 6.5, is related to the fact that the different grades of steel obtained from the BEDEC [207] database have the same amount of emissions. In the case of the CO_2 optimization, different elastic limit values are obtained for structural steel without producing essential variations in its objective emission function, but the highest in terms of cost.

In Table 6.8 the design variables results have been shown for cost and CO_2 optimization objectives. As it can be seen, there are some differences between cost and CO_2 optimization design results. The first one is the yield stress (f_{yk}) obtained for the best individual. It is observed that cost optimization results from this variable 275 MPa while CO_2 optimization gets 460 MPa. This difference is due to the difference in structural steel's cost and emission values. As shown in Table 6.1 as the cost increase, as the value of the yield stress increases, the value is the same for

Table 6.7: CO_2 minimization comparison for 30 executions of the discrete transfer function and discrete hybrid SCA and CS algorithms.

	SA		Transfer SCA		Transfer CS		Hybrid SCA		Hybrid CS	
Run	Cost (€)	CO_2(kg)	Cost (€)	CO_2(kg)	Cost (€)	CO_2(kg)	Cost (€)	CO_2(kg)	Cost (€)	CO_2(kg)
1	4103199.1	9394472.7	3826062.4	9388245.3	4531487.4	10115112.3	4420699.5	9384170.2	4421107.9	9384371.6
2	4104830.5	9393422.6	4107363.5	9398200	4931000.7	10230565.0	3828339.5	9386782.2	4091626.2	9384500.2
3	4095750.7	9386615.5	4106480.8	9419624.4	4789317.2	10033694.7	4092720.6	9385866.9	4093543.7	9385445.5
4	4101735.1	9390010.9	3830420.8	9390027.3	4607448.4	9710063.3	4092681.4	9385020.4	4421714.6	9384676.8
5	4431949.9	9390386.3	4423829.8	9388224.6	4724373.8	9870644.4	4428155.9	9387845.9	3823916.4	9384601.8
6	4428021.6	9387786.7	4104429.3	9413019.9	4735134.9	9912923.2	3829500.6	9387354.6	3823680	9384485.3
7	4428243.3	9393282.6	4444861.3	9427586	4730550.6	9924267.8	4427399.4	9387473	4091769.9	9384571.1
8	4424257.7	9387914.4	3845183.8	9417923.6	4503658.7	9765664.9	4093430.2	9385389.5	3823245	9384270.9
9	4099351.4	9395896.2	3828004.3	9391991.1	4212280.9	10052411.1	3831646.9	9388412.7	4421527.7	9384578.5
10	3836602.7	9407896.6	4434043.8	9399596.9	4666593.6	9725656.3	3827295.3	9386273.6	4093543.7	9385445.5
11	4436583.5	9399830.4	4440365	9405285.5	4841631.0	10686873.0	4091126.9	9384254.1	3824016.6	9384651.2
12	4099070.8	9391395.7	4098731.9	9398154.5	5058456.2	10525430.7	3824275.7	9384778.9	3823245	9384270.9
13	3837692.9	9394543.3	4097483.5	9395141.9	4257869.8	9838989.8	4093666.6	9385506.1	3826336.9	9385795.0
14	4098859.5	9394851.7	4447519.4	9406304.8	4957796.6	10944461.4	4091859.4	9385667.9	3827656.8	9386445.7
15	4092562.3	9385573.4	4149564.8	9501199.2	4721028.2	9992277.7	3828232.5	9386739.1	4426817	9387185.9
16	4437303.8	9398323.1	4111137.6	9411014.2	4925090.5	10312531.2	4091796.4	9384584.1	4096921.1	9387110.4
17	4100494.5	9392570.7	4103984.7	9401026.2	4977891.6	10121176.4	3829720	9387462.8	4101662	9389447.4
18	4424307.7	9386325.9	3852755.9	9455679.3	4552468.0	10031915.7	4090883.3	9384585.2	3824016.6	9384651.2
19	4102823.5	9396581.4	3831846.9	9398755	4611778.6	10355530.8	4100425.2	9388837.8	4093460.5	9385404.4
20	4428702.7	9390314.8	3853687	9444022.8	4928246.3	10324582.5	3823782.1	9384535.6	4423239.1	9385422.2
21	4430019.3	9392768.3	3834232.5	9393079.5	4894711.7	10129787.8	3825979.5	9385618.9	3825050.6	9385167.1
22	4102389.5	9391525.7	3843360.9	9430497.2	4878828.2	10058610.4	4096206.3	9386758	4568165.1	9384308.4
23	3829423.6	9390490.5	4132163.3	9459204.2	4891768.4	10229330.1	4094423	9385878.9	3823948.5	9384617.7
24	4106712.4	9395756.6	4111394.3	9413642.1	4598949.9	10406844.4	3826340.7	9385796.9	4092556.6	9384958.9
25	3833087.7	9391660.1	3835567.5	9409985.7	4763740.6	9977672.0	4095292.9	9386307.8	3826660.3	9385954.4
26	3823206.8	9384338.0	4109800.5	9405586.3	4614532.1	9738456.8	3828734.7	9386977.1	3823948.5	9384617.7
27	4428242.5	9392728.7	4442164.1	9424594.9	5249949.1	10943039.5	3823782.1	9384535.6	3832507.4	9388836.8
28	3832154.7	9388663.3	4108189.4	9406482.7	4371744.8	9740572.8	4100432.8	9388841.5	3825740.1	9388369.9
29	4428372.5	9397013.8	4445608.5	9410269.7	4872910.1	10028070.8	3828738.5	9386978.9	4090843.3	9384114.8
30	4096391.3	9387611.7	3837284.5	9401492.1	4576118.0	9997514.0	3832291.8	9388730.6	4092556.6	9384958.9
Average	4167411	9392617.2	4087917.4	9413528.6	4732578.5	10124155.7	4002995.3	9386265.5	4039167.5	9385469.5
Max	4437303	9407896.6	4447519.4	9501199.2	5249949.1	10944461.4	4428155.9	9388841.5	4568165.1	9389447.4
Min	3823206	9384338.0	3826062.4	9388224.6	4212280.9	9710063.3	3823782.1	9384170.2	3823245.0	9384114.8
Std	226692	4878	232227.7	24665.3	231256.6	328416.3	192413.8	1423.3	241158.4	1414.8.9
Wilcoxon p-value		2.7 e-4		1.2 e-4		2.7 e-6				

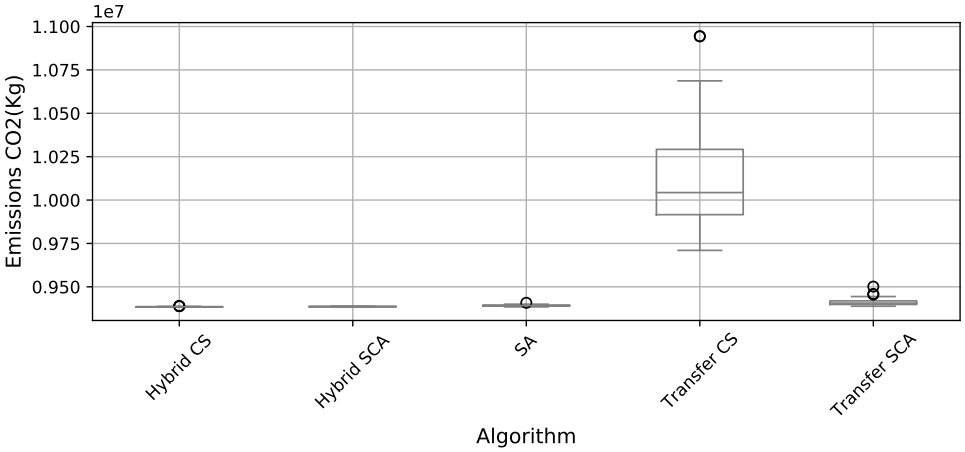

Figure 6.5: Emissions boxplots for SA, discrete transfer SCA, discrete transfer CS, discrete hybrid SCA, and discrete hybrid CS Algorithms.

emissions for all yield stress values. Thus, the CO_2 optimization takes a higher yield stress value because the strength capacity of these steels is higher and is capable of resisting more stresses with less material. Regarding cells dimensions it can be seen that CO_2 best design gets higher values for both upper (h_{c_1}) an lower (h_{c_1}) cells heights. In the case of the cost objective function, the best individual gives a null value to the height of the upper cell. The objective of these cells is to reduce the distance between stiffened zones to reduce the web plate's reduction. For cost optimization, the upper cell does not accomplish this function or is almost not enough to be relevant for the design, while for CO_2 emissions objective function, it allows a better cross-section behavior and takes a positive value. Regarding bottom flange stiffeners ($n_{s_{f_2}}$), both optimization objectives remove this elements for the optimum design. This is because, in negative bending moments, sections exist a concrete slab in the bottom flanges that do not allow the instability of the bottom flange plate, while in positive bending moment sections, this plate is in tension and, consequently, cannot buckle, and these elements are not necessary. Regarding the other variables, both optimization designs give a similar value being the higher difference in the beam height value (h_b), where CO_2 optimization takes a lower value due to the increase in the yield stress (f_{yk}) that allow reducing the Section by increasing the structural steel resistance.

Table 6.8: Design variables results for best, mean, minimum, maximum, and standard deviation values

		Cost optimization				CO_2 optimization			
Variables	**Unit**	**Best**	**Mean**	**Min**	**Max**	**Best**	**Mean**	**Min**	**Max**
b	m	7	7	7	7	7	7	7	7
$alpha_w$	deg	55	63	45	87	71	62.3	45	90
h_s	mm	200	200	200	200	200	200	200	200
h_b	cm	298	304	250	381	286	311	250	388
h_{fb}	mm	410	438	400	610	620	480	400	680
t_{f1}	mm	25	27	25	57	25	26	25	39
b_{f1}	mm	300	309	300	480	300	300	300	300
h_{c_1}	mm	0	264	0	960	9	333	0	830
t_{c_1}	mm	16	16	16	17	16	16	16	16
t_w	mm	16	16	16	16	16	16	16	16
h_{c_2}	mm	33	38.8	00	90	41	32.8	0	86
t_{c_2}	mm	18	19	16	25	18	19	16	25
b_{c_2}	mm	300	302	300	370	300	300	300	300
t_{f_2}	mm	25	25	25	29	25	25	25	25
h_{s_2}	mm	150	150	150	150	150	150	150	150
ϕ_{base}	mm	6	6	6	6	6	6	6	6
ϕ_{r_1}	mm	6	6	6	6	6	6	6	6
ϕ_{r_2}	mm	6	6	6	6	6	6	6	6
n_{r_1}	u	200	278.4	200	436	200	282	200	425
n_{r_2}	u	200	280	200	403	228	270.8	200	418
s_{f_2}	mm	300	322.1	200	550	200	328	200	550
$n_{s_{f_2}}$	u	0	0	0	0	0	0	0	0
s_w	mm	450	327.5	200	600	200	347.6	200	600
s_t	mm	240	306	200	600	200	322.6	200	600
d_{st}	m	3.3	2.407	1	4.2	2.52	1.2	1	5
d_{sd}	cm	6	6.5	4.1	9.7	4.8	6.3	4	9.9
b_{fb}	mm	1000	450	200	1000	200	430	200	1000
$t_{f_{fb}}$	mm	33	29	25	35	29	29	25	34
$t_{w_{fb}}$	mm	27	28	25	35	26	29	25	35
f_{ck}	MPa	25	25	25	25	25	25	25	25
f_{yk}	MPa	275	275	275	275	460	328	275	460
f_{sk}	Mpa	500	500	500	500	500	500	500	500
h_{sc}	mm	100	100	100	100	100	100	100	100
ϕ_{sc}	mm	16	17	16	22	16	16.3	16	22

6.5 Conclusions

The present work proposes a discrete hybrid KMDA method that uses the k-means unsupervised learning technique in conjunction with SCA and SC to solve a discrete optimization issue. It was specifically applied in this work to the design of a Steel-Concrete Composite Bridge. Two experiments were designed to demonstrate the superiority of KMDA in bridge optimization. The first experiment aims to compare the proposed approach to a baseline algorithm in which the discretization stage is executed by a random operator with fixed transition probabilities. $Random0.3$ and $Random0.5$. The results showed that the incorporation of the k-means operator allows obtaining better results, as well as the reduction of the dispersion of the objective values. In the comparison, it was obtained for cost optimization that Hybrid SCA reduced the value by 1.4% compared to $Random0.5$ and by 1.3% compared to $Random0.3$. In the comparison of the emissions of CO_2, considering cost optimization, the hybrid SCA managed to reduce emissions by 1.3% in both cases. The Wilcoxon statistical test showed that the difference is significant. Regarding the execution times, these were similar in the different algorithms.

In the second experiment, the result of the proposed hybrid technique was compared with another frequently used method to discretize algorithms, transfer functions. Additionally, a version of SA adapted to solve civil engineering optimization problems was included. In the case of transfer functions, the solution only uses its information to discretize, unlike k-means which first analyzes the group of solutions and then discretizes. From the results of the experiments, it is once again observed that the proposed hybrid technique is superior in the results obtained. Particularly in the case of cost optimization, it is observed that Hybrid SCA reduced costs on average compared to SA by 1.1 % and compared to transfer SCA by 0.57 %. In the case of Hybrid CS, the result was very similar to that of Hybrid SCA, the latter being 0.05% higher on average. In the case of CO_2optimization, we again observed that the hybrid algorithms were superior to those using transfer function and SA. Hybrid CS outperformed Transfer CS by 7.8%, and up to 0.07% compared to SA. In the case of Hybrid CSA, it outperforms Transfer CSA by 0.3% and SA by 0.07 %.

Finally, an analysis of the optimum obtained was conducted, observing that outstanding results are also obtained for CO_2 emissions when costs are optimized. However, the reciprocal, that is, when emissions are optimized, does not imply that costs are optimized. This was related to the fact that different steel grades have different costs but generate the same emissions.

As a new line of research, we identified that optimization consumes a significant amount of time, near to 8000(s), with which developing algorithms that allow reducing optimization times allows exploring a more significant number of configurations

and more complex situations. When an analysis of the execution times is carried out, we observe that the primary time is consumed to evaluate the constraints. It is hypothesized that by incorporating a deep learning model that does not have essential execution times, the constraints could be modeled and replaced, thereby improving the times used in optimization. Along the same lines, to try to reduce the number of calculations, another idea to explore is to use upper bound strategies (UBS) [277] to reduce the total number of structural analyzes in design optimization.

Chapter 7

Hybrid swarm intelligence optimization methods for low-embodied energy steel-concrete composite bridges

Authors:	D. Martínez-Muñoz , J. García, J.V. Martí, and V. Yepes
Status:	Manuscript published
Journal:	Mathematics, 11(1):140
Year:	2023
DOI:	10.3390/math11010140
JCR IF (2021):	2.592

JCR Category	Ranking	Quartile
Mathematics	21/333	Q1

Presentation:	Post-print (author version)

Abstract

Bridge optimization is a significant challenge, given the huge number of possible configurations of the problem. Embodied energy and cost were taken as objective functions for a box-girder steel–concrete optimization problem considering both as single-objective. Embodied energy was chosen as a sustainable criterion to compare the results with cost. The stochastic global search TAMO algorithm, the swarm intelligence cuckoo search (CS), and sine cosine algorithms (SCA) were used to achieve this goal. To allow the SCA and SC techniques to solve the discrete bridge optimization problem, the discretization technique applying the k-means clustering technique was used. As a result, SC was found to produce objective energy function values comparable to TAMO while reducing the computation time by 25.79%. In addition, the cost optimization and embodied energy analysis revealed that each euro saved using metaheuristic methodologies decreased the energy consumption for this optimization problem by 0.584 kW·h. Additionally, by including cells in the upper and lower parts of the webs, the behavior of the section was improved, as were the optimization outcomes for the two optimization objectives. This study concludes that double composite action design on supports makes the continuous longitudinal stiffeners in the bottom flange unnecessary.

Keywords: swarm intelligence; steel–concrete composite structures; bridges; optimization; metaheuristics; sustainability

7.1 Introduction

Structural engineering has been traditionally based on materialized safety solutions reducing the investment to the minimum. However, the current search for solutions that fall within the definition of sustainable development makes that criterion insufficient. Regarding this, other criteria have arisen to add the concept of sustainability to structures [221]. Introducing new design criteria in structural problems increases complexity, moving this problem to the decision-making field of knowledge. In order to assess the sustainability of solutions, life cycle assessment has become one of the most widely used tools to evaluate the social and environmental profile of a solution [278], [279]. Nevertheless, in order to approximate an environmental assessment, one representative criterion can be chosen as an alternative. The most used criteria in these cases are the CO_2 emissions and the energy consumption [280], [281]. Regarding this, structural optimization research in recent years has focused on applying different techniques to obtain optimal designs considering CO_2 emissions and embodied energy as well as cost as optimization objectives. In conclusion, in concrete

structures, many research studies have shown a clear relation between the three criteria [124], [173].

The energy required to build a structure, like CO_2 emissions, is an indicator of sustainability [282]. However, there are different definitions of the energy required in the case of a structure. Each definition implies a different method of calculation. Therefore, there has yet to be a consensus in the scientific community regarding a single definition and calculation methodology [283], [284]. Heuristic steel or composite structures were optimized in works such as Whitworth and Tsavdaridis [285]. In structures made of reinforced concrete, the reduction of the required energy can be accomplished optimizing the use of materials instead of directly changing traditional to new construction materials. Some authors have used energy as an objective function in structural optimization [286]–[288].

To address civil engineering optimization problems, particularly in the design of structures, heuristic methods have had interesting results [289]. One of the most representative structures of civil engineering is bridges because they can connect different geographical locations. This type of structure also stands out for its complexity in obtaining optimal solutions due to the high number of design possibilities. In order to obtain optimum designs, heuristic optimization techniques are put forth as an alternative to traditional experience-based design. These methods allow for reaching optimum designs ensuring compliance with the restrictions imposed by regulations, adding these as problem constraints. These methods were extensively applied in many types of structures, such as road vaults [212] or walls [172], among others.

Regarding bridge energy optimization, Penadés-Plà et al. [124] proposed a Kriging-based optimization approach that cut computing time by 99.06% and produced results that differed from heuristic optimization's use of simulated annealing by just 2.54%. This research work was applied to optimize the embodied energy of a three-span 40–50–40 m continuous box-section footbridge.

However, recent review works highlight a lack of knowledge in applying heuristic and metaheuristic techniques to steel–concrete composite bridges (SCCB) [189] compared to concrete bridges. The techniques applied to that type of structure are: set-based parametric design [106], harmony search (HS) [109], genetic algorithm (GA), and imperialist competitive algorithm [103], among others. In addition, some particle swarm algorithms were applied to carry out SCCB optimizations [109]. However, in those studies, the unique criterion taken as an objective function is the cost. Thus, researchers have only considered the economic pillar of sustainability in some isolated studies. This shows a lack in SCCB sustainable designs research, which is not in line with the current policy of countries that seek economically viable solutions and are environmentally and socially friendly.

Therefore, this study proposes to optimize a composite steel and concrete bridge using embodied energy as the objective function. The main purpose of this research is to obtain an energy-embodied optimum design. For this, two types of metaheuristics were applied in order to use the one that reaches the best behavior for this optimization problem. Due to the large number of variables that the bridge presents, it is an important challenge for optimization algorithms. Since this energy optimization problem has not been solved before and there is no comparison baseline, it has been proposed to use and compare two groups of techniques. The first one is based on a global stochastic search (threshold accepting with a mutation operator algorithm) and was used before in solving similar problems with good results. The second is based on hybrid methods that integrate machine learning algorithms in the discretization process of continuous swarm intelligence methods. This technique has been used to solve combinatorial problems with a binary representation [290]. The current work proposes a variation to address the discrete problem. In this work, first, an analysis of the contribution of the hybrid method to the optimization result is carried out through the comparison with random discretization methods. Additionally, the main parameter (β) used in the hybrid method is analyzed in order to identify its contribution to the optimization result. Subsequently, the hybrid method is compared with the threshold accepting with a mutation operator algorithm. The comparison is made through the minimization of the embodied energy and of the costs. Finally, the different solutions found in both optimizations are analyzed and compared. For this, in Section 7.2, the optimization problem variables, parameters, and constraints were defined. Section 7.3 describes the different optimization algorithms used and their tuning. Subsequently, Sections 7.4 and 7.5 show the results and the comparison with previous studies. As it can be seen in Section 7.6, results of the study show that the cost and the embodied energy are clearly related when optimizing cost; however, optimizing embodied energy does ot necessarily result in a cost-optimal solution.

In conclusion, it should be mentioned that other types of particle swarm optimization algorithms [291], [292] and other methods, such as differential evolution ones [293], [294], can be applied in future research to study their behavior for this optimization problem. Moreover, in the new studies, new sustainability criteria, such as the complete life cycle assessment, will be chosen for carrying out multi-objective optimization. As the calculation of more and higher complexity objective functions can increase the computational time, the use of metamodels generated with machine learning techniques will be taken into account.

7.2 Optimization Problem Description

The problem posed in this study is the minimization of the objective function that evaluates the embodied energy and the cost of a steel–concrete composite bridge (SCCB). To deal with this problem, the bridge was parameterized. In this case, cost and embodied energy criteria were considered as a single objective in order to compare the designs obtained from both optimizations. In Equation (7.1), the embodied energy target function was defined. Data for embodied energy considers cradle-to-gate analysis; thus, it considers all processes necessary from obtaining raw materials , their conversion into those elements that will allow performing the bridge resistant section, and their final placement on-site. Data of embodied energy and costs in Table 7.1 were obtained from the Construction Technology Institute of Catalonia by the BEDEC database [207]. Furthermore, the cost objective function is formulated in Equation (7.2). Both objective functions must meet the regulation and recommendation constraints' represented by Equation (7.3). Meeting these constraints will ensure the feasibility of the obtained solution from the optimization procedure. Expressions (7.1) and (7.2) represent the multiplication of each material measurement multiplied by the embedded energy (e_i) and price (p_i), respectively.

$$E(\vec{x}) = \sum_{i=1}^{n} e_i \cdot m_i(\vec{x}) \tag{7.1}$$

$$C(\vec{x}) = \sum_{i=1}^{n} p_i \cdot m_i(\vec{x}) \tag{7.2}$$

$$G(\vec{x}) \leq 0 \tag{7.3}$$

Table 7.1: Embodied energy and cost values for materials.

Material	Unit	Energy (kW·h)	Cost (€)
Concrete C25/30	m^3	402.44	88.86
Concrete C30/37	m^3	428.29	97.80
Concrete C35/45	m^3	429.95	101.03
Concrete C40/50	m^3	429.95	101.03
Precast pre-slab	m^2	175.87	27.10
Steel B400S	m^2	3.38	1.40
Steel B500S	m^2	3.38	1.42
Rolled steel S275	m^2	12.23	1.72
Rolled steel S355	m^2	12.23	1.85
Rolled steel S460	m^2	12.23	2.01
Shear-connector steel	m^2	13.52	1.70

7.2.1 Variables and Parameters

A 220 m continuous three-span box-girder steel and concrete composite bridge was defined as the optimization problem. According to the variables, these correspond to each bridge element's geometry, reinforcement, concrete, and steel grades. All of these variables were discretized in order to arrive at a real constructible solution, hence constituting a discrete optimization problem. The discretization of variables is defined in Table 7.2. The number of feasible optimization solutions is equal to 1.38×10^{46}

when this variable discretization is considered. Metaheuristic methods are appropriate for locating the best answer when so many combinations are possible. This bridge optimization problem's global formulation considers 34 different variables in total. These bridge variables are illustrated in Figure 7.1. The variables nature can be classified into six categories. First are the geometric variables of the transverse section, which are: distance between wings on top (b), angle between wings and flanges (α_w), thickness of the upper slab (h_s), depth of the steel section (h_b), floor beam lower value (h_{fb}), upper flange thickness (t_{f_1}), upper flange width (b_{f_1}), upper cells height (h_{c_1}) and thickness (t_{c_1}), wings thickness (t_w), low cells height (h_{c_2}), thickness (t_{c_2}), and width (b_{c_2}), and low slab thickness (h_{s_2}). Beam depth limits are defined as L/40 and L/25, L being the longest length of the spans.

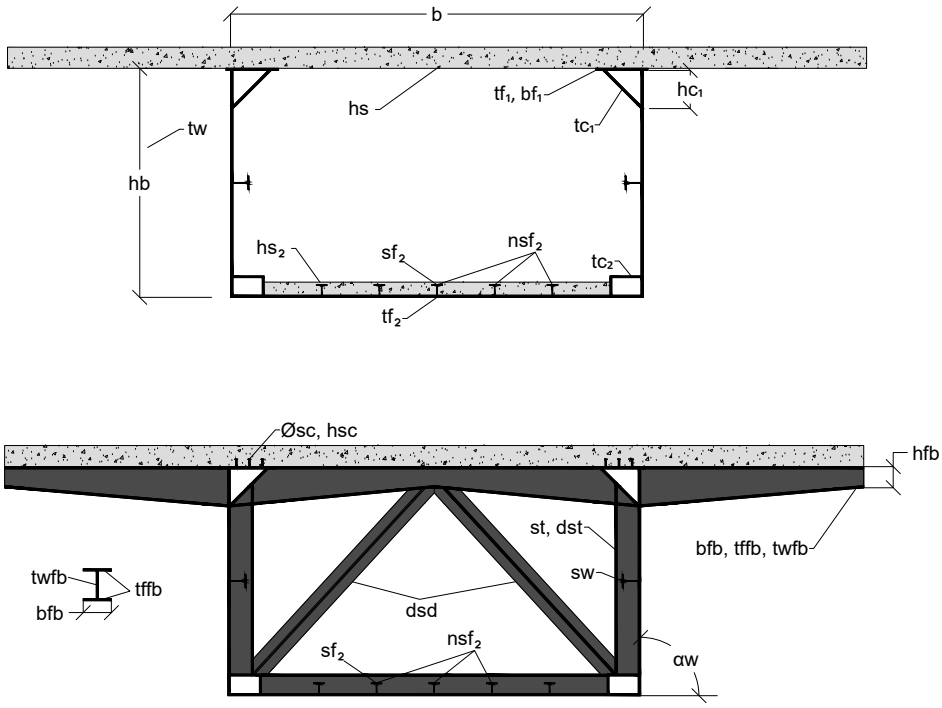

Figure 7.1: Transverse section variables for the optimization problem.

SCCBs can utilize materials more effectively, profiting from the material location. This is true in statically determined girders. In this case, the upper concrete slab is materialized along the whole length of the bridge. This upper slab is attached to the upper flanges by shear connectors. This reinforces the flange plate, preventing it from buckling. Moreover, in the case of isostatics, the lower flanges would be subjected to tensile stress, avoiding buckling instability problems. In this problem, negative bending stresses will arise in supported portions under the typical loads (mostly gravitational) to which road bridges are subjected. This will cause a reversal of forces and tensile strains in the upper concrete slab and compression in the lower flange. In this instance, to improve the behavior of the bridge's cross section, it was decided to realize a concrete bottom slab in this zone in addition to the reinforcement of the top slab. In order to optimize the reinforcement of the top slab, it was separated into a base reinforcement that is the least necessary by regulations [26], [237], [238] and two additional layers in negative bending sections, where the reinforcement is enhanced. Accordingly, the second group of variables corresponds to base rein-

forcement, first reinforcement and second reinforcement bar diameters (ϕ_{base}, ϕ_{r_1}, ϕ_{r_2}), and the corresponding bar number of the reinforcement areas (n_{r_1}, n_{r_2}).

In order to avoid buckling of steel plates, stiffeners were defined as the third category of the problem variables considering half IPE profiles for wings, bottom flange, and the transverse stiffeners (s_w, s_{f_2}, s_t). In order to allow the optimization procedure to define the number of stiffeners of the bottom flange ($n_{s_{f_2}}$), this is considered as a variable placing them evenly distributed over the width.

To finalize the geometrical variables definition, the shear connectors and floor beam geometry were defined through the width of the floor beam (b_{fb}), thicknesses of the flanges ($t_{f_{fb}}$) and webs ($t_{w_{fb}}$), and the shear connectors height (h_{sc}) and diameter (ϕ_{sc}). To determine the materials strength, the rolled steel tensile stress (f_{yk}), concrete strength (f_{ck}), and reinforcement steel tensile stress (f_{sk}) were also defined as variables.

Table 7.2: Optimization problem variables and boundaries.

Variables	Unit	Lower Limit	Upper Limit	Step Size	Possibilities
Geometrical variables					
b	m	7	10	0.01	301
α_w	deg	45	90	1	46
h_s	mm	200	400	10	21
h_b	cm	250 (L/40)	400 (L/25)	1	151
h_{fb}	mm	400	700	100	31
t_{f_1}	mm	25	80	1	56
b_{f_1}	mm	300	1000	10	71
h_{c_1}	mm	0	1000	1	101
t_{c_1}	mm	16	25	1	10
t_w	mm	16	25	1	10
h_{c_2}	mm	0	1000	10	101
t_{c_2}	mm	16	25	1	10
b_{c_2}	mm	300	1000	10	71
t_{f_2}	mm	25	80	1	56
h_{s_2}	mm	150	400	10	26
Stiffeners					
$n_{s_{f_2}}$	u	0	10	1	11
d_{st}	m	1	5	0.1	41
d_{sd}	m	4	10	0.1	61
s_{f_2}	mm	IPE 200-IPE 600 *			12
s_w	mm	IPE 200-IPE 600 *			12
s_t	mm	IPE 200-IPE 600 *			12
Floor beams					
b_{fb}	mm	200	1000	100	9
$t_{f_{fb}}$	mm	25	35	1	11
$t_{w_{fb}}$	mm	25	35	1	11
Reinforcement					
n_{r_1}	u	200	500	1	301
n_{r_2}	u	200	500	1	301
ϕ_{base}	mm	6, 8, 10, 12, 16, 20, 25, 32			8
ϕ_{r_1}	mm	6, 8, 10, 12, 16, 20, 25, 32			8
ϕ_{r_2}	mm	6, 8, 10, 12, 16, 20, 25, 32			8
Shear Connectors					
h_{sc}	mm	100, 150, 175, 200			4
ϕ_{sc}	mm	16, 19, 22			3
Material strength					
f_{ck}	MPa	25, 30, 35, 40			4
f_{yk}	MPa	275, 355, 460			3
f_{sk}	MPa	400, 500			2

*Following the standard series of IPE profiles [239].

Table 7.3 defines the parameters used for the bridge optimization problem. These parameters consider the Eurocode structural checks [26], [237], [238], the bridge spans length that corresponds to 60–100–60 m as can be seen in Figure 7.2, the deck width (B) of 16 m, and the upper and lower bound for the variables considering regulations [26], [237], [238] and design guides [25], [242].

Table 7.3: Parameters of the SCCB optimization problem.

Geometrical parameters		
Bridge deck width (W)	16	m
Span number	3	
Central span length	100	m
External span length	60	m
Minimum web thickness ($t_{w_{min}}$)	15	mm
Minimum flange thickness ($t_{f_2 min}$)	25	mm
Reinforcement cover	45	mm
Material parameters		
Maximum aggregate size	20	mm
Concrete longitudinal strain modulus (E_{cm})	$22 \cdot ((f_{ck} + 8)/10)^3$	MPa
Concrete transverse strain modulus (G_{cm})	$E_{cm}/(2 \cdot (1 + 0.2))$	MPa
Steel longitudinal strain modulus (E_s)	210,000	MPa
Steel transverse strain modulus (G_s)	80,769	MPa
Regulation requirement parameters		
Regulations	Eurocodes [26], [237], [238], [240], IAP-11 [241]	
Exposure environment	XD2	
Structural class	S5	
Service life	100	years
Loading parameters		
Reinforced concrete density	25	kN/m^3
Steel density	78.5	kN/m^3
Asphalt density	24	kN/m^3
Asphalt layer thickness	100	mm
Bridge traffic protections	5.6	kN/m
Traffic load	Eurocode 1 [240]	
Thermal load	Eurocode 1 [240]	
Wind load	Eurocode 1 [240]	

Upper and lower slab reinforcements were set with the minimum amount required for reinforcement in Eurocode 2 [238]. The connection was obtained considering the concrete slab stresses. Effective widths due to shear lag are calculated considering Eurocode 4 [26] as only this part is considered as resistant. The steel bar reinforcements (ϕ_{r_1}, ϕ_{r_2}) were placed only in the effective width. Lower slabs defined on

supports are placed on the first and last third of every span corresponding to the shear lag negative bending areas defined in Eurocode 4 [26].

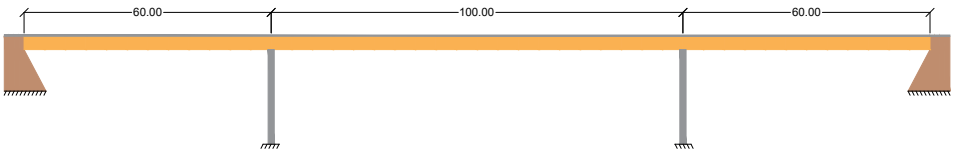

Figure 7.2: Bridge spans length of the SCCB bridge.

7.2.2 Structural Analysis and Constraints

The constraints of the optimization problem correspond to the structural safety and serviceability checks defined by the regulations [26], [237], [238]. Furthermore additional constraints were incorporated following some design guides [25], [242].

Constraints defined by Eurocodes correspond to ultimate limit states (ULS) and serviceability limit states (SLS). ULS correspond to the structural resistance of bridge sections, while SLS correspond to the defined materials stresses and deflection limits. The loads and combination defined correspond to those imposed by Eurocode 1 [240] and are summarized in Table 7.3.

For ULS checks, both local and global analyses were performed. For global analysis, the checks corresponded to: shear, flexure, torsion, and flexure–shear interaction. To obtain the sections resistance, the reductions due to shear lag [26] and slenderness of Class 4 sections [238] were considered. The precision of the Class 4 reduction iterative process was defined in 10^{-6}. Sections were homogenized considering the coefficient (n) between the longitudinal deflection modulus of concrete (E_{cm}) and steel (E_s) as defined in Equation (7.4). Concrete creep and shrinkage were defined following the Eurocodes [26], [237], [238] standard. For developing the floor beams and diaphragm behavior to ULS, local modeling was performed.

$$n = \frac{E_s}{E_{cm}} \tag{7.4}$$

Deflection, material's tension limit, and fatigue were defined as SLS constraints. The deflection limit was defined following Spanish regulation IAP-11 [241], fixing $L/1000$ as the maximum deflection value for live loads' frequent combination. In this case, L l represents each span length. Furthermore, restrictions for construction and geomet-

rical requirements were defined. All structural checks were defined using a numerical model programmed with Python language.

7.3 Optimization Algorithms

7.3.1 Trajectory-Based Algorithm: Threshold Accepting with a Mutation Operator (TAMO)

Duec and Scheuer [295] developed threshold accepting (TA), as an alternative to Kirpatricks' simulated annealing (SA) [244]. Both metaheuristics are within the trajectory-based group . These algorithms vary the problem variables and compare the objective functions obtained. The rejection or acceptance of the new solution depends on the criteria chosen. SA applies an acceptation criteria formula that gives the new solution a probability of being chosen, even worsening the objective function value. TA applies a more specific criterion by applying a threshold where the solution is directly accepted if its objective function value is inside. Accepting bad solutions enhances the optimization process and allows for avoiding local optimums. While the optimization process is performed, the threshold is reduced to exploit the optimum neighborhood. This study has applied threshold accepting with a mutation operator (TAMO) [296]. As the original TA, this algorithm starts with a random solution and an initial threshold. According to Medina's criterion [245], the initial threshold (U_0) is raised or lowered until the acceptability range is between 20% and 40%. The difference lies in the fact that in each iteration, the new solution can be modified, simulating the mutations of genetic algorithms. This modification allows adding exploration to the optimization process.

The TAMO algorithm has specific parameters that adjust it to the problem being solved. These parameters are variables number (VN), chain length (CL), standard deviation for mutation operator (SD), cooling coefficient (CC), and unimproved chains (UC). VN limits the number of variables changed in each iteration. CL defines the number of iterations run for each threshold. SD is related to the mutation operator's probability of mutation of the solution. CC defines the threshold reduction when the CL is reached. Finally, the UC defines the number of chains without improvement allowed before the optimization process is ended. In addition to UC, if the threshold arrives at 0.05% of the initial, then the optimization process is also finished. The parameters chosen for this optimization problem are those described in Section 7.3.5.

7.3.2 Sine Cosine Algorithm (SCA)

In [233], the sine cosine algorithm (SCA) was proposed. When exploring and using the search space, the swarm intelligence algorithm considers the sine and cosine functions. The procedure additionally employs P_j^t to relocate the solutions. It is the location of the final solution for iteration t and dimension j and is often the finest result thus far. Along with P_j^t, the technique uses three random numbers, $r_1, r_2, and r_3$, with values ranging from zero to one. Equations (7.5) and (7.6) illustrate the update method employed.

$$x_{i,j}^{t+1} = x_{i,j}^t + r_1 \times sin(r_2) \times |r_3 P_j^t - x_{i,j}^t| \tag{7.5}$$

$$x_{i,j}^{t+1} = x_{i,j}^t + r_1 \times cos(r_2) \times |r_3 P_j^t - x_{i,j}^t| \tag{7.6}$$

7.3.3 Cuckoo Search Algorithm

The cuckoo species is distinguished by depositing their eggs in other bird species nests; this way of behaving inspired the CS algorithm. Cuckoos are so sophisticated that they can imitate the colors and patterns of their chosen host species' eggs in some situations. An egg, in this instance, represents a solution. The analogy's premise is that the best solutions (cuckoos) should be used to replace those that do not function adequately. The CS algorithm is based on three fundamental rules:

1. One egg is laid by each cuckoo at a time, and it is placed in a nest that is chosen at random.
2. The best nests, or those that produce eggs of a high caliber, will be taken into consideration for the succeeding generation.
3. The number of available nests is a fixed value. With a chance of $p_a \in (0, 1)$, the cuckoo's egg will be found by the host bird.

$$x_{i,j}^{t+1} = x_{i,j}^t + \alpha \bigoplus \text{Lévy}(\lambda) \tag{7.7}$$

where $\alpha > 0$ is the step size that should be proportional to the problem's scales. The product $\bigoplus$ refers to entry-level multiplications. Through the use of a Lévy distribution to determine the random step length, the Lévy flight replicates a random walk, Lévy $\sim t^{-\lambda}$, $1 < \lambda \leq 3$.

7.3.4 Hybrid Swarm Intelligence: SCA and CS

Because both metaheuristics perform naturally in continuous domains, the hybrid method is used in the case of swarm intelligence metaheuristics. It takes the metaheuristic, MH, the list of discrete solutions acquired in the previous iteration, $lSol$, and a list of transition probabilities $transitionProbs$ as input parameters. It returns a new list of discrete solutions, $lSol$, as an output. In the first stage, the discretization method determines the MH's velocities. These velocities in the case of CSA and CS correspond to the component obtained by the difference between $|x_{i,j}^{t+1} - x_{i,j}^{t}|$ in Equations (7.5) to (7.7).

Following that, a k-means clustering technique is applied to convert the velocity values, which can take on values in $\mathbb{R}$, to transition probabilities values which take values in [0,1). The k-means technique clustering the velocities generating clusters in this specific case were five clusters. The clusters were sorted from the smallest to larger centroids. In the case of the smallest centroid, the smallest transition probability was assigned to all cluster velocities. The largest transition probability is assigned to all cluster points in the case of the largest centroid. Figure 7.3 shows a diagram with the k-means procedure. The values of transition probabilities used for this article were [0.1, 0.2, 0.4, 0.8, 0.9].

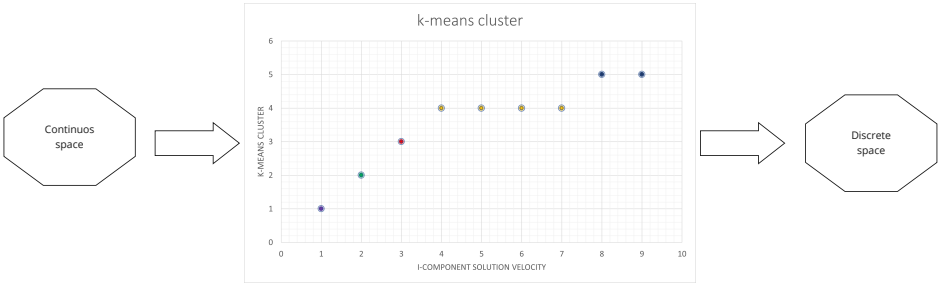

Figure 7.3: K-means discretization technique chart.

Then, for each dimension of each solution, a transition probability $DimSol\ Prob_{i,j}$ is obtained. If this probability is more significant than a random number, r_1, and a β parameter is greater than a random number, r_2, this dimension of the solution is updated with the value of the best solution obtained,until now. The procedure is updated with a random permitted value if the β condition is not fulfilled. In the case neither transition probability nor β condition is fulfilled, the dimension of the solution is not updated. This final option is intended to enhance the search space's exploration.

7.3.5 Parameter Tuning

The metaheuristics' results are dependent on the values of its parameters. As a result, a process of parameter selection is required to determine which parameters produce the greatest results for the goal function. This is highly dependent on the optimization problem. As a result, various optimization problems will provide a range of parameter values. Parameter tuning is the process of determining which parameters best fit the optimization problem.

TAMO Tuning

The number of parameters changes according to the metaheuristic. There are algorithms with more parameters than others, such as TAMO. Locating the most suitable ones might become a pretty hard job. As a result, current approaches enable the researcher to obtain the most statistically significant factors and concentrate the search on their variation. These are referred to as Design of Experiments (DoE). To obtain the TAMO parameter adjustment in this scenario, a 2^k fractional factorial design was used.

In factorial designs, each trial or replication examines all potential combinations of the factor levels. This enables the evaluation of the response's change as the factor level varies. This change is referred to as the factor's effect, and it is proportional to the factor's statistical significance [248]. Two levels must be allocated to the investigated algorithm parameters to carry out this operation. The parameters tested and the levels chosen are 100 and 100 for every step length, 0% and 30% for the standard deviation, 1 and 5 for the variable number change, 0.80 and 0.95 for the cooling coefficient, and 1 and 5 for the steps without improving.

Since each variable has two levels defined, 32 (2^5) runs are required to obtain a complete factorial design. Additionally, 5 replications are required to obtain the average and deviation for each experiment, resulting in a total of 160 runs. A fractional factorial DoE of resolution V was chosen to minimize the number of runs. This reduces the number of runs to 80 as the number of combinations is reduced to 16. Table 7.4, summarizes the parameter value combinations.

Table 7.4: Results for each parameter combination of the DoE.

	CL	SD	VN	CC	UC	Cost (€)	%Desv	Time (s)	%Desv
1	-	-	-	-	+	4,479,632.69	11.60%	1,066.43	7.42%
2	+	-	-	-	-	3,822,939.15	0.01%	8,945.34	1.66%
3	-	+	-	-	-	4,323,458.35	11.19%	1,074.43	3.73%
4	+	+	-	-	+	3,822,726.91	0.00%	8,707.18	2.27%
5	-	-	+	-	-	4,157,630.63	2.36%	373.77	8.33%
6	+	-	+	-	+	3,829,609.10	0.08%	2,776.87	10.37%
7	-	+	+	-	+	4,483,512.89	5.27%	376.63	11.12%
8	+	+	+	-	-	3,833,429.00	0.07%	2,768.47	2.72%
9	-	-	-	+	-	3,953,288.27	7.13%	2,668.19	5.68%
10	+	-	-	+	+	3,822,727.51	0.00%	23,570.64	0.88%
11	-	+	-	+	+	4,075,329.14	4.63%	2,743.15	5.30%
12	+	+	-	+	-	3,822,729.18	0.00%	23,265.95	0.76%
13	-	-	+	+	+	4,003,714.99	6.53%	1,180.30	2.97%
14	+	-	+	+	-	3,831,006.92	0.11%	10,347.75	5.33%
15	-	+	+	+	-	4,058,998.41	5.05%	1,295.28	16.48%
16	+	+	+	+	+	3,826,230.52	0.08%	10,059.03	2.73%

As shown in Table 7.4, the best results in terms of cost are obtained with Experiment 4. Furthermore, the deviation in cost is negligible. For these reasons, the parameters chosen for the TAMO algorithm correspond to those used in Experiment 4.

Hybrid Swarm Intelligence Methods Tuning

The process for choosing parameters employs four metrics to make an appropriate parameter selection: the best, the average, the worst value, and the time obtained in the different runs executed. Table 7.5 summarizes the parameters and their explored values. The Range column displays the values that were explored for each of the parameters. The Value column contains the currently selected value. We scanned eight parameter settings and repeated each setting five times.

Table 7.5: Scanned parameters for the cuckoo search algorithm.

Parameters	Description	Value	Range
N	Number of solutions	10	[10, 20]
Iteration Number	Maximum iterations	600	[600, 800]
β	Exploration–exploitation	0.8	[0.3, 0.5, 0.7, 0.8]
α	Step Length	0.01	0.01
λ	Levy distribution parameter	1.5	1.5
Transition probability	Transition probability	[0.1, 0.2, 0.4, 0.8, 0.9]	[0.1, 0.2,[0.4, 0.5],0.8, 0.9]

7.4 Results

This section details the results of the experiments carried out. Section 7.4.1 studies the contribution of the hybridization method to the final result of the optimization in addition to the value configured for the values of β. In addition to the tables, descriptive statistical analyzes are considered. In particular, descriptive statistics are combined with violin plot visualizations for a comprehensive study. The statistical significance of the results is also determined using the Kolmogorov–Smirnov–Lilliefors and Wilcoxon signed-rank statistical tests. The statistical methods described in Figure 7.4 [252] were used to select these tests. Later, in Section 7.4.2, the proposed hybrid algorithms CS and SCA are compared with TA; the latter was successfully used to solve other related optimization problems. Finally, Section 7.4.3 analyzes the results of the best value obtained.

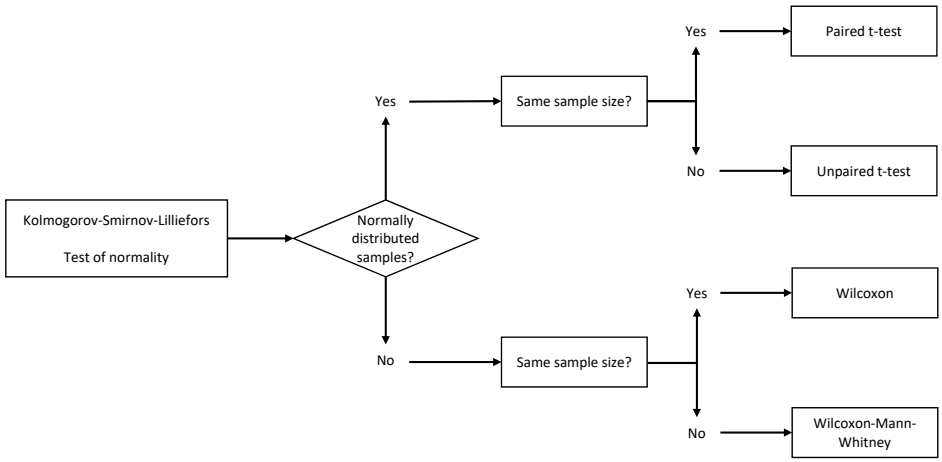

Figure 7.4: Statistical method.

7.4.1 Parameters Exploration of the Hybrid Algorithm

This section aims to identify the contribution of the k-means technique in the discretization process as well as to explore the importance of the β operator in the optimization result. To achieve the objective, two experiments were developed. The first corresponds to a comparison between the hybrid versions for SCA and CS with random discretization methods. The second involves comparing the results of using different values of the β parameter. For the construction of the random operator, in Algorithm 4, the getClusterProbability function was replaced by a uniform random number generator in Line 8 . This operation produces values ranging from zero to one. Line 9 of the method also sets up 2 values for $dimSolProb$; it sets the initial value in ($Random\,0.5$), which corresponds with a probability of transition of 50%. For the second value, the value is set to 0.7 ($Random\,0.3$), corresponding to a probability transition of 30%. For this experiment, the value of β used was 0.8. The result is displayed in Table 7.6.

Table 7.6 shows that for both CS and SCA the hybrid version is superior to both random versions. In the specific case of CS, which was the one that obtained the best result, when comparing it to its random versions, the average indicator in the hybrid version was 0.59% higher than $CS - Random\,0.5$ and 0.6% for the case of $CS - Random\,0.3$. The Wilcoxon statistical test indicates that the difference is significant in all cases. The experiment's main objective was to evaluate the impact of the clustering function (getClusterProbability); the experiment showed that the im-

pact on the optimization results is significant for the CS and SCA cases. The second experiment, which is detailed in Table 7.7, evaluates the impact of the parameter β used in Line 10 of Algorithm 4. Three conditions, $\beta = \{0.3, 0.5, 0.8\}$, were verified. Both metaheuristics were again evaluated. The parameter β determines if the movement is going to follow the best solution (Line 11) or considers a random movement (Line 13); the latter has the sense of developing an exploration of the search space. The higher the value is, the more limited the exploration will be. According to the results, the value that obtained the best results was 0.8. The differences were not as large as in the previous case; however, according to the Wilcoxon test, they were significant in all cases.

Algorithm 4 Hybrid algorithm.

1: **Function** Discretization($lSol$, MH,$transitionProbs$)
2: **Input** $lSol$, MH, $transitionProbs$
3: **Output** $lSol$
4: $vlSol \leftarrow$ getVelocities($lSol$, MH)
5: $lSolClustered \leftarrow$ appliedKmnsClust($vlSol$, K)
6: **for** (each Sol_i in $lSolClustered$) **do**
7: **for** (each $dimSol_{i,j}l$ in Sol_i) **do**
8: $dimSolProb_{i,j}$ = getClustProb($dimSol$, $transitionProbs$)
9: **if** $dimSolProb_{i,j} > r_1$ **then**
10: **if** $beta > r_2$ **then**
11: Update $lSol_{i,j}$ using the best.
12: **else**
13: Update $lSol_{i,j}$ using a random value allowed.
14: **end if**
15: **else**
16: Don't update the item in $lSol_{i,j}$
17: **end if**
18: **end for**
19: **end for**
20: **return** $lSol$

Table 7.6: Comparison of random with hybrid discretization algorithms in the embodied optimization problem.

	CS-Hybrid		CS-Random 0.5		CS-Random 0.3		SCA-Hybrid		SCA-Random 0.5		SCA-Random 0.3	
Run	**Cost (€)**	**Energy (kW·h)**	**Cost (€)**	**Energy (kW·h)**	**Cost (€)**	**Energy (kW·h)**	**Cost (€)**	**Energy (kW·h)**	**Cost (€)**	**Energy (kW·h)**	**Cost (€)**	**Energy kW·h**
1	4,096,945.7	26,685,288.4	4,144,609.5	26,924,597.2	3,901,827.4	27,054,482.8	4,093,040.7	26,675,993.4	3,893,662.8	26,993,377.1	3,960,137.9	27,344,487.5
2	3,825,898.2	26,677,834.4	4,128,651.0	26,827,502.2	4,158,129.4	27,012,480.6	3,833,087.9	26,694,948.0	3,922,221.6	27,158,981.4	3,894,003.8	26,994,996.4
3	4,094,985.4	26,680,668.9	3,848,284.2	26,782,468.4	4,488,718.2	26,920,032.6	4,093,055.8	26,676,029.4	3,939,000.7	27,237,960.1	3,902,733.6	27,041,432.2
4	4,092,167.0	26,673,913.8	4,128,797.8	26,825,120.9	4,158,129.4	27,012,480.6	4,431,425.5	26,696,563.9	3,896,661.8	27,081,425.9	3,882,735.9	26,890,936.9
5	4,090,639.1	26,670,276.8	4,099,424.2	26,706,958.3	3,847,222.5	26,744,603.2	3,832,058.8	26,692,528.2	3,882,294.8	27,047,746.5	3,872,531.6	26,870,535.1
6	4,428,019.7	26,688,457.2	4,457,224.7	26,803,634.0	3,848,295.5	26,782,495.4	3,827,006.3	26,680,472.1	3,870,409.1	26,896,521.3	3,853,870.1	26,865,455.3
7	4,092,030.9	26,673,589.7	4,512,757.8	27,010,214.1	3,901,410.8	27,051,726.7	4,097,544.0	26,686,759.0	3,856,030.7	26,794,705.4	3,895,172.4	27,033,901.0
8	4,090,639.1	26,670,276.8	4,429,502.6	26,708,460.1	3,888,138.1	26,923,550.4	3,824,911.8	26,676,124.8	3,841,775.5	26,763,858.5	3,882,310.3	26,973,266.3
9	3,828,638.3	26,684,356.6	3,828,880.8	26,699,699.6	4,511,638.5	26,992,955.9	4,420,381.8	26,670,276.8	3,871,312.6	26,935,825.3	3,859,508.9	26,891,452.3
10	4,098,046.3	26,687,908.1	3,900,002.1	27,088,694.5	4,534,699.3	27,057,884.7	3,831,043.8	26,691,335.4	3,866,380.4	26,912,272.5	3,867,904.2	26,868,955.3
11	3,822,723.1	26,670,276.8	4,108,676.9	26,746,543.2	4,478,184.2	26,862,464.8	4,424,708.5	26,680,575.6	3,900,122.2	27,021,209.4	3,896,980.1	27,049,283.8
12	3,822,723.1	26,670,276.8	4,118,910.4	26,771,292.7	4,473,260.4	26,857,346.9	4,094,550.7	26,679,759.9	3,869,631.8	26,854,424.5	3,893,663.9	26,913,646.3
13	4,428,645.6	26,689,947.1	4,098,320.3	26,703,158.2	4,469,122.9	26,832,577.3	3,829,345.5	26,686,040.1	3,945,317.9	27,483,275.5	3,847,065.1	26,784,215.9
14	3,822,723.1	26,670,276.8	4,490,894.9	26,969,332.4	447,8421.1	26,862,181.6	4,422,860.9	26,676,177.9	3,847,634.6	26,796,203.7	3,847,065.1	26,784,215.9
15	4,098,144.6	26,688,142.1	4,457,422.2	26,808,045.1	4,117,687.8	26,764,481.3	4,098,585.6	26,689,191.9	3,884,650.8	26,986,971.4	3,915,411.6	27,174,939.5
16	4,422,083.7	26,674,327.9	3,854,295.6	26,788,264.6	3,847,812.4	26,759,388.3	4,092,465.8	26,674,625.0	3,895,513.5	27,054,362.7	3,907,472.4	27,075,044.5
17	3,824,886.5	26,675,426.2	3,854,295.6	26,788,264.6	4,443,136.5	26,745,155.0	4,095,168.1	26,681,057.2	3,858,451.9	26,840,052.0	3,899,246.9	27,039,139.2
18	3,822,723.1	26,670,276.8	3,852,081.5	26,774,783.3	4,447,647.7	26,795,306.0	3,828,464.3	26,683,942.5	3,903,872.8	27,016,029.5	3,886,928.7	26,991,286.3
19	4,420,381.8	26,670,276.8	4,506,898.1	27,038,234.2	4,434,209.6	26,713,701.8	3,827,046.0	26,680,566.6	3,857,355.7	26,808,143.3	3,880,757.4	26,948,312.1
20	4,094,744.5	26,680,049.0	4,145,753.5	26,907,828.9	4,433,091.4	26,708,831.5	4099,757.7	26,691,981.7	3,866,415.5	26,856,837.2	3914,838.9	27,195,185.8
21	4,090,639.1	26,670,276.8	4,125,813.1	26,841,024.4	4,428,324.5	26,701,767.9	3,823,789.7	26,672,815.5	3,937,042.1	27,276,778.9	3,908,855.7	27,119,308.0
22	3,822,984.1	26,670,898.0	3,848,295.5	26,782,495.4	4,184,216.4	26,933,919.9	3,822,723.1	26,670,276.8	3,918,734.3	27,083,247.5	3,865,973.2	26,927,294.5
23	4,096,497.5	26,684,221.6	4,137,720.7	26,889,362.7	4,452,906.4	26,792,502.2	4,091,739.6	26,672,896.5	3,876,224.8	26,881,663.2	3,849,356.8	26,818,040.5
24	4,098,033.0	26,687,876.6	4,514,684.8	27,030,757.5	4,439,421.1	26,721,222.5	4,421,414.3	26,672,734.5	3,937,528.5	27,300,880.0	3,917,215.2	27129984.4
25	4,093,116.3	26,676,173.4	4,161,558.4	27,016,043.2	4,438,689.1	26,718,169.7	4,098,861.3	26,689,848.1	3,951,207.8	27,413,471.1	3,873,218.3	26,935,141.4
26	3,823,551.4	26,672,248.3	4,130,300.8	26,811,521.9	4,121,244.8	26,797,247.8	4,099,084.5	26,690,379.3	3,865,317.3	26,936,470.2	3,873,046.8	26,934,942.9
27	3,831,521.8	26,691,249.9	4,115,651.2	26,781,258.7	4,117,653.3	26,788,641.6	4,420,517.6	26,670,629.8	3,858,401.9	26,832,917.2	3,886,928.7	26,991,286.3
28	4,092,987.7	26,675,867.3	4,443,221.2	26,762,283.9	4,113,513.6	26,762,101.5	4,095,858.3	26,682,700.2	3,926,973.5	27,207,587.1	3,907,472.4	27,075,044.5
29	4,095,396.9	26,681,601.9	3,845,329.1	26,753,352.3	4,112,140.7	26,753,018.7	3,833,165.5	26,695,132.5	3,863,678.8	26,860,034.3	3,899,246.9	27,039,139.2
30	4,093,532.4	26,677,163.7	4,107,444.6	26,729,705.3	4,440,909.3	26,747,263.8	4,093,031.2	26,675,970.9	3,951,842.9	27,424,806.2	3,909,674.6	27,134,621.5
min	3,822,723.1	**26,670,276.8**	3,828,880.8	26,699,699.6	3,847,222.5	26,701,767.9	3,822,723.1	**26,670,276.8**	3,841,775.5	26,763,858.5	3,844,960.2	26,784,215.9
average	4,048,535	**26,677,980.8**	4,146,523.4	26,835,696.7	4,999,441.5	26,838,999.4	4,063,223.2	26,681,944.5	3,891,855.6	27,025,268	3,882,252.4	26,962,208.7
max	4,428,645.6	**26,691,249.9**	4,514,684.8	27,088,694.5	26,701,767.9	27,057,884.7	4,431,425.5	26,696,563.9	3,951,842.9	27,483,275.5	3,960,137.9	27,344,487.5
p-value				1.87×10^{-5}		2.32×10^{-5}				2.67×10^{-6}		5.21×10^{-5}

Table 7.7: Analysis of the β parameter for hybrid CS and hybrid SCA algorithms in the embodied optimization problem.

	CS-Hybrid 0.8		CS-Hybrid 0.5		CS-Hybrid 0.3		SCA-Hybrid 0.8		SCA-Hybrid 0.5		SCA-Hybrid 0.3	
Run	**Cost (€)**	**Energy (kW·h)**	**Cost (€)**	**Energy (kW·h)**	**Cost (€)**	**Energy (kW·h)**	**Cost (€)**	**Energy (kW·h)**	**Cost (€)**	**Energy (kW·h)**	**Cost (€)**	**Energy (kW·h)**
1	4,096,945.7	26,685,288.4	4,421,629.9	26,673,247.6	3,825,599.6	26,678,976.2	4,093,040.7	26,675,993.4	3,829,662.7	26,716,239.3	3,852,063.5	26,776,349.4
2	3,825,898.2	26,677,834.4	3,824,833.5	26,675,300.2	4,094,438.0	26,780,240.7	3,833,087.9	26,694,948.0	3,836,538.4	26,724,014.0	3,838,388.3	26,748,317.1
3	4,094,985.4	26,680,668.9	4,092,352.3	26,674,354.9	4,422,601.9	26,675,561.2	4,093,055.8	26,676,029.4	3,840,611.1	26,741,452.6	3,840,663.8	26,742,739.2
4	4,092,167.0	26,673,913.8	3,822,847.9	26,770,573.9	4,421,670.5	26,673,846.7	4,431,425.5	26,696,563.9	3,841,151.8	26,744,025.5	3,847,634.6	26,796,203.7
5	4,090,639.1	26,670,276.8	3,822,723.1	26,670,276.8	4,095,234.4	26,681,559.3	3,832,058.8	26,692,528.2	3,835,346.5	26,712,877.4	3,845,385.7	26,765,875.6
6	4,428,019.7	26,688,457.2	3,822,723.1	26,670,276.8	3,829,906.8	26,687,555.0	3,827,006.3	26,680,472.1	3,838,241.8	26,725,296.9	3,839,844.8	26,745,147.7
7	4,092,030.9	26,673,589.7	4,094,610.3	26,679,729.4	4,097,484.9	26,686,879.0	4,097,544.0	26,686,759.0	3,830,021.3	26,689,322.1	3,837,570.3	26,738,778.4
8	4,090,639.1	26,670,276.8	4,094,466.5	26,679,387.3	4,094,968.4	26,680,888.9	3,824,911.8	26,676,124.8	3,840,141.1	26,773,580.5	3,979,915.8	27,694,901.1
9	3,828,638.3	26,684,356.6	4,421,264.9	26,672,378.9	4,095,281.1	26,681,498.3	4,420,381.8	26,670,276.8	3,831,809.5	26,714,597.9	3,837,811.0	26,715,356.9
10	4,098,046.3	26,687,908.1	4,422,378.7	26,675,030.1	4,427,962.4	26,688,613.0	3,831,043.8	26,691,335.4	3,834,422.1	26,712,377.7	3,844,114.5	26,749,794.7
11	3,822,723.1	26,670,276.8	3,822,723.1	26,670,276.8	4,090,840.2	26,670,957.4	4,424,708.5	26,680,575.6	3,838,997.9	26,749,285.6	3,860,551.2	26,812,438.0
12	3,822,723.1	26,670,276.8	4,090,639.1	26,670,276.8	4,421,846.9	26,673,764.3	4,094,550.7	26,679,759.9	3,832,276.8	26,708,331.7	3,832,242.2	26,734,012.5
13	4,428,645.6	26,689,947.1	4,420,760.4	26,671,178.1	3,833,836.5	26,697,654.5	3,829,345.5	26,686,040.1	3,822,878.2	26,671,004.0	3,837,078.2	26,722,390.6
14	3,822,723.1	26,670,276.8	4,093,831.1	26,677,874.9	4,099,807.9	26,692,617.8	4,422,860.9	26,676,177.9	3,833,610.5	26,732,750.5	3,880,757.4	26,948,312.1
15	4,098,144.6	26,688,142.1	3,831,013.4	26,690,010.2	4,101,920.0	26,698,535.8	4,098,585.6	26,689,191.9	3,831,631.1	26,720,405.2	3,915,723.6	27,289,381.2
16	4,422,083.7	26,674,327.9	3,822,938.7	26770790.0	3,830,424.7	26,788,928.1	4,092,465.8	26,674,625.0	3,838,434.6	26,741,872.9	3,849,356.8	26,818,040.5
17	3,824,886.5	26,675,426.2	3,828,880.8	26,684,933.8	4,421,068.2	26,672,104.2	4,095,168.1	26,681,057.2	3,830,766.1	26,710,390.1	3,843,137.6	26,777,082.8
18	3,822,723.1	26,670,276.8	4,422,163.1	26,674,517.0	3,829,894.7	26,694,327.8	3,828,464.3	26,683,942.5	3,842,429.7	26,755,365.9	3,827,737.8	26,701,775.3
19	4,420,381.8	26,670,276.8	4,421,096.6	26,671,978.3	4,094,847.7	26,780,908.6	3,827,046.0	26,680,566.6	3,832,170.7	26,707,620.9	3,854,353.3	26,779,597.7
20	4,094,744.5	26,680,049.0	4,420,381.8	26,670,276.8	3,828,383.1	26,684,286.1	4,099,757.7	26,691,981.7	3,826,311.6	26,692,093.6	3,846,577.9	26,819,795.3
21	4,090,639.1	26,670,276.8	4,091,717.0	26,672,842.5	4,091,181.4	26,672,974.8	3,823,789.7	26,672,815.5	3,857,112.2	26,818,332.1	3,845,166.9	26,786,016.9
22	3,822,984.1	26,670,898.0	4,091,035.8	26,671,251.0	4,422,529.3	26,676,586.8	3,822,723.1	26,670,276.8	3,832,154.6	26,716,933.8	3,846,331.7	26,806,453.6
23	4,096,497.5	26,684,221.6	4,422,781.5	26,675,988.9	4,091,923.9	26,674,600.6	4,091,739.6	26,672,896.5	3,830,030.8	26,702,518.8	3,841,512.6	26,788,509.8
24	4,098,033.0	26,687,876.6	4,421,425.6	26,672,761.5	4,092,847.1	26,676,393.4	4,421,414.3	26,672,734.5	4,175,468.7	29,169,891.1	3,832,590.9	26,713,656.9
25	4,093,116.3	26,676,173.4	4,092,652.7	26,675,099.5	4,425,736.9	26,686,155.0	4,098,861.3	26,689,848.1	3,829,702.6	26,709,870.0	3,862,680.1	26,851,899.7
26	3,823,551.4	26,672,248.3	4,427,045.8	26,786,139.1	4,422,166.5	26,674,525.0	4,099,084.5	26,690,379.3	3,832,923.7	26,714,515.0	3,847,190.0	26,747,850.2
27	3,831,521.8	26,691,249.9	4,091,183.7	26,671,573.2	4,429,755.7	26,694,284.9	4,420,517.6	26,670,629.8	3,834,191.9	26,702,712.9	3,872,021.5	26,806,869.8
28	4,092,987.7	26,675,867.3	4,091,251.8	26,671,735.2	4,095,770.6	26,683,352.3	4,095,858.3	26,682,700.2	3,829,805.4	26,703,590.3	3,844,960.2	26,799,370.1
29	4,095,396.9	26,681,601.9	3,822,723.1	26,770,276.8	3,823,680.0	26,672,733.5	3,833,165.5	26,695,132.5	3,832,418.3	26,724,789.7	3,853,668.0	26,877,301.7
30	4,093,532.4	26,677,163.7	4,092,443.1	26,674,571.0	3,833,038.7	26,705,152.8	4,093,031.2	26,675,970.9	3,842,743.9	26,761,566.9	3,848,918.1	26,787,319.3
min	3,822,723.1	**26,670,276.8**	3,822,723.1	**26,670,276.8**	3,823,680.0	26,670,957.4	3,822,723.1	**26,670,276.8**	3,822,878.2	26,671,004.0	3,827,737.8	26,701,775.3
average	4,048,535.0	**26,677,980.8**	4,121,950.6	26,687,830.2	4,122,888.3	26,692,882.1	4,063,223.2	26,681,944.5	3,846,133.5	26,805,587.5	3,853,537.6	26,828,051.3
max	4,428,645.6	**26,691,249.9**	4,427,045.8	26,786,139.1	4,429,755.7	26,788,928.1	4,431,425.5	26,696,563.9	4,175,468.7	29,169,891.1	3,979,915.8	27,694,901.1
Wilcoxon *p*-value				0.014		1.1×10^{-4}				3.4×10^{-5}		7.2×10^{-4}

7.4.2 Embodied Energy and Cost Optimization Methods Comparison

This section describes and analyzes the energy minimization results achieved by the TAMO, discrete CS, and discrete SCA algorithms. Table 7.8 shows the outcomes of the 30 executions of each of the algorithms. The results correspond to the minimization of the steel–concrete embodied energy of the structure. The minimum value of embodied energy obtained throughout the execution is represented in the Energy column. The Cost column represents the structure's cost that was minimized. The Time corresponds to the amount of time it takes to achieve the minimum in seconds.

When analyzing the table, it is observed that concerning the best value obtained, all three algorithms obtain the same value, 26,670,276.8 kW·h. In the case of the average indicator, TAMO obtained a slight superiority, with a value of 26,671,471.6 kW·h, followed by CS with a value of 26,677,980.8 kW·h, and finally SCA with 26,681,944.4 kW·h. In the case of the worst value obtained, TAMO again obtained the best value, followed by CS and finally SCA. The Wilcoxon test compared TAMO-CS and TAMO-SCA to determine whether this difference is significant. The result indicates that the difference is not significant since it delivers values greater than 0.05 in the p-value. When the times are analyzed, the situation changes. A notable difference is observed where CS obtains the best result with an average of 7305 s, CSA with an average of 7960 s, and TAMO with an average of 9399 s. In addition, in the table, we must highlight the dispersion of the results obtained for the costs in the three algorithms. For example, in the case of TAMO, some energy optimizations obtain costs of 3,822,723 and, in other cases, values of 4,422,594.

Table 7.8: Embodied energy minimization results for 30 executions of TAMO, hybrid CS, and hybrid SCA algorithms.

	TAMO			Hybrid CS			Hybrid SCA		
Run	**Cost (€)**	**Energy (kW·h)**	**Time(s)**	**Cost (€)**	**Energy (kW·h)**	**Time(s)**	**Cost (€)**	**Energy (kW·h)**	**Time(s)**
1	3,823,571.1	26,672,341.6	10,279.2	4,096,945.7	26,685,288.4	7,879.9	4,093,040.7	26,675,993.4	8,082.0
2	4,421,229.7	26,672,341.6	10,300.6	3,825,898.2	26,677,834.4	7,935.3	3,833,087.9	26,694,948.0	8,071.9
3	3,822,723.1	26,670,276.8	8,491.2	4,094,985.4	26,680,668.9	7,954.9	4,093,055.8	26,676,029.4	8,049.9
4	4,420,387.1	26,670,319.2	8,401.6	4,092,167.0	26,673,913.8	7,943.6	4,431,425.5	26,696,563.9	8,083.9
5	4,093,735.5	26,677,693.6	9,413.9	4,090,639.1	26,670,276.8	6,210.6	3,832,058.8	26,692,528.2	8,068.3
6	4,420,381.8	26,670,276.8	9,673.1	4,428,019.7	26,688,457.2	7,931.1	3,827,006.3	26,680,472.1	7,982.8
7	4,421,453.6	26,672,857.9	10,329.4	4,092,030.9	26,673,589.7	7,943.5	4,097,544.0	26,686,759.0	7,920.5
8	3,822,723.1	26,670,276.8	7,197.4	4,090,639.1	26,670,276.8	5,819.4	3,824,911.8	26,676,124.8	8,040.6
9	4,420,387.1	26,670,319.2	9,833.4	3,828,638.3	26,684,356.6	7,936.6	4,420,381.8	26,670,276.8	6,843.4
10	4,420,390.1	26,670,343.1	10,301.9	4,098,046.3	26,687,908.1	7,938.0	3,831,043.8	26,691,335.4	8,041.0
11	3,822,728.4	26,670,319.2	8,970.8	3,822,723.1	26,670,276.8	4,391.3	4,424,708.5	26,680,575.6	7,816.5
12	4,091,044.5	26,671,288.4	10,190.0	3,822,723.1	26,670,276.8	7,432.1	4,094,550.7	26,679,759.9	7,970.6
13	3,822,728.4	26,670,319.2	8,764.4	4,428,645.6	26,689,947.1	7,947.4	3,829,345.5	26,686,040.1	7,943.1
14	4,090,814.6	26,670,724.3	9,583.6	3,822,723.1	26,670,276.8	3,696.5	4,422,860.9	26,676,177.9	8,058.6
15	4,090,644.4	26,670,319.2	8,901.5	4,098,144.6	26,688,142.1	7,851.8	4,098,585.6	26,689,191.9	7,998.2
16	3,822,728.4	26,670,319.2	8,943.7	4,422,083.7	26,674,327.9	7,878.0	4,092,465.8	26,674,625.0	7,877.0
17	4,090,647.4	26,670,343.1	9,023.6	3,824,886.5	26,675,426.2	7,956.7	4,095,168.1	26,681,057.2	7,955.3
18	4,420,897.7	26,671,534.5	9,810.1	3,822,723.1	26,670,276.8	4,146.4	3,828,464.3	26,683,942.5	8,033.3
19	3,825,015.1	26,675,732.3	9,418.1	4,420,381.8	26,670,276.8	6,630.4	3,827,046.0	26,680,566.6	7,989.0
20	4,421,340.2	26,672,587.8	9,636.9	4,094,744.5	26,680,049.0	7,928.1	4,099,757.7	26,691,981.7	8,085.7
21	4,090,639.1	26,670,276.8	9,307.2	4,090,639.1	26,670,276.8	6,688.8	3,823,789.7	26,672,815.5	8,069.1
22	4,422,594.3	26,675,543.2	9,135.0	3,822,984.1	26,670,898.0	7,869.7	3,822,723.1	26,670,276.8	7,700.6
23	3,822,731.4	26,670,343.1	10,188.8	4,096,497.5	26,684,221.6	7,899.5	4,091,739.6	26,672,896.5	7,954.8
24	3,822,751.1	26,670,373.2	10,339.3	4,098,033.0	26,687,876.6	7,922.8	4,421,414.3	26,672,734.5	8,083.7
25	4,090,639.1	26,670,276.8	8,644.7	4,093,116.3	26,676,173.4	7,878.3	4,098,861.3	26,689,848.1	8,008.9
26	4,420,381.8	26,670,276.8	8,094.5	3,823,551.4	26,672,248.3	7,897.7	4,099,084.5	26,690,379.3	8,066.2
27	4,092,119.4	26,673,830.1	9,663.9	3,831,521.8	26,691,249.9	7,858.2	4,420,517.6	26,670,629.8	8,043.6
28	4,420,381.8	26,670,276.8	8,717.0	4,092,987.7	26,675,867.3	7,902.9	4,095,858.3	26,682,700.2	7,941.9
29	3,823,185.3	26,671,423.4	10,032.6	4,095,396.9	26,681,601.9	7,935.4	3,833,165.5	26,695,132.5	7,970.4
30	3,823,012.1	26,670,994.4	10,402.4	4,093,532.4	26,677,163.7	7,952.5	4,093,031.2	26,675,970.9	8,059.3
min	3,822,723.1	**26,670,276.8**	7,197.4	3,822,723.1	**26,670,276.8**	**3,696.5**	3,822,723.1	**26,670,276.8**	7,700.6
average	4,113,800.2	**26,671,471.6**	9,399.6	4,048,535.0	26,677,980.8	**7,305.2**	4,063,223.2	26,681,944.4	7,960.3
max	4,422,594.3	**26,677,693.6**	10,402.4	4,428,645.6	26,691,249.9	**7,956.7**	4,431,425.5	26,696,563.9	8,085.7
Wilcoxon *p*-value					0.087			0.064	

In Figure 7.5, the results of Table 7.8 are complemented with violin charts. The chart on the left shows the results of embodied energy, and the graph on the right shows the cost in euros for each configuration obtained. In the chart on the left, it can be seen that in the case of TAMO, the dispersion is less than that of CS and CSA; it should be noted that the scale is in the fourth digit. CS and SCA have similar distributions; however, according to the shape of the distribution obtained and the interquartile range, CS consistently produces better results than SCA. When analyzing the costs resulting from the configurations obtained by minimizing energy, we see that the dispersion of values is substantial and similar in the three algorithms. However, TAMO generates more sparse configurations than CS and SCA. In the case of CS and SCA, the distributions are similar.

In Table 7.9, the results of the cost optimization are shown. Regarding the algorithms and their results, something similar to the previous experiment occurs. In the best value, which corresponds to the minimum, they all obtain the value 3,822,723.1. Later in the average and the worst value, TA obtains the best results, closely followed

by CS and then SCA. The statistical test indicates that the difference is not significant in the TAMO-CS and TAMO-SCA comparison. When analyzing the convergence times, the result is a little different since the best times in the minimum, average, and maximum are for the SCA, followed by the CS and at the end, TAMO. Another interesting point that marks a difference concerning the previous results is that in this case, the energy results for cost optima are good and very similar to those obtained in energy minimization. In this case, TAMO obtained the best values, but the values obtained by CS and SCA were very close. This effect will be analyzed in the next section.

Table 7.9: Cost minimization results for 30 executions of TAMO, hybrid CS and hybrid SCA algorithms.

	TAMO			Hybrid CS			Hybrid SCA		
Run	**Cost (€)**	**Energy (kW·h)**	**Time(s)**	**Cost (€)**	**Energy (kW·h)**	**Time(s)**	**Cost (€)**	**Energy (kW·h)**	**Time(s)**
1	3,822,774,9	26,670,446.6	9,283	3,825,644.2	26,626,556.8	7,975	3,830,092.8	26,693,576.1	7,836
2	3,822,728.4	26,670,319.2	8,803	3,825,115.3	26,675,970.9	7,976	3,864,892.6	26,947,434.0	7,932
3	3,822,878.9	26,670,694.2	8,936	3,825,644.8	26,677,231.2	7,892	3,826,395.0	26,685,077.6	7,873
4	3,823,185.3	26,671,423.4	8,989	3,830,529.3	26,688,857.8	7,959	3,825,919.0	26,677,883.9	7,930
5	3,822,731.4	26,670,343.1	7,685	3,822,875.9	26,670,670.3	7,930	3,823,801.1	26,673,916.7	7,916
6	3,822,728.4	26,670,319.2	6,602	3,827,681.4	26,682,079.0	7,984	3,835,442.1	26,703,151.7	7,911
7	3,822,984.1	26,670,898.0	8,983	3,824,141.4	26,673,652.7	8,008	3,826,324.6	26,687,619.9	7,920
8	3,824,088.1	26,673,555.6	9,202	3,827,522.6	26,681,700.9	7,972	3,826,206.4	26,678,568.1	7,936
9	3,823,937.2	26,673,166.6	8,475	3,827,541.5	26,681,745.9	7,949	3,830,234.3	26,688,155.7	7,858
10	3,825,711.7	26,677,437.0	9,073	3,825,756.9	26,683,046.9	8,056	3,825,188.7	26,676,175.3	7,932
11	3,822,887.3	26,670,697.3	8,951	3,824,519.6	26,674,553.0	8,267	3,828,878.5	26,684,928.3	7,749
12	3,822,723.1	26,670,276.8	6,477	3,831,847.4	26,691,995.2	8,293	3,831,864.4	26,692,035.7	7,720
13	3,822,723.1	26,670,276.8	7,330	3,828,029.4	26,682,907.2	8,167	3,823,462.5	26,672,036.8	7,638
14	3,823,619.5	26,672,410.4	9,412	3,823,891.8	26,673,058.6	8,268	3,828,178.8	26,683,620.9	7,819
15	3,822,984.1	26,670,898.0	9,305	3,825,444.4	26,677,712.0	8,149	3,826,902.0	26,680,253.4	7,762
16	3,822,731.4	26,670,343.1	8,173	3,823,063.7	26,672,698.4	8,210	3,824,311.6	26,674,057.8	7,687
17	3,823,598.3	26,672,389.8	9,244	3,832,782.3	26,723,089.8	8,308	3,822,723.1	26,670,276.8	6,165
18	3,823,676.2	26,672,545.4	8,499	3,828,246.8	26,683,424.9	8,370	3,824,024.1	26,673,373.7	7,768
19	3,822,728.4	26,670,319.2	7,017	3,831,724.5	26,691,702.6	8,250	3,824,115.0	26,673,947.8	7,918
20	3,822,728.4	26,670,319.2	9,366	3,824,459.1	26,674,408.9	8,236	3,829,979.1	26,688,085.1	7,891
21	3,822,723.1	26,670,276.8	8,797	3,830,466.9	26,688,709.3	7,898	3,823,245.0	26,671,519.2	7,870
22	3,824,379.7	26,674,219.9	8,614	3,825,593.7	26,677,109.7	7,645	3,828,654.6	26,687,985.8	7,945
23	3,823,525.7	26,672,233.6	8,612	3,826,446.6	26,679,318.8	7,912	3,827,333.5	26,681,250.8	7,896
24	3,823,981.4	26,673,318.4	9,302	3,827,796.8	26,682,353.6	7,915	3,824,394.2	26,669,105.1	7,876
25	3,823,079.4	26,671,171.3	9,420	3,822,766.6	26,670,380.3	7,897	3,830,913.2	26,689,771.6	7,856
26	3,822,723.1	26,670,276.8	7,891	3,822,723.1	26,670,276.8	7,024	3,829,366.5	26,687,342.8	7,669
27	3,822,728.4	26,670,319.2	8,318	3,822,723.1	26,670,276.8	5,219	3,833,463.0	26,701,586.6	7,731
28	3,822,728.4	26,670,319.2	7,088	3,825,907.6	26,677,856.9	7,943	3,824,394.8	26,674,255.9	7,845
29	3,822,731.4	26,670,343.1	8,513	3,823,593.0	26,672,347.4	7,924	3,823,562.7	26,672,275.4	7,696
30	3,823,015.1	26,671,018.3	8,802	3,830,083.2	26,688,753.5	7,914	3,830,124.4	26,688,997.7	7,948
Min	**3,822,723.1**	26,670,276.8	6,477	3,822,723.1	26,670,276.8	5,219	3,822,723.1	26,669,105.1	6,165
Average	**3,823,192.1**	26,671,419.2	8,505	3,826,485.4	26,678,814.9	7,917	3,828,479.6	26,690,942.2	7,783
Max	**3,825,711.7**	26,677,437.0	9,420	3,832,782.3	26,723,089.8	8,370	3,864,892.6	26,947,434.0	7,948
Wilcoxon *p*-value					0.091			0.093	

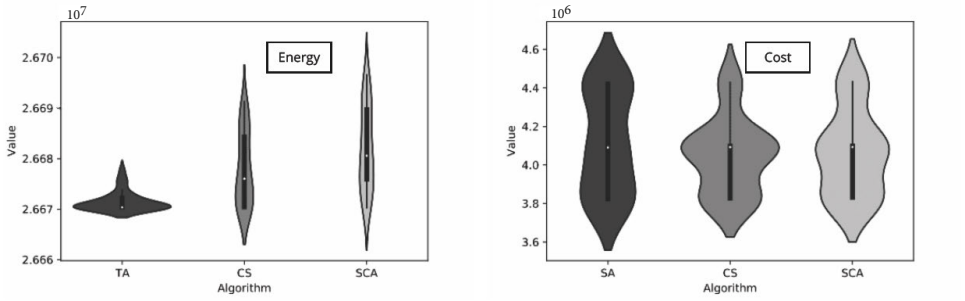

Figure 7.5: Embodied energy and cost result violin plots.

7.4.3 Optimization Results

The objective of this section is to compare the results obtained for embodied energy and cost optimizations. As it can be seen in Tables 7.8 and 7.9, the three algorithms obtain the same best result. If the average results are compared, TAMO obtains the lower cost and energy values. However, if the computation time is taken into account, it can be seen that for cost optimization, SCA is 14.27% faster than TAMO, while CS results in a 25.79% faster energy optimization with little increase in the objective function. These variations correspond to 0.21% and 0.02% if SCA is considered for cost optimization and CS for energy optimization, respectively. For these reasons, SCA and CS were chosen to compare their optimization results. Results of the optimization problem variables are shown in Table 7.10.

The first finding is related to the number of optimums found by both algorithms. Table 7.8 shows that CS found the same minimum value of energy several times but with different results in terms of costs. This is in line with Figure 7.6 that shows that the same results in energy can yield different cost values. This is because the embodied energy of steel does not depend on the yield stress. On the contrary, as the yield stress of steel rises , the cost increases. This comparison can be observed in Table 7.1. This allows the energy optimization to increase the yield stress without penalizing the objective function and, consequently, to obtain an optimum design with higher yield stress. On the contrary, the cost optimization searches for solutions with lower yield stresses to reduce the overall structure cost. Nevertheless, if we consider the relation between the cost and energy optimization obtained in the regression plots of Figure 7.6 we see that by reducing the cost by one EUR, the energy is reduced by 0.584 kW·h in this optimization problem.

Comparing the variables obtained from both optimizations, it can be observed that the upper part of the steel beam trends in every case to 7 m, matching the lower bound defined for this variable. Regarding the angle of the webs, it can be observed that the embodied energy profits more from the inertia of these elements obtaining, as a result, angles closer to 90 degrees which imply a greater perpendicularity between webs and flanges. Regarding the cells, the central part of the optimum designs gives a positive value for both upper and lower cells, which implies that these elements improve the cross section's behavior. As can be seen, the optimum designs obtained by the two algorithms are pretty similar. The differences are mainly in the transverse beams and in the thicknesses of some elements. Finally, it is worth noting that the optimization removes the stiffeners of the lower wing. This is due to the double composite action of the slabs in the support zones.

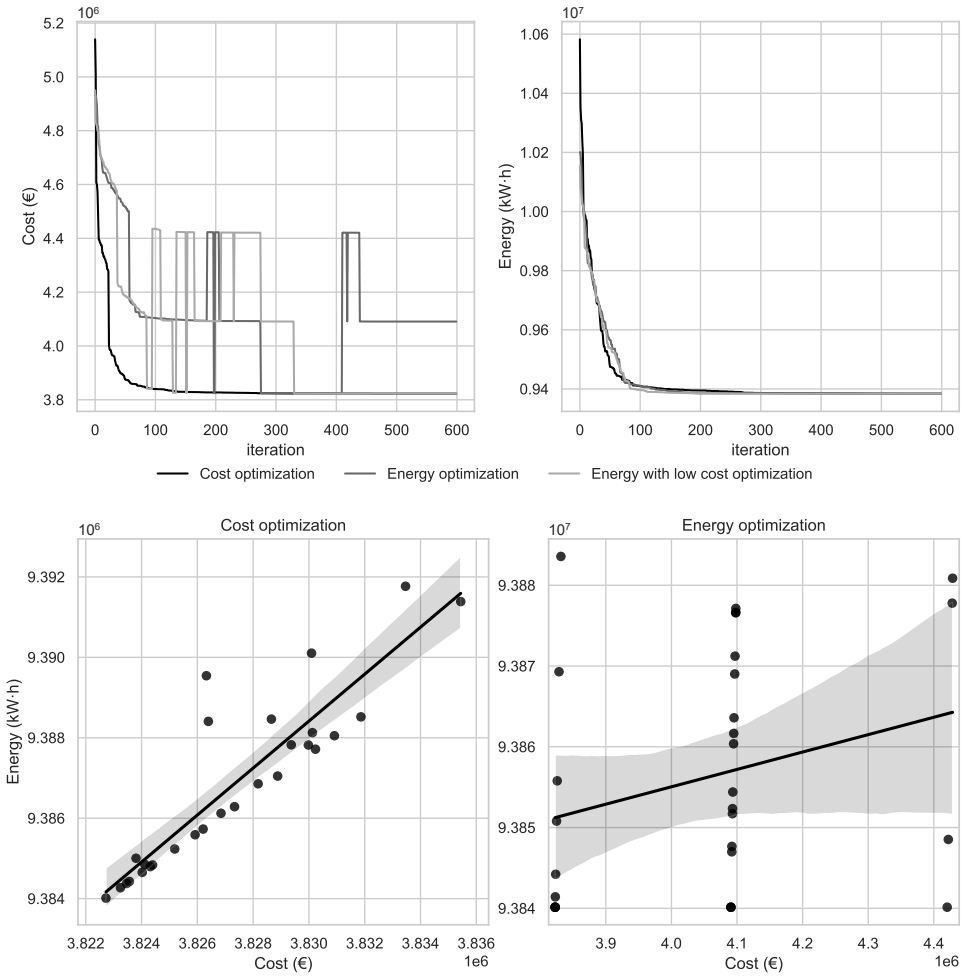

Figure 7.6: Optimization results from both cost and energy optimization criteria.

Table 7.10: Design variables minimum and maximum values for best cost and energy optimization results.

		Cost Optimization			Energy Optimization			
Variables	**Unit**	**Best**	**Min**	**Max**	**Mean**	**Mode**	**Min**	**Max**
b	m	7	7	7	7	7	7	7
α_w	deg	55	45	87	64	79	45	90
h_s	mm	200	200	200	200	200	200	200
h_b	cm	298	250	381	312	-	255	397
h_{fb}	mm	410	400	610	460	450	400	660
t_{f_1}	mm	25	25	57	25	25	25	25
b_{f_1}	mm	300	300	620	300	300	300	300
h_{c_1}	mm	330	0	960	420	-	0	980
t_{c_1}	mm	18	16	17	16	16	16	16
t_w	mm	16	16	16	16	16	16	16
h_{c_2}	mm	330	0	900	610	640	80	900
t_{c_2}	mm	18	16	25	17	16	16	24
b_{c_2}	mm	300	300	370	300	300	300	300
t_{f_2}	mm	25	25	29	25	25	25	25
h_{s_2}	mm	150	150	150	150	150	150	150
$n_{s_{f_2}}$	u	0	0	0	0	0	0	0
d_{st}	m	3.3	1	4.9	2.86	-	1	4.8
d_{sd}	m	6	4.1	9.9	6.43	7.6	4	9.6
b_{fb}	mm	1000	200	1000	540	500	200	1000
$t_{f_{fb}}$	mm	33	25	35	30	29	25	35
$t_{w_{fb}}$	mm	27	25	35	28	26	25	35
n_{r_1}	u	200	200	436	200	200	200	390
n_{r_2}	u	200	200	403	200	200	200	367
ϕ_{base}	mm	6	6	10	6	6	6	6
ϕ_{r_1}	mm	6	6	6	6	6	6	6
ϕ_{r_2}	mm	6	6	6	6	6	6	6
s_{f_2} *	mm	300	200	550	335	220	200	600
s_w *	mm	450	200	600	295	200	200	450
s_t *	mm	240	200	600	279	200	200	500
h_{sc}	mm	100	100	100	100	100	100	100
ϕ_{sc}	mm	16	16	22	16	16	16	22
f_{ck}	MPa	25	25	25	25	25	25	25
f_{yk}	MPa	275	275	275	328	275	275	460
f_{sk}	MPa	500	500	500	500	500	500	500

* Values of the standard series of IPE profiles [239]. Note: Min and Max correspond to the maximum and minimum values obtained. Best corresponds to the value obtained for the best individual for cost, and Mean and Mode refers to the statistics of the best values obtained from energy optimization. The cost optimization data were obtained from Hybrid SinCos, while the energy optimization ones were obtained from the Hybrid CS.

7.5 Discussion

In the literature, three studies have optimized steel–concrete composite box-girder bridges. These studies are [97], [109]. This section will compare the results obtained in Section 7.4 with those found in previous optimization studies. The value of concrete strength (f_{ck}) obtained from both cost and energy optimizations were 25 MPa. The high inertia of the section produces this due to its height. In negative bending moment zones, the concrete is not considered in the calculation, following the method proposed by Eurocode 4 [26], while in positive bending moments, the high inertia of the cross section produces a reduction in the stresses. Because of this, higher concrete strength is not necessary.

In the comparison focused on steel yield stress (f_{yk}), it can be seen that in [109] the results give a design value for steel yield stress of 275 MPa when optimizing cost. This is in line with the results of this optimization problem when optimizing cost. In contrast, if the energy optimization steel stress results are compared, it can be seen that there is some disparity between the yield stress results. This is because the energy and the emissions produced for manufacturing different yield stress steels are the same. Optimizing energy has the same result as optimizing cost, depending on the yield stress chosen by the optimization procedure. Comparing the results with [97], it can be seen that the tensile stress chosen is a parameter and does not vary in this study. This yield stress corresponds with 355 MPa, the expected value for steel bridges.

Finally, a variable comparison was made with [109]. Regarding the lower flange stiffeners, these studies' results align with the ones obtained in this study. In all cases, these elements are eliminated from the cross section. By comparing the different results, a compromise solution can be found that optimizes the costs and energy criteria by applying multi-objective optimization techniques.

7.6 Conclusions

There is a clear trend in bridge design to consider criteria other than cost to obtain new alternatives for structural design. Consequently, many studies consider different techniques and objectives in concrete bridge optimization to obtain more sustainable alternative bridges. In contrast, the optimization studies of steel–concrete composite bridges were focused on weight and cost reduction, leaving aside other pillars of sustainability (e.g., the environmental pillar). There are few studies of SCCB optimization. Three optimization algorithms were proposed to compare its results in terms of computation time and minimization results. One of these algorithms was a threshold

accepting with a mutation operator (TAMO), which belongs to trajectory-based algorithms. The other two metaheuristics fit in the swarm intelligence algorithms family, the sine cosine algorithm (SCA) and the cuckoo search (CS). A hybridization machine learning strategy was applied to swarm algorithms to improve their performance.

This study shows a box-girder steel–concrete composite bridge optimization considering cost and embodied energy as single optimization objectives. The first part of the study compares the performance of the three algorithms proposed using the best tuning obtained for each algorithm. As a result of this part of the study, the SCA algorithm obtained similar results as TAMO, but on average, the computation time for cost optimization was higher. For energy optimization, the same occurs with CS compared with TAMO. Consequently, these algorithms were chosen to carry out both cost and energy single objective optimization. In both optimizations, the number of stiffeners defined at the end of the optimization process achieved the value of 0 due to the structural behavior produced by the double composite action design. Furthermore, in steel plates, upper and lower cells shorten the distance between non-stiffened zones and increase section stress resistances. Additionally, as demonstrated by past research on bridges, there is a direct connection between cost and energy optimization. In this case, 0.584 kW·h of energy reduction can be obtained for every EUR optimized when applying heuristic optimization techniques. This relation is only produced in the way of cost optimization. If embodied energy is optimized, it is not possible to ensure that an optimal solution will be found in relation to cost.

This work allows the structural researcher to enlarge their knowledge of SCCB optimization by considering new methods and target functions. It opens the door to using those elements to obtain new design criteria for more sustainable and efficient steel–concrete composite bridge alternatives. In future research, other machine learning techniques will be applied to study its performance and accelerate the computation time. Furthermore, this proposed study will consolidate or discard the addition of cells in the cross section and eliminate stiffeners in the bottom flange in this type of box-girder SCCB bridge.

Regarding the study of the algorithm, it is interesting to carry out a time complexity analysis. We must consider that the hybrid algorithm has a complexity of the metaheuristic $\mathcal{O}(MH)$ plus $\mathcal{O}$(K-means), which is $\mathcal{O}(n^2)$, plus the discretization process, which is also $\mathcal{O}(n^2)$. The preceding suggests carrying out a time analysis study where, on the one hand, the structure can be varied by increasing its complexity to analyze how the different algorithms behave in convergence times. On the other hand, we can vary the analysis by maintaining the same design, but making the search space more complex, for example, increasing the number of discrete elements to evaluate the different algorithms at convergence times.

Chapter 8

Deep learning approach for life cycle optimization of steel-concrete composite bridges

Authors:	D. Martínez-Muñoz, J. García, J.V. Martí, and V. Yepes
Status:	Manuscript sent
Journal:	Applied Soft Computing
Year:	2023
DOI:	–
JCR IF (2021):	8.263

JCR Category	Ranking	Quartile
Computer Science, Artificial Intelligence	23/145	Q1
Computer Science, Interdisciplinary Applications	11/112	Q1

Presentation:	Manuscript

Abstract

Being able to carry out life cycle analysis of complex structures is of vital environmental and social importance. Calculating and comparing optimal structures under these criteria allows to understand the critical points of the design and make better decisions when faced with a problem of this type. On the other hand, by including the life cycle, the objective functions of the optimization problem become more complex. This results in longer computation times. Therefore, the above is an interesting challenge for machine learning and optimization techniques to speed up computations. This article proposes a methodology to build deep learning models to speed up the calculations of the structural constraints when solving an optimization problem considering the structure's life cycle. Different hyperparameters are analyzed to obtain the most robust model that speeds up a concrete and steel composite bridge calculations. Subsequently, the best model integrates with three different metaheuristics. The Old Bachelor Acceptance with a Mutation Operator (OBAMO) algorithm, the Cuckoo search algorithm (CS), and the sine cosine algorithms (SCA) have been used. The results show that, in the best case, using the deep learning model allows one to speed up the calculations 50 times. Finally, the best obtained deep learning model performs an optimal comparison based on costs and environmental and social life cycle assessment. The results regarding the life cycle assessment show an increase in steel yield strength for optimal solutions for both environmental and social objective functions.

Keywords: neural networks; sustainability; optimization; bridges; machine learning; composite structures.

8.1 Introduction

Most countries' economic viability and social growth are closely related to their infrastructure's development, reliability, and durability [297]. Infrastructure is critical because it significantly impacts economic activity, growth, and employment. However, these activities can have a tremendous environmental and social impact, have irreversible consequences, and potentially endanger the present and future of society. Because construction is a carbon-intensive [3] business, much of the research has focused on minimizing emissions, as it is increasingly crucial to minimize the environmental effect of construction projects. In a search for state-of-the-art, studies have been carried out on sustainable building [167], [169], optimization of energy consumption [298], in addition to the analysis of the life cycle of CO2 emissions from concrete structures [282], [299], [300].

However, we must note that regardless of the criteria that researchers consider to represent the sustainability of structures, it is widely agreed that a complete evaluation of sustainability must cover the entire life cycle of the structure [185], [206], [278], [301]. This means, on the one hand, considering the three sustainability pillars: economic, environmental and social. Therefore, in defining the objective function that guides this optimization, the complete life cycle analysis must be considered dividing the life cycle in four stages. This stages are: Manufacturing, Construction, Use and Maintenance, and End of Life [145]. Furthermore, all structural designs involve variability and uncertainty [302], [303]. This implies that the optimization process becomes more complicated due to the increase on the complexity of the objective functions, therefore, a crucial point is to be able to speed up the calculations.

One way to speed up these calculations is to use machine learning techniques. For example, dimensionality reduction techniques can be used to simplify the search space's dimensionality or objective function. Another way is to replace the objective function or the constraints with some model that emulates them. For example, in the case of replacing the objective function in [124], the kriging technique was used to reduce the computing times of a concrete box-girder bridge. In [304], neural networks were used to model viscosity and conductivity values and further integrated into NSGA-II (nondominated sorting genetic algorithm II) to perform optimization.

Structural field studies have used neural networks to predict the transfer length in prestressed concrete [305]. Similarly, neural networks were applied to predict the energy consumption for building heating, ventilation, and air conditioning systems. Then, a multi-objective genetic algorithm was used to find the optimal consumption conditions [306]. As a result, the multi-objective optimization shows better results regarding thermal comfort and energy consumption when compared to the base case design.

Considering the research lines presented in the previous paragraphs, this article proposes a model based on deep learning techniques to replace the restrictions defined in the design of a steel-concrete composite bridge (SCCB) and accelerate the optimization calculations. Subsequently, once the model is adjusted for simple objective functions, an environmental and social life cycle analysis is applied, which implies more complex objective functions.

Specifically, the contribution of this article includes:

- A methodology for the construction and tuning of the deep learning model.
- The model is integrated into different metaheuristic algorithms, evaluating their performance in terms of time and quality of the solutions obtained.

- An environmental and social life cycle analysis is carried out.

The results show that the deep learning model is capable of speeding up calculations by a factor of 50 when using swarm-type algorithms and by a factor of 37 when using trajectory algorithms. Furthermore, the results regarding life cycle assessment show an increase in steel yield stress for optimum solutions for both environmental and social objective functions. This is because the increase in yield strength does not result in an increase in impact. Conversely, for cost optimization results, an increase in the steel resistance is translated directly as an increase in cost, and optimum solutions get lower yield stress values.

A brief structure of contents is as follows: In Section 8.2, the deep learning techniques used, the optimization techniques applied, the objective functions considered as well as the definition of the optimization problem are detailed. The results obtained are described in Section 8.3, first, the different experiments developed to achieve the appropriate model that accelerates the calculations are detailed, and later the results obtained in the analysis of the life cycle of the structure are detailed. Finally, in Section 8.4, the main conclusions and the suggested next steps are stated.

8.2 Deep Learning metamodel assisted optimization

Structural problems are often characterized by high complexity, which results in high computational costs. The model is often of such complexity that the high computational cost implies eliminating some constraints of the initial model or simplifying the associated objective functions. Additionally, multiple runs of these complex structural models are required during optimization processes to obtain the optimal result. To reduce computation time, this research proposes a Deep Neural Network (DNN) metamodel, explained in Section 8.2.1, to predict the feasibility of structural solutions for a steel-concrete composite bridge (SCCB) deck. This metamodel has been applied to various metaheuristics described in Section 8.2.2 to compare the results obtained. Moreover, this study considers three objective functions, defined in Section 8.2.3, to compare the results regarding the three pillars of sustainability, treated as single objective optimizations.

8.2.1 Deep neural networks model

This section explains the proposed methodology to train the deep neural network model that will speed up the optimization calculations. It should be noted that the built model solves the problem of whether or not the bridge to be optimized complies with the imposed constraints. In this sense, the model will solve a binary classification problem. The essential components of the developed methodology for the construction of the classification model comprise Deep learning-based methods. Mainly there are three points to develop. The first point corresponds to the construction of the training dataset; the second point corresponds to the network topology definition and the hyperparameters used. Finally, the third point is defining the metrics and evaluating the best configuration. The above points will be developed in this section.

Methodology used for the construction of the training data set

This section explains the construction of the dataset used for training different deep neural network models. Various data sets were built for the calibration of the networks to evaluate the best way to carry out the training. Because different optimization techniques were used, a complete execution was considered for OBAMO and SCA. In each of the optimizations developed, the data was recorded, identifying whether or not they complied with the standard established for the structure. Due to the fact that there was an imbalance between the conditions that were met and those that did not, it was decided to test cases where the data were not balanced vs. cases where the training data sets were balanced with the synthetic minority over-sampling technique (SMOTE). Additionally, performing independent training for OBAMO, SCA, and a hybrid one where both data sets were integrated was compared. Data integration is tested for both the unbalanced and SMOTE-balanced cases. The sampling strategy parameter in the case of SMOTE was set to one.

Topology network definition, hyper-parameters explored and metrics used

For the definition of the network topology, multilayer perceptron neural networks with the TensorFlow framework were considered. For the definition of the topology, initially, a one-layer network with different numbers of nodes was tested; specifically, 64, 128, and 256 nodes were tested. Once the first layer was established, the case of a second layer was evaluated by the number of nodes in the first layer divided by two. In the event that the second layer generates improvements in the metrics defined with respect to the network of one layer, a third layer is explored where the number of nodes corresponds to $\frac{n}{4}$ of the number of nodes of the first layer. On the other hand, the explored hyperparameters corresponded to the optimization algorithm, the

batch size, and the number of epochs. In the case of optimization algorithms, three techniques were explored, SGD, RMSprop, and Adam. For the case of batch size, three configurations, 32, 64, and 128, were explored. Finally, in the epochs, 100 and an early stopping were used as the maximum value, with the rule that if the test set does not improve after 10 cases, the process ends with the training. In the case of the metrics used, both false positives and false negatives were significant to minimize; therefore, it was decided to use the F1-score metric, which generates the harmonic average between precision and recall.

8.2.2 Hybrid metaheuristics

This section describes the metaheuristics used in this study, which can be divided into two main groups: trajectory-based and swarm intelligence. All algorithms in this study have been hybridized. Trajectory-based techniques involve minor changes to the variable vector to modify the solution and search for the optimum. Mutation operators have been added to these algorithms as part of the hybridization process to improve the exploration of the optimization process. Swarm intelligence techniques involve varying the solution by moving the variables to search for a specific characteristic of the best individual in the population. In this case, hybridization has been achieved through a k-means clustering technique. It is worth noting that all algorithms have been modified to accommodate the discrete nature of the optimization problem.

In addition, all structural optimization methods require a structural check module to verify the feasibility of the solution, which typically consumes approximately 80% of the computation time for each iteration of the optimization problem. To reduce computation time, a DNN model has been trained to predict the feasibility of the solution. Details of the DNN model are provided in Section 8.2.1. While it is possible that the model may fail, after the optimization is complete, the constraints of the structural problem are checked using software developed in Python [243].

Trajectory-based: Old Bachelor Acceptance with a Mutation Operator

The searching strategy employed by such algorithms involves making small changes to the variable vector and assessing the resulting changes in the objective function. These metaheuristics accept inferior solutions in certain stages of the optimization process to prevent getting stuck in local optima and promote exploration. A threshold must be defined to limit the acceptance of solutions that fall outside acceptable boundaries. In this study, the threshold was modified dynamically during optimization, increasing or decreasing based on the acceptance rate of solutions. The Old

Bachelor Acceptance with a Mutation Operator (OBAMO2) is an adaptive threshold algorithm used in other structural optimization problems [307]. In this study, the OBAMO2 method was hybridized with a characteristic of Genetic Algorithms, specifically, the mutation operator, which allows certain mutations to occur during optimization to promote exploration.

The Old Bachelor Acceptance (OBA) algorithm is an iterative heuristic optimization method proposed by Hu et al. [308]. These procedures start with an initial solution and modify it by moving. If the new solution is inside the defined threshold, it is accepted even if its objective function is worse. In contrast to Simulated Annealing (SA) [244], which uses a monotonically decreasing acceptance scheme with decreasing temperature, the acceptance criterion employed by OBA is based on a dynamically changing threshold that follows the principle of "decreasing expectations". After each failure to improve the solution, the threshold is increased to allow switching to somewhat worse solutions. Conversely, with successive improvements in the solutions, the threshold is lowered. Hu et al. [308] highlight some benefits of OBA over SA, such as the non-monotonic acceptance scheme, the self-adjusting growth and decay of the thresholds, and the adaptation to a preset calculation time.

The OBA algorithm was chosen for this study because it has been previously applied to other structural optimization problems [309]. In order to enhance exploration during the optimization process, a mutation operator was incorporated, following recent research [307]. OBAMO is a hybrid algorithm that combines the algorithm presented in Algorithm 5 with a mutation operator. The algorithm is dependent on five parameters, namely, the number of iterations (N), the threshold updating parameter (Δ), the limit of movements without improvement (δ), the standard deviation (SD), and the number of variables (VN) allowed to change between iterations. The best combination of these parameters was obtained using a Design of Experiments method [248], resulting in values of 20,000, 0.3, 1, 100, and 9 for N, SD, VN, Δ, and δ, respectively.

Swarm intelligence: SCA and CS

Swarm intelligence methods mimic the behavior of natural systems to search for optimal solutions. These methods create populations of individuals that interact with each other, imitating the behavior of certain species. Two such algorithms that have been proposed are the Sine Cosine Algorithm (SCA), which uses sine and cosine functions to simulate the movements of individuals, and Cuckoo Search (CS), which models the behavior of natural cuckoo populations. Moreover, recent structural optimization studies have shown that adding a hybridization technique, such as K-means clustering, can improve the behavior of these metaheuristics [310], [311].

Algorithm 5 Old Bachelor Acceptance 2 [308]

M = Maximum iteration number
Δ = Threshold updating parameter
δ = Limit of movements without improvement
$count$ = Counter of consecutive movements accepted
T_0 = 0; $prev\_age$ = M
Choose of random solution s_0
for i=0 to M-1 **do**
    Choose a random neighboring solution s'
    if $f(s') < f(s_i) + T_i$ **then**
        $s_{i+1} = s'$
        age = 0
        if $prev\_age < \delta$ **then**
            $count$ = $count$ + 1
        else
            $count$ = 1
        end if
        T_{i+1} = $T_i - count \cdot \Delta \cdot (1 - i/M)$
    else
        s_{i+1} = s_i
        age = age + 1
        T_{i+1} = $T_i + \Delta/\delta \cdot (1 - i/M)$
    end if
    $prev\_age$ = age
end for
s_i = s_i corresponding with minimum $f(s_i)$ with $0 \leq i \leq M$

Sine Cosine Algorithm (SCA) The SCA is a swarm intelligence method developed by Mirjalili [233] that employs sine and cosine functions to explore the solution space. The movement of individuals is controlled by P_j^t, which typically uses the best solution found at the location of the best solution for iteration t and dimension j. Additionally, the algorithm uses three random numbers r_1, r_2, and r_3. The values

of these numbers determine whether the movement of the solutions is executed by a sine or a cosine function, as shown in Equations 8.1 and 8.2, respectively.

$$x_{i,j}^{t+1} = x_{i,j}^{t} + r_1 \times sin(r_2) \times \mid r_3 P_j^t - x_{i,j}^t \mid \tag{8.1}$$

$$x_{i,j}^{t+1} = x_{i,j}^{t} + r_1 \times cos(r_2) \times \mid r_3 P_j^t - x_{i,j}^t \mid \tag{8.2}$$

$\mathrm{Cuckoo\ Search\ (CS)}$ The CS algorithm is inspired by the cuckoo bird species, which lays its eggs in the nests of other bird species and sometimes mimics the hues and patterns of the host species' eggs. In this algorithm, an egg represents a solution, and the basic idea is to replace inadequate solutions with better ones, analogous to cuckoos replacing the host bird's eggs. The CS algorithm is based on three essential principles:

1. Each cuckoo lays one egg at a time, which is randomly placed in a nest.
2. Only the best nests, which produce high-quality eggs, are considered for the next generation.
3. The number of available nests is fixed, and the host bird has a probability $p_a \in (0, 1)$ of discovering the cuckoo's egg.

$$x_{i,j}^{t+1} = x_{i,j}^{t} + \alpha \bigoplus \text{Lévy}(\lambda) \tag{8.3}$$

The step size $\alpha > 0$ should be chosen proportionally to the scales of the problem. The operator $\bigoplus$ denotes element-wise multiplication. To simulate a random walk, the Lévy flight draws the step length from a Lévy distribution Lévy $\sim t^{-\lambda}$, where $1 < \lambda \leq 3$.

$\mathrm{Hybridization\ technique:\ K\text{-}means\ clustering}$ The hybrid method is utilized for swarm intelligence metaheuristics since both methods are naturally suited for continuous domains. The hybrid method takes the metaheuristic MH, the list of discrete solutions obtained in the previous iteration $lSol$, and a list of transition probabilities $transitionProbs$ as input parameters, and returns a new list of discrete solutions $lSol$ as an output. In the first stage, the discretization method calculates the velocity of MH. For CSA and CS, this velocity corresponds to the component obtained by the difference between $|x_{i,j}^{t+1} - x_{i,j}^{t}|$ in Equations 8.1 to 8.3.

Next, a transfer function is applied to convert the velocity values, ranging from $\mathbb{R}$, to values between [0, 1). A v-shape transfer function, $|\tanh(v)|$, is used in this case.

Then, for each solution and dimension, the value of $lSolProbability$ obtained by applying the transfer function is compared with a random number r_1 between [0,1). If the value of $lSolProbability$ is greater than the random number, an update occurs in that dimension; otherwise, it is not modified.

The update procedure has two possibilities: a β value is considered, and a random number r_2 is generated. If r_2 is less than β, the value is replaced by the value of the best solution obtained for that dimension. Otherwise, a random update is performed to enhance the exploration of the search space.

After that, a k-means clustering technique is used to convert the velocity values, ranging from $\mathbb{R}$, to transition probabilities values that take values in [0,1). The k-means technique generates clusters, in this case, five clusters, and sorts them from the smallest to the largest centroids. The most negligible transition probability is assigned to all cluster velocities in the case of the smallest centroid. In contrast, the most considerable transition probability is assigned to all cluster points in the case of the largest centroid. Figure 8.1 illustrates the k-means procedure. The transition probability values used for this article were [0.1, 0.2, 0.4, 0.8, 0.9].

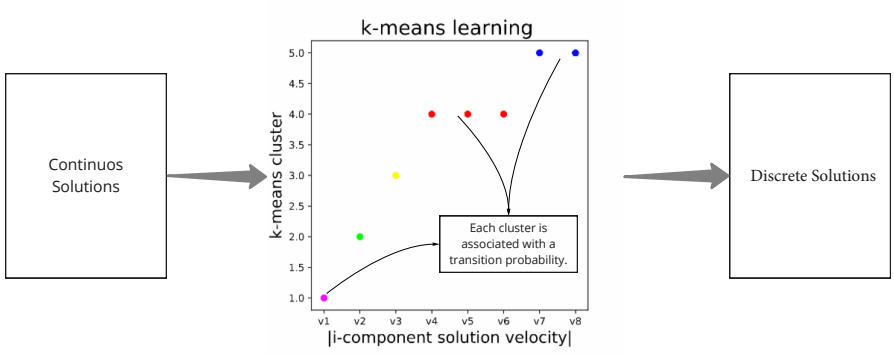

Figure 8.1: K-means discretization techniques diagram.

For each dimension of every solution, the transition probability $DimSolProb_{i,j}$ is computed. Suppose the probability is higher than a random number r_1, and β is more significant than a random number r_2. In that case, the solution's dimension value is updated with the best solution found until that point. If the condition for β is not satisfied, the procedure updates the dimension with a randomly permissible value. If

neither the transition probability nor the β condition is satisfied, the dimension of the solution is not updated. This final option is included to increase the exploration of the search space.

Algorithm 6 Hybrid algorithm

Function Discretization($lSol$, MH,$transitionProbs$)
Input $lSol$, MH, $transitionProbs$
Output $lSol$
$vlSol \leftarrow$ getVelocities($lSol$, MH)
$lSolClustered \leftarrow$ appliedKmeansClustering($vlSol$, K)
for (each Sol_i in $lSolClustered$) **do**
    for (each $dimSol_{i,j}l$ in Sol_i) **do**
        $dimSolProb_{i,j}$ = getClusterProbability($dimSol$, $transitionProbs$)
        if $dimSolProb_{i,j} > r_1$ **then**
            if $beta > r_2$ **then**
                Update $lSol_{i,j}$ considering the best.
            else
                Update $lSol_{i,j}$ with a random value allowed.
            end if
        else
            Don't update the element in $lSol_{i,j}$
        end if
    end for
end for
return $lSol$

8.2.3 Objective functions

The optimization problem at hand involves finding the optimal design of an SCCB while ensuring sustainability through the use of objective functions that represent the pillars of sustainability. Specifically, we evaluate the economic cost, as well as the environmental and social life cycle assessments of the SCCB's deck, using equations 8.4, 8.5, and 8.6, respectively.

Table 8.1: Cost values of every construction unit for SCCB

Construction unit	Unit	Cost (€)
Concrete C25/30	m^3	88.86
Concrete C30/37	m^3	97.80
Concrete C35/45	m^3	101.03
Concrete C40/50	m^3	104.08
Precast pre-slab	m^3	27.10
Reinforcement steel B400S	kg	1.40
Reinforcement steel B500S	kg	1.42
Rolled steel S275	kg	1.72
Rolled steel S355	kg	1.85
Rolled steel S460	kg	2.01
Shear-connector steel	kg	1.70

$$C(\vec{x}) = \sum_{i=1}^{n} p_i \cdot m_i(\vec{x}) \tag{8.4}$$

The objective cost function calculates the total cost of constructing the bridge by multiplying the unit cost of each required activity with its corresponding measurement. Table 8.1 contains a comprehensive list of all construction units and their respective costs obtained from the BEDEC database [207]. In equation 8.4, p_i refers to the price of each construction unit, and m_i represents its measurement.

$$ELCA(\vec{x}) = \sum_{i=1}^{n} \sum_{j=1}^{p} elca_j \cdot m_j(\vec{x}) \tag{8.5}$$

$$SLCA(\vec{x}) = \sum_{i=1}^{n} \sum_{j=1}^{p} slca_j \cdot m_j(\vec{x}) \tag{8.6}$$

The primary objective of the life cycle assessment (LCA) is to evaluate the environmental (ELCA) and social impact (SLCA) of the structure, taking into account all processes involved, from raw material extraction to demolition and transportation to a landfill site. In equations 8.5 and 8.6, i represents each life cycle stage, $elca_j$ and $slca_j$ correspond to the environmental and social impact of each process within a given stage, respectively, and m_j indicates the corresponding measurement of each process. Each process's environmental and social impact and their corresponding

measurement are detailed in Table 8.2. The LCA methodology has been described in section 8.2.3.

Table 8.2: Ecoinvent processes LCA environmental and social impact values

Process	**Unit**	$elca_i$ **(points)**	$slca_i$ **(mrh)**
concrete production 25MPa	m³	2.037E+01	1.254E+05
concrete production 30MPa	m³	2.631E+01	1.668E+05
concrete production 35MPa	m³	2.478E+01	1.554E+05
concrete production 40MPa	m³	2.585E+01	1.623E+05
steel production 71% of recycling rate	kg	1.523E-01	1.941E+03
steel production 98% of recycling rate	kg	1.036E-01	2.067E+03
transport, freight, lorry 16-32 metric ton, EURO6	t·km	2.502E-02	4.116E+01
transport, freight, lorry 3.5-7.5 metric ton, EURO6	t·km	7.755E-02	1.655E+02
welding, arc, steel	m	2.350E-02	2.535E+02
welding, gas, steel	m	2.303E-02	2.429E+02
diesel, burned in building machine	MJ	1.361E-02	8.764E+00
carbon dioxide	kg	4.369E-02	0.000E+00
rock crushing	kg	7.223E-05	8.305E-01

Life cycle assessment method

The life cycle assessment (LCA) evaluates the environmental and social impact of the processes involved in an activity or product, covering all stages necessary to complete it. For bridges, the ISO 14040:2006 [145] regulation is used to carry out the environmental LCA, while the Guidelines for Social Life Cycle Assessment of Products [224] guide the assessment of the social impact. Impact information from databases is required, along with a chosen life cycle impact assessment (LCIA) method to model the life cycle of a structure. This research uses the ReCiPe 2008 method [151] for environmental LCA and the social impacts weighting method (SIWM) for social impact. The ecoinvent v3.7.1 [199] and soca v2 [312] databases are used for environmental and social LCA, respectively, as they are reliable and frequently updated [200]. Moreover, the soca database allows for the association of ecoinvent processes with the PSILCA [313] database social impacts, making it useful for scientists [279].

In this research, four stages are defined: manufacturing, construction, use, and end-of-life to assess the impact of an SCCB, which are similar to those in previous LCA studies on bridges [279]. The manufacturing phase involves transforming raw materials into products needed for construction and transporting them to the building site while considering waste generated during these activities. The impact of recycled steel on the SCCB's global environmental impact is significant, particularly in producing steel products [279]. It is essential to distinguish between structural and

reinforcement steel, as the recycling percentages differ. For instance, the recycling rate of reinforcement steel is 71%, while that of structural steel is 98% in developed countries such as the US [193].

The construction phase includes actions required to build the bridge, such as equipment and building style, and location. Formwork, scaffolding, vibrators, and concrete pouring must be considered, and procedures for welding the steel sections should be established for steel and steel-concrete composite bridges. The diesel consumption of machinery during construction, based on manufacturer information, literature, or other sources, is included in the LCA model for modeling construction activities.

The use and maintenance stage encompasses all the activities required throughout the structure's lifetime. Recent research has investigated the potential for concrete carbonation to sequester CO_2 [164], [176]. García-Segura et al. [177] developed an expression for concrete carbonation, given by equation 8.7. This equation considers the service life t and carbonation coefficient k, the exposed area A and the amount of cement C in one cubic meter of concrete. Additionally, the amount of clinker in the cement is represented by *k*.

$$CO_2 fixed\,(kg) = 0.383 \cdot \frac{k\left(\frac{mm}{\sqrt{year}}\right) \cdot \sqrt{t(year)}}{1000} \cdot A(m^2) \cdot C\left(\frac{kg}{m^3}\right) \cdot k(\%) \quad (8.7)$$

The end-of-life stage includes the procedures that occur after the structure's lifetime, specifically the dismantling of the structure. This stage involves using machinery to demolish the structure and transporting and treating the waste generated during this process. The distances between the building site and the landfill or waste treatment facilities must be specified as part of the analysis. Depending on the properties of the waste materials, there are three primary options for their disposal: reuse, recycling, or landfilling. Concrete and steel are the most commonly used materials in bridge construction, and waste treatment options depend on the region and population's needs.

The inventory analysis involves collecting data on all the materials and energy consumed during the bridge life cycle. Considering these processes' outputs allows for determining the product's environmental impact. Figure 8.2 shows the processes involved in each stage.

The LCA impact was assessed using a Python script incorporating data from Ecoinvent version 3.7.1 [199] and soca version 2 [312]. One unit of each product was modeled using GreenDelta's OpenLCA software, an open-source tool widely used in the scientific community for LCA [198].

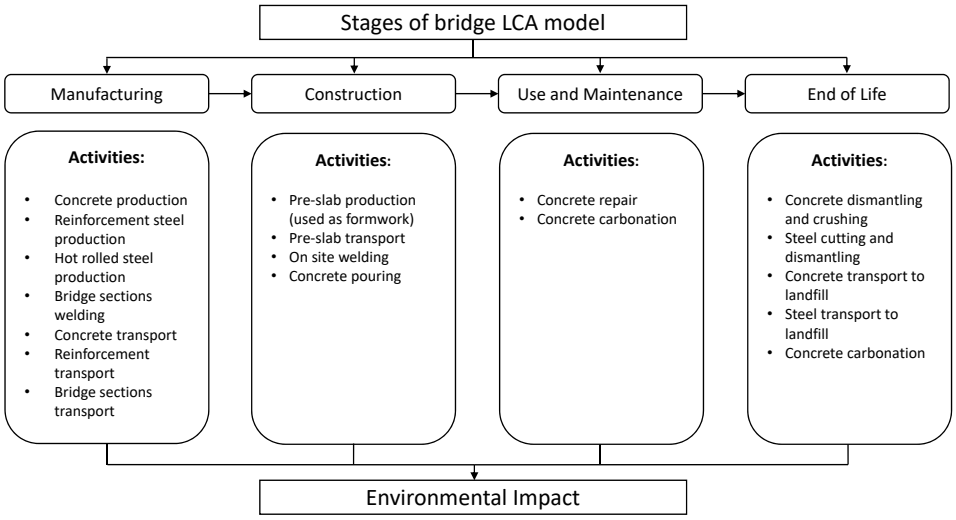

Figure 8.2: Bridge life cycle model stages and activities

8.2.4 Problem definition

This study aims to optimize the structure of a 60-100-60 meter SCCB deck with a box-girder geometry. Prior research has defined the optimization problem and employed single-objective metaheuristic optimization methods to evaluate cost, CO_2 emissions, and embodied energy [298], [310], [311]. In this paper, we present a metamodel-assisted strategy that utilizes deep neural networks (DNN) to conduct environmental and social life cycle assessment (LCA) optimization. Our approach enables us to compare the computational costs and design changes associated with considering a complete social and environmental impact profile.

Variables and parameters

The structural problem for this research involves a 60-100-60 meter SCCB deck with a box-girder geometry. The problem includes 34 design variables considering the bridge's cross-section, stiffeners geometry, slab reinforcement, and material strength. The variables are grouped into four categories: cross-section geometry variables (b, α_w, h_s, h_b, h_{fb}, t_{f_1}, b_{f_1}, h_{c_1}, t_{c_1}, t_w, h_{c_2}, t_{c_2}, b_{c_2}, t_{f_2}, h_{s_2}); stiffener and floor beam variables ($n_{s_{f_2}}$, d_{st}, d_{sd}, s_{f_2}, s_w, s_t, h_{fb}, b_{fb}, $t_{f_{fb}}$, $t_{w_{fb}}$), which define the stiffeners' and transverse elements' position and geometry; reinforcement and shear connector variables (n_{r_1}, n_{r_2}, ϕ_{base}, ϕ_{r_1}, ϕ_{r_2}, h_{sc}, ϕ_{sc}); and material strength vari-

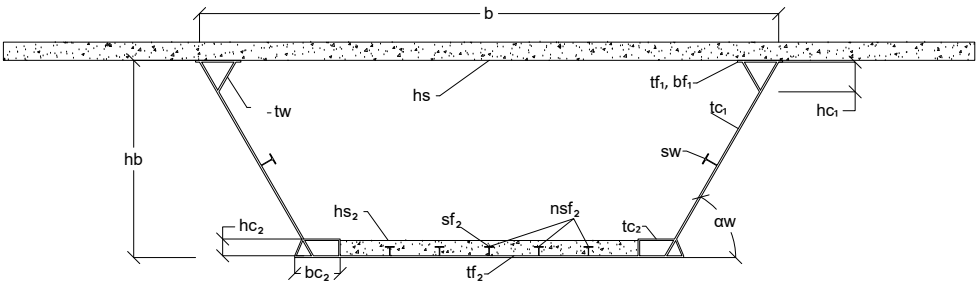

Figure 8.3: SCCB structural optimization problem cross-section variables

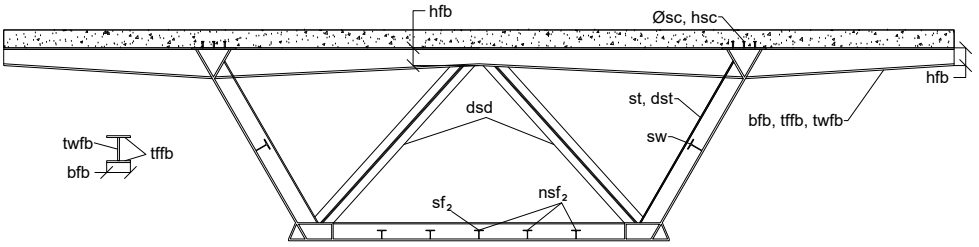

Figure 8.4: SCCB structural optimization stiffeners and floor beam variables

ables (f_{ck}, f_{yk}, f_{sk}). The geometric variables' position in the cross-section is shown in Figure 8.3, while the floor beams and stiffeners variables are presented in Figure 8.5. The optimization problem is discrete, as previously reported in related research on this optimization problem [311]. Lower and upper bounds and step sizes have been defined for all SCCB variables, and the discretization of the variables is summarized in Table 8.3. Considering all possible combinations, the number of designs is equal to 1.38×10^{46}.

Additionally, the optimization problem includes parameters that remain constant throughout the optimization process and are referred to as fixed parameters. These parameters are the same as those defined in the original problem [279]. The first fixed parameters are the bridge length and width. The bridge spans a total length of 200 m, with two lateral spans of 60 m and one central span of 100 m, and has a width (W) of 16 m. The bounds of the variables defined in Table 8.3 are also considered fixed parameters. Moreover, other parameters define the position and minimum values for specific elements, such as the reinforcement areas, lower flange, web thicknesses, and lower slab distributions shown in Figure 8.5. The minimum values of the web and bottom flange thicknesses ($t_{w_{min}}$, t_{f_2min}) are determined to be 15 mm and 25 mm,

Table 8.3: Optimization problem variables and boundaries

Variables	Unit	Lower Limit	Upper Limit	Step Size	Possibilities
Geometrical variables					
b	m	7	10	0.01	301
α_w	deg	45	90	1	46
h_s	mm	200	400	10	21
h_b	cm	250 (L/40)	400 (L/25)	1	151
t_{f_1}	mm	25	80	1	56
b_{f_1}	mm	300	1000	10	71
h_{c_1}	mm	0	1000	1	101
t_{c_1}	mm	16	25	1	10
t_w	mm	16	25	1	10
h_{c_2}	mm	0	1000	10	101
t_{c_2}	mm	16	25	1	10
b_{c_2}	mm	300	1000	10	71
t_{f_2}	mm	25	80	1	56
h_{s_2}	mm	150	400	10	26
Stiffeners and floor beams					
$n_{s_{f_2}}$	u	0	10	1	11
d_{st}	m	1	5	0.1	41
d_{sd}	m	4	10	0.1	61
s_{f_2}	mm		IPE 200 – IPE 600 *		12
s_w	mm		IPE 200 – IPE 600 *		12
s_t	mm		IPE 200 – IPE 600 *		12
h_{fb}	mm	400	700	100	31
b_{fb}	mm	200	1000	100	9
$t_{f_{fb}}$	mm	25	35	1	11
$t_{w_{fb}}$	mm	25	35	1	11
Reinforcement and shear connectors					
n_{r_1}	u	200	500	1	301
n_{r_2}	u	200	500	1	301
ϕ_{base}	mm		6, 8, 10, 12, 16, 20, 25, 32		8
ϕ_{r_1}	mm		6, 8, 10, 12, 16, 20, 25, 32		8
ϕ_{r_2}	mm		6, 8, 10, 12, 16, 20, 25, 32		8
h_{sc}	mm		100, 150, 175, 200		4
ϕ_{sc}	mm		16, 19, 22		3
Material strength					
f_{ck}	MPa		25, 30, 35, 40		4
f_{yk}	MPa		275, 355, 460		3
f_{sk}	MPa		400, 500		2

* Following the series of IPE profiles defined in [239].

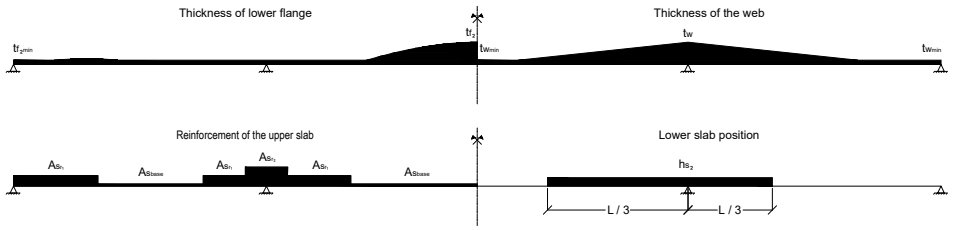

Figure 8.5: Reinforcement, thicknesses and lower slabs distribution in bridge spans

respectively, according to specific design guidelines [25], [242]. The last geometrical parameter is the reinforcement coating, which is set to 45 mm by Eurocode 2 [238] for an XD2 environment.

In addition, the following parameters define the characteristics of the concrete according to Eurocode 2 [238] regulations. These parameters include the maximum aggregate size, fixed at 20 mm, and the steel and concrete Young's longitudinal and transverse moduli. The parameter values for steel are fixed at 210,000 MPa and 80,769 MPa, respectively, while for concrete, they depend on the strength, with the expressions $22 \cdot ((f_{ck} + 8)/10)^3$ and $E_{cm}/(2 \cdot (1 + 0.2))$.

Finally, the last set of parameters defines the bridge service life, structural class, and loading parameters. The service life for this type of structure is set at 100 years, while the structural class is determined to be S5 following Eurocodes [240]. The loads considered in the bridge include self-weight, dead loads, traffic, temperature variation, and wind, with all loads defined per Eurocode 1 [240].

Constraints

The optimization problem is subject to constraints that ensure structural safety (ULS) and serviceability (SLS), as prescribed by Eurocodes [26], [237], [238]. Specific design guidelines [25], [242] were also considered to establish additional constraints.

Structural resistance of the bridge sections falls under ULS constraints, while SLS constraints relate to prescribed stresses and deflection limitations of materials and the structure. Load and combination prescriptions were taken from Eurocode 1.

Both local and global structural models were utilized to perform ULS checking. The global analysis evaluated shear, flexure, torsion, and flexure-shear interaction, check-

ing for solution feasibility. Shear lag [26] and Class 4 section slenderness [238] were taken into account when determining section resistance. A 10^{-6} accuracy was specified for the iterative Class 4 reduction method. Homogenization of sections was done by considering the coefficient (n) between the longitudinal deflection modulus of steel (E_s) and concrete (E_cm) according to Equation 8.8. Concrete creep and shrinkage was determined according to Eurocodes [26], [237], [238]. Local modeling was employed to assess floor beam and diaphragm response to ULS.

$$n = \frac{Es}{Ecm} \tag{8.8}$$

Regarding SLS constraints, the deflection limit was determined according to Spanish regulation IAP-11 [241], which stipulates a maximum deflection value of L/1000 for frequent combinations of live loads, where L denotes the length of each span. Structural and geometrical constraints were also specified. All structural tests were performed using a Python-programmed numerical model [243].

The ULS and SLS checking coefficients were determined based on the difference between the design values of the effects of actions (E_d) and their corresponding resistance values (R_d), as illustrated by Equation 8.9. The section satisfies the constraints if these coefficients are greater than or equal to one.

$$\frac{R_d}{E_d} \geq 1 \tag{8.9}$$

8.3 Results and discussion

This section details the main experiments carried out when integrating the deep learning model within the optimization algorithms described above. This results section has been divided into two sub-sections for a better understanding. The first, section 8.3.1, details the central experiments that make it possible to build the deep learning model and later, with the best model obtained, describes the results of the times and minimums obtained by applying the deep learning model to the different optimization algorithms. Once the best configurations have been identified, in the second sub-section, the algorithms are applied to environmental and social life cycle analysis. The comparison and discussion of these results are detailed in sub-section 8.3.2.

8.3.1 Algorithm Analysis

This section aims to detail the methodology used to achieve the deep learning model. The primary hyperparameters and techniques used to achieve the model are described. Subsequently, a comparison of different metaheuristics that solve the optimization problem with and without the deep learning model is made.

Neural Network models comparison

For the construction of the classification model, multilayer perceptron networks, [314], were considered. As input variables, the value of the 34 variables was considered (Table 8.3), that define the design of a bridge. Multilayer perceptron networks have a series of parameters that need to be explored for proper tuning. Among the relevant parameters, the number of layers and the optimization method used to perform the learning of the network stand out. Additionally, because there is an imbalance between the classes, SMOTE, [315] was used as an oversampling method. Additionally, an essential point for constructing the model corresponds to the data set used for the training. This type of problem is not trivial to build a good data set. There are several difficulties, such as the imbalance of classes and the fact that values close to the minimum of the objective functions usually have fewer points. In this sense, experiments were carried out in the way the training set was constructed. Two types of heuristic techniques were used to generate the data set, one based on trajectory, OBAMO, and another swarm class, SCA. Three scenarios were tested: a dataset generated by OBAMO, one generated by SCA, and one that integrates both datasets.

The data set hybrid used has approximately 20,000 bridges that satisfy the constraints of the structural problem and 7,000 points that do not meet the conditions. Table 8.4 shows the results of the 5-fold cross-validation considering 1, 2, and 3 hidden layers and using oversampling with SMOTE. The test set was generated prior to performing the oversampling process. It is also important to consider that the Batch Size parameter, the optimization method, and the type of dataset used (hybrid) remained fixed in the experiment. When looking at the F1-score, it is clear from the table that using three hidden layers performs better when using the original data set or the oversampled dataset. We also observe that the oversampling case is higher than the standard model in the four indicators analyzed.

Models	Data							
	Training				Testing			
	Accuracy	Precision	Recall	F1-score	Accuracy	Precision	Recall	F1-score
1 hidden layer (128)	0.62	0.61	0.75	0.67	0.61	0.60	0.74	0.67
2 hidden layer (128-64)	0.79	0.73	0.93	0.82	0.78	0.84	0.72	0.78
3 hidden layer (128-64-32)	0.85	0.94	0.76	0.84	0.85	0.94	0.76	0.85
1 hidden layer-SMOTE	0.84	0.94	0.75	0.83	0.84	0.94	0.75	0.83
2 hidden layer-SMOTE	0.83	0.79	0.93	0.85	0.83	0.79	0.93	0.85
3 hidden layer-SMOTE	0.93	0.93	0.94	0.93	0.92	0.92	0.93	0.92

Table 8.4: Neural network configurations explored. The parameters used in the structure of the networks were ADAM as optimization algorithm, 128 as batch size, and integrated data set.

Another relevant experiment aims to quantify whether the hybrid dataset obtains better metrics than the other datasets. Table 8.5 summarizes the results using a batch size of 128, ADAM, and a three-layer network topology. The table shows that the hybrid case is more robust than each of the datasets separately in the four indicators. Finally, in Table 8.6, three techniques are evaluated to carry out the learning process, keeping the rest of the parameters constant. From the table, it can be seen that the ADAM method works better than Rmsprop and SGD. From the above, it is observed that the training set, the number of layers, and the oversampling are essential to obtain a model with good metrics. From now on, the model with three layers, Adam, batch size 128, will continue to be used.

Models	Data							
	Training				Testing			
	Accuracy	Precision	Recall	F1-score	Accuracy	Precision	Recall	F1-score
OBAMO dataset	0.87	0.90	0.85	0.87	0.87	0.90	0.85	0.87
SCA dataset	0.86	0.80	0.97	0.88	0.86	0.80	0.97	0.88
Hybrid dataset	0.93	0.93	0.94	0.93	0.92	0.92	0.93	0.92

Table 8.5: Exploration of different data sets. The network configuration was ADAM, with three hidden layers and a batch size of 128 and SMOTE oversampling.

Models	Data							
	Training				Testing			
	Accuracy	Precision	Recall	F1-score	Accuracy	Precision	Recall	F1-score
SGD	0.88	0.82	0.93	0.87	0.87	0.81	0.92	0.86
RmsProp	0.90	0.90	0.91	0.90	0.90	0.89	0.90	0.89
ADAM	0.93	0.93	0.94	0.93	0.92	0.92	0.93	0.92

Table 8.6: Exploration of different optimization algorithms. The network configuration was three hidden layers and a batch size of 128, SMOTE oversampling and integrated data set.

Time and optimization values analysis

Once the model that classifies whether the bridge complies with the constraints has been defined, we proceed to integrate it into the different algorithms described in section 8.2.2. The fundamental objective of the classification model is to speed up the calculations. This section's objective is to evaluate the effectiveness in the acceleration of the calculations through the times that the executions of the optimization last. For the evaluation to be fair, a correction factor must be incorporated in the case of the algorithm that uses the classification model. The above is because the model can be wrong, and the final result could be invalid. Each algorithm must generate 30 valid executions; in the case of the models that incorporate the DNN model, the times of all the executions will be added and divided by the times of the valid executions. That gives us a factor greater than one, which will be applied to the time of each valid execution made by the algorithm. The results with the application of the correction factor are shown in table 8.7, the objective function used in this case was the cost. From the table, it can be seen that the execution times are significantly reduced. In the case of OBAMO, the algorithm with DNN is 37 times faster; in the case of CS and SCA, it was 50 times faster. In absolute terms, CS was the fastest, followed by SCA. Another relevant point is that the optimization values are improved; on average, all the models with DNN obtain better values, and the dispersion of the values also decreases. The next step is to use the algorithms with DNN but with more complex objective functions.

	OBAMO	OBAMO_DNN	CS_Hybrid	CS_Hybrid_DNN	SCA_Hybrid	SCA_Hybrid_DNN
Min value	3826142.7	3822723.1	3822723.1	3822723.1	3822723.1	3822723.1
Mean value	3829815.0	3822726.0	3831446.3	3824305.2	3831247.4	3825153.7
Std	101135.9	2.7	27182.9	1309.7	16274.2	1715.3
Min Time (s)	8716.4	240.3	7911.0	158.4	7924.6	158.1
Mean Time (s)	9112.4	244.5	8083.6	159.1	7939.1	159.5

Table 8.7: Comparison of results with and without deep learning model for cost optimization.

8.3.2 Objective functions results comparison

One of the goals of this research is to obtain a sustainable and optimal design for an SCCB. For this purpose, the effects of different variables and material amounts have been analyzed. To compare the outcomes of three distinct single-objective optimization sets that consider cost, ELCA, and SLCA, 100 iterations were carried out. However, as the number of feasible solutions varied for each optimization objective, only the top 30 results were chosen for comparison to guarantee a fair and consistent assessment of solutions across all objectives. Additionally, this section includes a comparison with recent studies on SCCB optimization.

Initially, we studied the primary parameters of the cross-section and transverse stiffeners. As shown in Figure 8.6, the results were similar in terms of the distance of stiffeners and diaphragms (d_{st}, d_{sd}), with values ranging from 2 to 3.5 m for the three objectives for transverse stiffeners and 5.5 to 8 m for diaphragms. The most significant difference was observed in the web angle α_w, where ELCA had values ranging from 60 to 75 degrees, while both cost and SLCA resulted in higher ranges, ranging from 60 to 85 degrees. The height of the steel beam tended to have lower values for ELCA and SLCA objective functions. Upon analyzing the distribution of values, it was found that for SLCA and ELCA, higher groupings had lower heights. This is because the design of the cost objective looked for solutions with lower yield strength, which necessitated an increase in the cross-section height to avoid exceeding the tension limit.

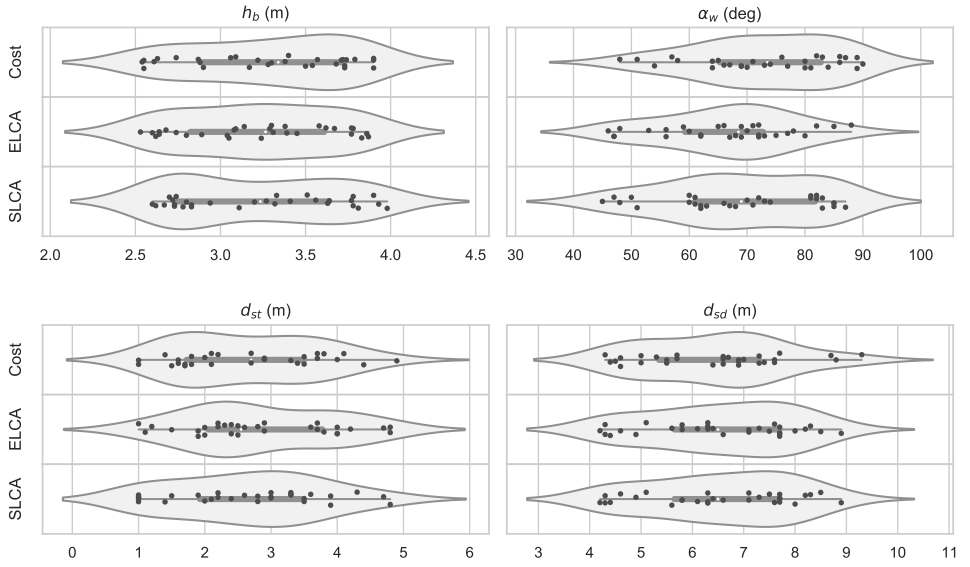

Figure 8.6: Cross-section main variables results for Cost, ELCA and SLCA objective functions

The following variables analyzed in this study pertain to the proposed cell values for the design. As shown in Figure 8.7, the height variables (h_{c_1}, h_{c_2}) for both upper and lower cells exhibited positive values, affirming the effectiveness of these elements in reducing the distance between steel plate webs without stiffening. Additionally, the thickness of these elements was minimal for the upper cell t_{c_1}, while for the bottom one, values ranged from 17 to 22. These elements aided in improving the flexural behavior of the cross-section, reducing the section reduction that is often classified as class 4 [237].

This study compares the amounts of main materials and objective function values reached by each optimization function. The results are summarized in Figures 8.8 and 8.9. It is observed that all optimization functions produced the same amount of structural steel, while the amount of reinforcing steel was higher for SLCA and ELCA. However, the increase in these amounts was not significant enough to indicate a clear difference between the functions. When focusing on the speed of material reduction, it was found that ELCA and Cost optimizations decreased the amount of structural steel at a slower rate than SLCA. This decrease was caused by the amount of recycled steel (steel scrap) considered in the manufacturing process. Recent studies [279] have shown that the trend in steel production is to increase the use of steel scrap to reuse the maximum amount of material possible. However, this generates

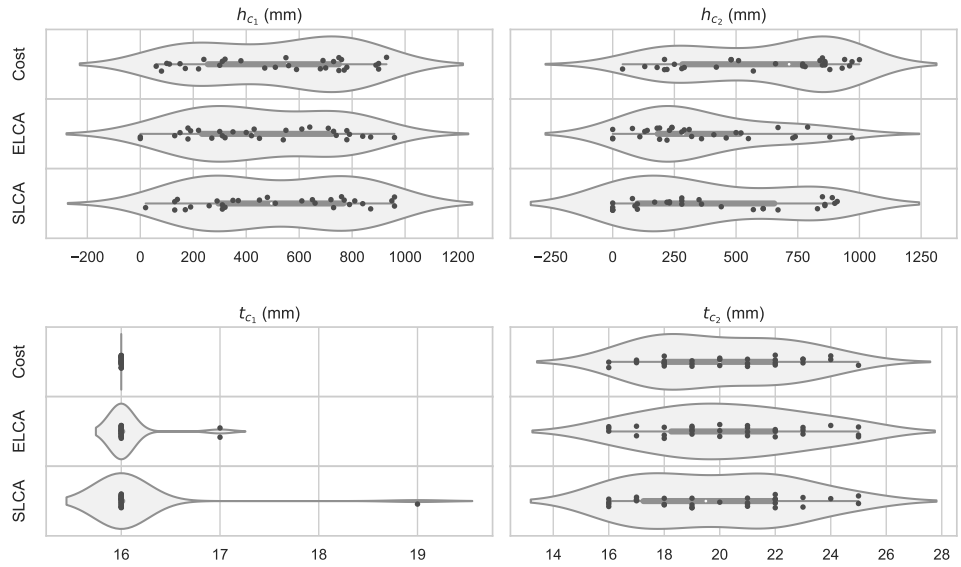

Figure 8.7: Cross-section cells geometry and thicknesses results for Cost, ELCA and SLCA objective functions

a higher impact on the social pillar of sustainability, resulting in an overall increase in impact. Considering that structural steel has the most significant impact on the objective functions, social optimization reduces the quantity of steel to minimize its impact. Another consequence of the amount of steel scrap used in the steel manufacturing process is shown in Figure 8.9. Recent studies that solve this optimization problem while considering CO_2 and embodied energy as sustainable criteria [298], [310], [311], and the LCA of SCCB [279], indicate that the environmental and social impact of steel is independent of the yield stress; it only depends on the amount of steel scrap used in the manufacturing process. In contrast, cost depends strongly on the yield strength. This is due to the usual yield stress of commercial profiles being 275 MPa, and the demand for higher yield strength steels being lower, resulting in lower production and higher cost. This clear difference is shown in Figure 8.9, where it can be seen that cost reduction gives an ELCA and SLCA reduction, but not necessarily the opposite. This results are in line with the ones obtained by Martínez-Muñoz et al. [298], [311] this confirms that the CO_2 emissions and the embodied energy can be a good approximation to environmental sustainability. The best individual results comparison have been show that ELCA and SLCA reach solutions with higher yield stress than cost, and obtaining a compromise solution can only be done by applying

a multi-objective optimization strategy, which will be interesting to consider in future studies.

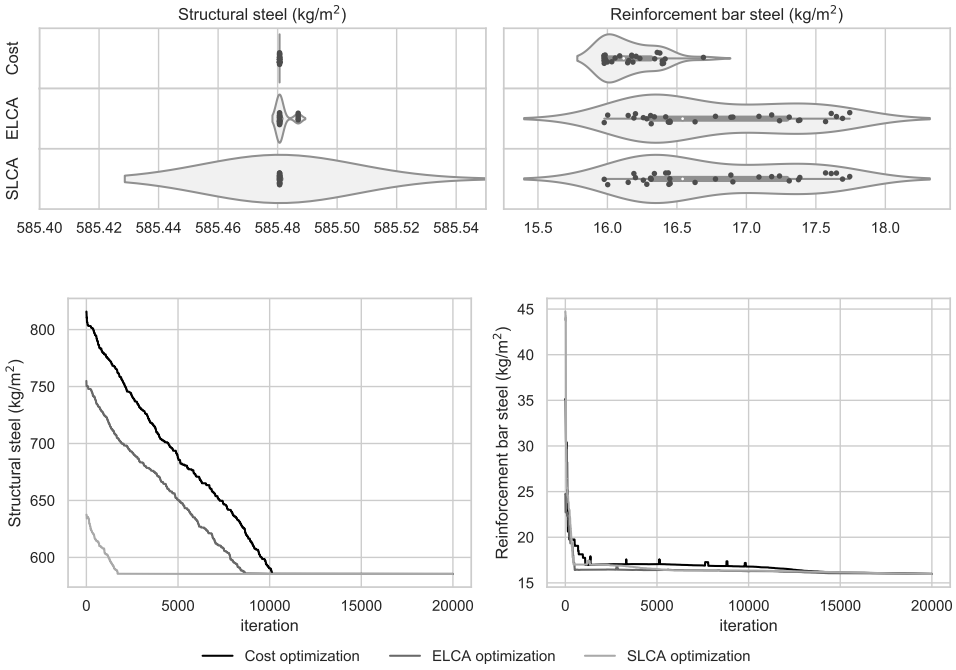

Figure 8.8: Steel amounts results an trajectories for Cost, ELCA and SLCA objective functions

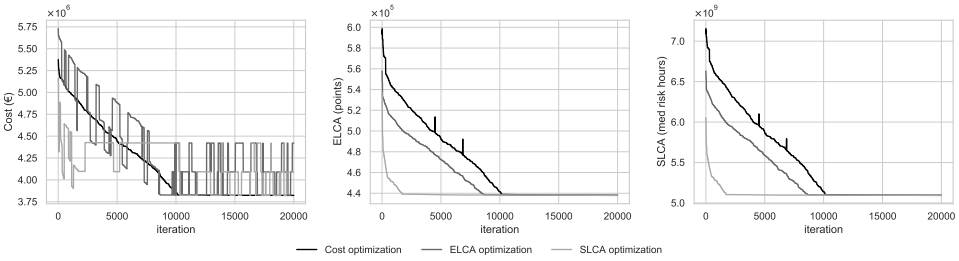

Figure 8.9: Cost, ELCA and SLCA variation for every objective function

Table 8.8 displays the results of the best individuals obtained through metamodel-assisted optimizations. These are the best feasible individuals selected from 100 algorithm runs. The table shows that the primary difference lies in the yield stress values. The best individuals for ELCA and SLCA exhibit higher values since there

is no penalty for increasing resistance in the objective function. Although the steel distribution across the cross-section differs, the total material amount remains unchanged. These results are comparable to those obtained in previous studies by Martínez-Muñoz et al. [298], [311] that consider CO_2 and embodied energy as environmental impact indicators. Moreover, a comparison with recent SCCB optimization studies indicates that the number of stiffeners in the lower flange is reduced to zero in this optimization problem. However, this outcome depends heavily on the chosen construction method.

Table 8.8: Best solutions obtained for cost, ELCA and SLCA objective functions

Variables	Unit	Cost	ELCA	SLCA
b	m	7	7	7
α_w	deg	64	71	73
h_s	mm	200	200	200
h_b	cm	255	262	363
h_{fb}	mm	400	590	530
t_{f_1}	mm	25	25	25
b_{f_1}	mm	300	300	300
h_{c_1}	mm	690	430	370
t_{c_1}	mm	16	16	16
t_w	mm	16	16	16
h_{c_2}	mm	840	0	0
t_{c_2}	mm	18	22	19
b_{c_2}	mm	300	300	300
t_{f_2}	mm	25	25	25
h_{s_2}	mm	150	150	150
$n_{s_{f_2}}$	u	0	0	0
d_{st}	m	3.7	2.6	1
d_{sd}	m	5.7	6.3	4
b_{fb}	mm	500	900	500
$t_{f_{fb}}$	mm	29	26	30
$t_{w_{fb}}$	mm	27	31	25
n_{r_1}	u	200	200	200
n_{r_2}	u	204	200	200
ϕ_{base}	mm	6	6	6
ϕ_{r_1}	mm	6	6	6
ϕ_{r_2}	mm	6	6	6
${s_{f_2}}^*$	mm	300	500	450
${s_w}^*$	mm	300	360	240
${s_t}^*$	mm	360	600	400
h_{sc}	mm	100	100	100
ϕ_{sc}	mm	19	22	16
f_{ck}	MPa	25	25	25
f_{yk}	MPa	275	460	355
f_{sk}	MPa	500	500	500
Structural steel	kg	2,060,892	2,060,892	2,060,892
Reinforcement steel	kg	56,271	56,239	56,239
Concrete	m³	528	528	528

8.4 Conclusions

This research have used a deep neural network metamodel for accelerating the optimization of a SCCB. This metamodel has been applied to SCA, CS and OBAMO algorithms to carry out the optimization and comparing the perfomance. The neural network model used in this study has demonstrated significant improvements in optimization speed, with a range of 37 to 50 times faster than traditional optimization methods. While the neural network model may lead to non-feasible solutions, the calculation speed increases so that such errors can be tolerated.

Furthermore, the optimization process using the validation model yielded more feasible results for ELCA and SLCA due to the increase in the steel yield stress. However, since the environmental and social impact of the design is not dependent on the yield stress, solutions that consider these as objective functions resulted in higher yield stress.

Overall, the solutions obtained using different objective functions consistently involved the use of cells in the cross-section of the bridge. This study suggests that deep learning models have great potential in optimizing complex engineering designs, particularly in reducing the computational time required for optimization. However, the trade-off between speed and accuracy must be carefully considered in practical applications. Future work will apply this DL acceleration to multi-objective and robust optimization techniques in order to get compromise solutions designs. On the other hand, it is also interesting to consider the methodology and apply it to other types of structural design problems to analyze the generality of this methodology.

Chapter 9

Game theory approach for environmental and social LCA multi-objective optimization of steel-concrete composite bridges

Authors:	D. Martínez-Muñoz, J.V. Martí, and V. Yepes		
Status:	Manuscript sent		
Journal:	Engineering Structures		
Year:	2023		
DOI:	–		
JCR IF (2021):	5.582		
	JCR Category	Ranking	Quartile
	Engineering, Civil	20/138	Q1
Presentation:	Manuscript		

Abstract

The design of bridges must balance sustainability and construction simplicity. A game theory-based optimization method was applied in this research to find a sustainable steel-concrete composite bridge design. The sustainability was evaluated through cost and environmental and social impact using the Life Cycle Assessment method. The optimization process considered four criteria simultaneously, using a discrete version of the SCA algorithm and a transfer function for discretization. The preferred solutions were selected using the Minkowski distances approach. Results showed a decrease in slab reinforcement and an increase in the amount of steel in the cross-section, leading to only an 8.2‰ increase in cost compared to similar studies. Regarding the cross-section, the geometry obtained considers cells in the upper and lower parts of the webs to improve the bending resistance. The proposed method allows for the simultaneous optimization of multiple criteria and provides a sustainable yet simple bridge design solution.

Keywords: game theory; multi-objective optimization; steel-concrete composite structures; bridges; metaheuristics; sustainability.

9.1 Introduction

Engineering problems involve selecting the optimal solution based on various criteria, such as cost, environmental and social impact, and construction simplicity. Balancing these criteria adds complexity to the decision-making process, requiring the use of techniques and tools to achieve practical solutions [316], [317]. To reach a compromise solution that considers the decision-making process and educates stakeholders, multi-objective optimization (MOO) techniques are applied [318]–[320]. MOO techniques allow for balancing all criteria and considering the relative importance of each in the decision-making process.

The civil engineering industry is known for considering multiple criteria in finding the best solution. Projects often have a significant economic impact and concerns regarding their environmental and social impact, given the large scale of these projects. One example is structure design problems, where researchers have been using multi-objective strategies to find optimal solutions [321]. Ghasemof et al. [322] have applied multi-objective optimization (MOO) to achieve a performance-based design for buildings. The same method has also been used to optimize seismic performance in structures, as demonstrated in the study by Rastegaran et al. [323], resulting in effective risk-based designs.

Furthermore, several other studies have focused on optimizing the geometric design of various structural components, including wind turbine foundations [230], reinforced concrete (RF) frames in bridges [324], and cable-stayed bridge tendons [325], among others. In the case of cable-stayed bridges, the optimization criteria considered include the structure's cost, sustainability, ease of construction, and safety. These studies often incorporate CO2 emissions as a criterion for sustainability, resulting in a design that optimizes cost and environmental impact.

Recent research in steel-concrete composite structures has shown that a single-objective optimization (SOO) approach, using either CO_2 emissions or embodied energy as the criteria, may not necessarily lead to an optimal cost solution. This is because increasing the yield stress of structural steel does not affect its emissions or embodied energy [298], [310].

Current studies in steel-concrete composite bridge (SCCB) optimization need to gain comprehensive knowledge from various fields. One limitation is using only one indicator for sustainability, such as CO_2 emissions or embodied energy [298], [310]. More advanced methods, such as the structure's Life Cycle Assessment (LCA), can provide a more comprehensive evaluation of the environmental impact profile. Additionally, existing studies have only considered sustainability's economic and environmental aspects, ignoring the social impact. Moreover, the optimization of SCCB has primarily been performed using SOO criteria, as demonstrated in the study by Briseghella [97] and noted in review articles [189].

This research presents a MOO strategy, utilizing a game theory approach, for designing a three-span Steel-Concrete Composite Bridge (SCCB) with a box-girder cross-section. The design includes adding four cells at the flange-web contact zone to reduce the distance between stiffened zones and minimize material usage.

The optimization problem is defined in section 9.2.3 to obtain a sustainable design that enhances construction ease. The MOO method, described in section 9.2, includes the use of a game theory-based approach and an objective function that considers the environmental and social impact, as well as cost, through a Life Cycle Assessment (LCA) of the structure, as outlined in section 9.2.2.

The optimization procedure involves using the Sine Cosine Algorithm (SCA), adjusted to the discrete nature of the problem through a transfer function discretization technique, as discussed in section 9.2.4. The final step of selecting the best solution among the obtained results is using a Minkowski family distances-based approach, described in section 9.2.5.

This research aims to improve the knowledge and understanding of SCCB design by proposing a MOO strategy that balances sustainability and construction ease.

9.2 Multi-objective optimization

As a general definition, a multi-objective minimization problem can be defined as choosing a solution vector $\vec{X}$ with n variables that minimizes the k objective function chosen subject to m certain constraints as defined in equations 9.1 to 9.3.

$$\vec{X} = x_1, x_2, \ldots, x_n \tag{9.1}$$

$$min(f_i(\vec{X})) = min(f_1(\vec{X}), f_2(\vec{X}), \ldots, f_k(\vec{X})) \tag{9.2}$$

$$g_j(X) \geq 1 \tag{9.3}$$

In this study, the optimization problem consists of an SCCB deck. The structure has three spans, of which the lateral ones have a length of 60 m while the central span is 100 m. The structural optimization problem variables, parameters, and constraints have been defined in section 9.2.3. The objective functions chosen for the MOO have been the three pillars of sustainability, represented by the cost (economy), the environmental (environment) and the social (society) LCA, and the constructive ease of the RC slabs. All the objective functions have been defined in section 9.2.2. A game theory-based procedure has been selected to reach the optimal compromise solutions. This method has been described in section 9.2.1. Figure 9.1 summarizes the complete MOO process carried out in this research.

9.2.1 Game theory approach

Game theory is a brand of applied mathematics that allows studying the interaction in formalized incentive structures. The name given to this structure corresponds to *games*. The players represent the objective functions $f_i(\vec{X})$ in this problem. Players can change problem variables vector $\vec{X}$ for changing the value of the objective function. The goal of every player is to minimize the objective function. However, the value of every player's objective function can also be influenced by the decisions of other players regarding the variables vector.

Considering the above, it can be concluded that a game theory problem encompasses interest among players. Thus, it gives two possibilities for problem resolution. In the first one, players are guided by selfishness and, consequently, try to decrease their objective function without considering the consequences for the rest of the players. This, in game theory, is named a non-cooperative game. The point where the

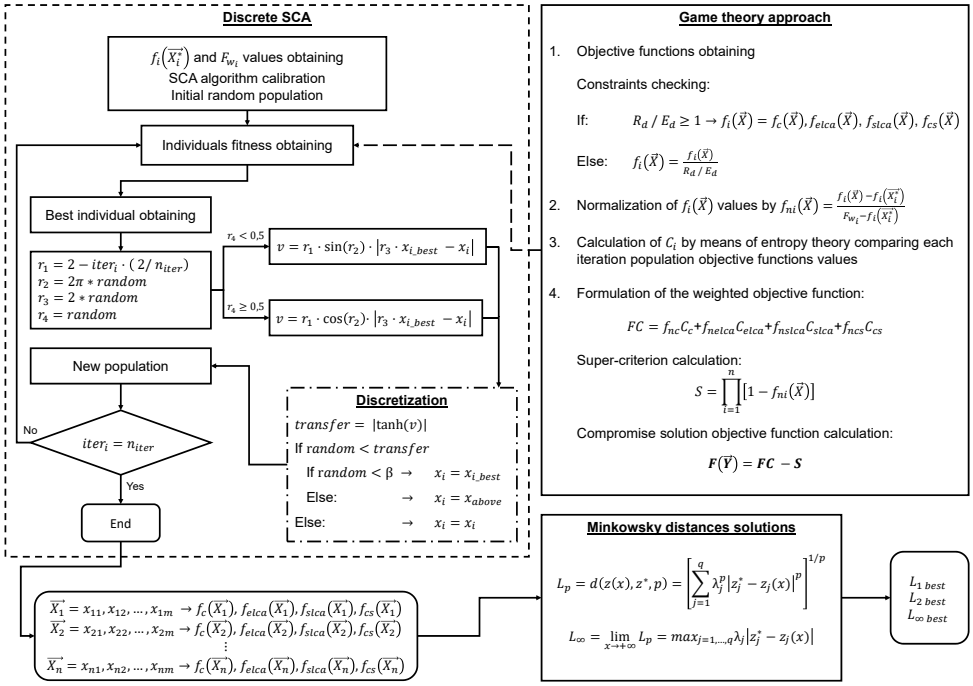

Figure 9.1: Game theory optimization process flowchart

players cannot modify the solution unilaterally to improve its corresponding criterion is called Nash equilibrium [326]. This equilibrium can be mathematically defined as given in equation 9.4 for n design variables and k criteria. This Nash equilibrium can be more than one point in the solution space and, in this case, $f_i(\vec{X})$ have different values for each Nash equilibrium point. If this situation is produced, the player that declares the moving of first place forces the others to move to the equilibrium point.

$$\begin{aligned} f_1(x_1^*, \ldots, x_n^*) &\leq f_1(x_1, x_2, \ldots, x_n^*) \\ f_2(x_1^*, \ldots, x_n^*) &\leq f_1(x_1^*, x_2, \ldots, x_n^*) \\ &\vdots \\ f_k(x_1^*, \ldots, x_n^*) &\leq f_k(x_1^*, x_2^* \ldots, x_n) \end{aligned} \tag{9.4}$$

The other option arises in which the players cooperate to find a better solution than the one reached in the Nash equilibrium. If the deciders take this strategy, this is defined as a cooperative game. As a consequence, this provides a space for so-

lutions. In order to allow the reduction of solutions, the Pareto-optimal concept can be applied. A multi-objective Pareto-optimal feasible solution $\vec{Y}$ accomplish that no exist another feasible solution $\vec{Z}$ which $f_i(\vec{Y}) \leq f_i(\vec{Z})$ for i = 1, 2, ..., k with almost one j that accomplish $f_j(\vec{Y}) < f_i(\vec{Z})$ [327]. The next step in the procedure is to choose the solution vector contained in the Pareto-optimal set that represents a compromise solution that benefits all players or at least is acceptable. This is made by defining specific negotiation rules between players that allow them to formulate a super-criterion. This super-criterion allows reformulating the MOO problem into a SOO that allows a compromise solution between players.

Game theory based optimization strategy

In this work, a game theory-based MOO has been applied to SCCB structural optimization. The methodology followed is the one proposed by Annamdas and Rao [328]. This method uses a cooperative game strategy in which the super-criterion maximizes the deviation between every objective function and its worst value. It should be noted that the method does not need the criteria introduced to be contrary to each other. It has taken good results in other engineering problems and consists of the following steps:

1. Minimize and maximize of the $k$objectives to get the best $f_i(\vec{X}_i^*)$ and the worst F_{w_i} value.

2. Normalize the current value of the $k$objective function $f_i(\vec{X})$ with respect to the best and worst value by means of equation 9.5.

$$f_{ni}(\vec{X}) = \frac{f_i(\vec{X}) - f_i(\vec{X}_i^*)}{F_{w_i} - f_i(\vec{X}_i^*)} \tag{9.5}$$

   This normalization avoids favoring any criteria by making the values of all criteria lie between zero and one when minimizing the objective function defined in 9.6.

3. Minimize an objective function $F(\vec{Y})$, defined in 9.6, that takes into account the compromise solution rules.

$$F(\vec{Y}) = FC - S \tag{9.6}$$

In this expression FC, defined in 9.7, represents a weighted objective function that includes the Pareto-optimal set.

$$FC = C_1 f_{n1}(\vec{X}) \ + \ \ldots \ + \ C_{k-1} f_{n(k-1)}(\vec{X}) \ + \ (1 - C_1 - \ldots - C_{k-1}) f_{nk}(\vec{X}) \quad (9.7)$$

with 0 $\leq C_i \leq$ 1 and $\sum_{i=1}^{n} C_i =$ 1

The super-criterion S, defined in 9.8, maximizes the deviation between every objective function and its worst.

$$S = \prod_{i=1}^{n} [1 - f_{ni}(\vec{X})] \quad (9.8)$$

The method proposed by Annamdas and Rao proposes to minimize FC for all possible combinations of weights C_i. This study has modified this method, assigning those weights to the values obtained through the entropy theory [329]. These weight values have been obtained by comparing the individuals generated in each population by the selected metaheuristic. The algorithm chosen is a discrete version of the sine cosine algorithm (SCA) which has been previously applied to this optimization problem considering different criteria as SOO [311]. This algorithm and its discretization technique have been defined in section 9.2.4.

9.2.2 Objective functions

The problem chosen for the MOO consists in reaching the optimum design of an SCCB involving four criteria as objective functions. Equations 9.9, 9.10, 9.11 and 9.12 assess the economic cost, the constructive simplicity of the slab, and the environmental and social life cycle assessment of the structure respectively.

$$C(\vec{x}) = \sum_{i=1}^{n} p_i \cdot m_i(\vec{x}) \quad (9.9)$$

The objective cost function multiplies the unit cost of every activity needed for constructing the bridge by its measurement. Table 9.1 includes all the construction units and their corresponding costs obtained from the BEDEC database [207]. In equation

Table 9.1: Cost values of every construction unit for SCCB

Construction unit	Unit	Cost (€)
Ccncrete C25/30	m^3	88.86
Concrete C30/37	m^3	97.80
Concrete C35/45	m^3	101.03
Concrete C40/50	m^3	104.08
Precast pre-slab	m^3	27.10
Reinforcement steel B400S	kg	1.40
Reinforcement steel B500S	kg	1.42
Rolled steel S275	kg	1.72
Rolled steel S355	kg	1.85
Rolled steel S460	kg	2.01
Shear-connector steel	kg	1.70

9.9, p_i corresponds with the price of every construction unit and m_i with its measurement.

$$CS(\vec{x}) = n_{layers} \cdot n_{bars} \tag{9.10}$$

The following objective function, defined in equation 9.10 considers the construction's simplicity of the RC slabs of the bridge. In this expression, n_{layers} and n_{bars} correspond to the number of reinforcement layers and bars. This criterion considers that a lower amount of both bars and reinforcement layers is simpler to carry out during construction. The number of bars has been considered in the support sections of the bridge. In this section, the bridge is subjected to negative bending moments and, consequently, traction in the upper slab. Furthermore, the structural resistant model defined in EN 1994-1-1 [26] only considers reinforcement to obtain the ultimate moment of the section, which favors the placement of a more significant amount of reinforcement.

$$ELCA(\vec{x}) = \sum_{i=1}^{n} \sum_{j=1}^{p} elca_j \cdot m_j(\vec{x}) \tag{9.11}$$

$$SLCA(\vec{x}) = \sum_{i=1}^{n} \sum_{j=1}^{p} slca_j \cdot m_j(\vec{x}) \tag{9.12}$$

LCA's objective is to assess the structure's environmental (ELCA) and social impact (SLCA), considering the processes needed, from the extraction of the raw material to the demolition of the structure and its transport to the landfill site. In equations 9.11 and 9.12, i represent every life cycle stage, $elca_j$ and $slca_j$ the environmental and social impact of every process needed in every stage respectively, and m_j the measurement of every process. The processes considered and their corresponding environmental and social impact are defined in Table 9.2. The LCA method has been described in detail in section 9.2.2.

Table 9.2: Ecoinvent processes LCA environmental and social impact values

Process	**Unit**	$elca_i$ **(points)**	$slca_i$ **(mrh)**
concrete production 25MPa	m³	2.037E+01	1.254E+05
concrete production 30MPa	m³	2.631E+01	1.668E+05
concrete production 35MPa	m³	2.478E+01	1.554E+05
concrete production 40MPa	m³	2.585E+01	1.623E+05
steel production 71% of recycling rate	kg	1.523E-01	1.941E+03
steel production 98% of recycling rate	kg	1.036E-01	2.067E+03
transport, freight, lorry 16-32 metric ton, EURO6	t·km	2.502E-02	4.116E+01
transport, freight, lorry 3.5-7.5 metric ton, EURO6	t·km	7.755E-02	1.655E+02
welding, arc, steel	m	2.350E-02	2.535E+02
welding, gas, steel	m	2.303E-02	2.429E+02
diesel, burned in building machine	MJ	1.361E-02	8.764E+00
carbon dioxide	kg	4.369E-02	0.000E+00
rock crushing	kg	7.223E-05	8.305E-01

Life cycle assessment method

The life cycle assessment is the evaluation of the contribution of the processes of one activity or product to its global impact. Together, these procedures cover all the steps needed to complete this product or activity. Depending on the scope of the LCA, the processes considered begin with the raw material extraction and finish in the different stages of the product's service life. In the case of bridges, the regulation that defines the procedure to carry out the environmental LCA is the ISO 14040:2006 [145]. In addition, the guide to follow to assess the social impact is the *Guidelines for Social Life Cycle Assessment of Products* [224]. To model the structure's life cycle, it is necessary to obtain the impacts from databases and choose a life cycle impact assessment (LCIA) method. The method chosen for this research is the ReCiPe 2008 method [151] for ELCA and the social impacts weighting method (SIWM) for SLCA. The databases contain information about the impact of processes. In this research, ecoinvent v3.7.1. [199] and soca v2 [312] have been chosen for ELCA and SLCA respectively. These databases are frequently upgraded and are very reliable

for the scientific community [200]. Furthermore, the soca database allows associating ecoinvent processes with the PSILCA [313] database social impacts, being a useful tool for scientists [279].

In order to assess the impact of the SCCB, four stages have been defined for obtaining the full impact of the bridge. These phases correspond to manufacturing, construction, use, maintenance, and end of life, which are similar to those defined in previous bridge LCA studies [279].

Manufacturing encompasses transforming the raw material into the products needed for construction and their transportation to the building site, considering the wastes generated during these activities. In the case of steel products production, recycled steel radically impacts the bridge global environmental impact in SCCB [279]. It is critical to distinguish between structural and rebar steel since, according to some studies, the reinforcement steel recycling percentage is 71%. In contrast, the structural steel recycling ratio is 98% in developed countries such as EEUU [193].

Construction includes the actions required to build the bridge, considering the equipment, depending on the building style and location of the structure, which is all included in the construction phase. Formwork, scaffolding, vibrators, and concrete pouring must be considered. Additionally, the procedures for welding the steel sections that were overlooked during the manufacturing phase must be established for steel and steel-concrete composite bridges. The diesel consumption of the machinery, which is based on information from the manufacturer, the literature, or other sources, is included in the LCA model for modeling construction activities.

All the tasks required throughout the structure's lifetime are included in the use and maintenance stage. Research has found that concrete can be carbonated to fix CO_2 [164], [176]. According to the study of García-Segura et al. [177], the expression of concrete carbonation is represented in equation 9.13. In this equation, t is the service life, and k is the carbonation coefficient. Concrete's exposed area is denoted by A, while C is the amount of cement contained in one concrete cubic meter. Finally, the amount of clinker in the cement is *k*.

$$CO_2 fixed\,(kg) = 0.383 \cdot \frac{k\left(\frac{mm}{\sqrt{year}}\right) \cdot \sqrt{t(year)}}{1000} \cdot A(m^2) \cdot C\left(\frac{kg}{m^3}\right) \cdot k(\%) \quad (9.13)$$

The dismantling of the structure, or the procedures that take place after the structure's life, is included in the end-of-life stage. The main operation is the machinery necessary to carry out the structure's demolition and the transportation and treatment of the waste products produced during that stage. As a result, the distances

between the building's site and the landfill or waste treatment facilities must be specified. Depending on the properties of the waste materials, there are three primary options for their disposal: reuse, recycling, or landfilling. Concrete and steel are the most common materials used in bridge construction. Waste treatment options are based on the population's needs and the region under consideration.

The inventory analysis constitutes the data gathering for all the materials and energy consumption required to develop all the processes involved in the bridge life cycle. When these processes' outputs are considered, the environmental impact of the product being evaluated can be determined. The processes used in every stage are shown in figure 9.2

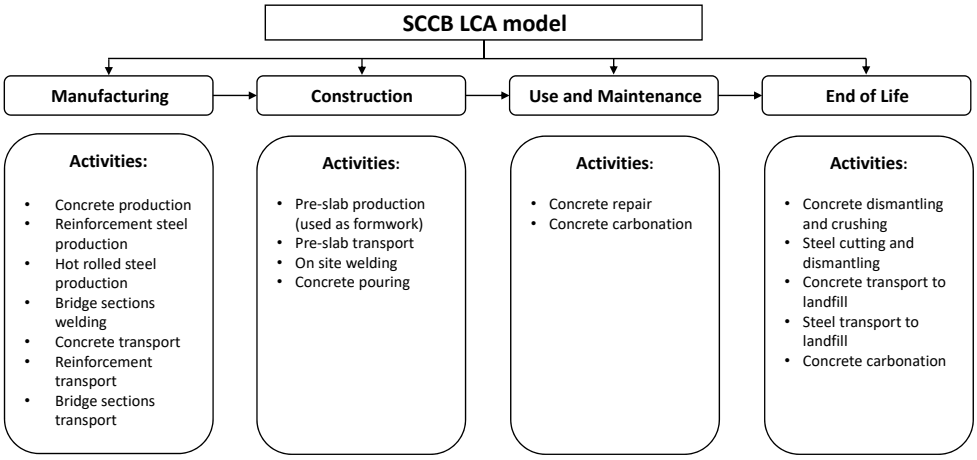

Figure 9.2: Bridge life cycle model stages and activities

The LCA impact was evaluated using a Python script created using information from Ecoinvent [199] in version 3.7.1. and soca in version 2 [312]. Data have been obtained modeling one unit of every product with GreenDelta's OpenLCA software. This tool, which is open source, enables the LCA, particularly for the scientific community [198].

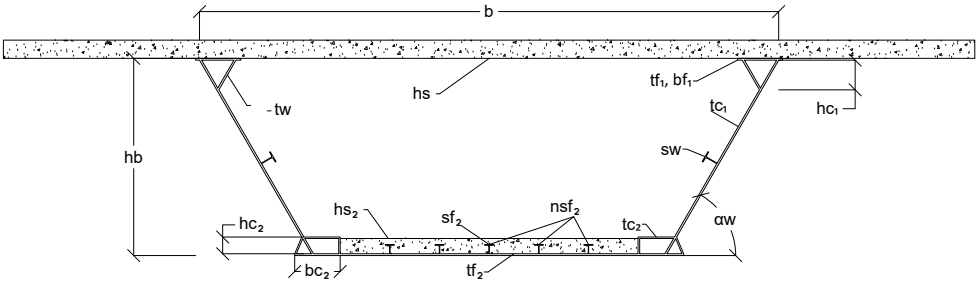

Figure 9.3: SCCB structural optimization problem cross-section variables

9.2.3 Problem definition

The structural optimization problem chosen for this research has been a 60-100-60 meter SCCB deck. The geometry of this deck is box-girder. The optimization problem has been defined previously in recent studies where SOO procedures have been applied [310]. This research applies a MOO game theory-based procedure to this existing optimization problem.

Variables and parameters

The structural problem considers a total of 34 design variables. These variables consider the bridge cross-section and stiffener geometry, the slabs' reinforcement, and the materials' strength. The variables are grouped in four groups corresponding to the cross-section geometry variables (b, α_w, h_s, h_b, h_{fb}, t_{f_1}, b_{f_1}, h_{c_1}, t_{c_1}, t_w, h_{c_2}, t_{c_2}, b_{c_2}, t_{f_2}, h_{s_2}), the stiffeners and floor beam variables ($n_{s_{f_2}}$, d_{st}, d_{sd}, s_{f_2}, s_w, s_t, h_{fb}, b_{fb}, $t_{f_{fb}}$, $t_{w_{fb}}$) which define the stiffeners and transverse elements position and geometry, the reinforcement and shear connectors variables (n_{r_1}, n_{r_2}, ϕ_{base}, ϕ_{r_1}, ϕ_{r_2}, h_{sc}, ϕ_{sc}) and the materials strenght variables (f_{ck}, f_{yk}, f_{sk}). Figure 9.3 shows the geometrical variables' position in the cross-section while 9.5 shows the floor beams and stiffeners variables. The optimization problem nature is discrete, as stated in previous research on this optimization problem [311]. All SCCB variables have been defined considering a lower, an upper bound, and step size. The discretization of the variables has been summarized in table 9.3. Considering all combination possibilities, the number of designs is equal to 1.38×10^{46}

Furthermore, the optimization problem is defined by some conditions that do not vary during the optimization problem. These conditions without variation are named parameters. This optimization problem considers the same parameters defined in the original problem [279]. The first parameters defined are bridge length and width. The

Table 9.3: Optimization problem variables and boundaries

Variables	Unit	Lower Limit	Upper Limit	Step Size	Possibilities
Geometrical variables					
b	m	7	10	0.01	301
α_w	deg	45	90	1	46
h_s	mm	200	400	10	21
h_b	cm	250 (L/40)	400 (L/25)	1	151
t_{f_1}	mm	25	80	1	56
b_{f_1}	mm	300	1000	10	71
h_{c_1}	mm	0	1000	1	101
t_{c_1}	mm	16	25	1	10
t_w	mm	16	25	1	10
h_{c_2}	mm	0	1000	10	101
t_{c_2}	mm	16	25	1	10
b_{c_2}	mm	300	1000	10	71
t_{f_2}	mm	25	80	1	56
h_{s_2}	mm	150	400	10	26
Stiffeners and floor beams					
$n_{s_{f_2}}$	u	0	10	1	11
d_{st}	m	1	5	0.1	41
d_{sd}	m	4	10	0.1	61
s_{f_2}	mm	IPE 200 – IPE 600 *			12
s_w	mm	IPE 200 – IPE 600 *			12
s_t	mm	IPE 200 – IPE 600 *			12
h_{fb}	mm	400	700	100	31
b_{fb}	mm	200	1000	100	9
$t_{f_{fb}}$	mm	25	35	1	11
$t_{w_{fb}}$	mm	25	35	1	11
Reinforcement and shear connectors					
n_{r_1}	u	200	500	1	301
n_{r_2}	u	200	500	1	301
ϕ_{base}	mm	6, 8, 10, 12, 16, 20, 25, 32			8
ϕ_{r_1}	mm	6, 8, 10, 12, 16, 20, 25, 32			8
ϕ_{r_2}	mm	6, 8, 10, 12, 16, 20, 25, 32			8
h_{sc}	mm	100, 150, 175, 200			4
ϕ_{sc}	mm	16, 19, 22			3
Material strength					
f_{ck}	MPa	25, 30, 35, 40			4
f_{yk}	MPa	275, 355, 460			3
f_{sk}	MPa	400, 500			2

* Following the series of IPE profiles defined in [239].

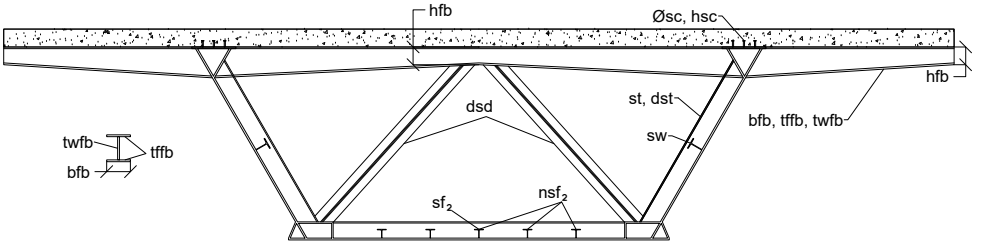

Figure 9.4: SCCB structural optimization stiffeners and floor beam variables

entire length of the bridge is 200 m, divided into two lateral spans of 60 and one central of 100, and its width (W) is 16 m. The following parameters are the variables' bounds defined in table 9.3. In addition, in this problem exist other parameters that define the position and the minimum values for some elements. This is the case of the reinforcement areas, lower flange, web thicknesses, and lower slab distributions represented in Figure 9.5. The minimum value of the web and bottom flange thicknesses ($t_{w_{min}}$, $t_{f_2 min}$) are defined in 15 a and 25 mm respectively by specific design guidelines [25], [242]. The last geometrical parameter is the reinforcement coating which is the one defined in Eurocode 2 [238] for an XD2 environment being 45 mm.

The following parameters define the characteristics of concrete following Eurocode 2 [238] regulation. These parameters are the maximum aggregate size, fixed in 20 mm, and the steel and concrete Young longitudinal and transverse modulus. For steel, these parameter values are fixed in 210,000 MPa and 80,769 MPa, respectively, while for concrete depend on the strength being the expressions $22 \cdot ((f_{ck} + 8)/10)^3$ and $E_{cm}/(2 \cdot (1 + 0.2))$.

Finally, the last parameters define the bridge service life, structural class, and loading parameters. Service life defined for this kind of structure is 100 years, while the structural class corresponds to S5 according to Eurocodes [240]. The loads considered in the bridge are self-weight, dead loads, traffic, temperature variation, and wind. All these loads have been defined following the Eurocode 1 [240].

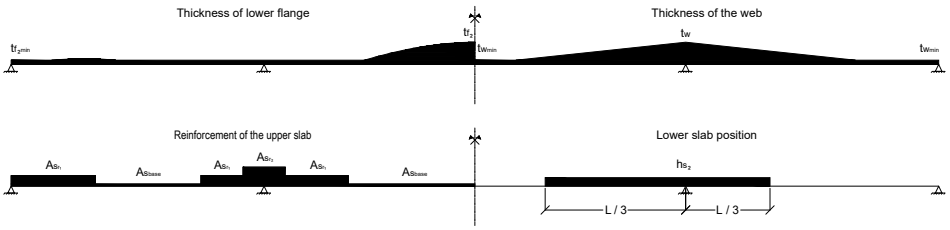

Figure 9.5: Reinforcement, thicknesses and lower slabs distribution in bridge spans

Constraints

The optimization problem's restrictions are related to the structural safety (ULS), and serviceability (SLS) constraints specified by the rules [26], [237], [238]. In addition, limitations were included by specific design guidelines [25], [242].

The ULS relates to the structural resistance of bridge sections, whereas the SLS corresponds to the prescribed stresses of the materials and structure deflection limitations. The prescribed loads and combinations correspond to those imposed by Eurocode 1.

Local and global structural models were undertaken for ULS checking. The feasibility of solutions is related to shear, flexure, torsion, and flexure-shear interaction checking in the case of global analysis. To determine the section's resistance, the shear lag [26] and slenderness of Class 4 sections [238] were taken into account. The accuracy of the iterative Class 4 reduction method was specified at 10^{-6}. Sections were homogenized by taking into account the coefficient (n) between the longitudinal deflection modulus of concrete (E_{cm}) and steel (E_s), as described by Equation 9.14. Creep and shrinkage of concrete were determined by the Eurocodes [26], [237], [238] standard. Local modeling was done to establish the floor beam and diaphragm response to ULS.

$$n = \frac{Es}{Ecm} \tag{9.14}$$

As SLS limitations, deflection, the material's tension limit, and fatigue were determined. The deflection limit was established by Spanish regulation IAP-11 [241], establishing L/1000 as the maximum deflection value for frequent combinations of live loads. In this instance, L denotes the length of each span. In addition, structural

limits and geometrical constraints were specified. All structural tests were specified using a Python-programmed [243] numerical model.

Both ULS and SLS checking coefficients relate to the difference between the design values of the effects of actions (E_d) and its associated resistance value (R_d), as shown by the equation 9.15. If these coefficient values are higher than or equal to one, the section satisfies the constraints defined in equation 9.3.

$$\frac{R_d}{E_d} \geq 1 \tag{9.15}$$

9.2.4 Sine cosine algorithm

The original Sine Cosine Algorithm (SCA) was proposed in 2016 by Mirjalili [233] and corresponds to a swarm intelligence class metaheuristic that uses sine and cosine functions to explore and utilize the search space. In addition, using P_j^t, which corresponds to the location of the target solution for iteration t and dimension j, to shift the solutions, the best solution so far is often employed. In addition, the method employs three numbers between 0 and 1 (r_1, r_2, and r_3). Equations 9.16 and 9.17 illustrate the updating mechanism used.

$$x_{i,j}^{t+1} = x_{i,j}^t + r_1 \times sin(r_2) \times \mid r_3 P_j^t - x_{i,j}^t \mid \tag{9.16}$$

$$x_{i,j}^{t+1} = x_{i,j}^t + r_1 \times cos(r_2) \times \mid r_3 P_j^t - x_{i,j}^t \mid \tag{9.17}$$

As the nature of the SCA algorithm is continuous, a discrete version of this algorithm has been used in this research. This discrete version has been proposed by Martínez-Muñoz et al. [310] and recently applied to this optimization problem with a SOO approach. This discrete version uses the velocities obtained for the second term of the equations 9.16 and 9.17, which is the one that controls the variables' vector change. It applies a v-shape transfer function $\mid \tanh(v) \mid$ to it as proposed by Hussien et al. [330]. The value obtained is compared with a random number between [0, 1). If the value of the random number is higher than the one obtained by the transfer function, the variable remains without changes; otherwise, a β value is defined and compared with a new random number to define if the variable takes the best value variable or change it to a near value. This β value has been tuned for this optimization problem in Martínez-Muñoz et al. [310] setting it in 0.8.

It should be noted that some individual solutions can be unfeasible due to the constraints applied to the optimization problem defined in section 9.2.3. When it occurs, a penalty function is applied to the objective function to increase its value proportionally to how far it is from meeting the constraint as defined in equation 9.18.

$$f_i(\vec{X}) = \frac{f_i(\vec{X})}{R_d/E_d} \tag{9.18}$$

9.2.5 Multi-objective preferred solutions selection

As the execution of the algorithm is repeated 30 times, different solutions are obtained. In SOO, the best is defined by the one that gets the lower objective function value. In this case, a method for the best individual selection must be followed, as four objective functions have been chosen for the MOO. The procedure applied for reaching the preferred solutions is proposed by Yepes et al. [331]. This strategy uses the three Minkowski metrics to choose the solution closest to the ideal point. This method applies the Manhattan (L_1), Euclidean (L_2), and Tchebycheff (L_∞). Equation 9.19 shows how the distance from any point $z(x) \in \mathbb{Z} \subset \mathbb{R}^q$ is evaluated in the p norm.

$$\begin{gathered} L_p = d(z(x), z^*, p) = \left[\sum_{j=1}^{q} \lambda_j^p \left| z_j^* - z_j(x) \right|^p \right]^{1/p}, \; p = 1, 2, \ldots \\ L_\infty = \lim_{p \to +\infty} Lp = max(\lambda_j \left| z_j^* - z_j(x) \right|), \; j = 1, \ldots, q \end{gathered} \tag{9.19}$$

In this expression (9.19) $z_j(x), j = 1, \ldots, q$ are the criteria chosen, $z^* = (z_1^*, \ldots, z_q^*)$ is the best values vector, and λ_j, $j = 1, \ldots, q$ the criteria weights defined in equation 9.20. These are composed of two components. The first corresponds to the values obtained from a multi-criteria decision-making process (w_j) and can contain a subjective component. The second component (δ_j) normalizes the criteria values. In Yepes et al. [331], the weights (w_j) are obtained by applying the analytic hierarchy process. In this case, the entropy theory [329] has been chosen to obtain the weights as this method does not require decision-makers and gives greater weight to the criterion that is better able to discriminate between alternatives. Furthermore, as all the objective functions are quantitative, no subjectivity is added to the process.

$$\lambda_j = \frac{w_j}{\delta_j} = \frac{w_j}{max \left| z_j(x) \right|}, \; x \in X \tag{9.20}$$

9.3 Results and discussion

This section analyzes and compares the results obtained for the game theory MOO approach strategy with a cost SOO procedure. Furthermore, the results obtained have been compared with recent SCCB optimization research. For this purpose, 100 runs of the algorithm have been done to reach optimum designs. The Minkowski distance methodology has been applied to these 100 optimal individuals to obtain the best for each distance.

As defined in section 9.2.1 the first step corresponds with the minimization and maximization of every objective function considered for the MOO problem. In this case, four objective functions have been considered whose expressions are defined in Equations 9.9 to 9.12. Five iterations have been carried out for every maximization and minimization to get the worst and best values, respectively. Table 9.4 shows the results obtained from the algorithm's runs for obtaining the maximum and minimum. The values chosen as best and worst correspond to the minimum and maximum of every five iterations. The algorithm used for the optimization process is the discrete SCA defined in section 9.2.4.

Table 9.4: Maximum and minimum values obtained from SOO of every objective function

	Minimization					Maximization			
Iteration	**C**	**ELCA**	**SLCA**	**CS**		**C**	**ELCA**	**SLCA**	**CS**
1	3.847E+06	4.387E+05	5.118E+09	4.221E+02		4.292E+07	4.690E+06	1.578E+10	1.063E+04
2	3.827E+06	4.404E+05	5.140E+09	4.140E+02		3.387E+07	1.071E+06	5.564E+10	8.327E+03
3	3.858E+06	4.396E+05	5.108E+09	4.140E+02		4.418E+07	1.700E+06	5.216E+10	1.065E+04
4	3.826E+06	4.423E+05	5.109E+09	4.341E+02		2.451E+07	4.389E+06	5.091E+10	4.181E+03
5	3.846E+06	4.413E+05	5.133E+09	4.542E+02		2.566E+07	3.604E+06	4.653E+10	1.020E+04
Min	3.826E+06	4.387E+05	5.108E+09	4.140E+02	**Max**	4.418E+07	4.690E+06	5.564E+10	1.065E+04

Results shown in table 9.4 correspond to the best $f_i(\vec{X}_i^*)$ and worst F_{w_i} values used in equation 9.5 for normalizing the objective functions' results. Once these values have been obtained, the game theory objective function is used for carrying out the MOO process using the discrete SCA algorithm. This procedure produces 100 optimum individuals. The Minkowski distance method has resulted in three best design solutions corresponding with the Manhattan (L_1), Euclidean (L_2), and Tchebycheff (L_∞) distances to the ideal point. This ideal point is defined by every of the lower values of every objective function shown in Table 9.4. For obtaining the values of the Minkowski distances, the weights associated have been calculated using the entropy theory [329]. The objective metrics preferred solution, weights, and the associated results of objective functions considered are shown in Table 9.5.

First, a comparison has been made for the variation of the objective function during the optimization problem comparing the MOO designs with a cost SOO procedure obtained following the method described in [311]. In Figure 9.6 it can be seen the

Table 9.5: Objective function and metrics values for preferred solutions

Best metric	Cost	ELCA	SLCA	CS	$\mathbf{L_1}$	$\mathbf{L_2}$	$\mathbf{L_\infty}$
L_1	3,829,816	438,661	5,103,214,053	434	**0.0069**	0.0064	0.0064
L_2	3,871,234	442,250	5,154,756,687	422	0.0087	**0.0044**	0.0026
L_∞	3,871,234	442,250	5,154,756,687	422	0.0087	0.0044	**0.0026**
Cost	3,830,396	439,182	5,105,214,208	882	0.1063	0.1057	0.1057
Weights	0.2479	0.2477	0.2479	0.2565			

comparison of the trajectories obtained. It should be noted that the best design obtained from L_2 and L_∞ is the same, and consequently, only one representation has been made. As seen, apparent differences can be observed in how the algorithm moves through the solution space to obtain the optimum. In cost optimization, the algorithm decreases costs and reduces ELCA and SLCA due to the cost reduction of the used material.

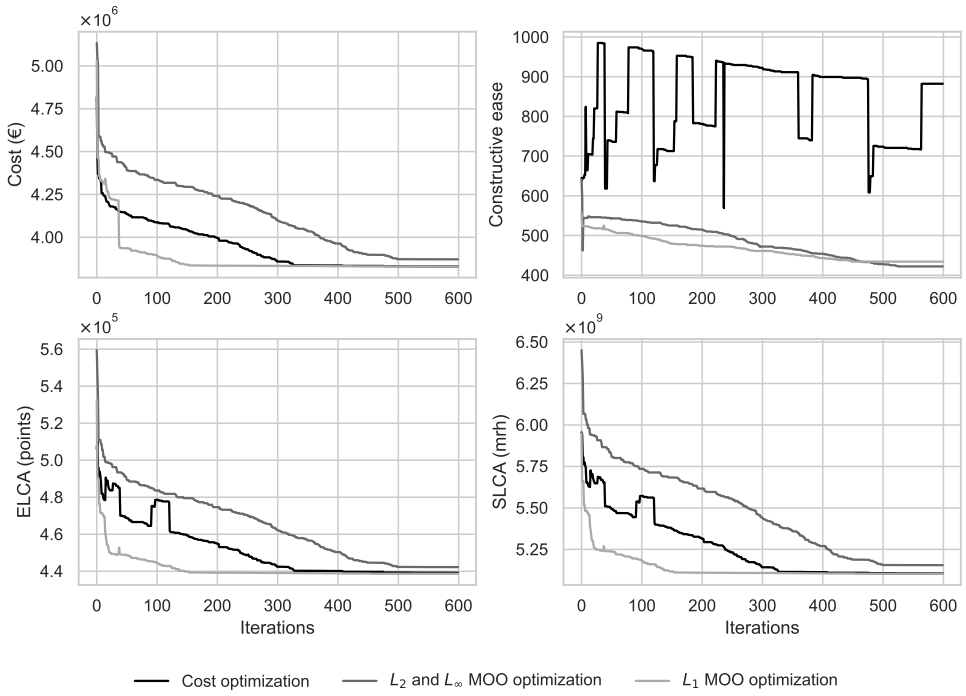

Figure 9.6: Objective functions variation during the optimization process for both MOO and cost SOO best individuals

Conversely, the value of the CS of the upper slab does not have a clear trend reaching the end of the process, a significant difference compared to the MOO design solutions. If the MOO design is obtained, it can be seen that from 500 iterations, all objective functions are stabilized. This validates the number of iterations used for the proposed method. Furthermore, it can be seen that the MOO procedure L_1 best individual decreases at the beginning of the process the cost, ELCA, and SLCA criteria in a more straightforward way. From 325 iterations, the value of these objective functions is stabilized. From that point, continues the CS of the RC slab reduction. The reasons for this can be observed in Figure 9.7. The essential material and, consequently, the most impacting is the rolled steel that materializes the steel beam in the bridge's cross-section is reduced drastically. On the contrary, the L_2 and L_∞ solutions reduce at the same time all criteria. The differences observed regarding the amounts of the materials can be seen in the box plot of Figure 9.7. In contrast to SOO, MOO produces a lower amount of reinforcing steel and increases the rolled steel amount to obtain a similar cross-section design strength.

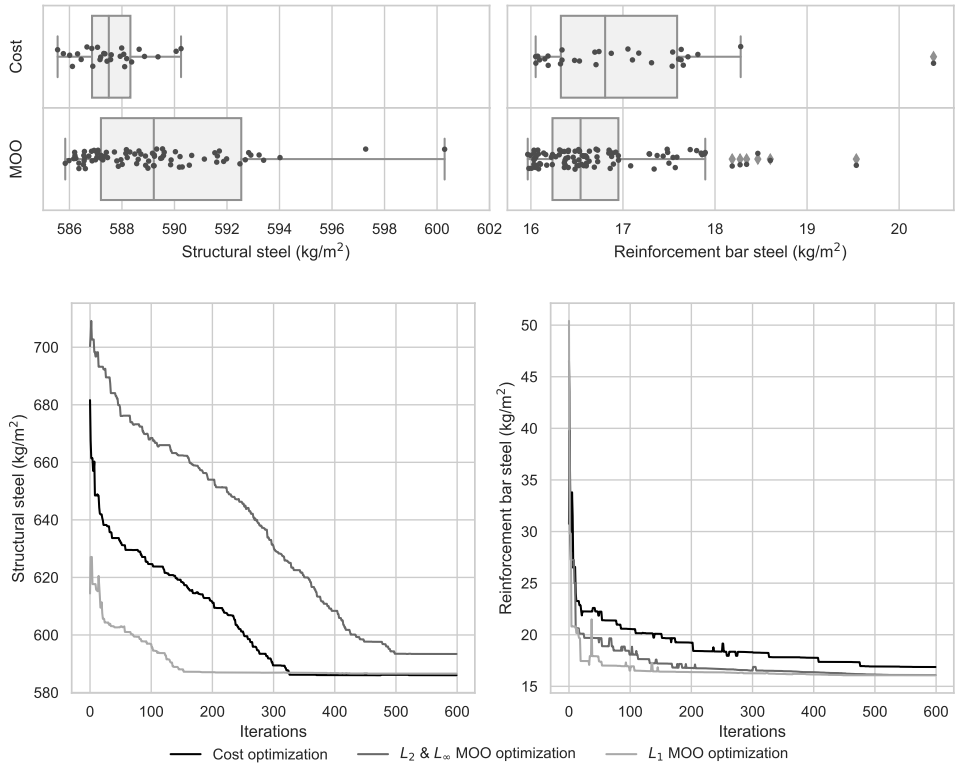

Figure 9.7: Reinforcements and rolled steel amounts data obtained from both MOO and SOO procedures

As shown in table 9.5, depending on the solution chosen, the MOO optimization can become even better in terms of cost than the SOO. If the L_1 metric solution is compared with the SOO, it can be seen that a reduction of 580 € is produced. Furthermore, suppose this is compared with the study of Martínez-Muñoz et al. [311] that applied SCA for both cost and CO_2 emissions SOOs to this structural problem. In that case, the cost SOO best individual takes the value of 3,829,666 €, compared with the best individual of MOO strategy applied in this research is lower in only 150 € (8.2 ‰ of the best cost individual). Furthermore, if the result is compared to the CO_2 emissions best design in the same study of Martínez-Muñoz et al. [311] it can be observed that it takes the cost value of 4,096,922 € increasing the best cost founded in a 6,98 %. The MOO strategy proposed is capable of finding sustainable and better constructive simplicity solutions that do not increase the cost for this optimization problem.

Table 9.6: Best solutions obtained for cost SOO and MOO L_1, L_2 and L_∞

Variables	**Unit**	**Cost**	L_1	L_2, L_∞
b	m	7	7	7
α_w	deg	49	70	87
h_s	mm	200	200	200
h_b	cm	315	252	381
h_{fb}	mm	420	440	610
t_{f_1}	mm	58	51	57
b_{f_1}	mm	560	480	620
h_{c_1}	mm	130	170	960
t_{c_1}	mm	21	18	17
t_w	mm	16	27	16
h_{c_2}	mm	490	270	900
t_{c_2}	mm	24	24	25
b_{c_2}	mm	300	710	370
t_{f_2}	mm	25	25	29
h_{s_2}	mm	150	150	150
$n_{s_{f_2}}$	u	0	0	0
d_{st}	m	1.1	2.9	2.4
d_{sd}	m	4.3	4.0	7.2
b_{fb}	mm	400	200	400
$t_{f_{fb}}$	mm	27	30	30
$t_{w_{fb}}$	mm	32	30	31
n_{r_1}	u	303	200	200
n_{r_2}	u	200	200	200
ϕ_{base}	mm	6	25	20
ϕ_{r_1}	mm	6	6	6
ϕ_{r_2}	mm	6	6	6
s_{f_2}	mm	400	220	300
s_w	mm	270	450	200
s_t	mm	600	550	600
h_{sc}	mm	100	100	100
ϕ_{sc}	mm	16	16	19
f_{ck}	MPa	25	25	25
f_{yk}	MPa	275	275	275
f_{sk}	MPa	500	500	500
Structural steel	kg	2,062,748	2,088,751	2,064,727
Reinforcement steel	kg	59,394	56,657	56,584
Concrete	m³	528	528	528

The results from a cost SOO and the best Minkowski metrics individuals of the MOO structural problem variables have been shown in Table 9.6. As described before, the difference in material amounts is an increase in the amount of structural steel to allow for the reduction of reinforcing steel. Focusing the analysis on the slab reinforcement, it can be observed that the base reinforcement bars' diameter takes a higher value allowing for reducing the number of bars. This reduction is produced to improve the constructive simplicity of the upper slab. Two principal reasons justify this. The first one is that the distance between bars increases, and consequently, the concrete's vibration can be done more efficiently. Moreover, reducing bars reduces the time of placement of these bars.

Consequently, this steel amounts variation directly impacts the values of the design variables of the problem, as shown in figures 9.8 to 9.10. First, the transverse section main variables have been compared in Figure 9.8. The main difference found is an increase in the depth of the steel beam h_b and the distance between transverse stiffeners d_{st} while the diaphragms d_{sd}, which control the torsional resistance of the bridge, increase. The results between SOO and MOO are similar concerning the angle of the webs (α_w).

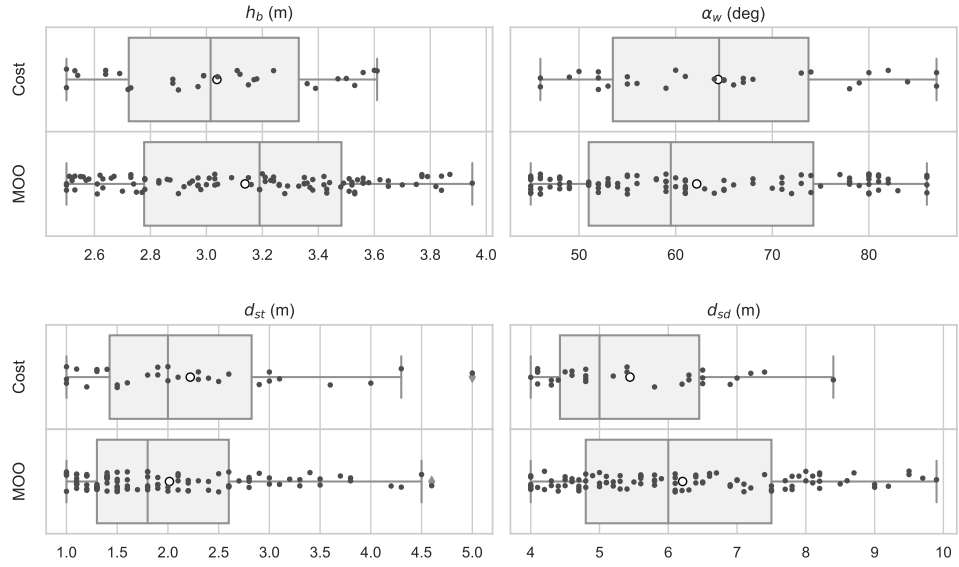

Figure 9.8: SOO and MOO strategies design cross-section variables values

The following analysis focuses on the thicknesses and widths of the bridge flanges. It can be seen in Figure 9.9 that the width of the top flange (b_{f_1}) increases while

its thickness (t_{f_1}) remains constant. This allows adding more inertia to resist the negative bending moments in supported zones and compensate for the loss due to the reduction of reinforcing steel. The bottom flange and web thicknesses (t_{f_2}, t_w) increase in the case of MOO design. Regarding the heights and thicknesses of the cells proposed for this design in section 9.2.3, it can be seen that the results shown in Figure 9.10 give positive values for the heights. This result is similar to the one obtained for SOO designs in this structural optimization problem [298], [310], [311]. It is observed an increase in the thicknesses (t_{c_1}, t_{c_2}) of these elements and an increase in the bottom cells' height (h_{c_2}) while the upper cell remains similar in terms of height.

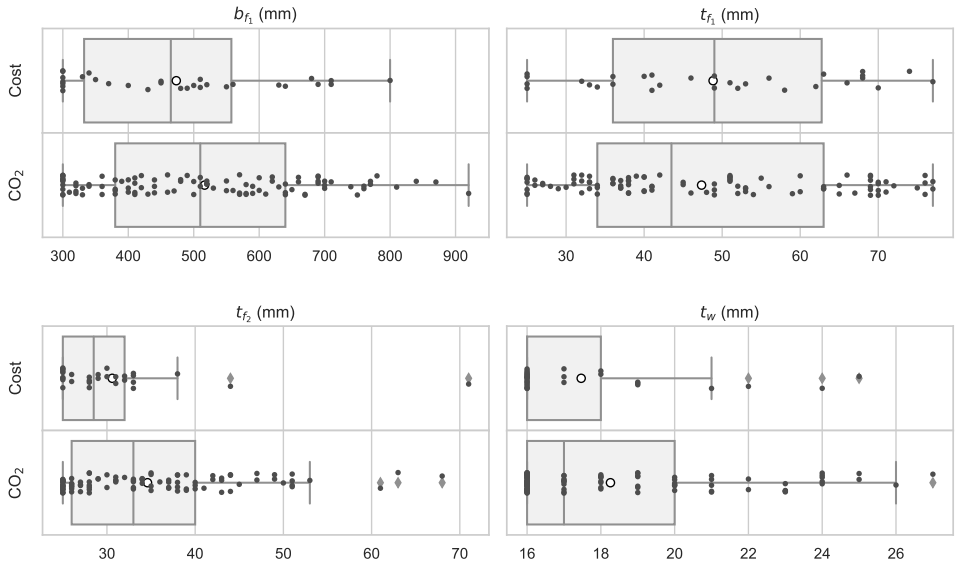

Figure 9.9: SOO and MOO strategies design flanges and webs variables values

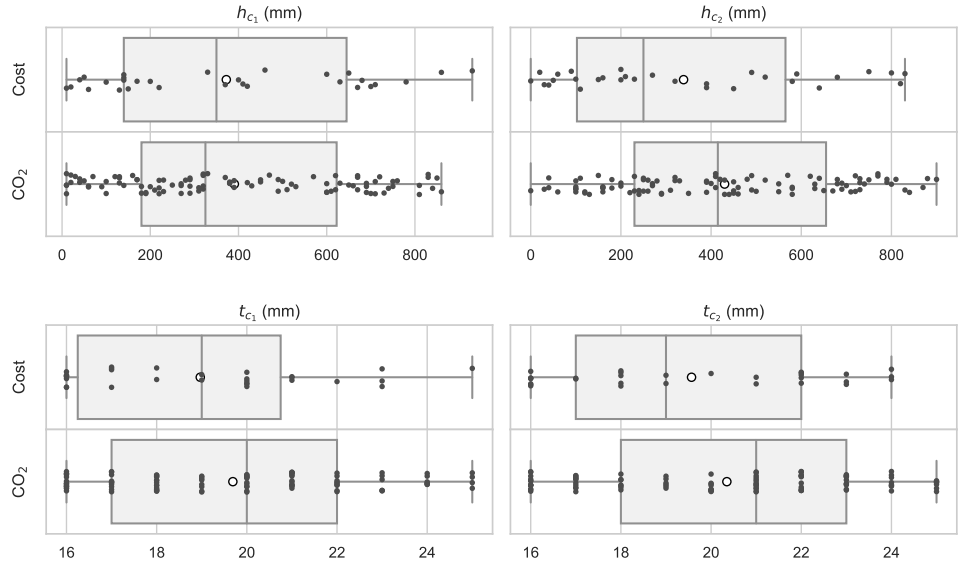

Figure 9.10: SOO and MOO strategies design cell variable results values

The variables that define the strength of the materials are the same for all designs obtained in this study. Concrete characteristic strength takes 25 MPa, corresponding with the lower value allowed by the concrete European regulation [238]. Regarding the reinforcement yield stress, the results are the same for all design alternatives taking 500 MPa as the value. Finally, a comparison of the structural steel yield stress has been made. When optimizing cost as SOO, the yield stress obtained is 275 MPa as the design reached by the MOO strategy. Conversely, in CO_2 [310], [311] and embodied energy [298] SOO studies that solve this structural problem, the yield stress increase. This is produced because the CO_2 and embodied energy associated with an increase in yield stress are null. This is also the case of ELCA and SLCA, where the impact does not increase for modeling higher-strength steels. The only thing that modifies the steel's impact is its recycling ratio for both environmental and social impacts [279].

9.4 Conclusions

This research has utilized a game theory approach to perform MOO on a steel-concrete composite bridge deck. The cooperative game strategy allows for finding a balance between various objectives. The structural problem defined involves 34 variables and 1.38×10^{46} combinations. The optimization algorithm employed is a discretized version of the Sine Cosine Algorithm (SCA), which was adjusted for discrete optimization by using a v-shape transfer function. The preferred solutions were then selected using a Minkowski distance method based on entropy theory to assign weights to the objectives, which included cost, environmental life cycle assessment (ELCA), social life cycle assessment (SLCA), and the ease of construction of the upper slab.

The results indicate that the MOO approach leads to similar cost increases of 8.2 ‰ compared to the single-objective optimization (SOO) approach based on cost. The most significant difference between the SOO and MOO designs is an increase in the amount of structural steel and a reduction in the reinforcement of the upper slab. This reduction was achieved by increasing the diameter of the bars, which improves the constructability of the slab and reduces the need for concrete vibration. The values of the steel beam variables were increased to compensate for the negative bending strength in the support zones.

In conclusion, the MOO approach can result in a sustainable design that also considers the ease of construction, as evidenced by the decreased reinforcement of the slab and the use of lower yield stress of the structural steel (275 MPa). This research demonstrates that the proposed method can be applied to complex structural problems to obtain sustainable designs, and in this case, without increasing cost. Future research can explore incorporating hybrid optimization algorithms or metamodels to improve performance and reduce computation time.

Chapter 10

Discussion

The dissertation presents several research inquiries regarding composite bridges' optimum sustainable design. The proposed methodology considers the complete life cycle assessment profile. To face these questions, this approach employs a metamodel-assisted, multi-objective strategy founded on Game and Entropy Theory. Figure 10.1 summarizes relation between the chapters and the research questions posed in this dissertation for reaching the SCCB study case sustainable design.

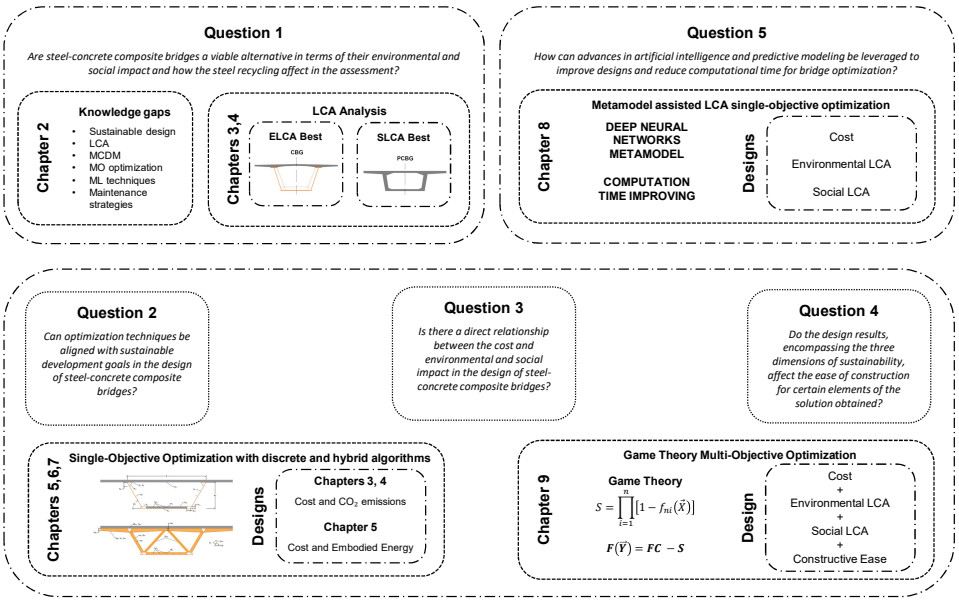

Figure 10.1: Dissertation research questions and chapter relations flowchart

10.1 Research Question Q1

> *Are steel-concrete composite bridges a viable alternative in terms of their environmental and social impact and how the steel recycling affect in the assessment?*

The doctoral thesis aims to address the research question by utilizing the life cycle analysis methodology. Specifically, the study compares a box-girder steel-concrete composite solution with slab and box-girder concrete alternatives, focusing on bridge spans ranging from 25 to 40 meters. Chapter 3 presents an Environmental Life Cycle

Assessment (ELCA) conducted following the ISO 14040 [145] methodology, consisting of four phases: goal and scope definition, inventory analysis, impact assessment, and result interpretation. For impact assessment, the ReCiPe 2008 [151] method is chosen, and the Ecoinvent v3.3 database is used to collect environmental impact data.

In addition, Chapter 4 applies both ELCA and Social Life Cycle Assessment (SLCA) to the bridge structures. The guidelines established in the *Guidelines for Social Life Cycle Assessment of Products* [224] are followed for SLCA. This chapter uses the Ecoinvent v3.7.1 and SOCA v2 databases for ELCA and SLCA, respectively.

Traditionally, the choice of bridge deck types has been driven by their economic feasibility [205]. For example, prestressed concrete solid and lightened slabs are commonly used for spans between 15 and 35 meters. Box-girder bridges are preferred for spans between 25 and 125 meters. The research in Chapters 3 and 4 faces the challenge of comparing bridge solutions' environmental and social impacts within the range of 25 to 40 meters for both concrete and steel-concrete alternatives.

The study reveals lightened slab solutions are the most environmentally sustainable for short bridge spans. However, as the span distance increases, the sustainability assessment results change significantly depending on the analyzed aspect. If a purely environmental approach is taken, composite solutions emerge as the most sustainable option for spans ranging from 25 to 40 meters. On the other hand, a purely social approach indicates that the impact of composite alternatives is higher than that of concrete box-girder solutions, even surpassing the concrete slab alternatives, which would be economically unfeasible. Another important observation is that updating the database to a current version leads to lower environmental impacts, indicating that the environmental impact improves as the technology of the processes improves.

One key difference in the study is related to the bridge structures' use and maintenance, and end-of-life phases. The environmental analysis shows a negative impact due to the effects of concrete carbonation, which is a process that occurs naturally and needs the environment to occur. This translates into an improvement in the environmental impact. However, from a social point of view, this phenomenon has no effect, and therefore, all impacts are positive.

Another main point of the analysis is the amount of recycled steel used in composite bridges as presented in Chapters 3 and 4, different steel recycling percentages have been taken into account for comparing the results regarding the span lengths of the study. These rates depend on the manufacturing process, such as BOF, EAF, and hot rolling processes. The trend in developed countries [147] is to manufacture steels

with an increasing amount of steel scrap, leading to higher recycling percentages. From an environmental point of view, this is a positive strategy. However, it may not be beneficial from a social perspective. The study results show that increasing the amount of recycled steel leads to a higher social impact.

The answer to the research question is clear. If we consider a purely environmental approach, the composite solution is the best, however, if the approach is social, a concrete solution should be chosen. However, the current trend is to obtain sustainable designs, i.e. solutions that integrate all dimensions of sustainability in the design. Therefore, the choice of solution becomes a multi-criteria decision making problem, where the solution chosen will depend on the weight assigned to each of the criteria being evaluated.

10.2 Research Question Q2

> *Can optimization techniques be aligned with sustainable development goals in the design of steel-concrete composite bridges?*

As previously mentioned, structures that consider all aspects of sustainability can be challenging. Therefore, this doctoral thesis proposes several strategies to tackle this problem. Chapters 5, 6, and 7 present a mono-objective optimization approach that considers both economic and environmental aspects to obtain an optimal design.

Discrete optimization techniques must be used to accommodate the discrete nature of the problem o achieve a feasible solution that can be implemented. The discretization of variables is based on construction feasibility. Some variables have fixed values according to design standards such as Eurocode2, Eurocode3, and Eurocode4, which specify the concrete resistance (f_{ck}), the elastic limit of steel reinforcement (f_{sk}) or structural steel (f_{yk}). This thesis proposes a strategy that uses transfer functions of the v-shape type, specifically a hyperbolic tangent ($\mid \tanh(v) \mid$), to adapt algorithms for discrete problems. This method is applied to swarm algorithms such as Jaya, Sine Cosine Algorithm (SCA), and Cuckoo Search (CS). Chapters 5, 6, and 7 show that these methods produce good results, outperforming traditional optimization methods for bridges such as Simulated Annealing with a Mutation Operator (SAMO) and Threshold Accepting with a Mutation Operator (TAMO).

Because the optimization problem is complex, hybridization techniques have been applied to enhance exploration and exploitation in certain optimization phases to find better solutions. This thesis uses the K-means technique, which groups solutions and assigns probabilities to choose the best alternatives. These techniques yield better results than classical alternatives such as TAMO and SAMO and with Jaya,

SCA, and CS algorithms without hybridization. Analyses of the results demonstrate that the solutions obtained are close to the global optimum in terms of cost since the best individual results are repeated several times.

Various approaches have been undertaken to achieve a sustainable solution. In chapters 5, 6, and 7, economic and environmental indicators such as cost, carbon emissions, and embedded energy were selected, resulting in differences in design when considering only one of the dimensions. It is noted that designs that consider economic factors and utilize automatic design processes lead to low emissions and embedded energy. However, low-cost values are not always achieved when emissions or energy are the optimization functions. Thus, it can be concluded that a mono-objective approach does not necessarily integrate all sustainability dimensions.

As a result, this thesis proposes a theory-based game strategy for addressing the structural optimization problem, as described in chapter 9. This approach employs the concept of cooperative games to search for a compromise solution that may worsen some criteria but ultimately leads to global sustainability improvement. The process involves a multi-criteria decision-making problem that necessitates weighing the importance of each criterion. As decision-makers cannot be involved in each iteration of the procedure, and alternatives proposed by Penadés-Plà et al. [332] would considerably increase computation time, weights are determined using the Entropy Theory. This method yields satisfactory results for all sustainability pillars, with a negligible increase in solution cost.

Therefore, it can be concluded that the proposed game theory-based method provides a comprehensive solution to the structural optimization problem of SCCBs, encompassing all sustainability dimensions.

10.3 Research Question Q3

> *Is there a direct relationship between the cost and environmental and social impact in the design of steel-concrete composite bridges?*

In the design of composite bridges, the material that has the most significant impact on the structure's life cycle is structural steel for both ELCA and SLCA, as explained in Chapters 3 and 4. Therefore, optimization techniques aim to reduce the use of this material. However, one crucial factor to consider is not just the material itself but its strength. The economic impact of steel increases as its yield strength increases. However, for the environmental and social aspects of sustainability, an increase in steel yield strength does not necessarily imply a change in its impact since the im-

pact depends on the percentage of recycled steel used for production. The same applies to the reinforcement rebars. These differences make the design of SCCBs significantly distinct from concrete bridges.

In concrete bridges, the most commonly used material is concrete itself. Increasing the bridge's strength requires increasing the amount of cement used in the concrete. As cement is the material that has the most significant impact on concrete manufacturing, increasing the strength of a concrete bridge directly leads to an increase in social and environmental impact. In contrast, for SCCBs, steel becomes the primary material, and the analysis of its impact becomes the primary objective. This distinction can be applied to all other composite or concrete structures. In optimizing an SCCB for cost, the solutions obtained would have lower steel yield strength. In comparison, solutions optimized for environmental and social impact require a higher steel yield strength. This concept is well-demonstrated in the results of Chapters 5 to 8.

In Chapter 8, we assess the ELCA and SCLA as objective functions that represent the environmental and social pillars, respectively. We observe that the results are similar when comparing the design obtained using the ELCA as an objective function to those obtained using emissions and embedded energy as objective functions. This indicates that more specific objective functions, such as emissions and energy, can provide an excellent approximation to the optimal environmental design of solutions. However, it is worth noting that the approach of these objective functions differs. The objective functions for emissions and energy take a cradle-to-gate approach, covering the earlier stages of the life cycle.

In contrast, the ELCA target function covers the cradle-to-grave approach, including the structure's demolition. As such, these more specific functions can be a good indicator of the environmental impact, especially given that maintenance and construction phases significantly impact the structure's life cycle. However, they do not take into account the maintenance phase.

Overall, it is clear that considering cost optimization leads directly to the optimization of emissions and embedded energy for the problem posed. Thus, these functions are good indicators of the performance of objective functions that evaluate the complete environmental life cycle. However, optimizing functions that represent sustainability's environmental and social dimensions only sometimes leads to directly optimizing the economic dimension. Nonetheless, compatible solutions address all three dimensions, as shown in Chapter 9. These solutions can be found by applying the methodology proposed in this doctoral thesis based on Game Theory.

10.4 Research Question Q4

Do the design results, encompassing the three dimensions of sustainability, affect the ease of construction for certain elements of the solution obtained?

The structural design results indicate that reducing the number of materials used can help minimize environmental impact, as higher consumption typically leads to a more significant impact. This observation is supported by the findings presented in chapters 3 and 4, which show the percentage impact of each phase of the life cycle. In particular, manufacturing materials, whether for concrete or composite solutions, is the most significant contributor to environmental impact, with the processes involved in material manufacturing having the most significant consumption. Therefore, reducing material consumption during this phase can help to minimize environmental impact.

With this in mind, two approaches can be taken to optimize the design of composite bridges. Firstly, it is possible to consider the arrangement of cross-section elements, as described in chapters 5 to 8. The optimization problem for SCCB raises the possibility of placing cells inside the box, which can increase the plates that do not require a reduction in the section for the resistant calculation of the assembly. In other words, the distribution of plates that make up the cross-section can be optimized to avoid instability and maximize the cross-section for resistance. This optimization not only impacts the service phase of the structure but also improves the behavior of the structure during construction, making better use of materials. Therefore, optimizing the cross-section of the trough can improve the construction process by minimizing material consumption.

Turning our attention to the design results for the number and diameter of the top slab bars, it is worth noting that single-objective design methods tend to reduce the diameter of the bars to a minimum and increase the number of bars to optimize the amount of reinforcing steel used. However, this can lead to difficulties during execution, as a large number of bars requires either the use of concrete with smaller aggregates or the placement of bars in successive layers, both of which can make the execution of the slab more challenging. Therefore, focusing solely on sustainability objectives in the design process can lead to complex and challenging executed designs.

This research proposes a solution based on a multi-objective optimization approach that includes a constructability function, as discussed in chapter 9 to address this problem. By incorporating this additional objective function alongside the sustain-

ability objectives, the proposed methodology generates sustainable designs that are easier to execute. This increases the complexity of the problem, as there are now three dimensions of sustainability and one dimension of constructive ease to consider. However, it also facilitates the evaluation of the best solution. The Minkowski distances are applied to obtain the optimal solution, resulting in two viable options. Using this methodology, the evaluation of the solutions with the method of Minkowski distances yields an optimal sustainable solution with better constructability that only incurs an 8.2 ‰ increase in cost compared to the solution obtained using the same algorithm.

10.5 Research Question Q5

> *How can advances in artificial intelligence and predictive modeling be leveraged to improve designs and reduce computational time for bridge optimization?*

The optimization of structures, as previously substantiated, poses a complex discrete optimization problem. Due to its complexity, using structural models to verify the structures poses a computational cost issue. Coupled with the high number of iterations required to reach an optimal solution, this presents a challenge. Computation time is a variable that depends on algorithmic characteristics. Upon analyzing computation times for different algorithms used, it is evident that algorithms based on trajectories are more costly than swarm algorithms. At the same time, the latter produces even better results. Thus, the algorithm's behavior in addressing the problem is the first consideration for algorithm selection. For this optimization problem, swarm algorithms generally produce better results than trajectory algorithms, with only a negligible difference when the optimal solution found is worse.

Additionally, it must be taken into account that one or several objective functions are necessary for any optimization. In sustainable bridge design, at least one function for each of the three dimensions is required to obtain a solution that integrates them. This is because, as substantiated in Chapters 3 and 4, the environmental and social pillars, particularly in the percentage of recycled steel, are contradictory. Conversely, comparing the results obtained from the single-objective optimization of Chapters 5 to 8, it is clear that optimizing the environmental and social pillars does not necessarily lead to cost optimization. This justifies using multi-objective techniques, such as those proposed in this doctoral thesis, and computational methods of artificial intelligence.

One approach to accelerate these computations is by leveraging machine learning techniques. For instance, dimensionality reduction techniques may simplify the search space's dimensionality or objective function. Another approach is substituting the objective function or constraints with a model that mimics them. For instance, in [124], the kriging technique was applied to diminish the computational time of a concrete box-girder bridge by replacing the objective function. In [304], neural networks were employed to simulate viscosity and conductivity values. These were then integrated into NSGA-II (nondominated sorting genetic algorithm II) for optimization.

Structural field studies have employed neural networks to anticipate the transfer length in prestressed concrete [305]. Similarly, neural networks were employed to forecast the energy usage of buildings' heating, ventilation, and air conditioning systems. Afterward, a multi-objective genetic algorithm was employed to identify the optimal consumption parameters [306]. The multi-objective optimization approach yielded superior thermal comfort and energy consumption outcomes compared to the base case design.

This research utilized a deep neural network metamodel to expedite the optimization of an SCCB. The metamodel was employed in SCA, CS, and OBAMO algorithms to execute the optimization and compare performance. The neural network model employed in this study exhibited remarkable improvements in optimization speed, clocking in at 37 to 50 times faster than traditional optimization methods. Though the neural network model may lead to infeasible solutions, the calculation speed acceleration is significant enough to tolerate such errors. The optimal solutions across various objective functions consistently featured cells in the bridge's cross-section. This study highlights the substantial potential of deep learning models in optimizing intricate engineering designs, particularly in reducing the computational time required for optimization.

Chapter 11

Conclusions and future work

This chapter can be divided into three parts: general conclusions, specific conclusions, and future lines of research. The general conclusions aim to encompass and unify all the work conducted in this dissertation. In contrast, the specific conclusions provide detailed information from each journal article. Additionally, potential avenues for future work are proposed.

11.1 General Conclusions

This dissertation is divided into two parts. The first part aims to assess the feasibility of SCCBs compared to other concrete alternatives. Chapter 3 focuses on conducting a complete environmental impact assessment using the Ecoinvent database and the ReCiPe method. The study considers four types of bridge alternatives: prestressed concrete solid slab, prestressed concrete lightened slab, prestressed concrete box-girder, and composite box-girder. These alternatives have been evaluated for span lengths ranging from 15 to 40 meters.

Additionally, the study evaluates the significance of the amount of steel scrap in the steel manufacturing process for both environmental impact and sustainability. In chapter 4, the social impact of these bridge alternatives is evaluated using the SOCA add-on and the social impact weighting method. The results indicate a clear difference between environmental and social impact results for the feasibility of bridge types. From an environmental perspective, the best alternative is the SCCB, while the concrete box-girder is the most socially impactful. Regarding the steel recycling ratio, a social approach shows that a higher amount of steel scrap in manufacturing leads to a higher social impact. In contrast, the environmental impact decreases with increasing steel scrap. The manufacturing stage incurs the highest impact in the life cycle assessment, indicating that reducing the number of materials can reduce the overall impact.

The second part of the study aims to achieve a sustainable design for an SCCB by utilizing metaheuristic optimization techniques. An SCCB with a box-girder cross section is considered a case study to accomplish this objective. The proposed algorithms are categorized into two main branches: trajectory-based and swarm intelligence. The trajectory-based branch employs Simulated Annealing, Threshold Accepting, and Old Bachelor Acceptance. The Swarm Intelligence branch, on the other hand, utilizes the Sine Cosine Algorithm, Jaya, and Cuckoo Search. The latter algorithms are specifically designed for solving continuous problems. However, a V-shape transfer function has been implemented to adapt them to the discrete nature of the structural optimization problem. Two hybridization techniques have been employed to improve the solutions, one for each algorithm branch. Firstly, mutation

operators have been incorporated into the trajectory-based algorithms to allow mutations in individuals during the optimization process, which increases exploration. Secondly, the K-means clustering technique has been applied to the swarm intelligence algorithms. This clustering technique facilitates the grouping of solutions. It assigns a higher acceptance probability to those closer to the best objective function values.

To model, the economic, environmental, and social dimensions of sustainability, cost, ELCA, and SLCA functions were selected, respectively. However, due to the complexity of LCA functions, emissions, and embedded energy were used as proxies for the environmental impact objective function to assess their suitability as indicators. The addition of these more complex functions, combined with the inherent complexity of the optimization problem, has presented a challenge in terms of the computational cost of solving the problem. To address this issue, a deep neural network model was trained to predict the feasibility of solutions without the need to obtain precise values. Data from different iterations of the optimization algorithms were used to train the deep neural network model, which employed multilayer perceptron networks to construct the classification model. The input variables comprised the 34 variables defining the SCCB design for the case study. The hybrid dataset included approximately 20,000 bridges satisfying the structural constraints and 7,000 points not meeting the conditions. A correction factor was incorporated into the algorithm that utilized the classification model to ensure a fair evaluation of computation time since the model could produce incorrect results. Each algorithm had to generate 30 feasible executions. The computation time for the models incorporating the deep neural network model was calculated by adding the times of all executions and dividing them by the times of the feasible executions. The results showed that deep neural network model optimization algorithms was between 37 and 50 times faster than the originals.

A multi-objective optimization using a game theory approach has been proposed to address the issue of unclear relationships between the objective functions of the environmental and social pillars and the cost function in single-objective optimization. This approach can be performed as either cooperative or non-cooperative games. In this case, a cooperative game has been chosen to find a compromise solution between the three dimensions of sustainability. An optimization problem has been formulated to define an objective function expressed as an aggregate function of the impact value for each criterion weighted by their importance. The entropy theory has been used to determine these weights, as it does not require decision-makers for their assignment. The method also utilizes the concept of super-criterion to search for a compromise solution.

Optimal design results that consider sustainability target functions are characterized by many bars in the top slab, which can impede its constructability. This is because

more bars increase placement time and complicate concrete vibration. A slab constructability function has been added to the optimization problem to address this issue. After applying the method, designs that do not compromise any sustainability pillars and improve constructability with only an 8.2

11.2 Specific conclusions

- All three dimensions of sustainability must be considered together using a multi-objective optimization approach.
- From an environmental perspective, composite bridges are better than concrete bridges for spans between 20 and 40 meters. However, from a social perspective, concrete bridges are more suitable.
- The amount of recycled steel used in composite bridges affects their environmental and social impact. Increasing the percentage of recycled steel reduces the environmental impact but increases the social impact.
- Optimizing the economic pillar can reduce composite bridges' environmental and social impact. However, there is no clear relationship between optimizing the environmental, social, and economic pillars when the latter is the target function.
- The optimal designs of composite bridges depend on the optimization objective. Designs with lower yield strength steel are favored when the cost is the criterion. However, when environmental or social criteria are the objectives, designs with higher yield strength steel are preferred.
- The characteristic strength of the concrete (f_{ck}) used in the bridge is always the minimum value specified by standards for optimum design, which is 25 MPa.
- The optimal designs for the bridge propose solutions that eliminate the need for longitudinal stiffening in the bottom flange of the deck. This finding aligns with previous optimization studies conducted on composite box girder bridges. However, the necessity of bottom flange stiffeners will vary based on the type and stage of the construction process. Further research is required in this field to gain a deeper understanding.
- The proposed cross-section design with interior cells in the web and flange contact zones enhances the stress resistance of the bridge by reducing the distances between panels and cross-section areas in class 4.

- More straightforward objective functions such as emissions and embedded energy are good environmental life cycle analysis approximations. However, complex functions considering all life cycle phases are necessary for a more comprehensive evaluation of the bridge's impact.
- Deep neural network models can significantly reduce computation time by 37 to 50 times, depending on the algorithm used.
- The proposed multi-objective optimization method enables the identification of compromise solutions that consider all three dimensions of sustainability in an aggregate objective function.
- The optimal design solutions generated by the proposed optimization problem feature many members in the top concrete slab to minimize material usage. However, this may affect the constructive ease of the element.
- Swarm intelligence algorithms perform better than trajectory algorithms in terms of computational time. Furthermore, hybridization and discretization techniques can enhance the optimal design results.

11.3 Future lines of research

The thesis employed a methodological approach that successfully achieved optimal sustainable designs, which effectively integrated all aspects of sustainability while considering the constructive simplicity of certain bridge elements. Additionally, the introduction of life cycle analysis as an objective function enabled a more comprehensive evaluation of the impact concerning the social and environmental dimensions for optimization. While this method was only applied to box-girder composite bridges, it could be used for designing other types of composite bridges, including slab and I-beam bridges and other structures. However, future research work could explore the performance of this methodology against traditional multi-objective optimization algorithms.

Currently, machine learning techniques are gaining popularity for improving computation times and predicting optimal designs. Although the current study used a model only to predict the feasibility of proposed solutions, a future research direction could be training artificial intelligence models that predict optimal designs directly as a function of the imposed boundary conditions. Additionally, while neural networks were used as the metamodel in this research, exploring other techniques could improve results.

In the proposed optimization strategy, the maintenance strategy of the structure could be included as an objective function in the optimization itself. Using the life cycle analysis methodology, the impact on each dimension of sustainability could be evaluated for each phase, and optimal maintenance could be generated along with an optimal design.

Although the results obtained from this study suggest that the global optimum of the problem has been reached or is close to it, the problem was posed with a fixed box shape for the edge of the structure. Further optimization could involve obtaining the cross-section's shape along the bridge's entire distance and exploring topological optimization to eliminate unnecessary steel sections. Finally, given the time reduction made possible by metamodels, searching for robust optimal solutions considering the reliability of various parameters could be considered.

Bibliography

[1] WCED, *Our common future*. World Commission on Environment and Development, 1987 (cit. on pp. 2, 12, 30, 58).

[2] A. Petek Gursel, E. Masanet, A. Horvath, and A. Stadel, "Life-cycle inventory analysis of concrete production: A critical review," *Cement and Concrete Composites*, vol. 51, pp. 38–48, 2014 (cit. on pp. 2, 31, 59).

[3] T. Ramesh, R. Prakash, and K. K. Shukla, "Life cycle energy analysis of buildings: An overview," *Energy and Buildings*, vol. 42, pp. 1592–1600, 2010 (cit. on pp. 2, 31, 59, 186).

[4] L. Y. Shen, W. Lu, H. Yao, and D. H. Wu, "A computer-based scoring method for measuring the environmental performance of construction activities," *Automation in construction*, vol. 14(3), pp. 297–309, 2005 (cit. on pp. 2, 31, 59).

[5] J.-h. Choi, "Strategy for reducing carbon dioxide emissions from maintenance and rehabilitation of highway pavement," *Journal of Cleaner Production*, vol. 209, pp. 88–100, 2019 (cit. on p. 2).

[6] A. P. Kyriacou, L. Muinelo-Gallo, and O. Roca-Sagalés, "The efficiency of transport infrastructure investment and the role of government quality: An empirical analysis," *Transport Policy*, vol. 74, pp. 93–102, 2019 (cit. on p. 2).

[7] A. Favier, C. De Wolf, K. Scrivener, and G. Habert, “A sustainable future for the european cement and concrete industry: Technology assessment for full decarbonisation of the industry by 2050,” ETH Zurich, Tech. Rep., 2018 (cit. on p. 2).

[8] D. Collings, *Steel–concrete composite bridges*. Thomas Telford Publishing, 2005 (cit. on pp. 2, 12).

[9] R. A. Smith, J. R. Kersey, and P. J. Griffiths, “The Construction Industry Mass Balance: resource use, wastes and emissions,” *Construction*, vol. 4, no. September, p. 680, 2002 (cit. on pp. 3, 12).

[10] J. H. Spangenberg, A. Fuad-Luke, and K. Blincoe, “Design for sustainability (dfs): The interface of sustainable production and consumption,” *Journal of Cleaner Production*, vol. 18, no. 15, pp. 1485–1493, 2010 (cit. on pp. 3, 12).

[11] H. Gervásio and L. S. da Silva, “Comparative life-cycle analysis of steel-concrete composite bridges,” *Structure and Infrastructure Engineering*, vol. 4, no. 4, pp. 251–269, 2008 (cit. on pp. 3, 13, 23).

[12] J. Bernabeu, *Evolución tipológica y estética de los puentes mixtos en Europa*. E.T.S.I. Caminos, Canales y Puertos (UPM), 2004 (cit. on pp. 3, 13).

[13] Y. I. Musa and M. A. Diaz, “Design optimization of composite steel box girder in flexure,” *Practice Periodical on Structural Design and Construction*, vol. 12, no. 3, pp. 146–152, 2007 (cit. on pp. 3, 13, 16, 19, 20, 83).

[14] I. Payá-Zaforteza, V. Yepes, F. González-Vidosa, and A. Hospitaler, “On the weibull cost estimation of building frames designed by simulated annealing,” *Meccanica*, vol. 45, no. 5, pp. 693–704, 2010 (cit. on pp. 3, 83, 84, 145).

[15] J. V. Martí, T. García-Segura, and V. Yepes, “Structural design of precast-prestressed concrete u-beam road bridges based on embodied energy,” *Journal of Cleaner Production*, vol. 120, pp. 231–240, 2016 (cit. on pp. 3, 19).

[16] A. M. Martins, L. M. Simões, and J. H. Negrão, “Optimization of cable-stayed bridges: A literature survey,” *Advances in Engineering Software*, vol. 149, p. 102 829, 2020 (cit. on pp. 3, 83).

[17] A. M. Martins, L. M. Simões, and J. H. Negrão, "Optimization of extradosed concrete bridges subjected to seismic action," *Computers & Structures*, vol. 245, p. 106 460, 2021 (cit. on p. 3).

[18] V. Penadés-Plà, T. García-Segura, J. V. Martí, and V. Yepes, "An optimization-lca of a prestressed concrete precast bridge," *Sustainability*, vol. 10, no. 3, p. 685, 2018 (cit. on pp. 3, 19).

[19] V. Penadés-Plà, J. V. Martí, T. García-Segura, and V. Yepes, "Life-cycle assessment: A comparison between two optimal post-tensioned concrete box-girder road bridges," *Sustainability*, vol. 9(10), p. 1864, 2017 (cit. on pp. 3, 38, 39, 59, 66).

[20] UN, *The future we want*. Rio de Janeiro: United Nations, 2012 (cit. on p. 13).

[21] C. de Jong, K. Klemp, and E. Mattie, *Ten Principles for Good Design: Dieter Rams: the Jorrit Maan Collection*. Prestel, 2017 (cit. on p. 13).

[22] IBM, *Ibm spss statistics for windows, version 25.0; ibm corp.: Armonk, ny, usa.* 2017 (cit. on pp. 14, 25).

[23] V. Penadés-Plà, T. García-Segura, J. V. Martí, and V. Yepes, "A review of multi-criteria decision-making methods applied to the sustainable bridge design," *Sustainability*, vol. 8, no. 12, p. 1295, 2016 (cit. on pp. 14, 15, 24).

[24] V. Belton and T. Stewart, *Multiple Criteria Decision Analysis: An Integrated Approach*. Springer, 2002 (cit. on p. 15).

[25] I. Vayas and A. Iliopoulos, *Design of steel-concrete composite bridges to Eurocodes*. Boca Raton: CRC Press, 2017 (cit. on pp. 15, 83, 92, 93, 120, 126, 130, 135, 164, 165, 202, 228, 229).

[26] CEN, *Eurocode 4: Design of composite steel and concrete structures*. Brussels, Belgium: European Committee for Standardization, 2013 (cit. on pp. 15, 16, 87–90, 92, 93, 120, 121, 130, 133–135, 161, 164, 165, 182, 202, 203, 222, 229).

[27] S.-i. Nakamura, Y. Momiyama, T. Hosaka, and K. Homma, “New technologies of steel/concrete composite bridges,” *Journal of Constructional Steel Research*, vol. 58, no. 1, pp. 99–130, 2002 (cit. on p. 18).

[28] Y. Xie, H. Yang, Z. Zuo, T. L. Sirotiak, and M. Yang, “Optimal steel section length of the composite rigid-frame bridge,” *Practice Periodical on Structural Design and Construction*, vol. 23, no. 3, p. 05 018 001, 2018 (cit. on p. 18).

[29] Y. Xie, H. Yang, Z. Zuo, and Z. Gao, “Optimal depth-to-span ratio for composite rigid-frame bridges,” *Practice Periodical on Structural Design and Construction*, vol. 24, no. 2, p. 05 019 001, 2019 (cit. on p. 18).

[30] A. Vasseghi, “Improving strength and ductility of continuous composite plate girder bridges,” *Journal of Constructional Steel Research*, vol. 65, no. 2, pp. 479–488, 2009 (cit. on p. 18).

[31] H.-Y. Kim and Y.-J. Jeong, “Steel–concrete composite bridge deck slab with profiled sheeting,” *Journal of Constructional Steel Research*, vol. 65, no. 8, pp. 1751–1762, 2009 (cit. on p. 18).

[32] H.-Y. Kim and Y.-J. Jeong, “Ultimate strength of a steel–concrete composite bridge deck slab with profiled sheeting,” *Engineering Structures*, vol. 32, no. 2, pp. 534–546, 2010 (cit. on p. 18).

[33] X. Shao, D. Yi, Z. Huang, H. Zhao, B. Chen, and M. Liu, “Basic performance of the composite deck system composed of orthotropic steel deck and ultrathin rpc layer,” *Journal of Bridge Engineering*, vol. 18, no. 5, pp. 417–428, 2013 (cit. on p. 18).

[34] L. Wu, J. Nie, J. Lu, J. Fan, and C. Cai, “A new type of steel–concrete composite channel girder and its preliminary experimental study,” *Journal of Constructional Steel Research*, vol. 85, pp. 163–177, 2013 (cit. on p. 18).

[35] J.-G. Nie, Y.-J. Zhu, M.-X. Tao, C.-R. Guo, and Y.-X. Li, “Optimized prestressed continuous composite girder bridges with corrugated steel webs,” *Journal of Bridge Engineering*, vol. 22, no. 2, p. 04 016 121, 2017 (cit. on p. 18).

[36] P. M. Esteves, J. F. Almeida, and J. J. Oliveira Pedro, “Steel–concrete hybrid bridge decks: Rational design models for connection regions,” *Proceedings of the Institution of Civil Engineers - Bridge Engineering*, vol. 171, no. 4, pp. 252–266, 2018 (cit. on p. 18).

[37] L. Peng-zhen, C. Lin-feng, L. Yang, L. Zheng-lun, and S. Hua, “Study on mechanical behavior of negative bending region based design of composite bridge deck,” *International Journal of Civil Engineering*, vol. 16, no. 5, pp. 489–497, 2018 (cit. on p. 18).

[38] V. Kodur, E. Aziz, and M. Dwaikat, “Evaluating fire resistance of steel girders in bridges,” *Journal of Bridge Engineering*, vol. 18, no. 7, pp. 633–643, 2013 (cit. on p. 18).

[39] J. Alos-Moya, I. Paya-Zaforteza, M. Garlock, E. Loma-Ossorio, D. Schiffner, and A. Hospitaler, “Analysis of a bridge failure due to fire using computational fluid dynamics and finite element models,” *Engineering Structures*, vol. 68, pp. 96–110, 2014 (cit. on p. 18).

[40] E. M. Aziz, V. K. Kodur, J. D. Glassman, and M. E. Moreyra Garlock, “Behavior of steel bridge girders under fire conditions,” *Journal of Constructional Steel Research*, vol. 106, pp. 11–22, 2015 (cit. on p. 18).

[41] J. Alos-Moya, I. Paya-Zaforteza, A. Hospitaler, and P. Rinaudo, “Valencia bridge fire tests: Experimental study of a composite bridge under fire,” *Journal of Constructional Steel Research*, vol. 138, pp. 538–554, 2017 (cit. on p. 18).

[42] J. Hu, A. Usmani, A. Sanad, and R. Carvel, “Fire resistance of composite steel & concrete highway bridges,” *Journal of Constructional Steel Research*, vol. 148, pp. 707–719, 2018 (cit. on p. 18).

[43] A. Astaneh-Asl and R. G. Black, “Seismic and structural engineering of a curved cable-stayed bridge,” *Journal of Bridge Engineering*, vol. 6, no. 6, pp. 439–450, 2001 (cit. on p. 18).

[44] S. Maleki, “Seismic energy dissipation with shear connectors for bridges,” *Engineering Structures*, vol. 28, no. 1, pp. 134–142, 2006 (cit. on p. 18).

[45] A. Dall'Asta and E. Tubaldi, "Transverse seismic response of continuous steel–concrete composite bridges exhibiting dual load path," *Earthquakes and Structures*, vol. 1, pp. 21–41, 2010 (cit. on p. 18).

[46] J. Seo and D. G. Linzell, "Horizontally curved steel bridge seismic vulnerability assessment," *Engineering Structures*, vol. 34, pp. 21–32, 2012 (cit. on p. 18).

[47] E. Tubaldi, M. Barbato, and A. Dall'Asta, "Influence of model parameter uncertainty on seismic transverse response and vulnerability of steel-concrete composite bridges with dual load path," *Journal of Structural Engineering*, vol. 138, no. 3, pp. 363–374, 2012 (cit. on p. 18).

[48] E. Tubaldi, A. Dall'Asta, and L. Dezi, "Reduced formulation for post-elastic seismic response of dual load path bridges," *Engineering Structures*, vol. 51, pp. 178–187, 2013 (cit. on p. 18).

[49] G.-F. Du, X.-M. Bie, Z. Li, and W.-Q. Guan, "Study on constitutive model of shear performance in panel zone of connections composed of cfsstcs and steel-concrete composite beams with external diaphragms," *Engineering Structures*, vol. 155, pp. 178–191, 2018 (cit. on p. 18).

[50] S. Carbonari, F. Gara, A. Dall'Asta, and L. Dezi, "Shear connection local problems in the seismic design of steel-concrete composite decks," in *Proceedings of Italian Concrete Days 2016*, Cham: Springer International Publishing, 2018, pp. 341–354 (cit. on p. 18).

[51] G. Abbiati, E. Cazzador, S. Alessandri, O. S. Bursi, F. Paolacci, and S. De Santis, "Experimental characterization and component-based modeling of deck-to-pier connections for composite bridges," *Journal of Constructional Steel Research*, vol. 150, pp. 31–50, 2018 (cit. on p. 18).

[52] J.-H. Ahn, C. Sim, Y.-J. Jeong, and S.-H. Kim, "Fatigue behavior and statistical evaluation of the stress category for a steel–concrete composite bridge deck," *Journal of Constructional Steel Research*, vol. 65, no. 2, pp. 373–385, 2009 (cit. on p. 18).

[53] B. Ovuoba and G. Prinz, "Investigation of residual fatigue life in shear studs of existing composite bridge girders following decades of traffic loading," *Engineering Structures*, vol. 161, pp. 134–145, 2018 (cit. on p. 18).

[54] C. Xu, K. Sugiura, and Q. Su, “Fatigue behavior of the group stud shear connectors in steel-concrete composite bridges,” *Journal of Bridge Engineering*, vol. 23, no. 8, p. 04 018 055, 2018 (cit. on p. 18).

[55] S. Yuan, J. Dong, Q. Wang, and J. Y. Ooi, “Fatigue property study and life assessment of composite girders with two corrugated steel webs,” *Journal of Constructional Steel Research*, vol. 141, pp. 287–295, 2018 (cit. on p. 18).

[56] Z. Zhu, T. Yuan, Z. Xiang, Y. Huang, Y. E. Zhou, and X. Shao, “Behavior and fatigue performance of details in an orthotropic steel bridge with uhpc-deck plate composite system under in-service traffic flows,” *Journal of Bridge Engineering*, vol. 23, no. 3, p. 04 017 142, 2018 (cit. on p. 18).

[57] F. Leitão, J. da Silva, P. da S. Vellasco, S. de Andrade, and L. de Lima, “Composite (steel–concrete) highway bridge fatigue assessment,” *Journal of Constructional Steel Research*, vol. 67, no. 1, pp. 14–24, 2011 (cit. on p. 18).

[58] J. Xu, H. Sun, S. Cai, W. Sun, and B. Zhang, “Fatigue testing and analysis of i-girders with trapezoidal corrugated webs,” *Engineering Structures*, vol. 196, p. 109 344, 2019 (cit. on p. 18).

[59] L. Deng, W. Yan, and S. Li, “Computer modeling and weight limit analysis for bridge structure fatigue using opensees,” *Journal of Bridge Engineering*, vol. 24, no. 8, p. 04 019 081, 2019 (cit. on p. 18).

[60] L. Deng and W. Yan, “Vehicle weight limits and overload permit checking considering the cumulative fatigue damage of bridges,” *Journal of Bridge Engineering*, vol. 23, no. 7, p. 04 018 045, 2018 (cit. on p. 18).

[61] S. Zhang, X. Shao, J. Cao, J. Cui, J. Hu, and L. Deng, “Fatigue performance of a lightweight composite bridge deck with open ribs,” *Journal of Bridge Engineering*, vol. 21, no. 7, p. 04 016 039, 2016 (cit. on p. 18).

[62] C. Xu, Q. Su, and K. Sugiura, “Mechanism study on the low cycle fatigue behavior of group studs shear connectors in steel-concrete composite bridges,” *Journal of Constructional Steel Research*, vol. 138, pp. 196–207, 2017 (cit. on p. 18).

[63] X. Wei, L. Xiao, and S. Pei, “Experiment study on fatigue performance of perforated shear connectors,” *International Journal of Steel Structures*, vol. 17, no. 3, pp. 957–967, 2017 (cit. on p. 18).

[64] G. Alencar, A. M. de Jesus, R. A. Calçada, and J. G. S. da Silva, “Fatigue life evaluation of a composite steel-concrete roadway bridge through the hot-spot stress method considering progressive pavement deterioration,” *Engineering Structures*, vol. 166, pp. 46–61, 2018 (cit. on p. 18).

[65] M. Arici, M. F. Granata, and M. Oliva, “Influence of secondary torsion on curved steel girder bridges with box and i-girder cross-sections,” *KSCE Journal of Civil Engineering*, vol. 19, no. 7, pp. 2157–2171, 2015 (cit. on p. 18).

[66] A. Camara and A. Ruiz-Teran, “Multi-mode traffic-induced vibrations in composite ladder-deck bridges under heavy moving vehicles,” *Journal of Sound and Vibration*, vol. 355, pp. 264–283, 2015 (cit. on p. 18).

[67] F. Sadeghi, A. Kueh, A. Bagheri Fard, and N. Aghili, “Vibration characteristics of composite footbridges under various human running loads,” *ISRN Civil Engineering*, vol. 2013, p. 817 384, 2013 (cit. on p. 18).

[68] M. Podworna and M. Klasztorny, “Vertical vibrations of composite bridge/track structure/high-speed train systems. part 1: Series-of-types of steel-concrete bridges,” *Bulletin of the Polish Academy of Sciences: Technical Sciences*, vol. 62, no. No 1, pp. 165–179, 2014 (cit. on p. 18).

[69] M. Podworna and M. Klasztorny, “Vertical vibrations of composite bridge/-track structure/high-speed train systems. part 2: Physical and mathematical modelling,” *Bulletin of the Polish Academy of Sciences: Technical Sciences*, vol. 62, no. No 1, pp. 181–196, 2014 (cit. on p. 18).

[70] M. Podworna and M. Klasztorny, “Vertical vibrations of composite bridge/-track structure/high-speed train systems. part 3: Deterministic and random vibrations of exemplary system,” *Bulletin of the Polish Academy of Sciences: Technical Sciences*, vol. 62, no. No 2, pp. 305–320, 2014 (cit. on p. 18).

[71] F. Sadeghi and A. B. Hong Kueh, “Serviceability assessment of composite footbridge under human walking and running loads,” *Jurnal Teknologi*, vol. 74, no. 4, 2015 (cit. on p. 18).

[72] Y. Li and S. He, “Research of steel-concrete composite bridge under blasting loads,” *Advances in Civil Engineering*, vol. 2018, p. 5 748 278, 2018 (cit. on p. 18).

[73] M. Yarnold, T. Golecki, and J. Weidner, “Identification of composite action through truck load testing,” *Frontiers in Built Environment*, vol. 4, Dec. 2018 (cit. on p. 18).

[74] Z. Li, X. Ma, J. Fan, and X. Nie, “Overhanging tests of steel-concrete composite girders with different connectors,” *Journal of Bridge Engineering*, vol. 24, no. 11, p. 04 019 098, 2019 (cit. on p. 18).

[75] F. A. Sofi and J. S. Steelman, “Nonlinear flexural distribution behavior and ultimate system capacity of skewed steel girder bridges,” *Engineering Structures*, vol. 197, p. 109 392, 2019 (cit. on p. 18).

[76] A. Gheitasi and D. K. Harris, “Overload flexural distribution behavior of composite steel girder bridges,” *Journal of Bridge Engineering*, vol. 20, no. 5, p. 04 014 076, 2015 (cit. on p. 18).

[77] A. Gheitasi and D. K. Harris, “Failure characteristics and ultimate load-carrying capacity of redundant composite steel girder bridges: Case study,” *Journal of Bridge Engineering*, vol. 20, no. 3, p. 05 014 012, 2015 (cit. on p. 18).

[78] V. Saraf and A. S. Nowak, “Proof load testing of deteriorated steel girder bridges,” *Journal of Bridge Engineering*, vol. 3, no. 2, pp. 82–89, 1998 (cit. on p. 18).

[79] Q. Su, C. Dai, and C. Xu, “Full-scale experimental study on the negative flexural behavior of orthotropic steel-concrete composite bridge deck,” *Journal of Bridge Engineering*, vol. 23, no. 12, p. 04 018 097, 2018 (cit. on p. 18).

[80] A. Zona, M. Barbato, A. Dall’Asta, and L. Dezi, “Probabilistic analysis for design assessment of continuous steel–concrete composite girders,” *Journal of Constructional Steel Research*, vol. 66, no. 7, pp. 897–905, 2010 (cit. on p. 18).

[81] F. Gara, G. Ranzi, and G. Leoni, “Simplified method of analysis accounting for shear-lag effects in composite bridge decks,” *Journal of Constructional Steel Research*, vol. 67, no. 10, pp. 1684–1697, 2011 (cit. on pp. 18, 19).

[82] J.-G. Nie and L. Zhu, “Beam-truss model of steel-concrete composite box-girder bridges,” *Journal of Bridge Engineering*, vol. 19, no. 7, p. 04 014 023, 2014 (cit. on p. 18).

[83] Y. Deng, B. M. Phares, and O. W. Steffens, “Experimental and numerical evaluation of a folded plate girder system for short-span bridges – a case study,” *Engineering Structures*, vol. 113, pp. 26–40, 2016 (cit. on p. 18).

[84] J. Buyu, Y. Xiaolin, Q. S. Yan, and Z. Yang, “Study on the system reliability of steel-concrete composite beam cable-stayed bridge,” *The Open Civil Engineering Journal*, vol. 10, pp. 418–432, 2016 (cit. on pp. 18, 19).

[85] T. Tong, Q. Yu, and Q. Su, “Coupled effects of concrete shrinkage, creep, and cracking on the performance of postconnected prestressed steel-concrete composite girders,” *Journal of Bridge Engineering*, vol. 23, no. 3, p. 04 017 145, 2018 (cit. on pp. 18, 19).

[86] D. K. Harris, “Assessment of flexural lateral load distribution methodologies for stringer bridges,” *Engineering Structures*, vol. 32, no. 11, pp. 3443–3451, 2010 (cit. on pp. 18, 19).

[87] D. K. Harris and A. Gheitasi, “Implementation of an energy-based stiffened plate formulation for lateral load distribution characteristics of girder-type bridges,” *Engineering Structures*, vol. 54, pp. 168–179, 2013 (cit. on pp. 18, 19).

[88] R. Melchers and A. Beck, *Structural Reliability Analysis and Prediction*. Wiley, 2018, ISBN: 9781119265993 (cit. on p. 18).

[89] M. Kleiber, T. Hien, H. Antunez, and P. Kowalczyk, *Parameter Sensitivity in Nonlinear Mechanics: Theory and Finite Element Computations*. Wiley, 1997, ISBN: 9780471968542 (cit. on p. 18).

[90] Y. Zhang and A. Der Kiureghian, “Dynamic response sensitivity of inelastic structures,” *Computer Methods in Applied Mechanics and Engineering*, vol. 108, no. 1, pp. 23–36, 1993 (cit. on p. 18).

[91] J. P. Conte, P. K. Vijalapura, and M. Meghella, “Consistent finite-element response sensitivity analysis,” *Journal of Engineering Mechanics*, vol. 129, no. 12, pp. 1380–1393, 2003 (cit. on p. 18).

[92] J. Conte, M. Barbato, and Q. gu, *Finite Element Response Sensitivity, Probabilistic Response and Reliability Analyses*. Jan. 2009, ISBN: 978-0-415-45261-8 (cit. on p. 18).

[93] V. Yepes, J. V. Martí, T. García-Segura, and F. González-Vidosa, “Heuristics in optimal detailed design of precast road bridges,” *Archives of Civil and Mechanical Engineering*, vol. 17, no. 4, pp. 738–749, 2017 (cit. on p. 19).

[94] V. Yepes, M. Dasi-Gil, D. Martínez-Muñoz, V. J. López-Desfilis, and J. V. Martí, “Heuristic techniques for the design of steel-concrete composite pedestrian bridges,” *Applied Sciences*, vol. 9(16), p. 3253, 2019 (cit. on pp. 19, 59, 126).

[95] M. Batikha, O. Ani, and T. Elhag, “The effect of span length and girder type on bridge costs,” *MATEC Web of Conferences*, vol. 120, p. 08 009, Jan. 2017 (cit. on pp. 19, 23).

[96] J. Surtees and D. Tordoff, “Optimum design of composite box girder bridge structures,” *Proceedings of the Institution of Civil Engineers*, vol. 63, no. 1, pp. 181–198, 1977 (cit. on p. 19).

[97] B. Briseghella, L. Fenu, C. Lan, E. Mazzarolo, and T. Zordan, “Application of topological optimization to bridge design,” *Journal of Bridge Engineering*, vol. 18, pp. 790–800, 2013 (cit. on pp. 19, 20, 120, 121, 126, 182, 217).

[98] M. P. Bendsøe and N. Kikuchi, “Generating optimal topologies in structural design using a homogenization method,” *Computer Methods in Applied Mechanics and Engineering*, vol. 71, no. 2, pp. 197–224, 1988 (cit. on pp. 19, 20).

[99] M. P. Bendsøe, “Optimal shape design as a material distribution problem,” *Structural optimization*, vol. 1, no. 4, pp. 193–202, 1989 (cit. on pp. 19, 20).

[100] O. Sigmund, “A 99 line topology optimization code written in matlab,” *Structural and Multidisciplinary Optimization*, vol. 21, no. 2, pp. 120–127, 2001 (cit. on pp. 19, 20).

[101] C. S. Edwards, H. A. Kim, and C. J. Budd, “An evaluative study on eso and simp for optimising a cantilever tie—beam,” *Structural and Multidisciplinary Optimization*, vol. 34, no. 5, pp. 403–414, 2007 (cit. on pp. 19, 20).

[102] Y. Xie and G. Steven, “A simple evolutionary procedure for structural optimization,” *Computers & Structures*, vol. 49, no. 5, pp. 885–896, 1993 (cit. on pp. 19, 20).

[103] R. L. Pedro, J. Demarche, L. F. F. Miguel, and R. H. Lopez, “An efficient approach for the optimization of simply supported steel-concrete composite i-girder bridges,” *Advances in Engineering Software*, vol. 112, pp. 31–45, 2017 (cit. on pp. 19, 20, 83, 127, 157).

[104] N. Lv and L. Fan, “Optimization of quickly assembled steel-concrete composite bridge used in temporary,” *Modern Applied Science*, vol. 8, no. 4, pp. 134–143, 2014 (cit. on pp. 19, 20, 83).

[105] A. Orcesi, C. Cremona, and B. Ta, “Optimization of design and life-cycle management for steel–concrete composite bridges,” *Structural Engineering International*, vol. 28, no. 2, pp. 185–195, 2018 (cit. on p. 20).

[106] R. Rempling, A. Mathern, D. Tarazona Ramos, and S. Luis Fernández, “Automatic structural design by a set-based parametric design method,” *Automation in Construction*, vol. 108, p. 102 936, 2019 (cit. on pp. 20, 83, 157).

[107] Y.-E. Nahm and H. Ishikawa, “A new 3d-cad system for set-based parametric design,” *The International Journal of Advanced Manufacturing Technology*, vol. 29, no. 1, pp. 137–150, 2006 (cit. on p. 20).

[108] A. C. Ward, J. K. Liker, J. J. Cristiano, and D. K. Sobek, “The second toyota paradox: How delaying decisions can make better cars faster,” *Long Range Planning*, vol. 4, p. 129, 1995 (cit. on p. 20).

[109] A. Kaveh, T. Bakhshpoori, and M. Barkhori, “Optimum design of multi-span composite box girder bridges using cuckoo search algorithm,” *Steel and Composite Structures*, vol. 17, no. 5, pp. 703–717, 2014 (cit. on pp. 20, 83, 120, 121, 126, 157, 182).

[110] A. Kaveh and M. M. M. Zarandi, “Optimal design of steel-concrete composite i-girder bridges using three meta-heuristic algorithms,” *Periodica Polytechnica Civil Engineering*, vol. 63, no. 2, pp. 317–337, 2019 (cit. on pp. 20, 83, 127).

[111] A. Kaveh and V. Mahdavi, “Colliding bodies optimization: A novel meta-heuristic method,” *Computers & Structures*, vol. 139, pp. 18–27, 2014 (cit. on p. 20).

[112] A. Kaveh and M. Ilchi Ghazaan, “Enhanced colliding bodies optimization for design problems with continuous and discrete variables,” *Advances in Engineering Software*, vol. 77, pp. 66–75, 2014 (cit. on p. 20).

[113] A. Kaveh and M. Ghazaan, “A new meta-heuristic algorithm: Vibrating particles system,” *Scientia Iranica*, vol. 24, pp. 551–566, Apr. 2017 (cit. on p. 20).

[114] P. Civicioglu, “Backtracking search optimization algorithm for numerical optimization problems,” *Applied Mathematics and Computation*, vol. 219, no. 15, pp. 8121–8144, 2013 (cit. on p. 20).

[115] X.-S. Yang, “Firefly algorithm,” in 2010, pp. 221–230 (cit. on p. 20).

[116] J. H. Holland, *Adaptation in Natural and Artificial Systems*. Ann Arbor, MI: University of Michigan Press, 1975 (cit. on p. 20).

[117] E. Atashpaz-Gargari and C. Lucas, “Imperialist competitive algorithm: An algorithm for optimization inspired by imperialistic competition,” *2007 IEEE Congress on Evolutionary Computation*, pp. 4661–4667, 2007 (cit. on p. 20).

[118] M. S. Gonçalves, R. H. Lopez, and L. F. F. Miguel, "Search group algorithm: A new metaheuristic method for the optimization of truss structures," *Computers & Structures*, vol. 153, pp. 165–184, 2015 (cit. on p. 20).

[119] X. Yang, *Nature-inspired Metaheuristic Algorithms*. Luniver Press, 2010 (cit. on p. 20).

[120] F. Glover and G. Kochenberger, *Handbook of Metaheuristics* (International Series in Operations Research & Management Science). Springer US, 2003 (cit. on p. 20).

[121] J. Kennedy, R. Eberhart, and Y. Shi, *Swarm Intelligence* (Evolutionary Computation Series). Elsevier Science, 2001 (cit. on p. 20).

[122] T. García-Segura, V. Penadés-Plà, and V. Yepes, "Sustainable bridge design by metamodel-assisted multi-objective optimization and decision-making under uncertainty," *Journal of Cleaner Production*, vol. 202, pp. 904–915, 2018 (cit. on pp. 20, 59).

[123] V. Yepes, T. García-Segura, and J. Moreno-Jiménez, "A cognitive approach for the multi-objective optimization of rc structural problems," *Archives of Civil and Mechanical Engineering*, vol. 15, no. 4, pp. 1024–1036, 2015, ISSN: 1644-9665 (cit. on p. 20).

[124] V. Penadés-Plà, T. García-Segura, and V. Yepes, "Accelerated optimization method for low-embodied energy concrete box-girder bridge design," *Engineering Structures*, vol. 179, pp. 556–565, 2019 (cit. on pp. 20, 84, 97, 157, 187, 249).

[125] F. Arnold and K. Sörensen, "What makes a vrp solution good? the generation of problem-specific knowledge for heuristics," *Computers & Operations Research*, vol. 106, pp. 280–288, 2019 (cit. on p. 20).

[126] J. Martínez-Calzón and J. Ortiz-Herrera, *Construcción mixta: hormigón-acero*. Rueda, 1978 (cit. on p. 21).

[127] J. Asencio, "The construction process of composite bridges. experiences of dyc: Solutions and considerations (in spanish)," *2nd International Workshop*

on Composite Bridges, State of the art on technology and analysis, pp. 565–567, 1995 (cit. on p. 21).

[128] J. Strasky, "Segmentally erected structures (in spanish)," *Tendencies on Bridge Design*, pp. 297–327, 2000 (cit. on p. 21).

[129] J. Martínez-Calzón, "Innovations on bridge construction. a general view of new execution methods of steel and concrete composite bridges (in spanish)," *Tendencies on Bridge Design*, pp. 167–185, 2000 (cit. on p. 21).

[130] D. Poineau, J. Lacombe, and J. Berthellemy, "Cracking control in the concrete slab of the nevers composite bridge. composite construction–conventional and innovative," *IABSE*, pp. 199–204, 1997 (cit. on p. 21).

[131] J.-M. Ducret, "Etude du comportement réel des ponts mixtes et modélisation pour le dimensionnement," p. 185, 1997 (cit. on p. 21).

[132] A. Marí, E. Mirambell, and I. Estrada, "Effects of construction process and slab prestressing on the serviceability behaviour of composite bridges," *Journal of Constructional Steel Research*, vol. 59, no. 2, pp. 135–163, 2003 (cit. on p. 21).

[133] K. Jung, K. Kim, C. Sim, and J. J. Kim, "Verification of incremental launching construction safety for the ilsun bridge, the world's longest and widest prestressed concrete box girder with corrugated steel web section," *Journal of Bridge Engineering*, vol. 16, no. 3, pp. 453–460, 2011 (cit. on p. 21).

[134] R. Hällmark, H. White, and P. Collin, "Prefabricated bridge construction across europe and america," *Practice Periodical on Structural Design and Construction*, vol. 17, no. 3, pp. 82–92, 2012 (cit. on p. 21).

[135] H. Valipour, A. Rajabi, S. Foster, and M. Bradford, "Arching behaviour of precast concrete slabs in a deconstructable composite bridge deck," *Construction and Building Materials*, vol. 87, pp. 67–77, 2015 (cit. on p. 21).

[136] I. J. Navarro, J. V. Martí, and V. Yepes, "Reliability-based maintenance optimization of corrosion preventive designs under a life cycle perspective," *Environmental Impact Assessment Review*, vol. 74, pp. 23–34, 2019 (cit. on p. 22).

[137] P. Albrecht and A. Lenwari, “Fatigue strength of repaired prestressed composite beams,” *Journal of Bridge Engineering*, vol. 13, no. 4, pp. 409–417, 2008 (cit. on p. 22).

[138] I. Sugimoto, Y. Yoshida, and A. Tanikaga, “Development of composite steel girder and concrete slab method for renovation of existing steel railway bridges,” *Quarterly Report of RTRI*, vol. 54, no. 1, pp. 8–11, 2013 (cit. on p. 22).

[139] A. Gheitasi and D. K. Harris, “Performance assessment of steel–concrete composite bridges with subsurface deck deterioration,” *Structures*, vol. 2, pp. 8–20, 2015 (cit. on p. 22).

[140] A. Gheitasi and D. K. Harris, “Redundancy and operational safety of composite stringer bridges with deteriorated girders,” *Journal of Performance of Constructed Facilities*, vol. 30, no. 2, p. 04 015 022, 2016 (cit. on p. 22).

[141] J. C. Matos, V. N. Moreira, I. B. Valente, P. J. Cruz, L. C. Neves, and N. Galvão, “Probabilistic-based assessment of existing steel-concrete composite bridges – application to sousa river bridge,” *Engineering Structures*, vol. 181, pp. 95–110, 2019 (cit. on p. 22).

[142] J. Bernardo and A. Smith, *Bayesian Theory* (Wiley Series in Probability and Statistics). Wiley, 2009 (cit. on p. 22).

[143] L. Jacinto, L. C. Neves, and L. O. Santos, “Bayesian assessment of an existing bridge: A case study,” *Structure and Infrastructure Engineering*, vol. 12, no. 1, pp. 61–77, 2016 (cit. on p. 22).

[144] J. Widman, “Environmental impact assessment of steel bridges,” *Journal of Constructional Steel Research*, vol. 46, no. 1, pp. 291–293, 1998, Second World Conference on Steel in Construction (cit. on p. 23).

[145] ISO, *Environmental Management, Life Cycle Assessment Principles and Framework (ISO 14040:2006)*. International Organization for Standardization, 2006 (cit. on pp. 23, 32, 60, 187, 197, 223, 243).

[146] G. Du and R. Karoumi, “Environmental life cycle assessment comparison between two bridge types: Reinforced concrete bridge and steel composite bridge,” 2013 (cit. on p. 23).

[147] worldsteel, *Life Cycle Inventory Methodology report for steel products*. World Steel Association, 2017 (cit. on pp. 23, 31, 35, 64, 73, 76, 243).

[148] G. Du and R. Karoumi, “Life cycle assessment of a railway bridge: Comparison of two superstructure designs,” *Structure and Infrastructure Engineering*, vol. 9(11), pp. 1149–1160, 2013 (cit. on pp. 23, 31, 37, 39, 59, 65, 66).

[149] C. Milani and M. Kripka, “Evaluation of short span bridge projects with a focus on sustainability,” *Structure and Infrastructure Engineering*, vol. 16, no. 2, pp. 367–380, 2020 (cit. on pp. 23, 24).

[150] B. C. Lippiatt, “Selecting cost-effective green building products: Bees approach,” *Journal of Construction Engineering and Management*, vol. 125, no. 6, pp. 448–455, 1999 (cit. on p. 23).

[151] M. Goedkoop, R. Heijungs, M. Huijbregts, A. De Schryver, J. Struijs, and R. Van Zelm, *ReCiPe 2008. Report I: Characterisation*. Ministry of Housing, Spatial planning and Environment (VROM), 2009, pp. 1–44 (cit. on pp. 23, 32, 61, 67, 197, 223, 243).

[152] C. Hwang and K. Yoon, *Multiple Attribute Decision Making: Methods and Applications A State-of-the-Art Survey* (Lecture Notes in Economics and Mathematical Systems). Springer Berlin Heidelberg, 1981 (cit. on p. 24).

[153] L. Rosén, P.-E. Back, T. Söderqvist, *et al.*, “Score: A novel multi-criteria decision analysis approach to assessing the sustainability of contaminated land remediation,” *Science of The Total Environment*, vol. 511, pp. 621–638, 2015 (cit. on p. 24).

[154] R. Sebastian, C. Claeson-Jonsson, and R. Di Giulio, “Performance-based procurement for low-disturbance bridge construction projects,” *Construction Innovation*, vol. 13, no. 4, pp. 394–409, 2013 (cit. on p. 24).

[155] K. Ek, A. Mathern, R. Rempling, *et al.*, “Multi-criteria decision analysis methods to support sustainable infrastructure construction,” Mar. 2019 (cit. on p. 24).

[156] R. Saaty, “The analytic hierarchy process—what it is and how it is used,” *Mathematical Modelling*, vol. 9, no. 3, pp. 161–176, 1987 (cit. on p. 24).

[157] S. Opricovic and G.-H. Tzeng, “Compromise solution by mcdm methods: A comparative analysis of vikor and topsis,” *European Journal of Operational Research*, vol. 156, no. 2, pp. 445–455, 2004 (cit. on p. 24).

[158] V. Penadés-Plà, T. García-Segura, and V. Yepes, “Robust design optimization for low-cost concrete box-girder bridge,” *Mathematics*, vol. 8, no. 3, p. 398, 2020 (cit. on p. 24).

[159] V. Penadés-Plà, D. Martínez-Muñoz, T. García-Segura, I. Navarro, and V. Yepes, “Environmental and social impact assessment of optimized post-tensioned concrete road bridges,” *Sustainability*, vol. 12, p. 4265, 2020 (cit. on pp. 24, 31, 35, 59, 63, 73).

[160] M. Greenacre, *Correspondence Analysis in Practice, Third Edition* (Chapman & Hall/CRC Interdisciplinary Statistics). CRC Press, 2017 (cit. on p. 25).

[161] V. Årskog, S. Fossdal, and O. E. Gjørv, *Life-cycle asessment of repair and maintenance systems for concrete structures*. International Workshop on Sustainable Development and Concrete Technology, 2004 (cit. on pp. 31, 59).

[162] M. E. Boesch and S. Hellweg, “Identifying improvement potentials in cement production with life cycle assessment,” *Automation in construction*, vol. 44(23), pp. 9143–914, 2010 (cit. on p. 31).

[163] M. Taylor, C. Tam, and D. Gielen, *Energy Efficiency and* CO_2 *Emissions from the Global Cement Industry, Energy Technology Policy Division*. International Energy Agency. Energy Technology Policy Division, 2006 (cit. on p. 31).

[164] F. Collins, “Inclusion of carbonation during the life cycle of built and recycled concrete: Influence on their carbon footprint,” *The International Journal of Life*

Cycle Assessment, vol. 15(6), pp. 549–556, 2010 (cit. on pp. 31, 37, 65, 198, 224).

[165] T. García-Segura, V. Yepes, and D. M. Frangopol, "Multi-objective design of post-tensioned concrete road bridges using artificial neural networks," *Structural and Multidisciplinary Optimization*, vol. 56, pp. 139–150, 2017 (cit. on pp. 31, 83, 84).

[166] V. Yepes, J. V. Martí, and T. García-Segura, "Cost and CO_2 emission optimization of precast-prestressed concrete u-beam road bridges by a hybrid glowworm swarm algorithm," *Automation in Construction*, vol. 49, pp. 123–134, 2015 (cit. on pp. 31, 122).

[167] A. Serpell, J. Kort, and S. Vera, "Awareness, actions, drivers and barriers of sustainable construction in chile," *Technological and Economic Development of Economy*, vol. 19(2), pp. 272–288, 2013 (cit. on pp. 31, 186).

[168] L. A. Sierra, E. Pellicer, and V. Yepes, "Method for estimating the social sustainability of infrastructure projects," *Environmental Impact Assessment Review*, vol. 65, pp. 41–53, 2017 (cit. on p. 31).

[169] N. Yusof, N. Zainul Abidin, S. H. M. Zailani, K. Govindan, and M. Iranmanesh, "Linking the environmental practice of construction firms and the environmental behaviour of practitioners in construction projects," *Journal of Cleaner Production*, vol. 121, pp. 64–71, 2016 (cit. on pp. 31, 59, 186).

[170] T. García-Segura, V. Yepes, J. Alcala, and E. Pérez-López, "Hybrid harmony search for sustainable design of post-tensioned concrete box-girder pedestrian bridges," *Engineering Structures*, vol. 92, pp. 112–122, 2015 (cit. on p. 31).

[171] J. V. Marti, V. Yepes, and F. Gonzalez-Vidosa, "Memetic algorithm approach to designing precast-prestressed concrete road bridges with steel fiber reinforcement," *Journal of Structural Engineering*, vol. 141, 2015 (cit. on p. 31).

[172] F. Molina-Moreno, T. García-Segura, J. V. Martí, and V. Yepes, "Optimization of buttressed earth-retaining walls using hybrid harmony search algorithms," *Engineering Structures*, vol. 134, pp. 205–216, 2017 (cit. on pp. 31, 59, 157).

[173] D. Martínez-Muñoz, J. V. Martí, J. García, and V. Yepes, "Embodied energy optimization of buttressed earth-retaining walls with hybrid simulated annealing," *Applied Sciences*, vol. 11, no. 4, p. 1800, 2021 (cit. on pp. 31, 59, 129, 145, 157).

[174] V. Yepes, J. Alcalá, C. Perea, and F. González-Vidosa, "A parametric study of optimum earth-retaining walls by simulated annealing," *Engineering Structures*, vol. 30(3), pp. 821–830, 2008 (cit. on pp. 31, 82).

[175] V. Yepes, F. González-Vidosa, J. Alcalá, and P. Villalba, "CO_2-Optimization design of reinforced concrete retaining walls based on a VNS-Threshold Acceptance Strategy," *Journal of Computing in Civil Engineering*, vol. 26, pp. 378–386, 2012 (cit. on pp. 31, 122).

[176] A. Dodoo, L. Gustavsson, and R. Sathre, "Carbon implications of end-of-life management of building materials," *Resources, Conservation and Recycling*, vol. 53(5), pp. 276–286, 2009 (cit. on pp. 31, 37, 65, 198, 224).

[177] T. García-Segura, V. Yepes, and J. Alcalá, "Life cycle greenhouse gas emissions of blended cement concrete including carbonation and durability," *The International Journal of Life Cycle Assessment*, vol. 19, pp. 3–12, 2014 (cit. on pp. 31, 37–39, 65, 66, 198, 224).

[178] G. Du, M. Safi, L. Pettersson, and R. Karoumi, "Life cycle assessment as a decision support tool for bridge procurement: Environmental impact comparison among five bridge designs," *The International Journal of Life Cycle Assessment*, vol. 19, pp. 1948–1964, 2014 (cit. on pp. 31, 37–39, 59, 65, 66).

[179] A. Hettinger, J. Birat, O. Hechler, and M. Braun, *Sustainable bridges – LCA for a composite and a concrete bridge* (Economical Bridge Solutions Based on Innovative Composite Dowels and Integrated Abutments: Ecobridge). Springer Vieweg, 2015 (cit. on pp. 31, 38, 39, 66).

[180] R. Salvador, M. Barros, G. dos Santos, K. van Mierlo, C. Piekarski, and A. de Francisco, "Towards a green and fast production system: Integrating life cycle assessment and value stream mapping for decision making," *Environmental Impact Assessment Review*, vol. 87, p. 106 519, 2021 (cit. on p. 31).

[181] P. Vitale, R. Napolitano, F. Colella, C. Menna, and D. Asprone, "Cement-matrix composites using cfrp waste: A circular economy perspective using industrial symbiosis," *Materials*, vol. 14(6), p. 1484, 2021 (cit. on p. 31).

[182] L. Caneda-Martínez, M. Monasterio, J. Moreno-Juez, S. Martínez-Ramírez, R. García, and M. Frías, "Behaviour and properties of eco-cement pastes elaborated with recycled concrete powder from construction and demolition wastes," *Materials*, vol. 14(5), p. 1299, 2021 (cit. on p. 31).

[183] Q. Jiang, F. Wang, Q. Liu, J. Xie, and S. Wu, "Energy consumption and environment performance analysis of induction-healed asphalt pavement by life cycle assessment (lca)," *Materials*, vol. 14(5), p. 1244, 2021 (cit. on p. 31).

[184] P. Zastrow, F. Molina-Moreno, T. García-Segura, J. Martí, and V. Yepes, "Life cycle assessment of cost-optimized buttress earth-retaining walls: A parametric study," *Journal of Cleaner Production*, vol. 140, pp. 1037–1048, 2017 (cit. on pp. 31, 36).

[185] J. J. Pons, V. Penadés-Plà, V. Yepes, and J. V. Martí, "Life cycle assessment of earth-retaining walls: An environmental comparison," *Journal of Cleaner Production*, vol. 192, pp. 411–420, 2018 (cit. on pp. 31, 187).

[186] A. Sánchez-Garrido, I. Navarro, and V. Yepes, "Neutrosophic multi-criteria evaluation of sustainable alternatives for the structure of single-family homes," *Environmental Impact Assessment Review*, vol. 89, p. 106 572, 2021 (cit. on p. 31).

[187] L. Laiblová, J. Pešta, A. Kumar, *et al.*, "Environmental impact of textile reinforced concrete facades compared to conventional solutions—lca case study," *Materials*, vol. 12(19), no. 19, p. 3194, 2019 (cit. on p. 31).

[188] D. Kvočka, A. Lešek, F. Knez, *et al.*, "Life cycle assessment of prefabricated geopolymeric façade cladding panels made from large fractions of recycled construction and demolition waste," *Materials*, vol. 13(18), p. 3931, 2020 (cit. on p. 31).

[189] D. Martínez-Muñoz, J. V. Martí, and V. Yepes, "Steel-concrete composite bridges: Design, life cycle assessment, maintenance, and decision-making," *Advances*

in Civil Engineering, vol. 2020, p. 8 823 370, 2020 (cit. on pp. 31, 59, 83, 126, 157, 217).

[190] B. Rossi, S. Marquart, and G. Rossi, "Comparative life cycle cost assessment of painted and hot-dip galvanized bridges," *Journal of Environmental Management*, vol. 197, pp. 41–49, 2017 (cit. on p. 31).

[191] B. Pang, P. Yang, Y. Wang, A. Kendall, H. Xie, and Y. Zhang, "Comparative life cycle cost assessment of painted and hot-dip galvanized bridges," *The International Journal of Life Cycle Assessment*, vol. 20, pp. 1300–1311, 2015 (cit. on pp. 32, 37, 61, 65).

[192] M. Marceau, M. Nisbet, and M. Vangeem, *Life Cycle Inventory of Portland Cement Concrete* (Report 2137a). Portland Cement Association, 2002 (cit. on pp. 35, 64).

[193] SRI, *Construction | SRI - Steel Recycling Institute https://www.steelsustainability.org/construction*. accessed on 30 January 2021 (cit. on pp. 36, 65, 198, 224).

[194] J. Hammervold, M. Reenaas, and H. Brattebø, "Environmental life cycle assessment of bridges," *Journal of Bridge Engineering*, vol. 18, pp. 153–161, 2013 (cit. on pp. 37, 38, 65, 66).

[195] T. García-Segura and V. Yepes, "Multiobjective optimization of post-tensioned concrete box-girder road bridges considering cost, CO_2 emissions, and safety," *Engineering Structures*, vol. 125, pp. 325–336, 2016 (cit. on pp. 37, 65).

[196] B. Lagerblad, *Carbon dioxide uptake during concrete life cycle - State of the art*. Swedish Cement and Concrete Research Institute, 2005 (cit. on pp. 38, 39, 66).

[197] MFOM, *Instrucción de Hormigón Estructural (EHE-08)*. Madrid: Ministerio de Fomento, 2011 (cit. on pp. 39, 66).

[198] A. Ciroth, "ICT for environment in life cycle applications openlca - a new open source software for life cycle assessment," *The International Journal of Life Cycle Assessment*, vol. 12, p. 209, 2007 (cit. on pp. 40, 67, 198, 225).

[199] R. Frischknecht and G. Rebitzer, “The ecoinvent database system: A comprehensive web-based lca database,” *Journal of Cleaner Production*, vol. 13(13), pp. 1337–1343, 2005 (cit. on pp. 40, 67, 197, 198, 223, 225).

[200] J. Pascual-González, G. Guillén-Gosálbez, J. M. Mateo-Sanz, and L. Jiménez-Esteller, “Statistical analysis of the ecoinvent database to uncover relationships between life cycle impact assessment metrics,” *Journal of Cleaner Production*, vol. 112, pp. 359–368, 2016 (cit. on pp. 40, 67, 197, 224).

[201] S. Larsen, “Inclusion of uncertainty in environmental impact assessment in greenland,” *Environmental Impact Assessment Review*, vol. 89, p. 106 583, 2021 (cit. on p. 40).

[202] J. Hong, G. Q. Shen, Y. Peng, Y. Feng, and C. Mao, “Reprint of: Uncertainty analysis for measuring greenhouse gas emissions in the building construction phase: A case study in china,” *Journal of Cleaner Production*, vol. 163, S420–S432, 2017 (cit. on p. 40).

[203] A. Ciroth, S. Muller, B. Weidema, and P. Lesage, “Empirically based uncertainty factors for the pedigree matrix in ecoinvent,” *The International Journal of Life Cycle Assessment*, vol. 21, pp. 1338–1348, 2016 (cit. on p. 40).

[204] V. Yepes, J. Díaz, F. González-Vidosa, and J. Alcalá, “Statistical characterization of prestressed concrete road bridge decks,” *Revista de la construcción*, vol. 8(2), pp. 95–108, 2009 (cit. on pp. 40, 69).

[205] MFOM, *Obras de paso de nueva construcción*. Madrid: Ministerio de Fomento, 2000 (cit. on pp. 40, 69, 243).

[206] Y. Zhang, Y. Mao, L. Jiao, C. Shuai, and H. Zhang, “Eco-efficiency, eco-technology innovation and eco-well-being performance to improve global sustainable development,” *Environmental Impact Assessment Review*, vol. 89, p. 106 580, 2021 (cit. on pp. 42, 70, 187).

[207] *Catalonia* I*nstitute of* C*onstruction* T*echnology.* BEDEC ITEC *Materials Database https://metabase.itec.cat/vide/es/bedec*. accessed on 30 January 2021 (cit. on pp. 42, 70, 84, 122, 130, 149, 159, 196, 221).

[208] S. Yi, K. Kurisu, and K. Hanaki, “Life cycle impact assessment and interpretation of municipal solid waste management scenarios based on the midpoint and endpoint approaches,” *The International Journal of Life Cycle Assessment*, vol. 16, pp. 652–668, 2011 (cit. on p. 43).

[209] P. Khatri, S. Jain, and S. Pandey, “A cradle-to-gate assessment of environmental impacts for production of mustard oil using life cycle assessment approach,” *Journal of Cleaner Production*, vol. 166, pp. 988–997, 2017 (cit. on p. 44).

[210] WCED, *Transforming our world: The 2030 agenda for sustainable development*. New York, NY, USA: World Commission on Environment and Development, 2015 (cit. on p. 58).

[211] F. J. Martínez, F. González-Vidosa, A. Hospitaler, and V. Yepes, “Heuristic optimization of rc bridge piers with rectangular hollow sections,” *Computers & Structures*, vol. 88, no. 5, pp. 375–386, 2010 (cit. on p. 59).

[212] A. Carbonell, F. González-Vidosa, and V. Yepes, “Design of reinforced concrete road vaults by heuristic optimization,” *Advances in Engineering Software*, vol. 42, no. 4, pp. 151–159, 2011 (cit. on pp. 59, 157).

[213] N. Ata-Ali, V. Penadés-Plà, D. Martínez-Muñoz, and V. Yepes, “Recycled versus non-recycled insulation alternatives: Lca analysis for different climatic conditions in spain,” *Resources, Conservation and Recycling*, vol. 175, p. 105 838, 2021 (cit. on p. 59).

[214] K. Murphy, “The social pillar of sustainable development: A literature review and framework for policy analysis,” *Sustainability: Science, Practice and Policy*, vol. 8, no. 1, pp. 15–29, 2012 (cit. on p. 59).

[215] L. Montalbán-Domingo, T. García-Segura, M. A. Sanz, and E. Pellicer, “Social sustainability criteria in public-work procurement: An international perspective,” *Journal of Cleaner Production*, vol. 198, pp. 1355–1371, 2018 (cit. on p. 59).

[216] S. Vallance, H. C. Perkins, and J. E. Dixon, “What is social sustainability? a clarification of concepts,” *Geoforum*, vol. 42, no. 3, pp. 342–348, 2011 (cit. on p. 59).

[217] R. Valdes-Vasquez and L. E. Klotz, "Social sustainability considerations during planning and design: Framework of processes for construction projects," *Journal of Construction Engineering and Management*, vol. 139, no. 1, pp. 80–89, 2013 (cit. on p. 59).

[218] E. Almahmoud and H. Doloi, "Assessment of social sustainability in construction projects using social network analysis," *Journal of International Business Research and Marketing*, vol. 3, no. 6, pp. 35–46, 2018 (cit. on p. 59).

[219] I. J. Navarro, V. Penadés-Plà, D. Martínez-Muñoz, R. Rempling, and V. Yepes, "Life cycle sustainability assessment for multi-criteria decision making in bridge design: A review," *Journal of Civil Engineering and Management*, vol. 26, no. 7, pp. 690–704, 2021 (cit. on p. 59).

[220] D. Martínez-Muñoz, J. V. Martí, and V. Yepes, "Comparative life cycle analysis of concrete and composite bridges varying steel recycling ratio," *Materials*, vol. 14, no. 15, p. 4218, 2021 (cit. on pp. 59, 61, 63, 64, 69–72).

[221] H. Gervásio and L. Simões da Silva, "A probabilistic decision-making approach for the sustainable assessment of infrastructures," *Expert Systems with Applications*, vol. 39, no. 8, pp. 7121–7131, 2012 (cit. on pp. 60, 156).

[222] S. Sabatino, D. M. Frangopol, and Y. Dong, "Sustainability-informed maintenance optimization of highway bridges considering multi-attribute utility and risk attitude," *Engineering Structures*, vol. 102, pp. 310–321, 2015 (cit. on p. 60).

[223] Z. Chen, A. B. Abdullah, C. J. Anumba, and H. Li, "Anp experiment for demolition plan evaluation," *Journal of Construction Engineering and Management*, vol. 140, no. 2, p. 06 013 005, 2014 (cit. on p. 60).

[224] C. Benoît and B. Mazijn, *Guidelines for Social Life Cycle Assessment of Products*. Paris, France: UNEP/SETAC Life Cycle Initiative,Sustainable Product and Consumption Branch, 2011, vol. 15 (cit. on pp. 60, 197, 223, 243).

[225] Y. Otsuki, D. Li, S. S. Dey, M. Kurata, and Y. Wang, "Finite element model updating of an 18-story structure using branch-and-bound algorithm with epsilon-constraint," *Journal of Civil Structural Health Monitoring*, vol. 11, no. 3, pp. 575–592, 2021 (cit. on p. 82).

[226] K. C. Sarma and H. Adeli, “Cost optimization of concrete structures,” *Journal of Structural Engineering*, vol. 124, no. 5, pp. 570–578, 1998 (cit. on p. 83).

[227] W. Hare, J. Nutini, and S. Tesfamariam, “A survey of non-gradient optimization methods in structural engineering,” *Advances in Engineering Software*, vol. 59, pp. 19–28, 2013 (cit. on p. 83).

[228] M. Afzal, Y. Liu, J. C. Cheng, and V. J. Gan, “Reinforced concrete structural design optimization: A critical review,” *Journal of Cleaner Production*, vol. 260, p. 120 623, 2020 (cit. on p. 83).

[229] J. Liu, P. Liu, L. Feng, W. Wu, D. Li, and Y. F. Chen, “Automated clash resolution for reinforcement steel design in concrete frames via q-learning and building information modeling,” *Automation in Construction*, vol. 112, p. 103 062, 2020 (cit. on p. 83).

[230] A. Mathern, V. Penadés-Plà, J. Armesto Barros, and V. Yepes, “Practical metamodel-assisted multi-objective design optimization for improved sustainability and buildability of wind turbine foundations,” *Structural and Multidisciplinary Optimization*, vol. 65, no. 2, p. 46, 2022 (cit. on pp. 83, 217).

[231] Z. Jaouadi, T. Abbas, G. Morgenthal, and T. Lahmer, “Single and multi-objective shape optimization of streamlined bridge decks,” *Structural and Multidisciplinary Optimization*, vol. 61, no. 4, pp. 1495–1514, 2020 (cit. on p. 83).

[232] V. T. Camacho, N. Horta, M. Lopes, and C. S. Oliveira, “Optimizing earthquake design of reinforced concrete bridge infrastructures based on evolutionary computation techniques,” *Structural and Multidisciplinary Optimization*, vol. 61, no. 3, pp. 1087–1105, 2020 (cit. on p. 83).

[233] S. Mirjalili, “Sca: A sine cosine algorithm for solving optimization problems,” *Knowledge-based systems*, vol. 96, pp. 120–133, 2016 (cit. on pp. 83, 97, 138, 167, 192, 230).

[234] R. Venkata Rao, “Jaya: A simple and new optimization algorithm for solving constrained and unconstrained optimization problems,” *International Journal of Industrial Engineering Computations*, vol. 7, pp. 19–34, 2016 (cit. on p. 83).

[235] A. G. Hussien, A. E. Hassanien, E. H. Houssein, M. Amin, and A. T. Azar, "New binary whale optimization algorithm for discrete optimization problems," *Engineering Optimization*, vol. 52, no. 6, pp. 945–959, 2020 (cit. on p. 83).

[236] K. K. Ghosh, R. Guha, S. K. Bera, N. Kumar, and R. Sarkar, "S-shaped versus v-shaped transfer functions for binary manta ray foraging optimization in feature selection problem," *Neural Computing and Applications*, 2021 (cit. on p. 83).

[237] CEN, *Eurocode 3: Design of steel structures*. Brussels, Belgium: European Committee for Standardization, 2013 (cit. on pp. 87, 89, 92, 93, 130, 133–135, 161, 164, 165, 202, 203, 208, 229).

[238] CEN, *Eurocode 2: Design of concrete structures*. Brussels, Belgium: European Committee for Standardization, 2013 (cit. on pp. 87–90, 92, 93, 120, 130, 133–135, 161, 164, 165, 202, 203, 228, 229, 239).

[239] CEN, *EN 10365:2017: Hot rolled steel channels, I and H sections. Dimensions and masses*. Brussels, Belgium: European Committee for Standardization, 2017 (cit. on pp. 88, 119, 163, 181, 201, 227).

[240] CEN, *Eurocode 1: Actions on structures*. Brussels, Belgium: European Committee for Standardization, 2019 (cit. on pp. 89, 92, 93, 134, 135, 164, 165, 202, 228).

[241] MFOM, *IAP-11: Code on the actions for the design of road bridges*. Madrid: Ministerio de Fomento, 2011 (cit. on pp. 89, 93, 134, 136, 164, 165, 203, 229).

[242] S. Monleón, *Diseño estructural de puentes (in Spanish)*. València: Universitat Politècnica de València, 2017 (cit. on pp. 89, 92, 93, 120, 130, 133, 135, 164, 165, 202, 228, 229).

[243] G. Van Rossum and F. L. Drake, *Python 3 Reference Manual*. Scotts Valley, CA: CreateSpace, 2009, ISBN: 1441412697 (cit. on pp. 93, 190, 203, 230).

[244] S. Kirkpatrick, C. D. J. Gelatt, and M. P. Vecchi, "Optimization by simulated annealing," *Science*, vol. 220, no. 4598, pp. 671–680, 1983 (cit. on pp. 96, 166, 191).

[245] J. R. Medina, “Estimation of incident and reflected waves using simulated annealing,” *Journal of Waterway, Port, Coastal, and Ocean Engineering*, vol. 127, no. 4, pp. 213–221, 2001 (cit. on pp. 96, 166).

[246] R. Rao, “Jaya: A simple and new optimization algorithm for solving constrained and unconstrained optimization problems,” *International Journal of Industrial Engineering Computations*, vol. 7, no. 1, pp. 19–34, 2016 (cit. on p. 97).

[247] M. Aslan, M. Gunduz, and M. S. Kiran, “Jayax: Jaya algorithm with xor operator for binary optimization,” *Applied Soft Computing*, vol. 82, p. 105 576, 2019 (cit. on p. 97).

[248] D. C. Montgomery, *Design and analysis of experiments*. Hoboken: John Wiley & Sons, 2013 (cit. on pp. 100, 169, 191).

[249] Minitab, *Minitab 19 Statistical Software*. State College, PA, 2019 (cit. on p. 101).

[250] J. García, B. Crawford, R. Soto, C. Castro, and F. Paredes, “A k-means binarization framework applied to multidimensional knapsack problem,” *Applied Intelligence*, vol. 48, no. 2, pp. 357–380, 2018 (cit. on pp. 103, 129, 144).

[251] W. L. Hays and R. L. Winkler, “Statistics: Probability, inference, and decision,” Tech. Rep., 1970 (cit. on pp. 104, 143).

[252] J. M. Lanza-Gutierrez, B. Crawford, R. Soto, N. Berrios, J. A. Gomez-Pulido, and F. Paredes, “Analyzing the effects of binarization techniques when solving the set covering problem through swarm optimization,” *Expert Systems with Applications*, vol. 70, pp. 67–82, 2017 (cit. on pp. 104, 171).

[253] A. Richardson, *Nonparametric statistics for non-statisticians: A step-by-step approach by gregory w. corder, dale i. foreman*, 2010 (cit. on p. 104).

[254] R. Mundry and J. Fischer, “Use of statistical programs for nonparametric tests of small samples often leads to incorrect pvalues: Examples from animal behaviour,” *Animal behaviour*, vol. 56, no. 1, pp. 256–259, 1998 (cit. on p. 104).

[255] W. Dillen, G. Lombaert, and M. Schevenels, “A hybrid gradient-based/metaheuristic method for eurocode-compliant size, shape and topology optimization of steel structures,” *Engineering Structures*, vol. 239, p. 112 137, 2021 (cit. on p. 126).

[256] K. Korus, M. Salamak, and M. Jasiński, “Optimization of geometric parameters of arch bridges using visual programming fem components and genetic algorithm,” *Engineering Structures*, vol. 241, p. 112 465, 2021 (cit. on p. 126).

[257] R. Belevičius, A. Juozapaitis, D. Rusakevičius, and S. Žilėnaitė, “Parametric study on mass minimization of radial network arch pedestrian bridges,” *Engineering Structures*, vol. 237, p. 112 182, 2021 (cit. on p. 126).

[258] X. Zhao, Y. Lu, H. Liang, Y. Wang, and Y. Yan, “Optimal design of reinforced concrete columns strengthened with square steel tubes and sandwiched concrete,” *Engineering Structures*, vol. 244, p. 112 723, 2021 (cit. on p. 126).

[259] Y. Han, B. Xu, Q. Wang, and Y. Liu, “Bi-directional evolutionary topology optimization of continuum structures subjected to inertial loads,” *Advances in Engineering Software*, vol. 155, p. 102 897, 2021 (cit. on p. 126).

[260] E.-G. Talbi, “Combining metaheuristics with mathematical programming, constraint programming and machine learning,” *Annals of Operations Research*, vol. 240, no. 1, pp. 171–215, 2016 (cit. on p. 127).

[261] M. Caserta and S. Voß, “Metaheuristics: Intelligent problem solving,” in *Matheuristics*, Springer, 2009, pp. 1–38 (cit. on p. 127).

[262] A. A. Juan, J. Faulin, S. E. Grasman, M. Rabe, and G. Figueira, “A review of simheuristics: Extending metaheuristics to deal with stochastic combinatorial optimization problems,” *Operations Research Perspectives*, vol. 2, pp. 62–72, 2015 (cit. on p. 127).

[263] L. Calvet, J. de Armas, D. Masip, and A. A. Juan, “Learnheuristics: Hybridizing metaheuristics with machine learning for optimization with dynamic inputs,” *Open Mathematics*, vol. 15, no. 1, pp. 261–280, 2017 (cit. on p. 127).

[264] E.-G. Talbi, “Machine learning into metaheuristics: A survey and taxonomy,” *ACM Computing Surveys (CSUR)*, vol. 54, no. 6, pp. 1–32, 2021 (cit. on p. 127).

[265] M. López-Ibáñez, J. Dubois-Lacoste, L. P. Cáceres, M. Birattari, and T. Stützle, “The irace package: Iterated racing for automatic algorithm configuration,” *Operations Research Perspectives*, vol. 3, pp. 43–58, 2016 (cit. on p. 127).

[266] J. Ries and P. Beullens, “A semi-automated design of instance-based fuzzy parameter tuning for metaheuristics based on decision tree induction,” *Journal of the Operational Research Society*, vol. 66, no. 5, pp. 782–793, 2015 (cit. on p. 127).

[267] A. Shahzad and N. Mebarki, “Data mining based job dispatching using hybrid simulation-optimization approach for shop scheduling problem,” *Engineering Applications of Artificial Intelligence*, vol. 25, no. 6, pp. 1173–1181, 2012 (cit. on p. 127).

[268] B. Waschneck, A. Reichstaller, L. Belzner, *et al.*, “Optimization of global production scheduling with deep reinforcement learning,” *Procedia CIRP*, vol. 72, no. 1, pp. 1264–1269, 2018 (cit. on p. 128).

[269] M. Jiang, Z. Huang, L. Qiu, W. Huang, and G. G. Yen, “Transfer learning-based dynamic multiobjective optimization algorithms,” *IEEE Transactions on Evolutionary Computation*, vol. 22, no. 4, pp. 501–514, 2017 (cit. on p. 128).

[270] J. García, B. Crawford, R. Soto, and G. Astorga, “A clustering algorithm applied to the binarization of swarm intelligence continuous metaheuristics,” *Swarm and evolutionary computation*, vol. 44, pp. 646–664, 2019 (cit. on p. 128).

[271] J. García, E. Lalla-Ruiz, S. Voß, and E. L. Droguett, “Enhancing a machine learning binarization framework by perturbation operators: Analysis on the multidimensional knapsack problem,” *International Journal of Machine Learning and Cybernetics*, vol. 11, no. 9, pp. 1951–1970, 2020 (cit. on pp. 128, 129).

[272] S. Kazemzadeh Azad, “Enhanced hybrid metaheuristic algorithms for optimal sizing of steel truss structures with numerous discrete variables,” *Structural*

and Multidisciplinary Optimization, vol. 55, no. 6, pp. 2159–2180, 2017 (cit. on p. 128).

[273] S. K. Azad, "Monitored convergence curve: A new framework for metaheuristic structural optimization algorithms," *Structural and Multidisciplinary Optimization*, vol. 60, no. 2, pp. 481–499, 2019 (cit. on p. 128).

[274] B. Crawford, R. Soto, G. Astorga, J. García, C. Castro, and F. Paredes, "Putting continuous metaheuristics to work in binary search spaces," *Complexity*, vol. 2017, 2017 (cit. on pp. 129, 137).

[275] F. Wilcoxon, "Individual comparisons by ranking methods," in *Breakthroughs in statistics*, Springer, 1992, pp. 196–202 (cit. on p. 143).

[276] J. V. Martí, F. Gonzalez-Vidosa, V. Yepes, and J. Alcalá, "Design of prestressed concrete precast road bridges with hybrid simulated annealing," *Engineering Structures*, vol. 48, pp. 342–352, 2013 (cit. on p. 145).

[277] S. K. Azad and O. Hasançebi, "Upper bound strategy for metaheuristic based design optimization of steel frames," *Advances in Engineering Software*, vol. 57, pp. 19–32, 2013 (cit. on p. 154).

[278] Y. Yılmaz and S. Seyis, "Mapping the scientific research of the life cycle assessment in the construction industry: A scientometric analysis," *Building and Environment*, vol. 204, p. 108 086, 2021 (cit. on pp. 156, 187).

[279] D. Martínez-Muñoz, J. V. Martí, and V. Yepes, "Social impact assessment comparison of composite and concrete bridge alternatives," *Sustainability*, vol. 14, no. 9, p. 5186, 2022 (cit. on pp. 156, 197, 200, 208, 209, 224, 226, 239).

[280] N. Abdou, Y. EL Mghouchi, S. Hamdaoui, N. EL Asri, and M. Mouqallid, "Multiobjective optimization of passive energy efficiency measures for net-zero energy building in morocco," *Building and Environment*, vol. 204, p. 108 141, 2021 (cit. on p. 156).

[281] Y. Xu, G. Zhang, C. Yan, G. Wang, Y. Jiang, and K. Zhao, "A two-stage multiobjective optimization method for envelope and energy generation systems

of primary and secondary school teaching buildings in china," *Building and Environment*, vol. 204, p. 108 142, 2021 (cit. on p. 156).

[282] T. Wang, I.-S. Lee, A. Kendall, J. Harvey, E.-B. Lee, and C. Kim, "Life cycle energy consumption and ghg emission from pavement rehabilitation with different rolling resistance," *Journal of Cleaner Production*, vol. 33, pp. 86–96, 2012 (cit. on pp. 157, 186).

[283] X. G. Casals, "Analysis of building energy regulation and certification in europe: Their role, limitations and differences," *Energy and Buildings*, vol. 38, no. 5, pp. 381–392, 2006 (cit. on p. 157).

[284] M. K. Dixit, J. L. Fernández-Solís, S. Lavy, and C. H. Culp, "Identification of parameters for embodied energy measurement: A literature review," *Energy and Buildings*, vol. 42, no. 8, pp. 1238–1247, 2010 (cit. on p. 157).

[285] A. Whitworth and K. Tsavdaridis, "Embodied energy optimization of steel-concrete composite beams using a genetic algorithm," *Procedia Manufacturing*, vol. 44, pp. 417–424, 2020 (cit. on p. 157).

[286] D. Yeo and R. D. Gabbai, "Sustainable design of reinforced concrete structures through embodied energy optimization," *Energy and Buildings*, vol. 43, no. 8, pp. 2028–2033, 2011 (cit. on p. 157).

[287] C. Quaglia, N. Yu, A. Thrall, and S. Paolucci, "Balancing energy efficiency and structural performance through multi-objective shape optimization: Case study of a rapidly deployable origami-inspired shelter," *Energy and Buildings*, vol. 82, pp. 733–745, 2014 (cit. on p. 157).

[288] D. Miller, J.-H. Doh, and M. Mulvey, "Concrete slab comparison and embodied energy optimisation for alternate design and construction techniques," *Construction and Building Materials*, vol. 80, pp. 329–338, 2015 (cit. on p. 157).

[289] J. Liu, Y. Liu, Y. Shi, and J. Li, "Solving resource-constrained project scheduling problem via genetic algorithm," *Journal of Computing in Civil Engineering*, vol. 34, no. 2, p. 04 019 055, 2020 (cit. on p. 157).

[290] J. García, J. Lemus-Romani, F. Altimiras, *et al.*, "A binary machine learning cuckoo search algorithm improved by a local search operator for the set-union knapsack problem," *Mathematics*, vol. 9, no. 20, p. 2611, 2021 (cit. on p. 158).

[291] D. N. Hama Rashid, T. A. Rashid, and S. Mirjalili, "Ana: Ant nesting algorithm for optimizing real-world problems," *Mathematics*, vol. 9, no. 23, p. 3111, 2021 (cit. on p. 158).

[292] F. Pace, A. Santilano, and A. Godio, "A review of geophysical modeling based on particle swarm optimization," *Surveys in Geophysics*, vol. 42, no. 3, pp. 505–549, 2021 (cit. on p. 158).

[293] V. Santucci, M. Baioletti, and G. Di Bari, "An improved memetic algebraic differential evolution for solving the multidimensional two-way number partitioning problem," *Expert Systems with Applications*, vol. 178, p. 114 938, 2021 (cit. on p. 158).

[294] W. Deng, S. Shang, X. Cai, H. Zhao, Y. Song, and J. Xu, "An improved differential evolution algorithm and its application in optimization problem," *Soft Computing*, vol. 25, no. 7, pp. 5277–5298, 2021 (cit. on p. 158).

[295] G. Dueck and T. Scheuer, "Threshold accepting: A general purpose optimization algorithm appearing superior to simulated annealing," *Journal of Computational Physics*, vol. 90, no. 1, pp. 161–175, 1990 (cit. on p. 166).

[296] G. Dueck and T. Scheuer, "Design of open reinforced concrete abutments road bridges with hybrid stochastic hill climbing algorithms," *Informes de la Construcción*, vol. 67, no. 540, e114, 2015 (cit. on p. 166).

[297] D. M. Frangopol, "Life-cycle performance, management, and optimisation of structural systems under uncertainty: Accomplishments and challenges 1," *Structure and infrastructure Engineering*, vol. 7, no. 6, pp. 389–413, 2011 (cit. on p. 186).

[298] D. Martínez-Muñoz, J. García, J. V. Martí, and V. Yepes, "Hybrid swarm intelligence optimization methods for low-embodied energy steel-concrete composite bridges," *Mathematics*, vol. 11, no. 1, p. 140, 2023 (cit. on pp. 186, 199, 209, 211, 217, 238, 239).

[299] J. M. Barandica, G. Fernández-Sánchez, Á. Berzosa, J. A. Delgado, and F. J. Acosta, "Applying life cycle thinking to reduce greenhouse gas emissions from road projects," *Journal of cleaner production*, vol. 57, pp. 79–91, 2013 (cit. on p. 186).

[300] E. Wang and Z. Shen, "A hybrid data quality indicator and statistical method for improving uncertainty analysis in lca of complex system–application to the whole-building embodied energy analysis," *Journal of cleaner production*, vol. 43, pp. 166–173, 2013 (cit. on p. 186).

[301] I. J. Navarro, V. Yepes, J. V. Martí, and F. González-Vidosa, "Life cycle impact assessment of corrosion preventive designs applied to prestressed concrete bridge decks," *Journal of Cleaner Production*, vol. 196, pp. 698–713, 2018 (cit. on p. 187).

[302] M. S. Phadke, *Quality engineering using robust design*. Prentice Hall PTR, 1995 (cit. on p. 187).

[303] G. Taguchi, "Introduction to quality engineering, asian productivity organization," *Dearborn, Michigan: American Supplier Institute Inc*, 1986 (cit. on p. 187).

[304] M. H. Esfe, P. Razi, M. H. Hajmohammad, *et al.*, "Optimization, modeling and accurate prediction of thermal conductivity and dynamic viscosity of stabilized ethylene glycol and water mixture al2o3 nanofluids by nsga-ii using ann," *International Communications in Heat and Mass Transfer*, vol. 82, pp. 154–160, 2017 (cit. on pp. 187, 249).

[305] J. R. Marti-Vargas, F. J. Ferri, and V. Yepes, "Prediction of the transfer length of prestressing strands with neural networks," *Computers and Concrete*, vol. 12, no. 2, pp. 187–209, 2013 (cit. on pp. 187, 249).

[306] P. Satrio, T. M. I. Mahlia, N. Giannetti, K. Saito, *et al.*, "Optimization of hvac system energy consumption in a building using artificial neural network and multi-objective genetic algorithm," *Sustainable Energy Technologies and Assessments*, vol. 35, pp. 48–57, 2019 (cit. on pp. 187, 249).

[307] F. J. Martínez-Martín, V. Yepes, F. González-Vidosa, A. Hospitaler, and J. Alcalá, "Optimization design of RC elevated water tanks under seismic loads," *Applied Sciences*, vol. 12, no. 11, p. 5635, 2022 (cit. on p. 191).

[308] T. C. Hu, A. B. Kahng, and C.-W. A. Tsao, "Old bachelor acceptance: A new class of non-monotone threshold accepting methods," *ORSA Journal on Computing*, vol. 7, no. 4, pp. 417–425, 1995 (cit. on pp. 191, 192).

[309] A. Ruiz-Vélez, J. Alcalá, and V. Yepes, "Optimal design of sustainable reinforced concrete precast hinged frames," *Materials*, vol. 16, no. 1, p. 204, 2023 (cit. on p. 191).

[310] D. Martínez-Muñoz, J. García, J. V. Martí, and V. Yepes, "Discrete swarm intelligence optimization algorithms applied to steel–concrete composite bridges," *Engineering Structures*, vol. 266, p. 114 607, 2022 (cit. on pp. 191, 199, 209, 217, 226, 230, 238, 239).

[311] D. Martínez-Muñoz, J. García, J. V. Martí, and V. Yepes, "Optimal design of steel–concrete composite bridge based on a transfer function discrete swarm intelligence algorithm," *Structural and Multidisciplinary Optimization*, vol. 65, no. 11, p. 312, 2022 (cit. on pp. 191, 199, 200, 209, 211, 221, 226, 232, 235, 238, 239).

[312] GreenDelta GmbH, "Soca v. 2 add-on: Adding social impact information to ecoinvent," *Description of methodology to map social impact information from PSILCA v3 to ecoinvent v. 3.7.1*, 2021 (cit. on pp. 197, 198, 223, 225).

[313] A. Ciroth and F. Eisfeldt, "PSILCA – A product social impact life cycle assessment database," *Database version*, vol. 1, pp. 1–99, 2016 (cit. on pp. 197, 224).

[314] F. Murtagh, "Multilayer perceptrons for classification and regression," *Neurocomputing*, vol. 2, no. 5-6, pp. 183–197, 1991 (cit. on p. 204).

[315] N. V. Chawla, K. W. Bowyer, L. O. Hall, and W. P. Kegelmeyer, "Smote: Synthetic minority over-sampling technique," *Journal of artificial intelligence research*, vol. 16, pp. 321–357, 2002 (cit. on p. 204).

[316] E. Zavadskas, T. Vilutienė, Z. Turskis, and J. Šaparauskas, "Multi-criteria analysis of projects' performance in construction," *Archives of Civil and Mechanical Engineering*, vol. 14, no. 1, pp. 114–121, 2014 (cit. on p. 216).

[317] M. Medineckiene, E. Zavadskas, F. Björk, and Z. Turskis, "Multi-criteria decision-making system for sustainable building assessment/certification," *Archives of Civil and Mechanical Engineering*, vol. 15, no. 1, pp. 11–18, 2015 (cit. on p. 216).

[318] A. Altuzarra, P. Gargallo, J. M. Moreno-Jiménez, and M. Salvador, "Influence, relevance and discordance of criteria in ahp-global bayesian prioritization," *International Journal of Information Technology & Decision Making*, vol. 12, no. 04, pp. 837–861, 2013 (cit. on p. 216).

[319] J. M. Moreno-Jiménez, J. Cardeñosa, C. Gallardo, and M. Á. de la Villa-Moreno, "A new e-learning tool for cognitive democracies in the knowledge society," *Computers in Human Behavior*, vol. 30, pp. 409–418, 2014 (cit. on p. 216).

[320] J. M. Moreno-Jiménez, C. Pérez-Espés, and M. Velázquez, "E-cognocracy and the design of public policies," *Government Information Quarterly*, vol. 31, no. 1, pp. 185–194, 2014 (cit. on p. 216).

[321] C. Fang, Y. Ping, Y. Gao, Y. Zheng, and Y. Chen, "Machine learning-aided multi-objective optimization of structures with hybrid braces – framework and case study," *Engineering Structures*, vol. 269, p. 114 808, 2022 (cit. on p. 216).

[322] A. Ghasemof, M. Mirtaheri, and R. Karami Mohammadi, "Multi-objective optimization for probabilistic performance-based design of buildings using fema p-58 methodology," *Engineering Structures*, vol. 254, p. 113 856, 2022 (cit. on p. 216).

[323] M. Rastegaran, S. Beheshti Aval, and E. Sangalaki, "Multi-objective reliability-based seismic performance design optimization of smrfs considering various sources of uncertainty," *Engineering Structures*, vol. 261, p. 114 219, 2022 (cit. on p. 216).

[324] F. J. Martinez-Martin, F. Gonzalez-Vidosa, A. Hospitaler, and V. Yepes, "Multi-objective optimization design of bridge piers with hybrid heuristic algorithms,"

Journal of Zhejiang University SCIENCE A, vol. 13, no. 6, pp. 420–432, 2012 (cit. on p. 217).

[325] N. Soto, C. Cid, A. Baldomir, and S. Hernández, "Fail-safe optimum cable system under cable breakage in cable-stayed bridges. application to the queensferry crossing bridge," *Engineering Structures*, vol. 279, p. 115 557, 2023 (cit. on p. 217).

[326] J. Nash, "Non-cooperative games," *Annals of Mathematics*, vol. 54, no. 2, pp. 286–295, 1951 (cit. on p. 219).

[327] S. S. Rao, *Engineering optimization theory and practice*. Hoboken, NJ, USA: John Wiley & Sons, Ltd., 2019 (cit. on p. 220).

[328] K. K. Annamdas and S. S. Rao, "Multi-objective optimization of engineering systems using game theory and particle swarm optimization," *Engineering Optimization*, vol. 41, no. 8, pp. 737–752, 2009 (cit. on p. 220).

[329] M. Zeleny, *Multiple Criteria Decision Making*. McGraw-Hill, 1982 (cit. on pp. 221, 231, 232).

[330] A. G. Hussien, A. E. Hassanien, E. H. Houssein, M. Amin, and A. T. Azar, "New binary whale optimization algorithm for discrete optimization problems," *Engineering Optimization*, vol. 52, no. 6, pp. 945–959, 2020 (cit. on p. 230).

[331] V. Yepes, T. García-Segura, and J. Moreno-Jiménez, "A cognitive approach for the multi-objective optimization of RC structural problems," *Archives of Civil and Mechanical Engineering*, vol. 15, no. 4, pp. 1024–1036, 2015 (cit. on p. 231).

[332] V. Penadés-Plà, V. Yepes, and T. García-Segura, "Robust decision-making design for sustainable pedestrian concrete bridges," *Engineering Structures*, vol. 209, p. 109 968, 2020 (cit. on p. 245).